HUMANIZED MOUSE MODELS TO STUDY IMMUNE RESPONSES TO HUMAN INFECTIOUS ORGANISMS

EDITED BY: Qingfeng Chen, Jianzhu Chen and Yan Li
PUBLISHED IN: Frontiers in Immunology

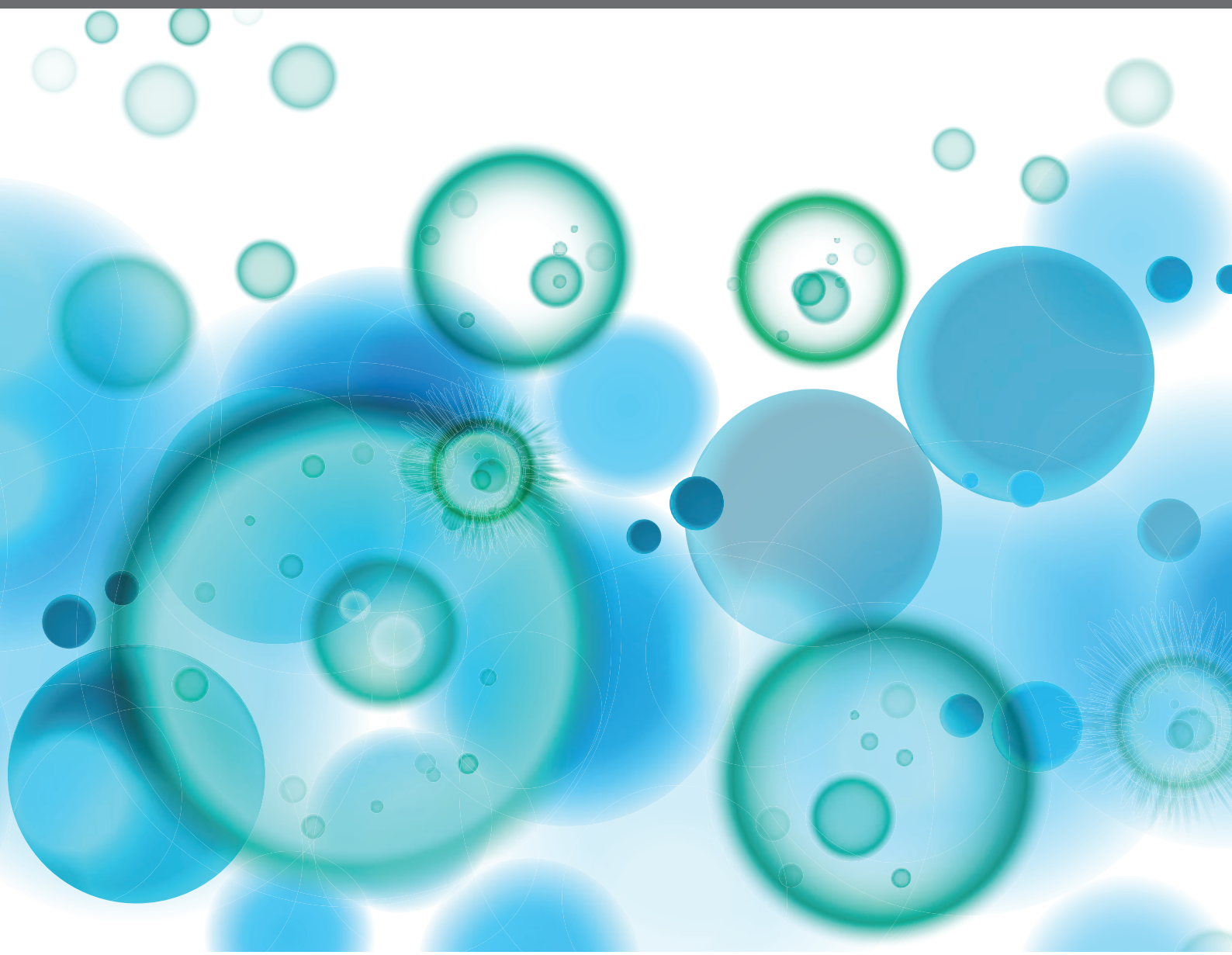

frontiers Research Topics

frontiers

ISSN 1664-8714
ISBN 978-2-88974-822-8
DOI 10.3389/978-2-88974-822-8

About Frontiers

Frontiers is more than just an open-access publisher of scholarly articles: it is a pioneering approach to the world of academia, radically improving the way scholarly research is managed. The grand vision of Frontiers is a world where all people have an equal opportunity to seek, share and generate knowledge. Frontiers provides immediate and permanent online open access to all its publications, but this alone is not enough to realize our grand goals.

Frontiers Journal Series

The Frontiers Journal Series is a multi-tier and interdisciplinary set of open-access, online journals, promising a paradigm shift from the current review, selection and dissemination processes in academic publishing. All Frontiers journals are driven by researchers for researchers; therefore, they constitute a service to the scholarly community. At the same time, the Frontiers Journal Series operates on a revolutionary invention, the tiered publishing system, initially addressing specific communities of scholars, and gradually climbing up to broader public understanding, thus serving the interests of the lay society, too.

Dedication to Quality

Each Frontiers article is a landmark of the highest quality, thanks to genuinely collaborative interactions between authors and review editors, who include some of the world's best academicians. Research must be certified by peers before entering a stream of knowledge that may eventually reach the public - and shape society; therefore, Frontiers only applies the most rigorous and unbiased reviews.
Frontiers revolutionizes research publishing by freely delivering the most outstanding research, evaluated with no bias from both the academic and social point of view. By applying the most advanced information technologies, Frontiers is catapulting scholarly publishing into a new generation.

What are Frontiers Research Topics?

Frontiers Research Topics are very popular trademarks of the Frontiers Journals Series: they are collections of at least ten articles, all centered on a particular subject. With their unique mix of varied contributions from Original Research to Review Articles, Frontiers Research Topics unify the most influential researchers, the latest key findings and historical advances in a hot research area! Find out more on how to host your own Frontiers Research Topic or contribute to one as an author by contacting the Frontiers Editorial Office: frontiersin.org/about/contact

HUMANIZED MOUSE MODELS TO STUDY IMMUNE RESPONSES TO HUMAN INFECTIOUS ORGANISMS

Topic Editors:
Qingfeng Chen, Institute of Molecular and Cell Biology (A*STAR), Singapore
Jianzhu Chen, Massachusetts Institute of Technology, United States
Yan Li, Nanjing University, China

Citation: Chen, Q., Chen, J., Li, Y., eds. (2022). Humanized Mouse Models to Study Immune Responses to Human Infectious Organisms. Lausanne: Frontiers Media SA. doi: 10.3389/978-2-88974-822-8

Table of Contents

frontiers in Immunology

EDITORIAL
published: 10 March 2022
doi: 10.3389/fimmu.2022.860029

Editorial: Humanized Mouse Models to Study Immune Responses to Human Infectious Organisms

Melissa Xin Yu Wong[1,2] *and Qingfeng Chen*[2,3]*

[1] Cardiovascular and Metabolic Disorders, Duke-NUS Graduate Medical School, Singapore, Singapore, [2] Institute of Molecular and Cell Biology, Agency for Science, Technology and Research (ASTAR), Singapore, Singapore, [3] Department of Microbiology and Immunology, Yong Loo Lin School of Medicine, National University of Singapore, Singapore, Singapore

Keywords: humanized mouse models, infectious diseases, human specificity, inflammation, liver humanization

Editorial on the Research Topic

Humanized Mouse Models to Study Immune Responses to Human Infectious Organisms

This Research Topic is a collection of 9 articles covering the latest development in humanized mice technologies pertaining to immune responses towards infectious organisms. Ranging from bacterial infections that rapidly rot tissue and bone, to chronic viral infections with the ability to evade eradication for decades - each organism distinctly interacts and manipulates the human immune response depending on the environment. This begets the need for a model that can faithfully capture the human immune signature and the host-pathogen interaction. This Topic discusses the advances in 2 types of humanized mice: liver-humanized mice, and mice reconstituted with components of the human immune system.

Vector-borne diseases account for close to 20% of all infectious diseases worldwide. There were an estimated 241 million cases of malaria worldwide, resulting in hundreds of thousands of deaths, especially in children under 5. Modelling the life cycle of malaria parasites has been challenging as human red blood cells (hRBCs) are rapidly eliminated *in vivo*. Existing immunodeficient models require daily transfusions to replenish hRBCs, drastically limiting the scope of preclinical testing for therapeutics. Yamaguchi et al. present a novel NOG sub-strain harboring a murine C3 mutation preventing rejection of hRBCs *in vivo*. This allows hRBCs to be retained in humanized mice up to a remarkable 30 days, thus expanding the scenarios that can be studied *in vivo*, such as vaccinations and co-infections.

Zika virus (ZIKV) is another vector-borne virus known for its devastating neurological and obstetric complications. The search for a ZIKV vaccine remains a highly active field of research. Tarbe et al. demonstrate that memory CD8 T cells generated from Japanese Encephalitis Virus (JEV) immunization are cross-reactive against ZIKV infection in HLA-transgenic mice. Live attenuated JEV vaccinations, along with other vector-borne disease vaccines, have been well studied and used clinically. This discovery is an important step in understanding whether cross-protection among these vaccines exist. Perhaps the solution to a longstanding global health problem could lie in evidence-based repurposing of existing resources, making it not too far out of reach.

Hepatitis B virus (HBV) is notoriously difficult to model *in vivo* due to its strong human hepatotropism. Lai et al. discuss how human liver chimeric mice, among a small handful of animals that successfully harbour HBV infection, remain at the forefront of *in vivo* modelling due to their cost efficiency and availability. With current technologies optimized to produce liver humanization exceeding 70%, researchers are now able to study the life cycle of HBV in a large number of animals.

Edited and reviewed by:
Claire Anne Chougnet, Cincinnati Children's Research Foundation, United States

***Correspondence:**
Qingfeng Chen
qchen@imcb.a-star.edu.sg

Specialty section:
This article was submitted to Viral Immunology, a section of the journal Frontiers in Immunology

Received: *22 January 2022*
Accepted: *16 February 2022*
Published: *10 March 2022*

Citation:
Wong MXY and Chen Q (2022) Editorial: Humanized Mouse Models to Study Immune Responses to Human Infectious Organisms. Front. Immunol. 13:860029. doi: 10.3389/fimmu.2022.860029

Furthermore, headway has been made into dual humanization models, which provides a powerful pre-clinical platform for recapitulating parts of the human immune response to HBV and therapeutic effects.

Despite the discovery of antiretroviral therapy, Human Immunodeficiency Virus-1 (HIV-1) has evaded eradication for decades and remains a lifelong disease. Gillgrass et al. succinctly summarise the plethora of humanized mouse models that have been developed to understand the pathogenesis of HIV-1, and how it sustains its reservoir in humans. Critically, the article also discusses the use of humice in dissecting the many confounding factors in patient prognosis, including co-infections, the efficacy of HIV vaccines, and immune system interaction with the endogenous microbiome. Gillgrass' review dovetails nicely with Abeynaike and Paust's article on novel HIV-1 therapies studied in humanized mice, featuring gene-editing strategies like CRISPR/Cas9, as well as immune-based therapies such as Chimeric Antigen Receptor (CAR) T cell immunotherapy.

The strength of current humanized mice technology infectious lies in its ability to initiate innate immune responses and antigen-specific T cell responses. However, the full spectrum of humoral response to diseases is limited by the lack of mature B cells and hence antibody class switching. To address this, Cheng et al. presents a proof-of-concept study where TLR9 agonist CpG-B, in combination with co-stimulatory molecule CD40 targeting, triggers a more efficient transition human B cell maturation in humanized mice. This promotes isotype switching from IgM to IgG, the latter playing an essential role in measuring the human response against infectious diseases, thus adding a new dimension to disease modelling capabilities.

Improved B cell maturation in humanized mice also spells good news for researchers studying lymphoproliferative infectious diseases such as Epstein Barr virus (EBV). The two EBV strains vary in their tissue tropism, thus influencing their oncogenic properties. Schuchmachers and Münz review how humanized mice have allowed researchers to tease out the functional significance of viral structures, and how they interact with host genomics and other co-infections to produce malignancy.

Finally, humanized mice have lent great insight into the pathogen-host interaction in tissue infections. Tackling the study of polymicrobial synergy and dysbiosis of the subgingivial microbiota is no easy feat. Rojas et al. discuss at great length the new ways researchers have inoculated Their article covers the immunotherapies that have sprung forth from such studies. Muthukrishnan et al. also present original research on a model recapitulating S. aureus pathogenesis during osteomyelitis, bringing fresh hope for non-antibiotic interventions to combat implant-associated osteomyelitis, as well as to curb rampant multi-drug resistance.

Humanized mice encompass a powerful platform for interrogating the complexity of infectious disease interactions using an *in vivo* biological system. With infectious diseases evolving so rapidly in an interconnected world, technology must swiftly advance to suit the complexity of real-world issues. Constant sharing of knowledge and a strong network will be crucial in maintaining replicability between models and definitively drive progress in an exciting and dynamic field.

AUTHOR CONTRIBUTIONS

All authors contributed to the article and approved the submitted version.

FUNDING

MW is supported by Duke-NUS MD. Ph.D. program. QC is funded by the National Research Foundation Singapore Fellowship (NRF-NRFF2017-03, NRF-ISF joint grant (NRF2019-NRF-ISF003-3127) and National Medical Research Council- OF-LCG (OFLCG19May-0038).

Conflict of Interest: QC is the scientific founder of two biotech companies.

The remaining author declare that the research was conducted in the absence of any commercial or financial relationships that could be construed as a potential conflict of interest.

Publisher's Note: All claims expressed in this article are solely those of the authors and do not necessarily represent those of their affiliated organizations, or those of the publisher, the editors and the reviewers. Any product that may be evaluated in this article, or claim that may be made by its manufacturer, is not guaranteed or endorsed by the publisher.

frontiers in Immunology

ORIGINAL RESEARCH
published: 25 September 2020
doi: 10.3389/fimmu.2020.577546

Japanese Encephalitis Virus Vaccination Elicits Cross-Reactive HLA-Class I-Restricted CD8 T Cell Response Against Zika Virus Infection

Marion Tarbe[1,2†], Wei Dong[3†], Guang Hu[1,2†], Yongfen Xu[1,2†], Jing Sun[4†], Solene Grayo[1,2], Xianyang Chen[3], Chengfeng Qin[5], Jincun Zhao[4], Li Liu[1,2], Xiuzhen Li[1,2] and Qibin Leng[1,2,3*]*

[1] The Joint Center for Infection and Immunity, Guangzhou Institute of Pediatrics, Guangzhou Women and Children's Medical Center, Guangzhou Medical University, Guangzhou, China, [2] Institut Pasteur of Shanghai, University of Chinese Academy of Sciences, Chinese Academy of Sciences, Shanghai, China, [3] Affiliated Cancer Hospital & Institute of Guangzhou Medical University, State Key Laboratory of Respiratory Disease, Guangzhou, China, [4] State Key Laboratory of Respiratory Disease, Guangzhou Institute of Respiratory Health, The First Affiliated Hospital of Guangzhou Medical University, Guangzhou, China, [5] Department of Virology, State Key Laboratory of Pathogens and Biosecurity, Beijing Institute of Microbiology and Epidemiology, Beijing, China

OPEN ACCESS

Edited by:
Qingfeng Chen,
Institute of Molecular and Cell Biology (A*STAR), Singapore

Reviewed by:
Mingzhao Zhu,
Institute of Biophysics (CAS), China
Honglin Xu,
National Vaccine and Serum Institute, China

***Correspondence:**
Xiuzhen Li
13725100840@163.com
Qibin Leng
qbleng@sibs.ac.cn

[†] These authors have contributed equally to this work

Specialty section:
This article was submitted to Viral Immunology, a section of the journal Frontiers in Immunology

Received: 29 June 2020
Accepted: 07 September 2020
Published: 25 September 2020

Citation:
Tarbe M, Dong W, Hu G, Xu Y, Sun J, Grayo S, Chen X, Qin C, Zhao J, Liu L, Li X and Leng Q (2020) Japanese Encephalitis Virus Vaccination Elicits Cross-Reactive HLA-Class I-Restricted CD8 T Cell Response Against Zika Virus Infection. Front. Immunol. 11:577546. doi: 10.3389/fimmu.2020.577546

Japanese encephalitis virus (JEV) exposure or vaccination could elicit cross-reactive CD8 T cell immunity against heterologous flaviviruses in humans. In addition, cross-reactive CD8 T cells induced by dengue virus (DENV) have been shown to play a protective role against Zika virus (ZIKV). However, how JEV exposure or vaccination affects ZIKV infection in humans remains unclear. In this report, epitope prediction algorithms were used to predict the cross-reactive CD8 T cell epitope restricted to human HLA between JEV and ZIKV. We found that these predicted CD8 T cell epitopes are immunogenic and cross-reactive in humanized HLA transgenic mice. Moreover, JEV vaccine immunization provided cross-protection against ZIKV infection. Furthermore, CD8 T cells were involved in the protection against ZKIV infection *in vivo*. Our results have an important clinical implication that vaccination with JEV SA14-14-2 may provide protection against ZIKV infection in humans.

Keywords: JEV, Zika, cross-reactive, epitope, CD8 T cells, HLA-A2 transgenic mice, heterologous immunity

INTRODUCTION

Zika virus (ZIKV) is a global health threat due to its association with severe congenital malformations and its widespread transmission (1, 2). Nevertheless, the spreading of ZIKV is limited in China and South-East Asia (3–5) despite the presence of ZIKV transmission-competent mosquitoes and the circulation of other flaviviruses, including dengue viruses (DVs) and Japanese encephalitis virus (JEV). Several hypotheses have been suggested to explain the low incidence of ZIKV infection in Asia: low burden of public health prior to the Micronesia epidemic in 2007, misdiagnosis even in the laboratory due to the presence of other flaviviruses, endemic of ZIKV in Asia for several decades potentially providing long-lasting immunity, and/or cross-protective immunity provided by other endemic flaviviruses (6). While cross-reactivity of DV immunity with ZIKV infection has been reported because of the presence of DV in South America (7–9), little is

known about immunologic cross-reactivity of JEV to ZIKV and whether JEV pre-existing immunity may provide protection or contribute to ZIKV pathogenesis.

JEV is an arthropod-borne virus transmitted mainly through the bite of Culex species mosquitoes, primarily *Culex tritaeniorhynchus*. JEV is endemic to South and South-East Asia and epidemic in North Asia. It is reported that JEV seropositivity in adults in Korea range from 79–94% (10). Thus, JEV circulates from Pakistan to Japan and from Korea to Indonesia, as well as through east Pacific regions and northern Australia (11). JEV infection induces disease mainly during childhood. Approximately 10% of infected children develop mild febrile illness, and 0.1 to 1% of them progress to encephalitis, of which 20–30% are fatal and 30–50% result in permanent neurologic sequelae (12). The remainder of JEV infections in humans are clinically silent. The overwhelming majority of JEV-exposed individuals thus develop long-lasting immunity.

Live attenuated JEV vaccine (SA14-14-2) is widely used in China and other Asian countries (13). This vaccine is able to elicit both humoral and cellular immunity. Interestingly, while JEV vaccination in children provides high and long-lasting protection through neutralizing antibodies (14, 15). The vaccination in adults provides a T cell immune response that is more potent than a humoral response (16). Additionally, CD8 T cells in JEV-vaccinated and JEV-exposed healthy human subjects cross-react with DVs (16, 17) and other flaviviruses. Furthermore, Recent studies have revealed that murine MHC I-restricted CD8 T cells from mice infected with JEV or vaccine strain are indeed cross-reactive with ZIKV (18, 19). These evidences suggest JEV vaccination may elicit cross-reactive T cell immunity against ZIKV and thereby affect ZIKV pathogenesis in humans. To test this hypothesis, we performed bioinformatic analysis to predict the cross-reactive epitope between JEV and ZIKV. Then, the immunogenicity of these epitopes and the cross-protective role of CD8 T cells against ZIKV infection were determined in HLA-transgenic mice. Our results imply that JEV vaccination has a potential to protect ZIKV infection in humans by cross-reactive CD8 T cell immunity against these epitopes.

RESULTS

Prediction of Potential Cross-Reactive Epitope to ZIKV Restricted to Human MHCs

Human leukocyte antigen (HLA)-B*58:01(B58), HLA-A*02:01 (A2), HLA-A*11:01 (A11) and HLA-A*24:02 (A24) are prevalent MHC-I molecules in the Asian population. Moreover, HLA-A*02:01 is the most prevalent MHC-I in the Caucasian population. As JEV SA14-14-2 and ZIKV polyproteins share 56% sequence homology, we wondered whether JEV vaccination could induce cross-reactive CD8 T cell response against ZIKV infection in humans. To determine the potential JEV/ZIKV cross-reactive epitope restricted to human MHC-I, we predicted antigenic peptides from the JEV SA14-14-2 polyprotein using Immune Epitope Database Analysis Resource (IEDAR) software and selected candidates presenting IEDAR scores under 4, thereby obtaining 196, 185, 207, and 184 epitopes restricted to HLA B58, HLA A2, HLA A11, and HLA A24, respectively. We then aligned the sequences of the JEV SA14-14-2 polyprotein with ZIKV MR766 (reference strain) and ZIKV SPH2015 (Brazilian strain) to determine identical or similar (no more than 2 mutations) antigenic peptides in BLAST software. Further analysis with IEDAR revealed that 42 HLA B58, 21 HLA A2, 39 HLA A11 and 39 HLA A24-binding candidates were predicted, respectively (**Figure 1A** and **Supplementary Tables 1–3**). Among them, 6 HLA B58, 4 HLA A2, 5 HLA A11 and 7 HLA A24-binding candidates were identical between SA14-14-2 and ZIKV (**Figure 1B**). Moreover, most of these cross-reactive candidates were located in E, NS3 and NS5 proteins of ZIKV (**Figure 1C**). These data imply that JEV vaccination may elicit a cross-reactive CD8 T cell response to ZIKV in humans.

A Dominant JEV Epitope Elicits Cross-Reactive CD8 T Cell Response to ZIKV Infection in HLA A2-Transgenic Mice

Considering the availability of HLA transgenic mice and HLA genotype prevalence in humans, we focused our study on the HLA A2-restricted epitopes and evaluated the immunogenic properties of these potential cross-reactive epitopes *in vivo*. HHD mice, which are transgenic mice with a C57B/L6 background that express the human MHC-I A2 epitope-binding site (20), were infected either with the JEV-attenuated strain SA14-14-2 or ZIKV SZ-WIV01. Seven days after infection, splenocytes were collected and stimulated with each HLA A2-restricted peptide in an IFNγ-ELISpot assay. As shown in **Figure 2A**, J2, Z2, J/Z11, J12, Z12, Z12' and Z14' peptides were immunogenic epitopes in JEV infection. However, in ZIKV infection, the T cell response to J2 and Z2 peptides was negligible. J12, Z12 and Z12' peptides are the most dominant epitopes in response to ZIKV infection (**Figure 2B**). An intracellular staining assay confirmed that CD8 T cells from ZIKV-infected HHD mice indeed responded to all J12, Z12 and Z12' peptides by producing IFNγ. Moreover, CD8 T cells that responded to J12, Z12 and Z12' peptides were polyfunctional because they produced both IFNγ and TNFα (**Figure 2C**).

To further determine the cross-reactivity between J12 and Z12-specific CD8 T cells, J12 and Z12 tetramer were used to stain CD8 T cells collected from ZIKV-infected mice. We found that Z12 and J12 dual -reactive cells are significantly higher than Z12-specific CD8 T cells (**Figure 2D**). These results indicate that Z12-specific CD8 T cells are cross-reactive with J12-specific CD8 T cells. Altogether, these results demonstrate that JEV vaccination induces cross-reactive HLA A2-restricted CD8 T cells to ZIKV.

JEV Vaccination Polarizes CD8 T Cell Response to the Cross-Reactive ZIKV Epitope

We next studied whether JEV vaccination could affect the CD8 T cell response to ZIKV infection *in vivo*. HHD mice were first immunized with the JEV SA14-14-2 vaccine and then

A

Name	Virus strains	Position	Sequence	Score (%)
Z1	ZIKV-shared	16	MLKRGVARV	2.5
J1	SA14	16	MLKRGLPRV	1.5
Z2	ZIKV-shared	283	LLIAPAYSI	0.7
J2	SA14	287	LLVAPAYSF	2.4
Z3	ZIKV-shared	741/745*	SLFGGMSWF	4.9
J3	SA14	745	TLFGGMSWI	1.4
Z4	MR766	1218	HLALVAAFK	3.8
J4	SA14	1222	HLALIAVFK	3.9
Z4'	SPH2015/SZWIV01	1222	HLALIAAFK	3.5
Z5	ZIKV-shared	1404/1408*	GLLIVSYVV	0.5
J5	SA14	1410	GLMAVSYVV	0.2
Z6	ZIKV-shared	1538/1542*	VMQEGVFHT	1.7
J6	SA14	1544	VMYENVFHT	0.8
Z/J7	ZIKV (all strains) and JEV-shared	1812/1816/1818**	FMTATPPGT	3.1
Z8	ZIKV-shared	1856/1860*	KTVWFVPSV	1.8
J8		1862	KTVWFVASV	2.1
Z9	ZIKV-shared	2229/2233*	LLLVVLIPE	2.4
J9	SA14	2236	LLMVVLIPE	2.2
Z10	ZIKV-shared	2294/2298*	SMDIDLRPA	3.3
J10	SA14	2303	SMALDLRPA	3
Z/J11	ZIKV (all strains) and JEV-shared	2774/2778/2786**	NLGSGTRAV	1.1
Z12	MR766	2836	SLVNGVVRL	1.9
J12	SA14	2848	SLVNGVVKL	2.1
Z12'	SPH2015/SZWIV01	2840	SLINGVVRL	1.1
Z13	ZIKV-shared	2990/2994*	AIWYMWLGA	3.9
J13	SA14	3002	AIWFMWLGA	4
Z14	ZIKV-shared	2993/2997*	YMWLGARFL	0.4
J14	SA14	3005	FMWLGARYL	0.3
Z15	ZIKV-shared	3008/3012*	FLNEDHWMG	3.3
J15	SA14	3020	FLNEDHWLS	1.8
Z/J16	ZIKV (all strains) and JEV-shared	3291/3295/3305**	RLMANAICS	2.2
J/Z17	MR766/SA14	3292/3306	LMANAICSA	1.5
Z17'	SPH2015/SZWIV01	3296	LMANAICSS	6.8
Z18	MR766	3322	MTTEDMLMV	3
J18	SA14	3336	MTTEDMLQV	3.6
Z18'	SPH2015/SZWIV01	3326	MTTEDMLVV	3.4

B

	Total	Identical	Similar
B5801	196	6	36
A201	185	4	17
A1101	207	5	34
A2402	184	7	32

C

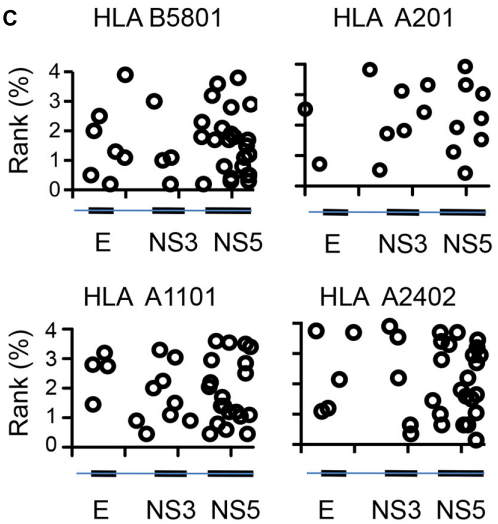

FIGURE 1 | Prediction of JEV and ZIKV-derived cross-reactive HLA-B*58:01, HLA-A*02:01, HLA-A*11:01 and HLA-A*24:02-restricted epitope candidates. **(A)** Sequence of predicted HLA-A*02:01-restricted JEV SA14, ZIKV MR766, ZIKVSPH2015 and ZIKVSZWIV01 cross-reactive epitopes. **(B)** Number of predicted JEV-derived HLA-B*58:01, HLA-A*02:01, HLA-A*11:01 and HLA-A*24:02-restricted epitopes and their comparison with ZIKV MR766-derived epitopes. **(C)** Location of predicted cross-reactive epitopes on the JEV polyprotein sequence and IEDB percentage ranks. *Starting position in MR766 (-/) and SPH2015/SZWIV01 (/-); **Starting position in MR766 (-/), SPH2015/SZWIV01 (/-/) and SA14 (/-).

infected with ZIKV 28 days later. Non-immunized HHD mice that received ZIKV infection were served as control group. Five days post ZIKV infection, splenocytes were harvested. ELISpot was used to determine the CD8 T cell response to ZIKV epitopes. As expected, T cells responded to J12, Z12, and Z12' peptides in Non-immunized group because of ZIKV infection. Notably, the responses to these peptides were 2 to 4 times higher in the JEV-immunized group than in the non-immunized group (**Figure 3A**).

We next used ICS assay to examine the IFNγ and TNFα production of CD8 T cells from JEV-immunized mice in response to peptide J12, Z12, and Z12'. As shown in the **Figure 3B**, the proportions of IFNγ producing CD8 T cells in the JEV-immunized group in response to J12, Z12 and Z12' peptides were approximately 4 times higher than that in the non-immunized group. Furthermore, IFNγ-producing T cells appeared polyfunctional, as nearly 50% of them also expressed TNFα (**Figures 3C,D**). In addition, the majority of IFNγ and TNFα-producing T cells expressed high levels of CD44 molecules (**Figures 3E,F**), a memory phenotype, indicating the T cell responses are a recall response. These data suggest that JEV vaccination polarizes CD8 T cell response to a dominant epitope that cross-reacts with ZIKV.

JEV-Specific CD8 T-Cells Provide Cross-Protection Against ZIKV Infection

Next, the protective potential of the JEV cross-reactive CD8 T cells against ZIKV infection was determined *in vivo*. We first generated HHD *Ifnar1*$^{-/-}$ mice that are susceptible to ZIKV by crossing HHD mice with *Ifnar1*$^{-/-}$ mice. HHD *Ifnar1*$^{-/-}$ mice were immunized twice with JEV on days 1 and 28, and then mice were challenged with ZIKV 14 days after the second immunization. The non-immunized mice lost approximately 17% of their body weight from day 4 to day 7 after ZIKV infection (**Figure 4A**). Eighty percent of these mice died 10 days after ZIKV infection (**Figure 4B**). In contrast, the immunized mice lost little body weight, and only 1 out of 7 mice died after ZIKV infection

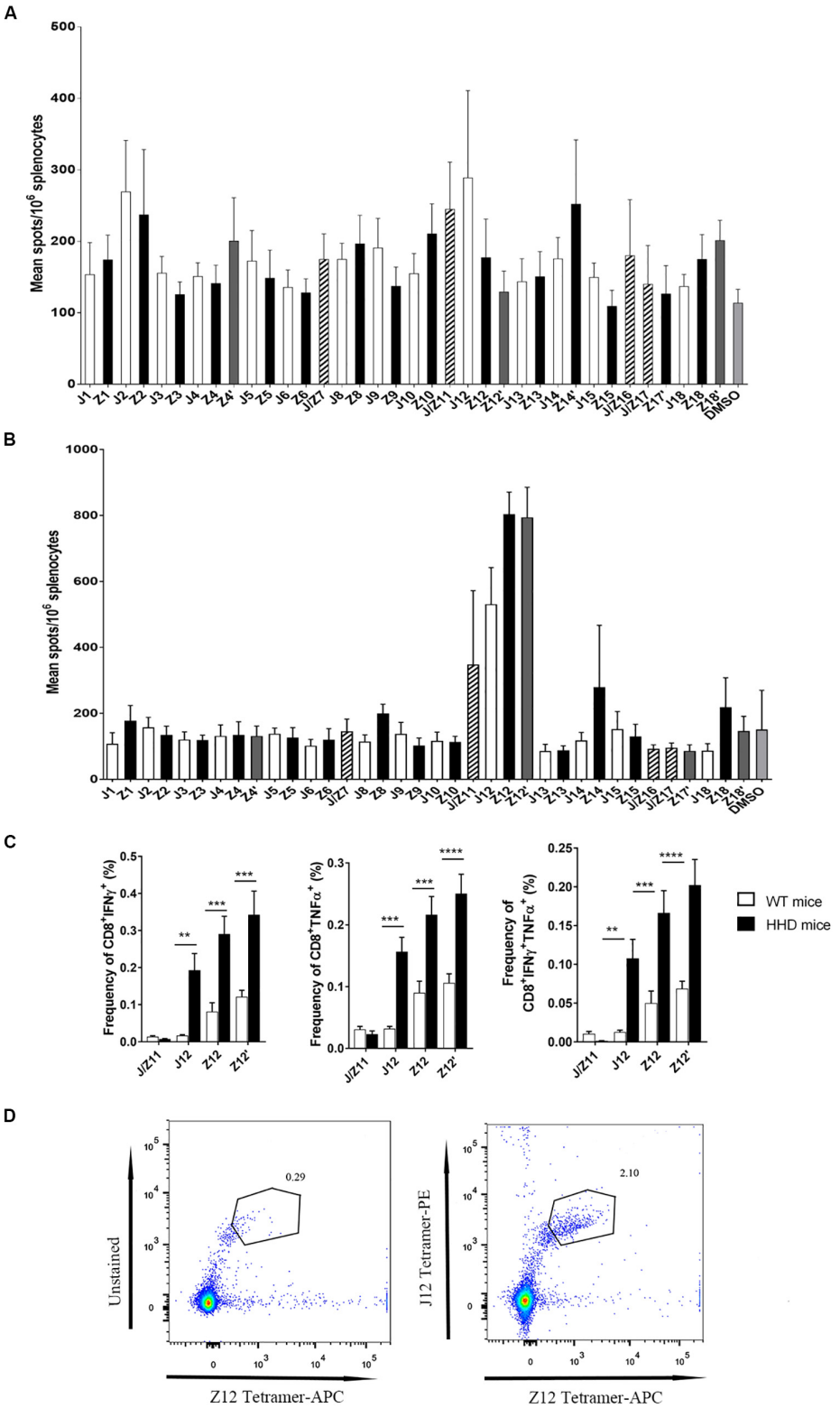

FIGURE 2 | Identification of JEV and ZIKV epitopes recognized by JEV- and ZIKV-specific $CD8^+$ T cells in HHD mice. **(A)** IFNγ ELISpot assay of splenocytes from JEV SA14-14-2-immunized HHD mice ($n = 5$) stimulated with the indicated peptides. **(B)** IFNγ ELISpot assay of splenocytes from ZIKV SZWIV01-infected HDD mice stimulated with the indicated peptides. **(C)** Intracellular staining of splenocytes from ZIKV SZWIV01-infected HDD mice. Splenocytes were stimulated with J/Z11, J12, Z12 and Z12' peptides. ZIKV SZWIV01-infected WT mice served as negative controls. Cells were gated on both CD8 and TCRβ positive. **(D)** HLA A2-J12 and Z12 tetramer staining of splenocytes from ZIKV SZWIV01-infected HDD mice.

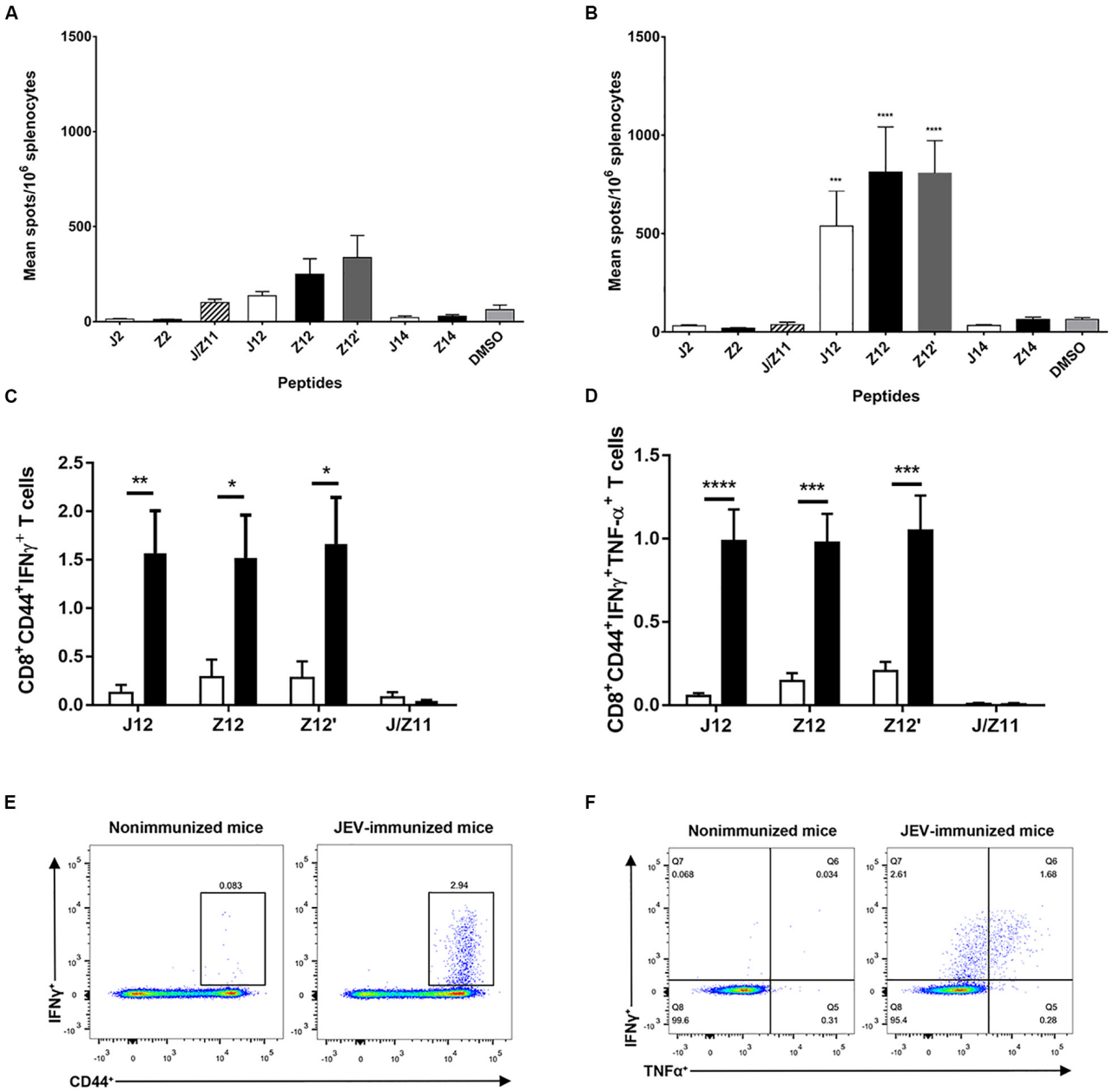

FIGURE 3 | JEV-specific CD8 T cells are recalled upon ZIKV infection in HHD mice. **(A,B)** IFNγ ELISpot assay of indicated epitopes with splenocytes from HHD mice (n = 5 each) that were immunized without **(A)** or with **(B)** the JEV SA14-14-2 vaccine once and then infected with ZIKV. **(C,D)** Intracellular staining of splenocytes from HHD mice (n = 5 each) that were immunized with or without the JEV SA14-14-2 vaccine once and then infected with ZIKV. The splenocytes were cultured with indicated peptides before intracellular staining. The averages of $IFN\gamma^+$ **(C)** and $IFN\gamma^+TNF\alpha^+$ **(D)** gated on CD8 T cells. **(E,F)** Representative plot of IFNγ and TNFα expression in CD8 T cells.

(**Figures 4A,B**). These observations suggest that JEV vaccination protects humanized HHD transgenic mice from ZIKV infection.

To determine the cross-protective role of CD8 T cells against ZIKV infection, we transferred purified CD8 T cells from JEV-immunized mice to naïve HHD *Ifnar1*$^{-/-}$ mice prior to ZIKV infection. After ZIKV challenge, all the control mice lost more than 20% of their initial weight in the first week and had to be sacrificed on day 7 or 8 post infection. Mice that were adoptively transferred with JEV-specific CD8 T cells showed similar weight loss as control mice, but three mice (30%) in this group started to recover from day 6 post infection onward (**Figures 5A,B**).

To further confirm the protective role of CD8 T cells against ZIKV infection, we performed CD8 T cell depletion study in HHD transgenic mice. As shown in **Figures 5C,D**, JEV-immunized mice that received isotype control antibody slightly loss weight and recovered rapidly after day 8 post-infection,

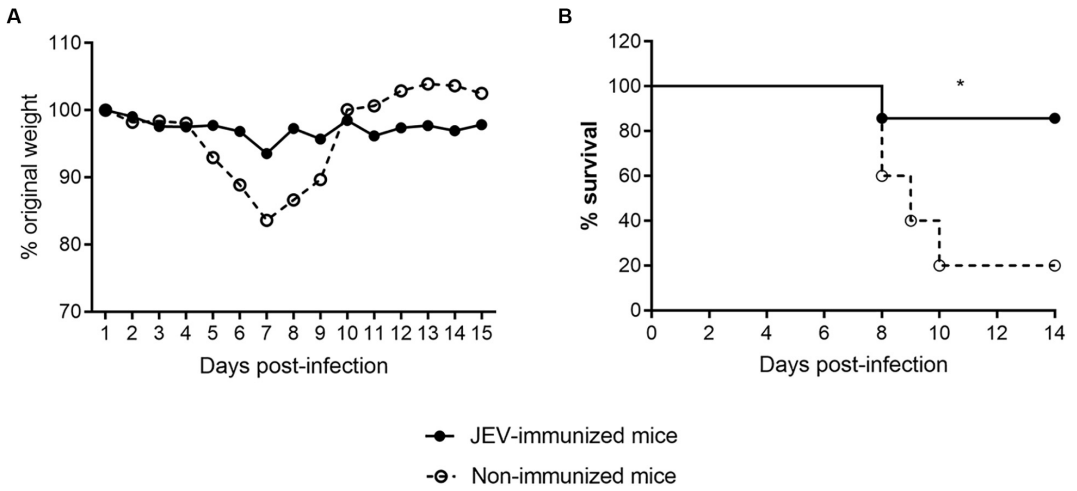

FIGURE 4 | JEV immunization provides protection against ZIKV infection in HHD *Ifnar1*$^{-/-}$ mice **(A,B)**. Body weight **(A)** and survival rate **(B)** of HHD *Ifnar1*$^{-/-}$ mice (n = 5 each) that were injected with JEV SA14-14-2 vaccine (n = 7) or mock (n = 5) two times on days 0 and 28 and then infected with ZIKV on day 14 after the boost.

and all the mice survived. At the opposite, when CD8 T cells were depleted in JEV-immunized group, all the mice in this group continuously lost weight and none of them survived after day 12 post ZIKV infection. Collectively, these data indicate that memory CD8 T cells generated from JEV immunization could provide cross-protection against ZIKV infection in HHD transgenic mice.

DISCUSSION

In this study, we found abundant cross-reactive epitope candidates that have the potential to be presented by the most prevalent MHC-I molecules in the Asian population. Consistent with previous studies, most of these epitope candidates were mainly located in the E, NS3 and NS5 proteins (21–23). We used HLA-transgenic mice to validate those HLA A2-restricted candidates. Among the candidates, the J12 peptide SLVNGVVKL from JEV appeared to be the most immunogenic and immunodominant epitope. Additionally, JEV vaccination induced memory CD8 T cells that can recognize ZIKV analogs SLINGVVRL and SLVNGVVRL, whereas ZIKV-specific CD8 T cells could also cross-react with J12-specific CD8 T cells. Furthermore, adoptively transfer JEV-specific CD8 T cells also could provide cross-protection against ZIKV infection in HLA-A2 transgenic mice. Taken together, these observations suggest that JEV vaccine immunization induce JEV-specific CD8 T cells, having the potential to provide cross-protection against ZIKV infection in humans.

Previous studies by us and others have independent shown that antibodies against JEV are cross-reactive to ZIKV, but passive transfer of JEV antisera fails to protect ZIKV infection in *Ifnar1*$^{-/-}$ mice (18, 24). Thus, antibody response is unlikely to mediate the protection of JEV vaccine-immunized HLA-transgenic or non-transgenic *Ifnar1*$^{-/-}$ mice from ZIKV infection. Although JEV antibodies exhibit antibody-dependent enhancement (ADE) of infection *in vitro*, the ADE effect was not observed in JEV vaccine-immunized mice or JEV antisera transferred mice (18, 24). It has been shown in Dengue virus infection, efficient CD8 T cells response is sufficient to inhibit ADE in infected mice. Our present study together with previous findings (18, 24) all suggest that cross-reactive JEV-specific CD8 T cells are protective to ZIKV infection in wild-type mice that are not HLA-transgenic (18, 19, 25). Thus, JEV vaccine can be clinically used for the prevention of ZIKV infection and also is at low risk of ADE induction in immune-competent humans.

In this study, we found that JEV vaccine immunization can provide cross-protection, but the adoptive transfer of CD8 T cells from JEV vaccine-immunized mice only partially protected naïve HHD *Ifnar1*$^{-/-}$ mice from ZIKV infection. One possible reason for this partial protection is that adoptive CD8 T cells failed to migrate into ZIKV-infected tissues due to a lack of micromilieu cues. Second, it is also possible that cross-reactive CD4 T cells are also important for cross-protection. Furthermore, JEV SA14-14-2 vaccine, as a live virus, could also activate some innate immune cells upon immunization in mice. Upon activation, innate immune cells become memory-like cells and respond to heterologous pathogens quickly and robustly within a few weeks to months. This process is named as trained immunity (26). Thus, it is also possible that JEV vaccination could induce trained immunity and thereby contribute to partial cross-protection against ZIKV infection.

Besides ZIKV, several flaviviruses, including West Nile virus, Usutu virus, Murray Valley encephalitis virus, Alfuy virus, and Spondweni virus, are also closely related to JEV (27). Whether JEV vaccination could elicit cross-protective immunity against these viruses remain unknown. Furthermore, vaccines for tick-borne encephalitis, yellow fever virus and dengue virus have also been clinically approved in humans (28). It is therefore of interest to study whether immunization of these vaccines in humans could affect other closely related flaviviruses. Understanding which mechanisms are involved in cross-protection against other

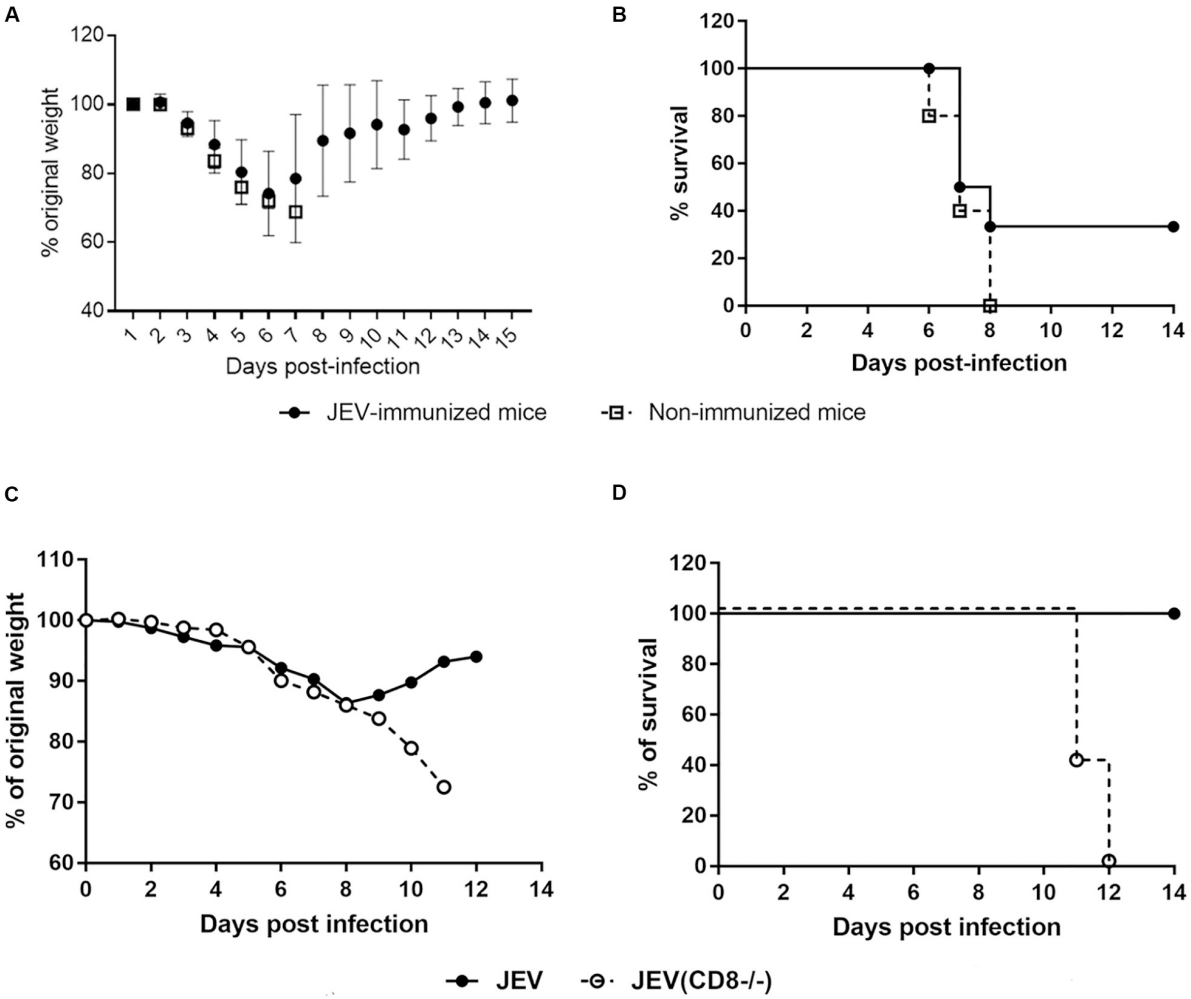

FIGURE 5 | JEV-specific CD8 T cells contribute to the cross-protection against ZIKV in HHD *Ifnar1*$^{-/-}$ mice **(A,B)**. Body weight **(A)** and survival **(B)** of HHD *Ifnar1*$^{-/-}$ mice (n = 5 each) that were injected with JEV SA14-14-2 vaccine (n = 7) or mock (n = 5) two times on days 0 and 28. CD8 T cells were purified and adoptively transferred to naïve mice before ZIKV infection, body weight (A) and survival rate **(B)** were monitored. **(C,D)** CD8 T cells in JEV SA14-14-2-immunized mice were depleted with antibody before ZIKV challenge, body weight **(C)** and survival rate **(D)** of HHD *Ifnar1*$^{-/-}$ mice (n = 6 each) were monitored.

closely related flavivirus is helpful for developing novel strategies to mitigate or prevent newly emerging flavivirus in future.

MATERIALS AND METHODS

Mice and Ethics Statement

HHD (C57BL/6 background) and WT C57BL/6 mice were originally obtained from Dr. F. Lemonnier (Institute Pasteur Paris) and the Shanghai Laboratory Animal Center (SLAC), respectively. AG6 mice deficient in both IFNAR1 and IFNGR were generated from C57BL/6 background *Ifngr1*$^{-/-}$ mice (Jackson laboratories, #003288) and *Ifnar1*$^{-/-}$ A129 mice (B&H company). AG6 mice were backcrossed to C57BL/6 background mice for more than 8 generations. HHD *Ifnar1*$^{-/-}$ mice were further generated by crossing AG6 mice with HHD mice. All mice were maintained and bred at the Institute Pasteur of Shanghai under standard pathogen-free conditions. Animal experiments were carried out in the animal biosafety level 2 laboratory and were approved by the Animal Care and Use Committee of the Institute Pasteur of Shanghai, CAS (Approval number: A2017017).

Peptide Synthesis

Peptides were synthesized by Genscript with a purity >95% confirmed by HPLC and mass spectrometry. All peptides were dissolved in DMSO at 10 mg/ml and stored at −20°C.

Viruses, Cells, and Reagents

The African Green kidney cell line Vero, Vero E6 and the Baby Hamster Kidney cell line BHK-21 were grown in Dulbecco's Modified Eagle Medium (DMEM, Gibco, Suzhou, United States), and human erythroleukemic K562 cells were grown in RPMI 1640 medium (Gibco, Suzhou, United States) at 37°C with 5%

CO_2. All media were supplemented with 10% heat-inactivated fetal bovine serum (FBS, Gibco, Suzhou, United States), 100 U/ml penicillin (Gibco, Suzhou, United States) and 100 μg/ml streptomycin (Gibco, Suzhou, United States). The live-attenuated vaccine strain Japanese encephalitis virus SA14-14-2 was gifted by Dr. Chengfeng Qin, and virus stocks were propagated on BHK-21 cells and titrated on Vero E6 cells by plaque-forming assay. The Zika virus strain SZ-WIV01 (GenBank number KU963796) was obtained from the Microorganisms & Viruses Culture Collection Center, Wuhan Institute of Virology, CAS, and virus stocks were propagated on Vero cells and titrated on Vero E6 cells by plaque-forming assay.

PMA and ionomycin were purchased from Sigma-Aldrich. Brefeldin A was purchased from Biotime. Antibodies against mouse CD8α, CD3, TCRβ, CD44, CD69, IFNγ and TNFα were purchased from eBioscience.

JEV Vaccine Immunization and Infection With ZIKV

JEV SA-14-14-2 (5×10^4 pfu/mouse) or ZIKV (1×10^4 pfu/mouse) was administered to 6- to 8-week-old HHD mice by intraperitoneal injection (i.p.) or retro-orbital injection. Seven days post infection, splenocytes were collected for flow cytometry analysis or ELISpot assay.

To detect JEV-specific CD8 T cells cross-reactive with ZIKV, 6- to 8-week-old HHD mice were immunized with SA-14-14-2 (i.p., 5×10^4 pfu/mouse) and infected with ZIKV (r.o., 1×10^4 pfu/mouse) 28 days after immunization. Five days post infection, splenocytes were collected for flow cytometry analysis or ELISpot assay.

Mouse IFNγ ELISpot Assay

Mouse IFNγ ELISpot assay was performed using the ELISpot kit (3321-2A, Mabtech) according to the manufacturer's instruction. Briefly, the day before the experiment, plates were coated with anti-IFNγ antibody AN18 at 4°C overnight. After the plates were washed with PBS and blocked with 10% FBS in RPMI, 0.4 μg of each peptide and 2.5×10^5 cells/well were added. The plates were incubated for 40 hours and then washed and visualized. Wells containing splenocytes in the presence of anti-CD3 and anti-CD28 antibodies were used as positive controls, while negative controls contained splenocytes in the presence of DMSO.

ZIKV Challenge in HHD *Ifnar1*$^{-/-}$ Mice

Four-week-old HHD *Ifnar1*$^{-/-}$ mice were immunized with two doses of 5×10^4 pfu JEV SA14-14-2 four weeks apart. Two weeks after the second immunization, the mice were infected with 10^4 pfu of ZIKV SZ-WIV01. Mouse survival, weight change and clinical score were monitored over 2 weeks. Clinical scores were graded as follows: 0 = healthy; 1 = ruffled fur; 2 = hunched position or reduced activity; 3 = limb weakness; 4 = paralyzed and 5 = moribund or dead.

For CD8 T cell adoptive transfer, 6- to 8-week-old HHD mice were immunized with 5×10^4 pfu of JEV SA14-14-2. Four weeks post immunization, splenocytes were collected, and CD8 T cells were isolated using the EasySep^{TM} Mouse CD8 + T Cell Isolation Kit according to the manufacturer's specifications. Then, 5-week-old HHD *Ifnar1*$^{-/-}$ mice were injected with 7.5 million purified CD8-positive splenocytes *via* the i.p. route. One day later, recipient mice were inoculated with 2×10^5 pfu ZIKV, and their survival and weight change were assessed for 2 weeks.

Flow Cytometry

Cells were washed and blocked in staining buffer (PBS, 0.3% BSA and 0.1% sodium azide) containing the anti-CD16/CD32 antibody for 10 min at 4°C and then stained with fluorophore-conjugated antibodies. After the cells were washed twice with staining buffer, data were collected on a Fortessa flow cytometer (BD Biosciences). For intracellular staining, 2.5 μg/ml BFA was added during the last 4 h of stimulation to block the secretion of cytokines. After the cells were washed and stained for cell-surface markers and fixated and permeabilized with the IC fixation buffer Kit (eBioscience) according to the manufacturer's protocol, the cells were stained with FITC-anti-mouse IFNγ or isotype control and analyzed with a Fortessa flow cytometer. The data were analyzed using FlowJo software.

Statistical Analyses

Statistical analyses for continuous data were performed with Prism6 for Windows software (Prism Graph-Pad Software Inc.). $P < 0.05$ was considered significant. Graphs were produced, and statistical analyses were performed using GraphPad Prism.

DATA AVAILABILITY STATEMENT

All datasets presented in this study are included in the article/**Supplementary Material**.

ETHICS STATEMENT

The animal study was reviewed and approved by Shanghai Laboratory Animal Center.

AUTHOR CONTRIBUTIONS

QL and XL designed this research. MT, WD, GH, YX, JS, SG, and XC performed the research. CQ, LL, and JZ contributed to reagents and animals. MT, WD, LL, and SG analyzed the data. MT, WD, and QL wrote the manuscript. All authors contributed to the article and approved the submitted version.

FUNDING

MT and WD were funded by the National Natural Science Foundation of China (81750110552 and 81901602, respectively). QL was funded by grants from the National Natural Science Foundation of China (31800735 and 31870829), and the National Key Project for Infectious Diseases of China (2018ZX10301-208).

ACKNOWLEDGMENTS

We wish to thank the staff in the flow cytometry and animal facilities at the State Key Laboratory of Respiratory Disease and Institut Pasteur of Shanghai.

SUPPLEMENTARY MATERIAL

The Supplementary Material for this article can be found online at: https://www.frontiersin.org/articles/10.3389/fimmu.2020.577546/full#supplementary-material

REFERENCES

1. Boggild AK, Geduld J, Libman M, Yansouni CP, McCarthy AE, Hajek J, et al. Surveillance report of Zika virus among *Canadian travellers* returning from the Americas. *CMAJ.* (2017) 189:E334–40. doi: 10.1503/cmaj.161241
2. Driggers RW, Ho CY, Korhonen EM, Kuivanen S, Jaaskelainen AJ, Smura T, et al. Zika virus infection with prolonged maternal viremia and fetal brain abnormalities. *N Engl J Med.* (2016) 374:2142–51. doi: 10.1056/NEJMoa1601824 doi: 10.1056/nejmoa1601824
3. Singapore Zika Study Group. Outbreak of Zika virus infection in Singapore: an epidemiological, entomological, virological, and clinical analysis. *Lancet Infect Dis.* (2017) 46:509–20. doi: 10.1016/S1473-3099(17)30249-9
4. Chu D-T, Ngoc VTN, Tao Y. Zika virus infection invietnam: current epidemic, strain origin, spreading risk, and perspective. *Eur J Clin Microbiol Infect Dis.* (2017) 36:2041–2. doi: 10.1007/s10096-017-3030-8
5. Duong V, Ong S, Leang R, Huy R, Ly S, Mounier U, et al. Low circulation of Zika virus, Cambodia, 2007-2016. *Emerg Infect Dis.* (2017) 23:296–9. doi: 10.3201/eid2302.161432
6. Duong V, Dussart P, Buchy P. Zika virus in Asia. *Int J Infect Dis.* (2017) 54:121–8.
7. Dejnirattisai W, Supasa P, Wongwiwat W, Rouvinski A, Barba-Spaeth G, Duangchinda T, et al. Dengue virus sero-cross-reactivity drives antibody-dependent enhancement of infection with Zika virus. *Nat Immunol.* (2016) 17:1102–8. doi: 10.1038/ni.3515
8. Wen J, Tang WW, Sheets N, Ellison J, Sette A, Kim K, et al. Identification of Zika virus epitopes reveals immunodominant and protective roles for dengue virus cross-reactive CD8+ T cells. *Nat Microbiol.* (2017) 2:17036. doi: 10.1038/nmicrobiol.2017.36
9. Priyamvada L, Quicke KM, Hudson WH, Onlamoon N, Sewatanon J, Edupuganti S, et al. Human antibody responses after Dengue virus infection are highly cross-reactive to Zika virus. *Proc Natl Acad Sci USA.* (2016) 113:7852–7. doi: 10.1073/pnas.1607931113
10. Choe YJ, Taurel AF, Nealon J, Seo HS, Kim HS. Systematic review of seroepidemiological studies on Japanese encephalitis in the Republic of Korea. *Int J Infect Dis.* (2018) 67:14–9. doi: 10.1016/j.ijid.2017.11.023
11. Wang H, Liang G. Epidemiology of Japanese encephalitis: past, present and future propestcs. *Therapeut Clin Risk Manag.* (2015) 11:435–48. doi: 10.2147/tcrm.s51168
12. Fischer M, Lindsey N, Staples E, Hills S. *Japanese Encephalitis Vaccines: Recommendations of the Advisory Committee on Immunization Practices (ACIP), Morbidity and Mortality Weekly Report (MMWR)(59(RR01))*. Atlanta, GA: Centers for Disease Control and Prevention CDC (2010). p. 1–27.
13. Yu Y. Phenotypic and genotypic characteristics of Japanese encephalitis attenuated live vaccine virus SA14-14-2 and their stabilities. *Vaccine.* (2010) 28:3635–41. doi: 10.1016/j.vaccine.2010.02.105
14. Zaman K, Naser AM, Power M, Yaich M, Zhang L, Ginsburg AS, et al. Lot-to-lot consistency of live attenuated SA 14-14-2 Japanese encephalitis vaccine manufactured in a good manufacturing practice facility and non-inferiority with respect to an earlier product. *Vaccine.* (2014) 32:6061–6. doi: 10.1016/j.vaccine.2014.09.012
15. Tandan JB, Ohrr H, Sohn YM, Yoksan S, Ji M, Nam CM, et al. Single dose of SA 14-14-2 vaccine provides long-term protection against Japanese Encephalitis: a case-control study in Nepalese children 5 years after immunization. *Vaccine.* (2007) 25:5041–5. doi: 10.1016/j.vaccine.2007.04.052
16. Turtle L, Tatullo F, Bali T, Ravi V, Soni M, Chan S, et al. Cellular immune responses to live attenuated Japanese encephalitis (JE) vaccine SA-14-14-2 in adults in a JE/Dengue co-endemic area. *PLoS Neglect Trop Dis.* (2017) 11:e0005263. doi: 10.1371/journal.pntd.0005263
17. Turtle L, Bali T, Buxton G, Chib S, Chan S, Soni M, et al. Human T cell responses to Japanese encephalitis virus in health and disease. *J Exp Med.* (2016) 213:1331–52. doi: 10.1084/jem.20151517
18. Zhang W, Xu Y, Zhao F, Tarbe M, Zhou S, Wang W, et al. The pre-existing cellular immunity to Japanese encephalitis virus heterotypically protects mice from Zika virus infection. *Sci. Bullet.* (2019) 65:6. doi: 10.1016/j.scib.2019.11.006
19. Chen D, Duan Z, Zhou W, Zou W, Jin S, Li D, et al. Japanese encephalitis virus-primed CD8+ T cells prevent antibody-dependent enhancement of Zika virus pathogenesis. *J Exp Med.* (2020) 217:e20192152. doi: 10.1084/jem.20192152
20. Pascolo S, Bervas N, Ure JM, Smith AG, Lemonnier FA, Perarnau B. HLA-A2.1-restricted education and cytolytic activity of CD8(+) T lymphocytes from beta2 microglobulin (beta2m) HLA-A2.1 monochain transgenic H-2Db beta2m double knockout mice. *J Exp Med.* (1997) 185:2043–51. doi: 10.1084/jem.185.12.2043
21. Lai L, Rouphael N, Xu Y, Natrajan MS, Beck A, Hart M, et al. Innate, T-, and B-cell responses in acute human zika patients. *Clin Infect Dis.* (2018) 66:1–10. doi: 10.1093/cid/cix732
22. Edupuganti S, Natrajan MS, Rouphael N, Lai L, Xu Y, Feldhammer M, et al. Biphasic zika illness with rash and joint pain. *Open Forum Infect Dis.* (2017) 4:ofx133. doi: 10.1093/ofid/ofx133
23. Waggoner JJ, Rouphael N, Xu Y, Natrajan M, Lai L, Patel SM, et al. Pericarditis associated with acute zika virus infection in a returning traveler. *Open Forum Infect Dis.* (2017) 4:ofx103. doi: 10.1093/ofid/ofx103
24. Wang R, Zhen Z, Turtle L, Hou B, Li Y, Wu N, et al. T cell immunity rather than antibody mediates cross-protection against Zika virus infection conferred by a live attenuated Japanese encephalitis SA14-14-2 vaccine. *Appl Microbiol Biotechnol.* (2020) 104:6779–89. doi: 10.1007/s00253-020-10710-z
25. Wang R, Zhen Z, Turtle L, Hou B, Li Y, Gao N, et al. Cross-protection against zika virus infection conferred by a live attenuated japanese encephalitis SA14-14-2 vaccine. *bioRxiv.* (2020). [Preprint]. doi: 10.1101/2020.02.14.950352
26. Netea MG, Giamarellos-Bourboulis EJ, Dominguez-Andres J, Curtis N, van Crevel R, van de Veerdonk FL, et al. Trained immunity: a tool for reducing susceptibility to and the severity of SARS-CoV-2 infection. *Cell.* (2020) 181:969–77. doi: 10.1016/j.cell.2020.04.042
27. Moureau G, Cook S, Lemey P, Nougairede A, Forrester NL, Khasnatinov M, et al. New insights into flavivirus evolution, taxonomy and biogeographic history, extended by analysis of canonical and alternative coding sequences. *PLoS One.* (2015) 10:e0117849. doi: 10.1371/journal.pone.0117849
28. Li G, Teleki C, Wang T. Memory T cells in flavivirus vaccination. *Vaccines (Basel).* (2018) 6:73. doi: 10.3390/vaccines6040073

Conflict of Interest: The authors declare that the research was conducted in the absence of any commercial or financial relationships that could be construed as a potential conflict of interest.

frontiers in Immunology

REVIEW
published: 19 February 2021
doi: 10.3389/fimmu.2021.638447

Establishment of Humanized Mice for the Study of HBV

Fritz Lai[1,2*], *Cherry Yong Yi Wee*[1] *and Qingfeng Chen*[1,3,4*]

[1] Institute of Molecular and Cell Biology, Agency for Science, Technology and Research (A*STAR), Singapore, Singapore, [2] Department of Medicine, Yong Loo Lin School of Medicine, National University of Singapore, Singapore, Singapore, [3] Key Laboratory for Major Obstetric Diseases of Guangdong Province, The Third Affiliated Hospital of Guangzhou Medical University, Guangzhou, China, [4] Department of Physiology, Yong Loo Lin School of Medicine, National University of Singapore, Singapore, Singapore

Viral hepatitis particularly Hepatitis B Virus (HBV) is still an ongoing health issue worldwide. Despite the vast technological advancements in research and development, only HBV vaccines, typically given during early years, are currently available as a preventive measure against acquiring the disease from a secondary source. In general, HBV can be cleared naturally by the human immune system if detected at low levels early. However, long term circulation of HBV in the peripheral blood may be detrimental to the human liver, specifically targeting human hepatocytes for cccDNA integration which inevitably supports HBV life cycle for the purpose of reinfection in healthy cells. Although there is some success in using nucleoside analogs or polyclonal antibodies targeting HBV surface antigens (HBsAg) in patients with acute or chronic HBV$^+$ (CHB), majority of them would either respond only partially or succumb to the disease entirely unless they undergo liver transplants from a fully matched healthy donor and even so may not necessarily guarantee a 100% chance of survival. Indeed, *in vitro/ex vivo* cultures and various transgenic animal models have already provided us with a good understanding of HBV but they primarily lack human specificity or virus-host interactions in the presence of human immune surveillance. Therefore, the demand of utilizing humanized mice has increased over the last decade as a pre-clinical platform for investigating human-specific immune responses against HBV as well as identifying potential immunotherapeutic strategies in eradicating the virus. Basically, this review covers some of the recent developments and key advantages of humanized mouse models over other conventional transgenic mice platforms.

Keywords: HBV, humanized mice, human immune system, human liver chimeras, chronic inflammation, liver fibrosis, HCC development, human hepatocyte

OPEN ACCESS

Edited by:
Kristina De Paris (Abel), University of North Carolina at Chapel Hill, United States

Reviewed by:
Masakazu Kamata, University of Alabama at Birmingham, United States
Ashraf Siddig Yousif, Ragon Institute of MGH, MIT and Harvard, United States

***Correspondence:**
Fritz Lai
mdcflsc@nus.edu.sg
Qingfeng Chen
qchen@imcb.a-star.edu.sg

Specialty section:
This article was submitted to Viral Immunology, a section of the journal Frontiers in Immunology

Received: *06 December 2020*
Accepted: *03 February 2021*
Published: *19 February 2021*

Citation:
Lai F, Wee CYY and Chen Q (2021) Establishment of Humanized Mice for the Study of HBV. Front. Immunol. 12:638447. doi: 10.3389/fimmu.2021.638447

INTRODUCTION

Hepatitis B Virus (HBV) infection remains a major health threat globally that contributes extensively to various types of liver diseases primarily due to development of acute hepatitis B which progresses into chronic hepatitis B (CHB) and subsequently causes liver fibrosis, cirrhosis and hepatocellular carcinoma (HCC). Based on the Global Hepatitis Report by WHO in 2015, it is estimated that 257 million people in the world are currently living with CHB (1). In fact, viral hepatitis was firmly responsible for 1.34 million deaths which was also the 6th leading cause

of death worldwide overtaking the number of deaths caused by HIV and tuberculosis which was ranked at 7th and 12th, respectively (2). HBV can be classified into 10 Genotypes (A to J) depending on various geographical regions for example, Genotype A is highly endemic in areas like Africa, Europe, India, and America whereas Genotypes B and C are commonly found in the Asia-Pacific region (3). Genotype D is prevalent in Africa, Europe, the Mediterranean region, and India but Genotype E is only identified in West Africa. On the other hand, Genotype F is limited to Central and South America. In addition, there have been reports of Genotype G profiles in France, Germany, and the Americas however, Genotype H is mainly found in Mexico and Central America. Finally, Southeast Asian countries like Vietnam and Laos did portray patients with HBV Genotype I whereas Genotype J has only been reported in Japan. Although some countries are more susceptible to specific HBV genotypes, it is vital to note the mode of viral spread particularly in Asian regions. Genotypes B and C are found in most Asian countries where HBV primarily infects infants at a perinatal stage or through mother-to-infant transmission (1, 4). Therefore, preventive measures like Hepatitis B vaccinations have been enforced worldwide (mandatory in most countries) during the first 5 years of the child's birth. It is especially important to provide vaccinations within this timeframe as the risk of HBV progression from acute to CHB can be as high as 95% at a perinatal period and 20–30% if infection occurs between the age of 1–5 (4). In fact, Singapore was one of the first countries in the world to have implemented the national childhood HBV immunization programme to all newborns as early as 1st September 1987 (5). This initiative had proven effective as the national hepatitis B seroprevalence study have recorded a significant reduction in HBV infection rates as well as increasing HBV immunity primarily in adult Singaporeans (aged 18–29 years) between 1998 and 2010. Of these young adults that were positive for hepatitis B surface antigen (HBsAg), none were positive for hepatitis B e antigen (HBeAg) in 2010 compared to 20.8% in 1998. Similarly, detection of hepatitis B core antigen (HBcAg) has also decreased significantly from 22.1 to 4.4% whereas immunized antibodies produced against HBsAg (anti-HBs) increased from 27.9 to 43.3%.

Despite implementation of such immunization programmes, an active infection can still occur. There is currently no curative treatment for patients with CHB but several antiviral agents like interferon (IFN)-α or pegylated (PEG)-IFN-α and nucleoside analogs (NUC) have been approved for long-term suppression of HBV viremia (6). Although these antiviral agents can reduce circulating HBV to below threshold of detection limit in majority of patients, complete eradication of HBV life cycle remained a challenge as intrahepatic replication proved to be primarily responsible for viral persistence, rebound of viremia during treatment withdrawal and ultimately progression of liver pathogenesis. In addition to the life-long physical symptoms of people living with CHB, the importance of psychosocial burden such as anxiety, financial loss, social discrimination, and rejection should also be recognized equally (7).

Therefore, many have utilized cell culture-based assays and various animal models to better understand specific aspects of the disease including HBV life cycle, virus-host interactions, immune responses, potential therapeutic targets, and more. It is clear that HBV naturally targets human hepatocytes which can be easily obtained commercially or isolated from liver resection of patients with CHB (6, 8). However, limited accessibility due to financial constraints, poor quality of liver tissues, individual preparation variabilities, etc., proved to be the biggest drawbacks. Hence, human hepatoma cell lines like Huh7 and HepG2 were widely used as an alternative to primary human hepatocytes (PHH) cultures to mainly study post-transcriptional involvement of HBV life cycle following transfection of plasmids carrying specific regions of HBV DNA. These cell lines are not actually susceptible to HBV infection due to the lack of expression of HBV receptors until the discovery of a key integral transmembrane protein, sodium taurocholate co-transporting polypeptide (NTCP) where viruses are known to enter human liver cells through binding of NTCP receptors at the basolateral membrane of hepatocytes prior to being engulfed (9, 10). This was further validated in NTCP-overexpressing cell lines that are more permissive to HBV infection which can be attenuated by gene silencing of NTCP or utilizing peptides like Mycludex B (MyrB) to block viral entry (10). In fact, NTCP was simply first identified through a basic understanding of the HBV genome being an enveloped virus encoding HBeAg, HBcAg, HBx, Pol, large surface (L), middle surface (M), and small surface (S) envelop proteins where the pre-S1 domain of the L protein was later recognized as a key determinant factor that promotes viral entry (9). Moreover, the full life cycle of HBV accomplished through generation of pregenomic RNA (pgRNA) during reverse transcription at overlength genome regions containing HBV core promoter is required for production of mature HBV viral particles (11). More importantly, the virological key to this endless infectious property of HBV is due to an intracellular HBV replication intermediate called covalently closed circular DNA (cccDNA) which is primarily responsible for viral persistence and reactivation following therapeutic withdrawal (12–14). Although the molecular mechanisms of cccDNA formation remains unclear, its fundamental characteristic in synthesizing new virions has already been described in cell culture settings as an episomal plasmid-like molecule that resides in host cell nucleus making it a prime target for elimination.

Indeed, both PHH and hepatoma cell lines have offered valuable insights on the study of HBV infection however, it is equally important to validate these findings *in vivo*. As we all know, HBV has a very limited host spectrum which makes investigation of viral tropism in animals very challenging. Only a handful of animals such as chimpanzee, Mauritian cynomolgus monkey, treeshrew, and woodchuck models have successfully harbor HBV infection to not only recapitulate liver disease pathogenesis (fibrosis, cirrhosis, and HCC) seen in HBV^+ patients but also offers a more accurate representation of viral-host interaction (15–19). However, handling of these larger animals requires strict ethics approval and involves high maintenance cost hence, most labs prefer using small animal models like mice as they reproduce in large numbers and can be easily purchased commercially. The evolution of various mouse strains over the last 20 years has clearly emphasized the

importance of having a reliable *in vivo* platform particularly evidenced by the constant improvement in generating a mouse model that encompasses human liver chimeras and/or human immune system to not only allow better identification of novel therapeutic strategies to combat HBV but also to elucidate mechanisms of human-specific viral-host immune responses. In this review, we will highlight some of the key humanized mouse model systems that have significantly enhanced the understanding of HBV research below.

THE EVOLUTION OF HUMANIZED MICE

Prior to mouse humanization, HBV transgenic mice were frequently utilized to mainly evaluate various methods of HBV clearance through molecular manipulation of specific regions of HBV using siRNA/shRNA (20, 21). However, the major drawbacks of utilizing this system is the absence of HBV cccDNA in mouse hepatocytes and failure of mice to exhibit HBV-induced liver pathogenesis. Subsequently, HBV DNA delivery by hydrodynamic injection (plasmid DNA) and viral vectors like Adenovirus, Baculovirus, Adeno-associated viruses (AAV) improved HBV transfection efficiency, stability as well as maintenance for longer periods (22–25). Unfortunately, HBV cccDNA was again not detected in mouse hepatocytes suggesting that there could be some forms of impairment in the HBV cccDNA intracellular recycling pathway. It was only until recently when recombinant HBV cccDNA was successfully generated in mice injected hydrodynamically through Cre-/Loxp-mediated recombination which functions similarly to real HBV cccDNA in the production of mature viruses (14, 25). More importantly, the improved stability and persistence of HBV severely damaged mice livers for the very first time which resulted in advanced liver pathogenesis evidenced by development of fibrosis (26). Although transgenic mice exhibiting such phenotype was considered a major breakthrough in the field of HBV *in vivo*, the study still revolved around a complete mouse host setting. Since human hepatocytes are the natural cellular target of HBV, the inevitable transition of mouse to human eventually gave rise to various establishments of human liver chimeric mice.

HBV-Trimera Mice

Mice engrafted with primary human cells have long been utilized for research such as xenograft transplants of human cancer cell lines into nude mice for the study of tumorigenesis *in vivo* (27). Over time, it was demonstrated that immunodeficient mouse recipients that lack mouse T, B and Natural Killer (NK) cells combined with an additional deletion of the common γ-chain of the interleukin 2 receptor (IL-2rγ) offered the most successful human engraftments with very low risk of rejection (28–30). So, the "Trimera" mouse was one of the earliest model involving the use of human hepatocytes in HBV study where wild-type mice were lethally irradiated prior to immediate injection of radioprotective bone marrow cells from SCID mouse followed by transplantation of *ex vivo* HBV-infected human liver tissues under the kidney capsule 10 days later (31). Although low levels of viremia were detected in these mice which can be reduced by human polyclonal anti-HBs antibody, Hepatect and reverse-transcriptase inhibitors, human hepatocytes only remained functional for a very short timeframe and that HBV persistence could not be fully established *in vivo*. Therefore, generation of a chimeric mouse liver model with robust expansion of human hepatocytes within the liver parenchyma would be key in permitting a stable HBV infection *in vivo*.

uPA-SCID Transgenic Mice

By taking advantage of the liver's regenerative property, Albumin-urokinase-type plasminogen activator (uPA) transgenic mouse was the first model to successfully demonstrate repopulation of adult human hepatocytes transplanted from a healthy donor into the liver of a diseased mouse recipient (32, 33). Basically, this system of hepatocytes renewal relied on the creative concept of deliberately inducing hepatic injury in particular, to mouse hepatocytes in order to make space for healthy ones to accommodate the damaged liver. It was reported that the constitutive expression of murine uPA gene driven by an albumin enhancer/promoter was responsible for hepatotoxicity, elevated plasma uPA levels, hypofibrinogenemia, spontaneous intestinal and intra-abdominal hemorrhaging in neonates which was eventually utilized to facilitate mouse liver damage (34). In addition to overexpressing uPA transgene, these mice were backcrossed with an immunodeficient strain such as the Severe Combined Immune Deficient (SCID) that lacks functional B, T and NK cells to better permit reconstitution of xenogenic human hepatocytes in the liver (33, 35, 36). These mice were also capable of harboring high levels of HBV replication which later became an *in vivo* forefront of hepatitis research particularly in pre-clinical assessments of novel antiviral therapeutics (37–39). Although many had utilized various mouse strains in generating a similar uPA mouse model, the uncontrolled constitutive expression of this toxic gene resulted in poor breeding efficiency, limited timeframe for transplantation and high mortality whenever the transplanted human hepatocytes were unable to compensate for mouse hepatocyte cell death (40–42). Hence, the unpredictability in mice maintenance and high cost demands somewhat restricted wide application of this model.

FRG Knockout Mice

Stability of the human liver chimeric mice system was gradually finetuned with the generation of Fah knockout (KO) mice in 2007 (43). Fumarylacetoacetate hydrolase (Fah) is a mouse-specific enzyme required for liver metabolism which primarily plays an important role in the last steps of the tyrosine catabolism pathway. Mice deficient in the Fah gene redirected its metabolic pathway to accumulate toxic tyrosine metabolic intermediates which subsequently damaged mouse hepatocytes (44–46). To maintain normal liver function, mice drinking water were supplemented with 2-(2-nitro-4-fluoromethylbenzoyl)-1,3-cyclohexanedione (NTBC), a chemical that has been approved to treat hereditary tyrosinemia type 1 (46). More importantly, NTBC drug can actually be passed down to pups through the mother's milk which greatly reduced the rate of mortality in pups of Fah KO mice. Unlike the uPA-overexpressed transgenic mice, NTBC cycling withdrawal offers a much better system in

controlling the severity of mouse liver damage depending on the proliferative capability of post-transplanted human hepatocytes which can also be measured via human albumin expression in the blood (6, 11, 29, 43). To avoid any immune rejection risk of human cells, Fah KO mice were crossed into a Rag2/IL-2rγ double knockout strain which has been demonstrated to reconstitute human hematopoietic cells efficiently (47, 48). The newly generated Fah/Rag2/IL-2rγ triple KO mouse termed as FRG KO, were not only able to expand human hepatocytes robustly but also sustained high production of HBV in the serum without displaying any cytopathic pathogenesis (43). In addition to NTBC withdrawal, these mice were also administered with a urokinase-expressing adenovirus (ad-uPA) prior to animal surgery to further induce cell-autonomous hepatotoxicity for an enhanced human hepatocyte engraftment (49). Therefore, FRG KO mice have proven to be one of the most sought-after *in vivo* platforms for studying mechanisms of HBV infection and identification of novel antiviral therapeutics. In fact, our group has also recently utilized FRG KO mice to further investigate the concerted actions of IFN-α and -γ signaling and identified IFN-α14 as a potent interferon subtype for suppressing HBV (50).

TK-NOG Transgenic Mice

A similar drug-induced human liver chimeric mouse model was established in 2011 where the herpes simplex virus type 1 thymidine kinase (UL23 or HSVtk) gene driven by a mouse albumin promoter was specifically expressed in livers of severely immunodeficient NOG mice (TK-NOG) (51, 52). TK-NOG mice were briefly exposed to the non-toxic drug ganciclovir (GCV) to selectively destroy mouse hepatocyte cells that were expressing the HSVtk transgene thereby allowing space for the transplanted human hepatocytes to repopulate the liver. As HSVtk only catalyzes GCV phosphorylation, any other mammalian cells lacking the transgene will remain unaffected. Similarly, TK-NOG mice also support strong HBV replication property which were mainly used for drug screening purposes (52, 53). However, the demand for this mouse model is nowhere near as high when compared to the FRG KO strain due to male mice being infertile which ultimately result in poor breeding efficiency. More notably, a male wild-type NOG mouse is required to mate with a female TK-NOG mouse in order to successfully breed new transgenic pups followed by a very labor intense genotyping validation process.

DUAL HUMANIZED MOUSE MODELS

Although majority of these immunodeficient human liver chimeric mice have provided valuable insights on virology, the lack of a functional immune system impedes the study of human-specific immune responses triggered by HBV infection and immunotherapeutic strategies. Therefore, several groups including us have attempted to overcome these limitations by developing a dual humanized mouse model reconstituted with both hepatocytes as well as immune system of human origin (54). In fact, our group was one of the frontier labs in South East Asia to have previously demonstrated successful co-engraftment of human fetal liver-derived hematopoietic stem cells (HSCs) and hepatoblasts in an immunodeficient NOD-SCID IL-2rγ$^{-/-}$ (NSG) mouse (HIL mouse) without any transgene modifications for the study of viral-related liver disease (55). These HIL mice were subjected to HCV inoculum before triggering HCV-specific immune responses which led to the development of liver pathogenesis like inflammation and fibrosis (56). Similarly, we have also utilized HIL mice to investigate the importance of intrahepatic CD206^{+} macrophages in HBV-induced liver inflammation and that liver fibrosis can be suppressed by anti-GM-CSF therapy (57, 58). While our HIL mice have indeed recapitulated most of the clinical symptoms observed in HBV/HCV patients, the weak liver chimerism gave rise to a much lower viral output when compared to some of the chimeric mice mentioned earlier. To overcome this obstacle, we have since utilized our own established immunodeficient NOD-SCID IL-2r$^{-/-}$ (NIKO) mouse strain (59) to generate mice lacking the Fah gene herein, termed as Fah-NIKO mice. Like the FRG KO mice, Fah-NIKO mice also adapted a similar approach of utilizing NTBC cycling to facilitate mouse hepatocyte cell death allowing transplanted human hepatocytes to repopulate. Our preliminary data indicated that Fah-NIKO mice could also achieve high levels of human liver engraftment and support HBV infection for long periods (unpublished data). Although our NIKO mice have demonstrated good human hematopoietic reconstitution which is comparable to NSG mice (unpublished data), we have yet to examine the dual humanization capability of NIKO mice in response to HBV infection. Therefore, mice engrafted with both mature human immune system and humanized liver could hold the key to better assess human-specific immune responses triggered by HBV of which some of the recent developments of dual humanized mice will be highlighted below.

AFC8-hu HSC/Hep Mice

In 2011, AFC8 mice became one of the first dual humanized mouse model to be established with human immune system and up to 30% repopulation of human hepatocytes in the mouse liver (60–62). Generation of these mice were actually quite similar to our HIL mice but with an added advantage of expressing a suicidal Caspase 8 inducible system to facilitate mouse hepatocyte cell death. Basically, immunodeficient Rag2/IL-2rγ KO mice in a BALB/c background were overexpressed with an albumin-driven Caspase 8 transgene which was fused with FK506 binding domain (FKBP) to specifically target mouse hepatocytes (AFC8 mice) (60). Following co-transplantation of human CD34^{+} HSCs and hepatocyte progenitor cells, these transgenic mice (AFC8-hu HSC/Hep mice) were administered with a FKBP dimerizer, AP20187 to induce hepatic injury for human liver engraftment. Similar to what we observed in HIL mice infected with HCV, AFC8-hu HSC/Hep mice also displayed human T cell responses to HCV and developed chronic liver inflammation/fibrosis which correlated with activation of stellate cells and human-specific fibrogenic genes (56, 60).

A2/NSG/Fas-hu-HSC/Hep Mice

Since several reports indicated that chronic HBV-associated pathologies were related to infiltration of T lymphocytes and

activated macrophages, the same group who generated AFC8-hu HSC/Hep mice developed another transgenic mouse model expressing HLA-A2 in an NSG background (A2/NSG) in order to study human antigen-specific T cell responses to HBV (63–65). They adapted a similar approach of transplanting HLA-A2 donor derived $CD34^+$ HSCs and hepatic progenitors into A2/NSG pups but used a murine Fas activating antibody Jo2 to induce hepatotoxicity for engraftment of human hepatocytes (A2/NSG/Fas-hu-HSC/Hep mice) (66, 67). Mice that were infected with HBV displayed long-term viral persistence, robust expansion of human lymphoid T cells isolated from lymphoid and liver tissues following HBV antigen stimulation, and developed HBV-induced liver pathogenesis including hepatitis and fibrosis. More importantly, HBV-infected A2/NSG/Fas-hu-HSC/Hep mice exhibited high accumulation of activated human M2-like macrophages particularly at the fibrotic regions of the liver which was similarly observed in both patients with CHB and acute liver failure further demonstrating the importance of M2 macrophages in the innate immune system involving tissue remodeling and wound repair (63, 68). Indeed, the development of antigen-specific T cell responses have provided a unique advantage of utilizing these haplotype-matched dual humanized mice models for the study of HBV. However, it was believed that such immunosuppressive or pro-inflammatory phenotypes can be further optimized with improved engraftment of human hepatocytes in yielding higher viral titers return.

uPA-NOG Transgenic Mice

As viral-induced liver pathogenesis including fibrosis, cirrhosis and even cancer can take decades to progress in humans, small animal models like dual humanized mice are ideal hosts to accelerate these processes for the study of its etiology. Hence, various groups have attempted to reconstitute functional human immune system in mice with high liver chimerism by tapping onto the uPA transgene technology and Fah KO strains (29, 54, 61, 69). For instance, the uPA transgene was expressed in a NOG mouse background instead of SCID to firstly stabilize its expression and expands the timeframe for a human cell transplantation (70). It was reported that the uPA expression in SCID mice would deteriorate with age which may affect the quality of liver humanization. Secondly, total body irradiation was replaced with treosulfan, a non-myeloablative conditioning method for engraftment of $CD34^+$ HSCs. Although irradiation of mouse cells has been widely used prior to HSCs transplantation, treosulfan provided a safer and well-tolerated alternative to the more invasive method which may cause occasional mortality long term. Lastly, uPA-NOG transgenic mice can be reconstituted with mature human hepatocytes and HLA-mismatched HSCs from two separate donors. One common phenotypic feature shared in most humanized mouse models following transplants of fetal hepatoblasts was the low hepatic repopulation levels and failure of these epithelial cells to differentiate into its mature form fully. Subsequent methods like delivery of adenoviral vector-expressing human hepatocyte growth factor (HGF) into uPA-NOG mice was performed in hope of improving engraftment of fetal liver cells but this strategy proved to be unsuccessful (71, 72).

Although many have reported that 3–5% of human hepatocyte engraftment is sufficient to trigger virus-mediated intrahepatic immune responses and pathological changes, a much higher liver chimerism is required to further elucidate these characteristics (56–58, 60, 70). To overcome this challenge, adult human hepatocytes were transplanted into uPA-NOG mice resulting in >70% humanization of mouse liver together with functional human immune system derived from mismatched fetal liver HSCs. Since the supply of fetal liver tissues are becoming scarce due to enforcements of human biomedical research acts, the mismatched sample compatibility meant that HSCs can be obtained from alternative sources like cord blood banks. In fact, $CD34^+$ HSCs successfully differentiated into specific immune cell subsets including $CD3^+$ lymphocytes with a CD4:CD8 ratio similar to those established in an NSG background as well as mature human B cells in a donor-dependent manner (70, 73–75). Furthermore, the absence of haplotype restrictions between the two grafts provided more flexibility in generation of dual humanized mice without evidence of hepatocyte rejection by the human immune system. Although there were mild liver damages in some old mice, expansion of $CD8^+$ T cells were absent and none of them developed signs of graft-vs.-host disease (GVHD) (70, 76). Hence, the successful engraftment of mismatched HSCs was clearly evidenced by low risk of cellular immune-mediated rejection of hepatocytes.

FRGN Mice

Another very minute modification was made in FRG KO mice in order to harbor decent human hematopoietic engraftment as well as liver humanization. Although NSG mice remained one of the most conventional hosts for engraftment of HSCs, it has been demonstrated that immunodeficient mice in NOD background conferred a more superior support for human hematopoiesis due to the identification of SIRP-α polymorphism which primarily enhanced human CD47 ligand binding on mouse macrophages (77). Hence, FRG KO mice were intercrossed with NOD strains until all generations were homozygous for the four alleles herein, termed as FRGN mice (78). In fact, several advantages were observed in FRGN mice compared to FRG KO ones. Firstly, complete humanization of mouse liver was achieved quicker in the FRGN strain. Secondly, the average litter size was almost doubled in FRGN breeders and lastly, the average body weights for both mouse genders were significantly heavier (∼5 g) than conventional FRG KO mice which may ultimately be critical for maintenance of a low mortality rate long-term. Like the use of treosulfan in uPA-NOG transgenic mice, FRGN mice were pre-conditioned with a DNA-damaging chemical, busulfan as well as ad-uPA prior to transplantation of mismatched $CD34^+$ HSCs and adult hepatocytes intrasplenically (70, 78–80). NTBC cycling was performed accordingly to facilitate mouse hepatocyte cell death which in turn allow repopulation of human ones (43). Although both HSCs and hepatocytes were from two separate donors, FRGN mice displayed high hematopoietic reconstitution in blood, spleen, thymus, bone marrow, and liver organs along with high human hepatocyte replacement. More importantly, human blood, mature B cells, T cells, and Kupffer cells which plays a major role in pro-inflammatory

TABLE 1 | Summary of humanized mouse models for the study of HBV.

Types	Advantages	Limitations	References
HBV-Trimera	• First immunodeficient mouse model transplanted with *ex vivo* human liver tissues isolated from HBV^+ patients • Hepatect and reverse transcriptase inhibitors reduced viremia *in vivo*	• Low viremia • Absence of HBV persistence • Very short lived functional human hepatocytes	(31)
uPA-SCID	• First transgenic mouse model to repopulate human hepatocytes in diseased livers of mouse recipients • Exhibited high levels of HBV replication • Good pre-clinical model for anti-viral applications	• Constitutive liver toxicity resulted in high mortality • Poor breeding capacity • Unpredictable mouse colonies	(32–42)
FRG KO	• Mouse hepatic injury can be controlled with NTBC cycling • Immunodeficient background to permit better human hepatocyte engraftments • Robust expansion of mature human hepatocytes (mg/ml hALB levels) • Exhibited high levels of viremia and persistent HBV • Suitable for studying HBV life cycle • Good pre-clinical model for anti-viral applications	• Absence of HBV-induced human immune responses • Absence of liver pathogenesis	(43, 50)
TK-NOG	• Immunodeficient background which requires non-toxic drug GCV to destroy mouse hepatocytes in order to accommodate human ones • Exhibited high levels of viremia • Mainly used for drug screening purposes	• Poor breeding capacity • Male mice are infertile. Requires genotyping for pups • Absence of HBV-induced human immune responses • Absence of liver pathogenesis	(51–53)
HIL	• Human immune liver mice generated by transplantation of $CD34^+$ HSCs derived from fetal liver • Exhibited functional human T cell responses toward HCV/HBV and developed liver pathogenesis • Identification of anti-GM-CSF therapy against HBV-induced liver fibrosis	• Very low human hepatocyte reconstitution • Low viremia	(56–58)
AFC8	• First dual humanized mouse model established with functional human immune system and up to 30% humanized mouse liver • Generated by co-transplantation of $CD34^+$ HSCs and hepatic progenitors from same donor • Exhibited functional human T cell responses toward HCV and developed liver inflammation	• Hepatic progenitors did not fully differentiate into mature human hepatocytes • Yet to be demonstrated in a HBV infection setting	(60, 62)
A2/NSG/Fas	• Transgenic mouse model expressing HLA-A2 to study antigen-specific T cell responses to HBV • Generated by co-transplantation of $CD34^+$ HSCs and hepatic progenitors from same donor • Murine Jo2 induced mouse liver damage • Mice displayed long term viral persistence • Mice developed HBV-induced liver fibrosis, infiltration of T lymphocytes and high accumulation of macrophages	• Hepatic progenitors did not fully differentiate into mature human hepatocytes • Persistent HBV but with low viral titers	(63–65)
uPA-NOG	• uPA expression on NOG mouse strain has longer lifespan compared to SCID background • Irradiation was replaced with treosulfan for HSC engraftment • Generated with HLA-mismatched HSCs and mature human hepatocytes from different donors • uPA-NOG mice displayed hemato-lymphoid reconstitution and expansion of human hepatocytes • No signs of GVHD	• Yet to be demonstrated in a viral infection setting	(70)
FRGN	• Quicker complete liver humanization than FRG KO mice • Larger litter size & body weight compared to FRG KO mice • Irradiation was replaced with busulfan • Generated with HLA-mismatched HSCs and mature human hepatocytes from different donors • Displayed hemato-lymphoid reconstitution and expansion of human hepatocytes • No signs of GVHD	• Yet to be demonstrated in a viral infection setting	(78)

(Continued)

TABLE 1 | Continued

Types	Advantages	Limitations	References
HIS-HUHEP	• Generated with HLA-mismatched HSCs and mature human hepatocytes from different donors • Displayed hemato-lymphoid reconstitution and expansion of human hepatocytes • No signs of GVHD • Exhibited high levels of viremia and persistent HBV • Nucleoside analogs reduced viral titers and restored naïve human immune profiles	• Detection of antigen-specific T cell responses was absent • Liver fibrosis and development of HCC was absent	(81–84)
FRGS	• Human hepatocyte-like cells (hHLCs) derived from hIPSCs can differentiate and expand in FRGS mice (∼40% liver chimerism) • Human bone mesenchymal stem cells (hBMSCs) can differentiate and expand in FRGS mice with ∼58.7% liver chimerism in addition to multiple human immune cell lineages • Exhibited high levels of viremia and persistent HBV • HBV-infected hBMSC-FRGS mice developed chronic inflammation, liver fibrosis and cirrhosis	• Development of HCC was absent	(87, 91)

responses were all detected in the liver of these mice (78). Although both uPA-NOG and FRGN mice demonstrated a marked improvement in dual reconstitution efficiency when utilizing mismatched HSCs and adult hepatocytes with minimal immune rejection, they were surprisingly not validated with some of the many potential applications such as HBV/HCV infection or metabolically induced steatohepatitis (70, 78).

HIS-HUHEP Mice

It was only until more recently when another transgenic mouse strain was generated for the engraftment of both human immune system and mismatched adult hepatocytes. Basically, dual reconstitution efficiency was compared between BALB/c Rag2/IL-2rγ KO NOD.sirpa uPA transgenic mice transplanted with $CD34^+$ fetal-derived HSCs alone (HIS), adult human hepatocytes alone (HUHEP), and both (HIS-HUHEP) (81). Similar to what was observed in the dual humanized mice models mentioned earlier, HIS-HUHEP mice hALB levels remained stable for long periods even in the presence of a supposedly allogeneic immune system, absolute numbers of blood leukocytes including $CD3^+$ T cells retained its naïve phenotype without any immune expansion or activation and pro-inflammatory immune cell infiltration was absent in hepatocyte grafts suggesting that HIS-HUHEP mice could be the best candidate for investigating HBV-induced immune responses and developing liver pathogenesis *in vivo*. Hence, it was later demonstrated that HIS-HUHEP mice could indeed support chronic HBV infection displaying up to 10^9 copies/ml viral DNA, both HBeAg and HBsAg measurements which was clinically equivalent in HBV^+ patients and detectable HBV cccDNA (82). In addition, clusters of both $CD3^+$ T cells and Kupffer cells were observed in HBV-infected HIS-HUHEP mice particularly around $HBcAg^+$ human hepatocytes throughout the liver parenchyma. The robust increase of intrahepatic cytotoxic $CD8^+$ T cells, activated NK cells and PD-1 mediated T cell exhaustion also indicated potential key effectors involved in an immunosuppressive environment (83). However, detection of antigen-specific T cell responses was absent due to the engraftment of HLA-mismatched grafts in HIS-HUHEP mice. Nevertheless, HBV-infected HIS-HUHEP mice treated with the nucleoside analog Entecavir (ETV) resulted in reduced HBV titers and restoration of naïve immune profiles evidenced by diminished liver immune cell infiltration suggesting that this dual humanized mouse model is suitable for potentially evaluating immunotherapeutic treatments (82, 84). One other aspect that remained to be investigated is HBV-mediated development of HCC. Although HBV-infected HIS-HUHEP mice could sustain high viremia and exhibited chronic inflammation phenotype, HCC development was not observed (82). Since HCC takes several decades to form, it may be difficult for dual humanized mice to recapitulate such HBV-associated liver pathology. Nevertheless, this *in vivo* platform could be helpful in elucidating tumorigenic pathways involving early phases of HCC initiation and progression.

hBMSC-FRGS Mice

As accessibility to PHHs becomes more limited due to affordability or simply lack of healthy donors, several labs have started sourcing for *in vitro* alternatives. One prime example was the generation of human hepatocyte-like cells (hHLCs) derived from human induced pluripotent stem cells (hiPSCs) which required a three-step procedure of endoderm priming, hepatic specification and maturation (85–90). Although these hHLCs required very distinct culture conditions for differentiation, expansion and maintenance, these cells were well-differentiated and fully functional. In addition, engraftment of mature hHLCs was also successful in FRG KO-BALB/c SCID (FRGS) mice (hHLC-FRGS) displaying ∼40% liver chimerism (87). More importantly, hHLCs and hHLC-FRGS mice were susceptible to chronic HBV infection completed with a full viral life cycle which was efficiently blocked by MyrB and ETV. The same research group then adapted a similar approach in exploring the possibility of generating a dual humanized mouse model by using human bone mesenchymal stem cells (hBMSCs) (91). Basically, hBMSCs were isolated from bone marrows of healthy male volunteers and cultured in multilineage (osteocytes, adipocytes and HLCs) differentiation media prior to transplantation

into FRGS mice (hBMSC-FRGS). Unlike hHLC-FRGS mice, hBMSC-FRGS actually displayed higher liver chimerism (58.7%) including HLA^+ cells that were also positive for mature human hepatocyte-specific markers. Furthermore, varying amounts of $hCD45^+$ cells were detected in bone marrows, thymus, lymph node, spleen, liver, and peripheral blood of hBMSC-FRGS mice. More notably, multiple human immune cell lineages such as T cells, B cells, NK cells, macrophages, and dendritic cells were present in the mouse liver following transplantation of hBMSCs. Similar to HIS-HUHEP mice as mentioned earlier, hBMSC-FRGS mice support persistence HBV infection with high levels of HBV DNA, HBsAg, HBeAg, as well as detectable intrahepatic HBV cccDNA (82, 91). Large production of human-derived pro-inflammatory cytokines/chemokines triggered by specific immune cell subsets was also released and sustained throughout the course of infection which may contribute to liver immunopathological injury. Critically, HBV-infected hBMSC-FRGS mice developed acute/chronic hepatitis patterns with varying degrees of lymphocytic portal inflammation, liver fibrosis, accumulations of scar tissues and ultimately progressed to liver cirrhosis which was similarly observed in CHB patients. Thus, this dual humanized mouse system could possibly be the most ideal model for evaluating viral immune pathophysiology and refining antiviral therapeutics.

CONCLUSION

Many research groups have deciphered some of the basic concepts of virus-host interactions by utilizing conventional platforms like *in vitro* culture systems as well as wild-type/transgenic mice which have been instrumental in the evolution of humanized mouse models. The generation of human liver chimeric mice was the first model to permit long term HBV persistence which were mainly used for understanding HBV life cycle and identification of potential antiviral drug targets. Over time, improvements led to the development of dual humanized mice engrafted with high liver chimerism and human immune cell lineages to better investigate HBV-triggered human immune responses. Concurrently, these HBV-infected mice developed severe pathological changes including chronic inflammation and fibrosis/cirrhosis further recapitulating liver pathogenesis observed in CHB patients. However, development of HCC *in vivo* remains elusive which is high likely due to its unpredictable proliferative nature to form over decades in humans. Although usage of dual humanized mice has yielded much progress in the field of HBV research as highlighted in this review (summarized in **Table 1**), improved models are required to incorporate the missing transition link of chronic HBV and HCC in hope of moving one step closer toward HBV cure.

AUTHOR CONTRIBUTIONS

FL took the lead in writing the manuscript. CW and QC contributed to writing. QC supervised the preparation of manuscript. All authors studied the literature and approved the submitted version.

FUNDING

This study was supported by the National Research Foundation Singapore Fellowship (NRF-NRFF2017-03), NRF-ISF joint grant (NRF2019-NRF-ISF003-3127), National Research Foundation Singapore Competitive Research Programme NRF2016-CRP001-103, Establishment of a scalable capability for autologous clinical cell therapy manufacturing (IAF-PP, H18/01/a0/022) from Agency for Science, Technology and Research (A*STAR), Gilead Sciences International Research Scholars Program in Liver Disease (to QC), Eradication of HBV TCR Program: NMRC/TCR/014-NUHS/2015, NMRC/OFLCG/003/2018 from National Medical Research Council, Singapore and National Medical Research Council-Clinician Scientist-Individual Research Grant (NMRC/CIRG/1427/2015).

REFERENCES

1. WHO. *April 2017 Global Hepatitis Report*. Geneva: World Health Organization (2017). p. 83.
2. Brown CR, MacLachlan JH, Cowie BC. Addressing the increasing global burden of viral hepatitis. *Hepatobiliary Surg Nutr.* (2017) 6:274–6. doi: 10.21037/hbsn.2017.05.02
3. Lin CL, Kao JH. Hepatitis B virus genotypes and variants. *Cold Spring Harb Perspect Med.* (2015) 5:a021436. doi: 10.1101/cshperspect.a021436
4. Li H, Yan L, Shi Y, Lv D, Shang J, Bai L, et al. Hepatitis B virus infection: overview. *Adv Exp Med Biol.* (2020) 1179:1–16. doi: 10.1007/978-981-13-9151-4_1
5. Ang LW, Cutter J, James L, Goh KT. Seroepidemiology of hepatitis B virus infection among adults in Singapore: a 12-year review. *Vaccine.* (2013) 32:103–10. doi: 10.1016/j.vaccine.2013.10.057
6. Zeisel MB, Lucifora J, Mason WS, Sureau C, Beck J, Levrero M, et al. Towards an HBV cure: state-of-the-art and unresolved questions–report of the ANRS workshop on HBV cure. *Gut.* (2015) 64:1314–26. doi: 10.1136/gutjnl-2014-308943
7. Tu T, Block JM, Wang S, Cohen C, Douglas MW. the lived experience of chronic hepatitis B: a broader view of its impacts and why we need a cure. *Viruses.* (2020) 12:515. doi: 10.3390/v12050515
8. Lai F, Chen Q. Humanized mouse models for the study of infection and pathogenesis of human viruses. *Viruses.* (2018) 10:643. doi: 10.3390/v10110643
9. Yan H, Zhong G, Xu G, He W, Jing Z, Gao Z, et al. Sodium taurocholate cotransporting polypeptide is a functional receptor for human hepatitis B and D virus. *Elife.* (2012) 1:e00049. doi: 10.7554/eLife.00049
10. Ni Y, Lempp FA, Mehrle S, Nkongolo S, Kaufman C, Falth M, et al. Hepatitis B and D viruses exploit sodium taurocholate co-transporting polypeptide for species-specific entry into hepatocytes. *Gastroenterology.* (2014) 146:1070–83. doi: 10.1053/j.gastro.2013.12.024
11. Li F, Wang Z, Hu F, Su L. Cell culture models and animal models for HBV study. *Adv Exp Med Biol.* (2020) 1179:109–35. doi: 10.1007/978-981-13-9151-4_5
12. Nassal, M. HBV cccDNA: viral persistence reservoir and key obstacle for a cure of chronic hepatitis B. *Gut.* (2015) 64:1972–84. doi: 10.1136/gutjnl-2015-309809

13. Newbold JE, Xin H, Tencza M, Sherman G, Dean J, Bowden S. The covalently closed duplex form of the hepadnavirus genome exists in situ as a heterogeneous population of viral minichromosomes. *J Virol.* (1995) 69:3350–57. doi: 10.1128/JVI.69.6.3350-3357.1995
14. Qi Z, Li G, Hu H, Yang C, Zhang X, Leng Q, et al. Recombinant covalently closed circular hepatitis B virus DNA induces prolonged viral persistence in immunocompetent mice. *J Virol.* (2014) 88:8045–56. doi: 10.1128/JVI.01024-14
15. Guidotti LG, Rochford R, Chung J, Shapiro M, Purcell R, Chisari FV. Viral clearance without destruction of infected cells during acute HBV infection. *Science.* (1999) 284:825–9. doi: 10.1126/science.284.5415.825
16. Dupinay T, Gheit T, Roques P, Cova L, Chevallier-Queyron P, Tasahsu SI, et al. Discovery of naturally occurring transmissible chronic hepatitis B virus infection among *Macaca fascicularis* from Mauritius Island. *Hepatology.* (2013) 58:1610–20. doi: 10.1002/hep.26428
17. Kock J, Nassal M, MacNelly S, Baumert TF, Blum HE, von Weizsacker F. Efficient infection of primary tupaia hepatocytes with purified human and woolly monkey hepatitis B virus. *J Virol.* (2001) 75:5084–9. doi: 10.1128/JVI.75.11.5084-5089.2001
18. Yan RQ, Su JJ, Huang DR, Gan YC, Yang C, Huang GH. Human hepatitis B virus and hepatocellular carcinoma. I. Experimental infection of tree shrews with hepatitis B virus. *J Cancer Res Clin Oncol.* (1996) 122:283–88. doi: 10.1007/BF01261404
19. Kulkarni K, Jacobson IM, Tennant BC. The role of the woodchuck model in the treatment of hepatitis B virus infection. *Clin Liver Dis.* (2007) 11:707–25. doi: 10.1016/j.cld.2007.08.012
20. Chisari FV. Hepatitis B virus transgenic mice: insights into the virus and the disease. *Hepatology.* (1995) 22:1316–25. doi: 10.1002/hep.1840220443
21. Uprichard SL, Boyd B, Althage A, Chisari FV. Clearance of hepatitis B virus from the liver of transgenic mice by short hairpin RNAs. *Proc Natl Acad Sci USA.* (2005) 102:773–8. doi: 10.1073/pnas.0409028102
22. Huang LR, Gabel YA, Graf S, Arzberger S, Kurts C, Heikenwalder M, et al. Transfer of HBV genomes using low doses of adenovirus vectors leads to persistent infection in immune competent mice. *Gastroenterology.* (2012) 142:1447–50 e1443. doi: 10.1053/j.gastro.2012.03.006
23. Lucifora J, Vincent IE, Berthillon P, Dupinay T, Michelet M, Protzer U, et al. Hepatitis B virus replication in primary macaque hepatocytes: crossing the species barrier toward a new small primate model. *Hepatology.* (2010) 51:1954–60. doi: 10.1002/hep.23602
24. Dion S, Bourgine M, Godon O, Levillayer F, Michel ML. Adeno-associated virus-mediated gene transfer leads to persistent hepatitis B virus replication in mice expressing HLA-A2 and HLA-DR1 molecules. *J Virol.* (2013) 87:5554–63. doi: 10.1128/JVI.03134-12
25. Yang D, Liu L, Zhu D, Peng H, Su L, Fu YX, et al. A mouse model for HBV immunotolerance and immunotherapy. *Cell Mol Immunol.* (2014) 11:71–8. doi: 10.1038/cmi.2013.43
26. Li G, Zhu Y, Shao D, Chang H, Zhang X, Zhou D, et al. Recombinant covalently closed circular DNA of hepatitis B virus induces long-term viral persistence with chronic hepatitis in a mouse model. *Hepatology.* (2018) 67:56–70. doi: 10.1002/hep.29406
27. Rygaard J, Povlsen CO. Heterotransplantation of a human malignant tumour to "Nude" mice. *Acta Pathol Microbiol Scand.* (1969) 77:758–60. doi: 10.1111/j.1699-0463.1969.tb04520.x
28. Iannacone M, Guidotti LG. Mouse models of hepatitis B virus pathogenesis. *Cold Spring Harb Perspect Med.* (2015) 5:a021477. doi: 10.1101/cshperspect.a021477
29. Grompe M, Strom S. Mice with human livers. *Gastroenterology.* (2013) 145:1209–14. doi: 10.1053/j.gastro.2013.09.009
30. Dandri M, Lutgehetmann M. Mouse models of hepatitis B and delta virus infection. *J Immunol Methods.* (2014) 410:39–49. doi: 10.1016/j.jim.2014.03.002
31. Ilan E, Burakova T, Dagan S, Nussbaum O, Lubin I, Eren R, et al. The hepatitis B virus-trimera mouse: a model for human HBV infection and evaluation of anti-HBV therapeutic agents. *Hepatology.* (1999) 29:553–62. doi: 10.1002/hep.510290228
32. Sandgren EP, Palmiter RD, Heckel JL, Daugherty CC, Brinster RL, Degen JL. Complete hepatic regeneration after somatic deletion of an albumin-plasminogen activator transgene. *Cell.* (1991) 66:245–56. doi: 10.1016/0092-8674(91)90615-6
33. Dandri M, Burda MR, Torok E, Pollok JM, Iwanska A, Sommer G, et al. Repopulation of mouse liver with human hepatocytes and *in vivo* infection with hepatitis B virus. *Hepatology.* (2001) 33:981–8. doi: 10.1053/jhep.2001.23314
34. Heckel JL, Sandgren EP, Degen JL, Palmiter RD, Brinster RL. Neonatal bleeding in transgenic mice expressing urokinase-type plasminogen activator. *Cell.* (1990) 62:447–56. doi: 10.1016/0092-8674(90)90010-C
35. Bissig KD, Wieland SF, Tran P, Isogawa M, Le TT, Chisari FV, et al. Human liver chimeric mice provide a model for hepatitis B and C virus infection and treatment. *J Clin Invest.* (2010) 120:924–30. doi: 10.1172/JCI40094
36. Dandri M, Lutgehetmann M, Volz T, Petersen J. Small animal model systems for studying hepatitis B virus replication and pathogenesis. *Semin Liver Dis.* (2006) 26:181–91. doi: 10.1055/s-2006-939760
37. Volz T, Lutgehetmann M, Allweiss L, Warlich M, Bierwolf J, Pollok JM, et al. Strong antiviral activity of the new l-hydroxycytidine derivative, l-Hyd4FC, in HBV-infected human chimeric uPA/SCID mice. *Antivir Ther.* (2012) 17:623–31. doi: 10.3851/IMP2075
38. Brezillon N, Brunelle MN, Massinet H, Giang E, Lamant C, DaSilva L, et al. Antiviral activity of Bay 41-4109 on hepatitis B virus in humanized Alb-uPA/SCID mice. *PLoS ONE.* (2011) 6:e25096. doi: 10.1371/journal.pone.0025096
39. Meuleman P, Leroux-Roels G. The human liver-uPA-SCID mouse: a model for the evaluation of antiviral compounds against HBV HCV. *Antiviral Res.* (2008) 80:231–8. doi: 10.1016/j.antiviral.2008.07.006
40. Lutgehetmann M, Mancke LV, Volz T, Helbig M, Allweiss L, Bornscheuer T, et al. Humanized chimeric uPA mouse model for the study of hepatitis B and D virus interactions and preclinical drug evaluation. *Hepatology.* (2012) 55:685–94. doi: 10.1002/hep.24758
41. Petersen J, Dandri M, Mier W, Lutgehetmann M, Volz T, von Weizsacker F, et al. Prevention of hepatitis B virus infection in vivo by entry inhibitors derived from the large envelope protein. *Nat Biotechnol.* (2008) 26:335–41. doi: 10.1038/nbt1389
42. Vanwolleghem T, Libbrecht L, Hansen BE, Desombere I, Roskams T, Meuleman P, et al. Factors determining successful engraftment of hepatocytes and susceptibility to hepatitis B and C virus infection in uPA-SCID mice. *J Hepatol.* (2010) 53:468–76. doi: 10.1016/j.jhep.2010.03.024
43. Azuma H, Paulk N, Ranade A, Dorrell C, Al-Dhalimy M, Ellis E, et al. Robust expansion of human hepatocytes in Fah-/-/Rag2-/-/Il2rg-/- mice. *Nat Biotechnol.* (2007) 25:903–10. doi: 10.1038/nbt1326
44. Grompe M, al-Dhalimy M, Finegold M, Ou CN, Burlingame T, Kennaway NG, et al. Loss of fumarylacetoacetate hydrolase is responsible for the neonatal hepatic dysfunction phenotype of lethal albino mice. *Genes Dev.* (1993) 7:2298–307. doi: 10.1101/gad.7.12a.2298
45. Overturf K, Al-Dhalimy M, Tanguay R, Brantly M, Ou CN, Finegold M, et al. Hepatocytes corrected by gene therapy are selected in vivo in a murine model of hereditary tyrosinaemia type I. *Nat Genet.* (1996) 12:266–73. doi: 10.1038/ng0396-266
46. Grompe M, Lindstedt S, al-Dhalimy M, Kennaway NG, Papaconstantinou J, Torres-Ramos CA, et al. Pharmacological correction of neonatal lethal hepatic dysfunction in a murine model of hereditary tyrosinaemia type I. *Nat Genet.* (1995) 10:453–60. doi: 10.1038/ng0895-453
47. Traggiai E, Chicha L, Mazzucchelli L, Bronz L, Piffaretti JC, Lanzavecchia A, et al. Development of a human adaptive immune system in cord blood cell-transplanted mice. *Science.* (2004) 304:104–07. doi: 10.1126/science.1093933
48. Gorantla S, Sneller H, Walters L, Sharp JG, Pirruccello SJ, West JT, et al. Human immunodeficiency virus type 1 pathobiology studied in humanized BALB/c-Rag2-/-gammac-/- mice. *J Virol.* (2007) 81:2700–12. doi: 10.1128/JVI.02010-06
49. Lieber A, Vrancken Peeters MJ, Meuse L, Fausto N, Perkins J, Kay MA. Adenovirus-mediated urokinase gene transfer induces liver regeneration and allows for efficient retrovirus transduction of hepatocytes *in vivo*. *Proc Natl Acad Sci USA.* (1995) 92:6210–14. doi: 10.1073/pnas.92.13.6210
50. Chen J, Li Y, Lai F, Wang Y, Sutter K, Dittmer U, et al. Functional comparison of IFN-alpha subtypes reveals potent HBV suppression by a concerted action of IFN-alpha and -gamma SIgnaling. *Hepatology.* (2020). doi: 10.1002/hep.31282

51. Hasegawa M, Kawai K, Mitsui T, Taniguchi K, Monnai M, Wakui M, et al. The reconstituted 'humanized liver' in TK-NOG mice is mature and functional. *Biochem Biophys Res Commun*. (2011) 405:405–10. doi: 10.1016/j.bbrc.2011.01.042
52. Kosaka K, Hiraga N, Imamura M, Yoshimi S, Murakami E, Nakahara T, et al. A novel TK-NOG based humanized mouse model for the study of HBV and HCV infections. *Biochem Biophys Res Commun*. (2013) 441:230–5. doi: 10.1016/j.bbrc.2013.10.040
53. Nakabori T, Hikita H, Murai K, Nozaki Y, Kai Y, Makino Y, et al. Sodium taurocholate cotransporting polypeptide inhibition efficiently blocks hepatitis B virus spread in mice with a humanized liver. *Sci Rep*. (2016) 6:27782. doi: 10.1038/srep27782
54. Allweiss L, Strick-Marchand H. *In-vitro* and *in-vivo* models for hepatitis B cure research. *Curr Opin HIV AIDS*. (2020) 15:173–9. doi: 10.1097/COH.0000000000000616
55. Chen Q, Khoury M, Limmon G, Choolani M, Chan JK, Chen J. Human fetal hepatic progenitor cells are distinct from, but closely related to, hematopoietic stem/progenitor cells. *Stem Cells*. (2013) 31:1160–9. doi: 10.1002/stem.1359
56. Keng CT, Sze CW, Zheng D, Zheng Z, Yong KS, Tan SQ, et al. Characterisation of liver pathogenesis, human immune responses and drug testing in a humanised mouse model of HCV infection. *Gut*. (2016) 65:1744–53. doi: 10.1136/gutjnl-2014-307856
57. Tan-Garcia A, Wai LE, Zheng D, Ceccarello E, Jo J, Banu N, et al. Intrahepatic CD206(+) macrophages contribute to inflammation in advanced viral-related liver disease. *J Hepatol*. (2017) 67:490–500. doi: 10.1016/j.jhep.2017.04.023
58. Tan-Garcia A, Lai F, Sheng Yeong JP, Irac SE, Ng PY, Msallam R, et al. Liver fibrosis and CD206(+) macrophage accumulation are suppressed by anti-GM-CSF therapy. *JHEP Rep*. (2020) 2:100062. doi: 10.1016/j.jhepr.2019.11.006
59. Chew M, Ye W, Omelianczyk RI, Pasaje CF, Hoo R, Chen Q, et al. Selective Expression of variant surface antigens enables *Plasmodium falciparum* to evade immune clearance *in vivo*. *bioRxiv [Preprint]*. (2020). doi: 10.1101/2020.07.22.215640
60. Washburn ML, Bility MT, Zhang L, Kovalev GI, Buntzman A, Frelinger JA, et al. A humanized mouse model to study hepatitis C virus infection, immune response, and liver disease. *Gastroenterology*. (2011) 140:1334–44. doi: 10.1053/j.gastro.2011.01.001
61. Allweiss L, Dandri M. Experimental in vitro and in vivo models for the study of human hepatitis B virus infection. *J Hepatol*. (2016) 64:S17–31. doi: 10.1016/j.jhep.2016.02.012
62. Bility MT, Zhang L, Washburn ML, Curtis TA, Kovalev GI, Su L. Generation of a humanized mouse model with both human immune system and liver cells to model hepatitis C virus infection and liver immunopathogenesis. *Nat Protoc*. (2012) 7:1608–17. doi: 10.1038/nprot.2012.083
63. Bility MT, Cheng L, Zhang Z, Luan Y, Li F, Chi L, et al. Hepatitis B virus infection and immunopathogenesis in a humanized mouse model: induction of human-specific liver fibrosis and M2-like macrophages. *PLoS Pathog*. (2014) 10:e1004032. doi: 10.1371/journal.ppat.1004032
64. Shultz LD, Saito Y, Najima Y, Tanaka S, Ochi T, Tomizawa M, et al. Generation of functional human T-cell subsets with HLA-restricted immune responses in HLA class I expressing NOD/SCID/IL2r gamma(null) humanized mice. *Proc Natl Acad Sci USA*. (2010) 107:13022–7. doi: 10.1073/pnas.1000475107
65. Wang S, Chen Z, Hu C, Qian F, Cheng Y, Wu M, et al. Hepatitis B virus surface antigen selectively inhibits TLR2 ligand-induced IL-12 production in monocytes/macrophages by interfering with JNK activation. *J Immunol*. (2013) 190:5142–51. doi: 10.4049/jimmunol.1201625
66. Mignon A, Guidotti JE, Mitchell C, Fabre M, Wernet A, De La Coste A, et al. Selective repopulation of normal mouse liver by Fas/CD95-resistant hepatocytes. *Nat Med*. (1998) 4:1185–8. doi: 10.1038/2681
67. Guidotti JE, Mallet VO, Parlier D, Mitchell C, Fabre M, Jaffray P, et al. Fas/CD95 pathway induces mouse liver regeneration and allows for highly efficient retrovirus-mediated gene transfer. *Hepatology*. (2001) 33:10–5. doi: 10.1053/jhep.2001.20678
68. Murray PJ, Wynn TA. Protective and pathogenic functions of macrophage subsets. *Nat Rev Immunol*. (2011) 11:723–37. doi: 10.1038/nri3073
69. Kremsdorf D, Strick-Marchand H. Modeling hepatitis virus infections and treatment strategies in humanized mice. *Curr Opin Virol*. (2017) 25:119–25. doi: 10.1016/j.coviro.2017.07.029
70. Gutti TL, Knibbe JS, Makarov E, Zhang J, Yannam GR, Gorantla S, et al. Human hepatocytes and hematolymphoid dual reconstitution in treosulfan-conditioned uPA-NOG mice. *Am J Pathol*. (2014) 184:101–9. doi: 10.1016/j.ajpath.2013.09.008
71. Delgado JP, Vanneaux V, Branger J, Touboul T, Sentilhes L, Mainot S, et al. The role of HGF on invasive properties and repopulation potential of human fetal hepatic progenitor cells. *Exp Cell Res*. (2009) 315:3396–405. doi: 10.1016/j.yexcr.2009.07.007
72. Okoye AA, Picker LJ. CD4(+) T-cell depletion in HIV infection: mechanisms of immunological failure. *Immunol Rev*. (2013) 254:54–64. doi: 10.1111/imr.12066
73. Choi B, Chun E, Kim M, Kim SY, Kim ST, Yoon K, et al. Human T cell development in the liver of humanized NOD/SCID/IL-2Rgamma(null)(NSG) mice generated by intrahepatic injection of CD34(+) human (h) cord blood (CB) cells. *Clin Immunol*. (2011) 139:321–35. doi: 10.1016/j.clim.2011.02.019
74. Lang J, Kelly M, Freed BM, McCarter MD, Kedl RM, Torres RM, et al. Studies of lymphocyte reconstitution in a humanized mouse model reveal a requirement of T cells for human B cell maturation. *J Immunol*. (2013) 190:2090–101. doi: 10.4049/jimmunol.1202810
75. Chang H, Biswas S, Tallarico AS, Sarkis PT, Geng S, Panditrao MM, et al. Human B-cell ontogeny in humanized NOD/SCID gammac(null) mice generates a diverse yet auto/poly- and HIV-1-reactive antibody repertoire. *Genes Immun*. (2012) 13:399–410. doi: 10.1038/gene.2012.16
76. Gorantla S, Makarov E, Finke-Dwyer J, Gebhart CL, Domm W, Dewhurst S, et al. CD8+ cell depletion accelerates HIV-1 immunopathology in humanized mice. *J Immunol*. (2010) 184:7082–91. doi: 10.4049/jimmunol.1000438
77. Takenaka K, Prasolava TK, Wang JC, Mortin-Toth SM, Khalouei S, Gan OI, et al. Polymorphism in Sirpa modulates engraftment of human hematopoietic stem cells. *Nat Immunol*. (2007) 8:1313–23. doi: 10.1038/ni1527
78. Wilson EM, Bial J, Tarlow B, Bial G, Jensen B, Greiner DL, et al. Extensive double humanization of both liver and hematopoiesis in FRGN mice. *Stem Cell Res*. (2014) 13:404–12. doi: 10.1016/j.scr.2014.08.006
79. Hayakawa J, Hsieh MM, Uchida N, Phang O, Tisdale JF. Busulfan produces efficient human cell engraftment in NOD/LtSz-Scid IL2Rgamma(null) mice. *Stem Cells*. (2009) 27:175–82. doi: 10.1634/stemcells.2008-0583
80. Wilkinson FL, Sergijenko A, Langford-Smith KJ, Malinowska M, Wynn RF, Bigger BW. Busulfan conditioning enhances engraftment of hematopoietic donor-derived cells in the brain compared with irradiation. *Mol Ther*. (2013) 21:868–76. doi: 10.1038/mt.2013.29
81. Strick-Marchand H, Dusseaux M, Darche S, Huntington ND, Legrand N, Masse-Ranson G, et al. A novel mouse model for stable engraftment of a human immune system and human hepatocytes. *PLoS ONE*. (2015) 10:e0119820. doi: 10.1371/journal.pone.0119820
82. Dusseaux M, Masse-Ranson G, Darche S, Ahodantin J, Li Y, Fiquet O, et al. Viral load affects the immune response to HBV in mice with humanized immune system and liver. *Gastroenterology*. (2017) 153:1647–61 e1649. doi: 10.1053/j.gastro.2017.08.034
83. Park J-J, Wong DK, Wahed AS, Lee WM, Feld JJ, Lok ASF, et al. Hepatitis B virus–specific global T-cell dysfunction in chronic hepatitis B. *Gastroenterology*. (2016) 150:684–95.e685. doi: 10.1053/j.gastro.2015.11.050
84. Boni C, Laccabue D, Lampertico P, Giuberti T, Viganò M, Schivazappa S, et al. Restored function of HBV-specific T cells after long-term effective therapy with nucleos(t)ide analogues. *Gastroenterology*. (2012) 143:963–73 e969. doi: 10.1053/j.gastro.2012.07.014
85. Basma H, Soto-Gutierrez A, Yannam GR, Liu L, Ito R, Yamamoto T, et al. Differentiation and transplantation of human embryonic stem cell-derived hepatocytes. *Gastroenterology*. (2009) 136:990–9. doi: 10.1053/j.gastro.2008.10.047
86. Xia Y, Carpentier A, Cheng X, Block PD, Zhao Y, Zhang Z, et al. Human stem cell-derived hepatocytes as a model for hepatitis B virus infection, spreading and virus-host interactions. *J Hepatol*. (2017) 66:494–503. doi: 10.1016/j.jhep.2016.10.009
87. Yuan L, Liu X, Zhang L, Li X, Zhang Y, Wu K, et al. A chimeric humanized mouse model by engrafting the human induced pluripotent stem cell-derived hepatocyte-like cell for the chronic hepatitis B virus infection. *Front Microbiol*. (2018) 9:908. doi: 10.3389/fmicb.2018.00908

88. Carpentier A, Tesfaye A, Chu V, Nimgaonkar I, Zhang F, Lee SB, et al. Engrafted human stem cell-derived hepatocytes establish an infectious HCV murine model. *J Clin Invest*. (2014) 124:4953–64. doi: 10.1172/JCI75456
89. Ang LT, Tan AKY, Autio MI, Goh SH, Choo SH, Lee KL, et al. A roadmap for human liver differentiation from pluripotent stem cells. *Cell Rep*. (2018) 22:2190–205. doi: 10.1016/j.celrep.2018.01.087
90. Esteban MA, Wang T, Qin B, Yang J, Qin D, Cai J, et al. Vitamin C enhances the generation of mouse and human induced pluripotent stem cells. *Cell Stem Cell*. (2010) 6:71–9. doi: 10.1016/j.stem.2009.12.001
91. Yuan L, Jiang J, Liu X, Zhang Y, Zhang L, Xin J, et al. HBV infection-induced liver cirrhosis development in dual-humanised mice with human bone mesenchymal stem cell transplantation. *Gut*. (2019) 68:2044–56. doi: 10.1136/gutjnl-2018-316091

Conflict of Interest: The authors declare that the research was conducted in the absence of any commercial or financial relationships that could be construed as a potential conflict of interest.

frontiers in Immunology

MINI REVIEW
published: 05 March 2021
doi: 10.3389/fimmu.2020.617516

Advances in Humanized Mouse Models to Improve Understanding of HIV-1 Pathogenesis and Immune Responses

Amy Gillgrass[1,2,3]*, *Jocelyn M. Wessels*[4], *Jack X. Yang*[1,2,3] *and Charu Kaushic*[1,2,3]

[1] Department of Medicine, McMaster University, Hamilton, ON, Canada, [2] McMaster Immunology Research Centre, McMaster University, Hamilton, ON, Canada, [3] Michael G. DeGroote Institute for Infectious Disease Research, McMaster University, Hamilton, ON, Canada, [4] Department of Obstetrics and Gynecology, McMaster University, Hamilton, ON, Canada

OPEN ACCESS

Edited by:
Yan Li,
Nanjing University, China

Reviewed by:
Larisa Y. Poluektova,
University of Nebraska Medical Center, United States
Masakazu Kamata,
University of Alabama at Birmingham, United States
Ramesh Akkina,
Colorado State University, United States

***Correspondence:**
Amy Gillgrass
gillgra@mcmaster.ca

Specialty section:
This article was submitted to Viral Immunology, a section of the journal Frontiers in Immunology

Received: 14 October 2020
Accepted: 30 December 2020
Published: 05 March 2021

Citation:
Gillgrass A, Wessels JM, Yang JX and Kaushic C (2021) Advances in Humanized Mouse Models to Improve Understanding of HIV-1 Pathogenesis and Immune Responses. Front. Immunol. 11:617516. doi: 10.3389/fimmu.2020.617516

Although antiretroviral therapy has transformed human immunodeficiency virus-type 1 (HIV-1) from a deadly infection into a chronic disease, it does not clear the viral reservoir, leaving HIV-1 as an uncurable infection. Currently, 1.2 million new HIV-1 infections occur globally each year, with little decrease over many years. Therefore, additional research is required to advance the current state of HIV management, find potential therapeutic strategies, and further understand the mechanisms of HIV pathogenesis and prevention strategies. Non-human primates (NHP) have been used extensively in HIV research and have provided critical advances within the field, but there are several issues that limit their use. Humanized mouse (Hu-mouse) models, or immunodeficient mice engrafted with human immune cells and/or tissues, provide a cost-effective and practical approach to create models for HIV research. Hu-mice closely parallel multiple aspects of human HIV infection and disease progression. Here, we highlight how innovations in Hu-mouse models have advanced HIV-1 research in the past decade. We discuss the effect of different background strains of mice, of modifications on the reconstitution of the immune cells, and the pros and cons of different human cells and/or tissue engraftment methods, on the ability to examine HIV-1 infection and immune response. Finally, we consider the newest advances in the Hu-mouse models and their potential to advance research in emerging areas of mucosal infections, understand the role of microbiota and the complex issues in HIV-TB co-infection. These innovations in Hu-mouse models hold the potential to significantly enhance mechanistic research to develop novel strategies for HIV prevention and therapeutics.

Keywords: HIV-1, humanized mouse, pathogenesis, immune response, mucosal infection, microbiota, co-infection, vaccines

INTRODUCTION

Currently approximately 38 million people are living with human immunodeficiency virus-type 1 (HIV-1), the underlying cause of acquired immune deficiency syndrome (AIDS) (1). Although treatment with antiretroviral therapy (ART) has transformed HIV from a deadly infection into a chronic disease, it does not clear the latent viral reservoir, therefore there is still no cure for HIV infection (2). Furthermore, even with ART, HIV infection increases risks of co-infection with other pathogens such as *Mycobacterium tuberculosis* (*Mtb*) (3). Additional research is required to advance the current state of HIV management and potential therapeutic strategies, in addition to understanding mechanisms of HIV pathogenesis. Although animal models such as non-human primates (NHP) have been used extensively in HIV research and have provided critical advances in knowledge within the field, there are several issues including host-restriction factors, ethics, and cost that can limit their use (4, 5). Furthermore, the human species-specific tropism of HIV-1 has prevented the use of traditional murine models leading to a lack of small animal models for *in vivo* HIV-1 research (6).

Humanized mouse (Hu-mouse) models, or immunodeficient mice engrafted with human immune cells and/or tissues, provide a cost-effective and practical approach to creating models for HIV-1 research. Unlike traditional mouse models, Hu-mouse models effectively sustain HIV-1 infections while also recapitulating relatively accurate *in vivo* immune responses to the infection due to the reconstitution with human immune cells when compared to other animal models (7). This review will outline the advances in Hu-mouse models that have made them useful in HIV-1 research and a convenient alternate to NHP. Furthermore, numerous novel modifications of Hu-mice demonstrate potential to advance knowledge in virus transmission, infection, evolution, pathogenesis, prevention, latency, cure, and disease interaction such as *Mtb* co-infection. Additionally, since the major physiological route of HIV-1 transmission in humans is by the mucosal route (intrarectally or intravaginally) (8), this review will detail the use of Hu-mice in elucidating mechanisms involving mucosal infections and discuss how microbiota may be involved.

HU-MOUSE MODELS FOR HIV-1 RESEARCH

Currently, some of the most widely used Hu-mouse models in HIV research take advantage of three major immunocompromised features which allow for the successful engraftment of human cells or tissues. NOD.Cg-Prkdc^{scid}Il2rg^{tm1Sug} (NOG) (9), NOD.Cg-Prkdc^{scid}Il2rg^{tm1Wjl} (NSG) (10, 11), and NOD.Cg-Rag1^{tm1MoM}Il2rg^{tm1Wjl} (NRG) (12) are on the non-obese diabetic (NOD) background that leads to suppressed mouse macrophage phagocytic activity. Mice with the *Prkdc*^{scid} or Rag1/Rag2 loci mutation lack mature T and B lymphocytes while the *Il2rg* gene mutation effectively eliminates mouse NK cell activity (13). The most common engraftment method of human cells is the intravenous or intrahepatic injection of CD34+ hematopoietic stem cells (14) into adult or newborn immunodeficient mice, respectively, after myeloablative irradiation or administration of myeloablative doses of drugs such as busulfan (15). This engraftment method has been performed in each model (NOG, NSG, NRG) yielding reconstitution of human CD4+ and CD8+ T cells, monocytes, macrophages, dendritic cells (DCs) and progenitor B cells in peripheral blood, primary and secondary lymphoid tissues (12, 16).

The unique engraftment method using surgical implantation of human fetal liver and thymus tissues followed by injection of matched CD34+ hematopoietic stem cells (HSCs) gave rise to the bone marrow liver thymus (BLT) model (17–19). The human thymic tissue allows for T cell education in the context of human cells (20). Both HSC-only and BLT methods are able to successfully reconstitute human monocytes, dendritic cells, T cells, and B cells in peripheral blood and tissues, but higher cell counts were observed in the BLT engraftment method (21, 22). The HSC-only method demonstrated better human B cell and myeloid cell development (21) while additional thymus support yielded higher $CD3^+$ T cell reconstitution in the spleen (21), gastrointestinal (GI) (22) and gut-associated lymphoid (GALT) tissues (18, 21, 23) (**Table 1**). Both methods have demonstrated similar susceptibility to HIV infection, trends in CD4+ T cell depletion, and persistent viral reservoirs *in vivo* (21). The major difference between the two methods is that BLT-engrafted mice have measurable T cell response against HIV-1 because the human thymic tissue allows the resulting T cells to respond to the HIV-1 antigen presentation by human leukocyte antigen (HLA) generating HLA-restricted anti-HIV-1 human T cell response, which is absent in the current HSC-only method (18, 48) (**Table 1**). This has led to the BLT model being the current gold standard for studying HIV-1 immune responses (17, 49, 50).

HSC ENGRAFTMENT MODELS (CURRENT GENERATION): NOG, NSG, NRG, DKO/BRG, NSG-BLT

NOG and NSG

The NOG and NSG mice differ in the IL-2 receptor gene (Il2rg) which is truncated in NOG and knocked-out in NSG. Both humanized NOG (hu-NOG) and humanized NSG (hu-NSG) mice have demonstrated successful engraftment of HSC with substantial human lymphoid repopulation (29, 51–53). Intraperitoneal and intravenous routes of HIV-1 infection into both types of mice demonstrated viremia and viral dissemination throughout lymphoid tissues (29, 51–54).

Hu-NOG mice have furthered the understanding of HIV-1 transmission as well as treatment testing and development. These mice can generate B cells that secrete isotype-switched, HIV-specific IgG antibodies (16). Studies using hu-NOG models investigated the role of human anti-viral factors in human transmission of HIV-1 (55) and treatment options with novel therapeutics such as zinc-finger nucleases (ZFN) showing reduced viral loads and increased CD4+ T cell counts (56). Additionally, viral evolution and replication kinetics have been

TABLE 1 | Summary of reported reconstitution of major human immune cell types within current generation and next generation hu-mice for HIV studies.

Humanized Mouse Model	Human immune cell reconstitution	References
Current Generation Models		
HSC-DKO/BRG	**PB:** CD45+ lymphocytes, CD4+ T cells, CD8+ T cells **BM:** CD45+ lymphocytes, mature and immature B cells **LT:** CD45+ lymphocytes, CD3+ T cells, CD4+ T cells, CD8+ T cells, T regulatory cells, mature and immature B cells	(24–27)
HSC-NOG	**PB:** CD45+ lymphocytes, CD3+ T cells, immature B cells **BM:** CD45+ lymphocytes, immature B cells **LT:** CD45+ lymphocytes, CD4+ T cells, CD8+ T cells, immature B cells	(16, 28)
HSC-NSG HSC-NRG	**PB:** CD3+ T cells, immature B cells **BM:** CD45+ lymphocytes, mature and immature B cells, immature NK cells **LT:** CD4+ T cells, CD8+ T cells, mature and immature B cells **FRT:** CD45+ cells, CD4+ T cells, CD68+ macrophages	(12, 29–31)
NSG-**BLT***	**PB:** CD3+ T cells, CD4+ T cells, CD8+ T cells, immature B cells **BM:** CD45+ lymphocytes, mature and immature B cells **LT:** CD4+ T cells, CD8+ T cells, mature and immature B cells **GI:** CD45+ lymphocytes, CD4+ T cells, CD8+ T cells, B cells, CD68+ macrophages, dendritic cells **FRT:** CD3+ T cells, CD4+ T cells, CD68+ macrophages, CD11c+ dendritic cells	(18, 32, 33)
Next Generation Models		
HSC-DRAG* HSC-DRAGA*	**PB:** CD3+ T cells, CD4+ T cells, CD8+ T cells, isotype switched mature B cells **BM:** CD45+ lymphocytes **LT:** CD45+ lymphocytes, CD4+ T cells, CD8+ T cells, T regulatory cells, dendritic cells **GI:** CD45+ lymphocytes, CD4+ T cells, CD8+ T cells, naïve and memory B cells **FRT:** CD4+ T cells, T follicular helper cells, naïve and memory B cells	(34–36)
HSC-BRGST HSC-BRGSA2DR2*	**PB:** CD45+ lymphocytes, CD3+ T cells, CD4+ T cells, CD8+ T cells, T follicular helper cells (HSC-BRGST only), isotype switched mature B cells **BM:** CD45+ lymphocytes, isotype switched B cells **LT:** CD45+ lymphocytes, CD4+ T cells, CD8+ T cells, isotype switched mature B cells, T follicular helper cells (HSC-BRGST only), central and effector memory T cells	(37, 38)
NSGW-NeoThy	**PB:** CD45+ lymphocytes, CD3+ T cells, CD4+ T cells, CD8+ T cells, regulatory T cells, B cells, monocytes/macrophages **BM:** CD45+ lymphocytes, CD3+ T cells, B cells **LT:** CD45+ lymphocytes, CD3+ T cells, regulatory T cells, B cells, monocytes/macrophages	(39)
HSC-NOG-EXL	**PB:** CD4+ T cells, CD8+ T cells, CD33+ myeloid cells, basophils, neutrophils, NK cells, monocytes, dendritic cells **BM:** CD3+ T cells, B cells, mast cells, basophils **LT:** CD3+ T cells, B cells, mast cells, basophils, dendritic cells **GI:** Mast cells, basophils	(40, 41)
HSC-NSGS/NSG-SGM3	**PB:** CD4+ T cells, B cells, T regulatory cells **BM:** CD3+ T cells, CD4+ T cells, T regulatory cells, B cells, dendritic cells **LT:** CD3+ T cells, CD4+ T cells, T regulatory cells, B cells, CD33+ myeloid cells	(42–44)
HSC-SRG-15	**PB:** CD45+ lymphocytes, mature NK cells **BM:** mature NK cells, CD45+ lymphocytes, CD3+ T cells, CD4+ T cells, CD8+ T cells **LT:** tissue-resident NK cells, CD45+ lymphocytes, CD3+ T cells, CD4+ T cells, CD8+ T cells	(31)
HSC-NSG-15	**PB:** mature NK cells, CD3+ T cells **BM:** mature NK cells, CD45+ lymphocytes, CD3+ T cells, CD4+ T cells, CD8+ T cells, B cells **LT:** mature NK cells, CD45+ lymphocytes, CD3+ T cells, CD4+ T cells, CD8+ T cells, B cells	(45)
HSC-MITRG HSC-MISTRG	**PB:** Monocytes, functional NK cells, CD45+ lymphocytes, CD3+ T cells, naïve CD4+ T cell, naïve CD8+ T cell, immature B cells **BM:** CD45+ lymphocytes, CD33+ myeloid cells, functional monocytes **LT:** functional NK cells, monocytes, dendritic cells **GI:** CD68+ myeloid cells	(46, 47)

PB, Peripheral blood; BM, Bone marrow; LT, Primary and secondary lymphoid tissue; GI, Gastrointestinal organs; FRT, Female reproductive tract.
**HLA-restricted immune responses observed.*

investigated using this model using various HIV-1 strains (57). Finally, hu-NOG mice were also used to investigate the efficacy of ART, long-acting antiretroviral compounds that showed reduced viral load and recovery of CD4+ T cell counts, and a latent viral reservoir with T cell depletion after treatment was stopped, similar to that seen in humans (58).

Numerous HIV-1 treatment methods have been tested on hu-NSG mice including combination ART (cART) (29, 59), highly

active antiretroviral therapy (HAART), and neutralizing antibody treatment (54). Similar to the response seen in hu-NOG mice, latent infection was established and persisted during treatment (29, 59). Resting memory CD4+ T cells were the major viral reservoir (29), unaffected by the length of cART treatment (59). A recent study using hu-NSG mice showed that HIV-1 hematopoietic stem/progenitor cell-based gene therapy targeting CCR5 and HIV-1 LTR could be used as anti-HIV strategy (60). Another study tested long-acting, slow-release antiviral therapy in combination with CRISPR-Cas9 gene editing to eliminate latent HIV-1 in Hu-mice, and was the first to demonstrate that permanent viral elimination is possible (61). Additionally, the hu-NSG model has been used to provide better understanding of HIV-1 pathogenesis. The model revealed that cell-to-cell viral transmission efficiently disseminated infection within tissues, suggesting anatomically localized spread would be an area of future investigation for targeted treatments (62). HIV-1 disease progression was also investigated in hu-NSG mice by tracking viral seeding into different tissue compartments providing a picture of the HIV-1 infection timeline (63). Although it has been demonstrated that hu-NSG mice successfully reconstitute human CCR5+ CD4+ T cells within the female reproductive tract (FRT) (29, 30), to date, HSC-engrafted NSG mice have not been utilized widely to study mucosal and sexual transmission of HIV-1 (30).

NRG and DKO (BRG)

Like the NSG model, the more radioresistant hu-NRG have similar successful engraftment of human peripheral blood mononuclear cells (PBMCs) or HSCs (12). HSC-engrafted NRG mice demonstrated successful mucosal HIV-1 challenge with viral dissemination throughout the FRT and lymphoid tissues (64, 65). An older, yet similar model without the NOD background termed $Rag1^{null}Il2rg^{null}$ or $Rag2^{null}Il2rg^{null}$ (DKO) mice (also known as BRG mice) (11, 66), also demonstrated susceptibility to both R5- and X4-tropic variants of HIV-1 *via* vaginal and rectal mucosal transmission with insights on therapy efficacy, latency and chronic infection (24–26, 67, 68). Furthermore, hu-DKO/hu-BRG mice have greatly contributed to cross-species transmission and viral evolution investigations (69, 70), as well as the development of Hu-mice based viral outgrowth assays to further the understanding of HIV latency (71, 72). Successful mucosal infection in hu-DKO and hu-NRG mice best models natural human routes of HIV-1 transmission and allows studies of microbiota alteration (65) and topical pre-exposure prophylaxis (PrEP) (67, 73–76).

Studies using hu-NRG mice investigated the role of plasmacytoid dendritic cells during infection (77) and HIV-1 latency, and revealed the persistence of type 1 interferon (IFN) signaling after cART treatment (78). Furthermore, therapeutics that enhance ART treatment such as broadly neutralizing antibodies (79) showed promise in this model for prevention of cell-to-cell HIV-1 transmission (80, 81). Novel CRISPR/CAS9 genome editing technology was used in PBMC-engrafted NRG mice and demonstrated excision of HIV-1 pro-viral DNA which reduced levels of HIV-1 (82). Additionally, single-cell RNA-sequencing was used in this model to characterize human innate immune cells in lymphoid tissues (83). Interestingly, despite the lack of isotype-switched mature B cells, hu-NRGs can still be a useful tool for certain vaccine investigations (84).

NSG-BLT Engraftment Model

Compared to HSC-engrafted DKO, NSG, and NRG, the BLT engrafted NSG (NSG-BLT) hu-mice have the best overall reconstitution and functional human immune system for studying immune responses to HIV-1 infection (18, 49, 85, 86). For this reason, the BLT mice are currently considered the gold standard for HIV-1 research in murine models (17, 49, 50). BLT mice have been shown repeatedly to sustain mucosal HIV-1 infection and CD4+ T cell reconstitution in the FRT (32, 87).

The NSG-BLT mice have been frequently used for testing HIV-1 prevention and therapy. Studies examining therapeutics such as the long-acting ART raltegravir (88), ultra-long-acting antiretroviral dolutegravir (89), and PreP therapies such as the nucleoside reverse transcriptase inhibitor (NRTI) 4'-ethynyl-2-fluoro-2'-deoxyadenosine (EFdA) take advantage of the reconstituted human immune cell population in the mucosa (90). These studies have demonstrated effective inhibition of HIV-1 replication, reduction of HIV-1 viral load, and protection from multiple high-dose HIV-1 challenges (87, 88, 89, 90). Other studies using the NSG-BLT model provided valuable insights into HIV-1 treatment, viral evolution, prevention strategies, dose testing, tissue concentration, and pharmacokinetic data (74, 91–95). NSG-BLT Hu-mice have also been used to investigate potential treatment methods including anti–human IFN receptor 2 (IFNR2) (96) and anti-IFN-α/β receptor (IFNAR) antibodies (78) in conjunction with ARTs to successfully diminish viral reservoir size in lymphoid tissue and delay viral rebound (78, 96). A novel therapeutic strategy using chimeric antigen receptor modified stem cells successfully repopulated NSG-BLT mice with HIV-specific lymphoid populations and demonstrates potential for use in HIV treatment and cure studies (97). The efficacy of both HIV-1 reverse transcriptase inhibitor EFdA (98) and latency-reversing agents such as panobinostat (99) were also studied within the lymphoid compartments to elucidate effects on viral reservoir and latency. Finally, the NSG-BLT model is among the Hu-mice that can be used to evaluate the efficacy of potential HIV vaccines as demonstrated through significant T cell protection upon gag-specific vaccine administration (100). The development of proof of concept vaccines for therapeutic treatment has also been tested in the NSG-BLT model. In a lentiviral-based DC vaccine, HIV-1 antigen (SL9 epitope) is expressed with CD40 ligand to stimulate DC responses and Programmed Death 1 (PD-1) to prevent checkpoint activation (101). This vaccine demonstrated the ability to induce antigen-specific T cells and memory (101). Although unable to induce protection it was able to decrease viral load in the short term (101). In a similar model (NRG with fetal thymus implanted), another therapeutic vaccine expressing 5 CD4 and CD8 HIV specific T cell epitopes with CD40 ligand and administered with TLR3 agonist PolyI:C was successful at inducing anti-HIV CD8 and CD4 T cell responses, reactivated HIV reservoirs in cART controlled HIV infected mice, and decreased cell associated viral DNA (102).

UNDERSTANDING MUCOSAL TRANSMISSION OF HIV-1 AND THE EFFECT OF MICROBIOTA USING HU-MOUSE MODELS

It is well recognized that more than 80% of HIV-1 infections occur through sexual transmission at mucosal surfaces, primarily the lower intestinal tract and female and male genital tract (8). While significant progress has been made in the understanding of mucosal transmission and pathogenic progression of HIV-1 through clinical studies and NHP models, the Hu-mice models present excellent model systems to recapitulate many features of mucosal infection in humans (103–106).

Most Hu-mouse experiments that have focused on mucosal (intrarectal or intravaginal) HIV-1 transmission have assessed prevention of infection using a wide variety of potential prophylactic agents. In these experiments, cell-free (including transmitted/founder strains) and cell-associated HIV-1 were used to challenge Hu-mice *via* the rectal or vaginal routes (24, 33, 64, 65, 94). While most of the mucosal prevention studies focused on the vaginal route of transmission, several have assessed the efficacy of PrEP preventions in Hu-mice challenged intrarectally. Topical microbicides (91), C5A in BLT mice (107), topically delivered ARVs (tenofovir disoproxil fumarate (TDF) and emtricitabine (FTC)) in BLT (108) are some of the prophylactic agents tested. Many studies tested various formulations, routes, pharmacokinetic and challenge routes. Different studies reported complete or partial protection against a single dose intrarectal challenge with HIV-1 (91, 94). Using the DKO model, tissue distribution of the interventions has also been assessed (73, 74). In studies focused on the vaginal route of transmission, many studies examined the efficacy of topical microbicides in DKO and BLT models (75, 92, 108–116). While most studies reported complete protection against single dose intravaginal challenge with HIV-1, others report only partial (89, 110, 113–117), or no protection (110).

Repeated, and often high dose, intravaginal exposure model has been tested to examine the effectiveness of the prophylactic intervention (88, 89, 94, 114). While it is likely that repeated, low dose viral challenges mimic vaginal transmission of HIV-1 in women more closely than high dose challenges, both experimental designs provide the opportunity to answer different research questions about prophylactic interventions. Interestingly, a few studies found delayed HIV-1 infection and dissemination when vaginal and systemic levels of drug were reduced or after drug cessation (112, 114, 115). Thus Hu-mice models can be useful in studying imperfect patient adherence and how this might impact HIV-1 transmission.

Work done by our group has highlighted the critical factors for successful mucosal transmission using a Hu-mouse model. We demonstrated that the frequency of circulating human CD45 + cells was the primary determinant of successful HIV-1 infection following intravaginal exposure in HSC-engrafted NRG mice. Furthermore, a significant correlation existed between peripheral blood CD45+ cells and HIV-1 target cells in the vaginal mucosa (64). This study highlighted that for successful HIV-1 infection through the intravaginal route, access to target cells in the mucosa is required. This highlights the importance of developing prophylactic interventions that limit target cells in mucosa, such as limiting tissue inflammation (118), to prevent HIV-1 infection.

The role of the microbiota in altering HIV susceptibility is a growing area of interest and the subject of many clinical studies. Hu-mice might be a useful model to examine the effect of the microbiota (vaginal and/or rectal) on HIV-1 acquisition, as a diverse vaginal microbiota low in *Lactobacillus* species is associated with a 4-fold increased risk of acquisition in women (119). If the next generation of Hu-mouse models engrafted with HSCs could be developed as gnotobiotic (germ-free) mice, this would allow for the reconstitution of Hu-mouse vagina/rectum/gut with human microbiota and assessment of HIV-1 acquisition risk. Although germ-free Hu-mice are not presently commercially available, a recent publication reported the generation of "pseudo-gnotobiotic" Hu-mice. NSG-BLT Hu-mice were treated with broad spectrum antibiotics, and subsequently transplanted with a human gut microbiota *via* fecal transplant; generating NSG-BLT mice reconstituted with human immune cells and a human gut microbiota. The authors found unique gut microbiota signatures in the mice that resembled those of the human donor, and they demonstrated that the human-like gut microbiota was stable in these mice for the duration of their study (14.5 weeks) (120). However, the relevance of this type of model and of other types of doubly-reconstituted Hu-mice (immune cells and microbiota) that we may be able to generate in the future is controversial at present. This is for a variety of reasons including, but not limited to, our lack of knowledge on generalizability of results obtained in mice to humans, a lack of standardized protocols, inter-donor, ethnic, and geographical microbial variability that makes replication of data challenging, and anatomical and physiological differences between mice and humans that might impact the microbiota (121). Nevertheless, germ-free humanized mouse models that can be reconstituted with a human-like microbiota may one day be key advancements that improve our understanding of the role of the vaginal, rectal and gut microbiota in mucosal HIV-1 transmission, epithelial barrier disruption, and inflammation. Furthermore, they may be useful in examining prophylactic interventions to decrease systemic inflammation and prevent HIV-1 transmission.

USING HU-MICE FOR UNDERSTANDING TUBERCULOSIS-HIV CO-INFECTION

Currently animal models for HIV co-infection with other pathogens are lacking. Although Hu-mice have been used to investigate HIV co-infection with pathogens such as Epstein–Barr virus and *Neisseria gonorrhoeae* (30, 122), co-infection with *Mycobacterium tuberculosis* (Mtb) is of particular interest as it is the most common cause of AIDS-related death (1). HIV-1 infection increases the risk of latent tuberculosis (TB) reactivation (123). HIV/TB co-infection increases morbidity and mortality while complicating therapies associated with both diseases due to multiple factors including the development of Immune Reconstitution Inflammatory Syndrome (IRIS) and TB drug resistance (124). The current inbred mouse *in*

vivo models of TB do not develop organized granulomas (125) and show inconsistent immune responses (126).

On the other hand, the use of Hu-mouse models (HSC-engrafted (127, 128) and BLT-engrafted (129) NSG mice) has demonstrated tremendous potential to recapitulate human TB infection, immune response, and formation of organized granulomas (127–129). With the vastly successful Hu-mice studies in HIV-1, they serve as a viable model for co-infection. In early HIV/TB co-infection studies, NSG-BLT mice were infected with HIV-1 followed by Mtb. HIV-1 was localized in pulmonary granulomas and exacerbated TB lesions and lung pathology were seen (130). A more recent study demonstrated that the same model can be used for studying TB relapse in co-infection by administration of HIV-1 intravenously after paucibacillary TB infection was established (131). Although only NSG-BLT model has been used thus far for TB-HIV co-infection, newer generation Hu-mouse models using the easier and more accessible HSC-only engraftment method for HIV/Mtb co-infection would allow for more widespread use of the model, thus addressing the lack of literature on HIV/TB co-infection studies *in vivo*.

IMPROVED HU-MOUSE MODELS FOR HIV-1 RESEARCH (NEXT GENERATION): NSG-A2, DRAG, DRAGA, AND BRGST

Addressing the Challenges With the BLT Model

Even though the BLT model is currently the gold standard for HIV-1 research, there are several disadvantages that limit its use. Xenogenic GvHD that develops post-engraftment (132, 133) remains a concern despite efforts to extend longevity using a triple-knockout model (134, 135). This reduces the sample population of mice in studies (17) and prevents long-term studies. Humanized BLT mice also lack high levels of B cell populations and hyper-mutated, class-switched IgG antibodies (136). Furthermore, the engraftment of human fetal liver and thymus tissue is time-consuming and requires great technical skill to execute. Finally, a major issue with using the fetal BLT method is material availability, as restrictions on the use of fetal tissue in research is of increasing concern (137). To address this shortcoming, a novel method of using neonatal thymus tissue to replace the use of fetal tissue was developed within NOD, B6.SCIDIl2rg$^{-/-}$Kit$^{W41/W41}$ (NSGW) mice (NSGW-NeoThy) (39, 138). The addition of the *Kit*$^{W41/W41}$ alleles offers the advantage of accepting HSC engraftment without prior irradiation (138, 139). Neonatal thymic samples are easier to obtain, and yield much larger quantities of tissue and can thus humanize more mice per sample compared to using fetal tissue (39). NSGW-NeoThy mice developed smaller thymic organoids but with either autologous or allogeneic HSC engraftment, the model successfully repopulated human myeloid and lymphoid populations comparable to fetal thymus-only engrafted NSG mice (39), thus demonstrating its potential for future use in HIV investigations. Some evidence also presented the potential of reduced GvHD in NSGW-NeoThy mice by administration of anti-human CD2 antibodies to remove GVHD-associated passenger thymocytes, but a more comprehensive study must be conducted to elucidate GvHD development in the model (39).

Next Generation of Transgenic Mice

NSG-A2 mice were developed from the NSG background strain and are transgenic for the human HLA class I-A2 molecule. When humanized with HLA-matched HSCs, this allows human CD8+ T cells to be functionally mature (140). However, neither total CD8+ T cell reconstitution levels nor B cell function were significantly better than NSG mice (140, 141). To improve the humoral immune response, the HLA class II transgene (specifically, HLA-DR4) molecule has been expressed in the NOG (142), NSG (143), and NRG mice (34). Here we are focusing on the more popularly used and radiation-tolerant NRG background termed DRAG mice.

Humanized DRAG (hu-DRAG) mice with HSC derived HLA-DR-matched umbilical cord blood engraftment resulted in significantly higher counts of human CD4+ and CD8+ T cells compared to its non-transgenic NRG counterpart (34) (**Table 1**). Human B cells were highly functional, and could undergo immunoglobulin (Ig) isotype class-switching (34). To adequately compare the benefits between transgenic HLA class I and II, a model co-expressing both the HLA-A2 and HLA-DR4 molecules, termed DRAGA mice was developed (35). Comparisons between NRG-A2, DRAG, and DRAGA models engrafted with HLA-matched HSCs demonstrated that both hu-DRAG and hu-DRAGA models had significantly better human T-cell reconstitution, CD4/CD8+ T cell function, and most importantly, significant B cell Ig class-switching when compared to NRG-A2 mice (35) and even the hu-BLT models (136) (**Table 1**). These results demonstrate that the HLA-DR4 transgene can confer more benefits in human lymphoid reconstitution compared to HLA-A2.

Recently the BRG background was altered to produce a promising model with consistent lymph node reconstitution and development addressing the shortcomings of secondary lymphoid tissue formation within current Hu-mouse models (37, 144). Balb/c *Rag2*$^{-/-}$*Il2rg*$^{-/-}$*Sirpa*^{NOD} (BRGS) mice (145) that express transgenic thymic-stromal-cell-derived lymphopoietin (TSLP), termed the BRGST model, boast robust human cellular and humoral responses (37). TSLP is similar in structure and function to IL-7, but is IL2rg independent and thus can promote B and T cell responses (39). In particular, when compared to the older hu-BRGS model, hu-BRGST mice demonstrated enhanced Ig-isotype class switching, central/effector memory T cell, and T follicular helper (TFH) cell development in secondary lymphoid tissues with pronounced B cell zones (37). When the BRGS background hosts HLA class I and II transgenes (termed BRGSA2DR2 mice), improvements in T and B cell development and functionality including Ig-isotype class switching and antigen-specific responses were also observed (38).

Hu-DRAG mice are capable of supporting HIV-1 infections when challenged intravaginally as the mucosa of the FRT and gut both repopulate with CD4+ T cells and TFH cells (36, 146). Hu-BRGST mice successfully sustain HIV-1 infection and replication

upon intraperitoneal inoculation (37). Viral reservoir and latency was also demonstrated after HAART administration, thus also offering possibilities in HIV latency and cure investigations (37). As hu-DRAG, hu-DRAGA, hu-BRGST, and hu-BRGSA2DR2 mice develop robust antigen-specific Ig responses, these models have tremendous potential for use in testing novel HIV-1 vaccine formulations. Immunization of both hu-DRAG and hu-DRAGA models for the investigation of other pathogenic viruses such as influenza (35, 147, 148) and Zika (149) have already yielded promising results (34, 35, 146–149). Therefore, the hu-DRAG and hu-DRAGA demonstrate tremendous potential for future use in HIV-1 therapeutic antibody and vaccine research.

Other Novel Models for HIV-1 Studies

The reconstituted human immune cell population in the current HSC-engrafted models for HIV-1 studies consist mainly of lymphoid cells with lower overall functional NK cell and myeloid repopulation (42, 150–152). Reduced myeloid populations may result in decreased endogenous cytokine signals, preventing the model from providing the full human inflammation process (42). Additionally, this may limit aspects of HIV-1 investigation such as innate immunity, antigen presentation interactions, or humoral immunity and vaccine studies. **Table 1** summarizes some of the novel models including, MITRG/MISTRG models (discontinued by the Jackson Laboratory- short life span of 10-16 weeks post engraftment), NSGS (also called NSG-SGM3) model (NSG mice expressing human myeloid promoting cytokines SCF, GM-CSF, and IL-3, life span issue after 20 weeks) (42–44), and NOG-EXL (NOG mice expressing GM-CSF and IL-3) (40, 41) for better human myeloid cell engraftment of monocytes/macrophages and NK cells reconstitution (46, 47). Furthermore, the NSG-15 (45) and SRG-15 (31) models have been developed to express transgenic human IL-15 specifically for improved NK cell development. Overall, these models have all demonstrated success in their use for HIV-1 investigations, and their myeloid and NK reconstitution improvements can further extend HIV-1 *in vivo* research capabilities. It is important for researchers to note that until all shortcomings of Hu-mouse models have been addressed, choosing the optimal model for a study will depend on the experiment itself with special considerations for study timeline and immune cells of interest.

CONCLUSION

In summary, the development of Hu-mouse models has provided a cost-effective and practical approach for HIV-1 research. These mice provide a useful pre-clinical tool, since they allow researchers to directly examine interactions between HIV-1 and the human immune system. Novel modifications in generating Hu-mice is increasing the feasibility of using these models to investigate more complex clinical problems, such as immune response in co-infections like HIV and TB, and understanding interactions between immune responses and microbiota in regulating HIV-1 susceptibility. As we continue to make improvements in humanization of mice by developing novel models with new features and gain better understanding of how to tailor the models to answer specific questions, we will continue to push the envelope and make breakthroughs in HIV-1 research.

AUTHOR CONTRIBUTIONS

AG and CK outlined the content of the review. JY and JW prepared the main body of the manuscript. AG and CK revised the manuscript. AG supervised the project. All authors contributed to the article and approved the submitted version.

FUNDING

CK's laboratory is funded by the Canadian Institutes of Health Research Operating Grant (FRN# SOP 159229). Salary support (JW) is provided by a Canadian Institutes of Health Research Postdoctoral Fellowship award (MFE 152502).

REFERENCES

1. UNAIDS. 2019 fact sheet. *Global HIV and AIDS statistics - 2019 fact sheet*. (2020). Available at: https://www.unaids.org/en/resources/fact-sheet.
2. Bachmann N, von Siebenthal C, Vongrad V, Turk T, Neumann K, Beerenwinkel N, et al. Determinants of HIV-1 reservoir size and long-term dynamics during suppressive ART. *Nat Commun* (2019) 10:1–11. doi: 10.1038/s41467-019-10884-9
3. Bell LCK, Noursadeghi M. Pathogenesis of HIV-1 and mycobacterium tuberculosis co-infection. *Nat Rev Microbiol* (2018) 16:80–90. doi: 10.1038/nrmicro.2017.128
4. Evans DT, Silvestri G. Nonhuman primate models in AIDS research. *Curr Opin HIV AIDS* (2013) 8:255–61. doi: 10.1097/COH.0b013e328361cee8
5. Sauter D, Kirchhoff F. Key Viral Adaptations Preceding the AIDS Pandemic. *Cell Host Microbe* (2019) 25:27–38. doi: 10.1016/j.chom.2018.12.002
6. Hatziioannou T, Evans DT. Animal models for HIV/AIDS research. *Nat Rev Microbiol* (2012) 10:852–67. doi: 10.1038/nrmicro2911
7. Shultz LD, Brehm MA, Victor Garcia-Martinez J, Greiner DL. Humanized mice for immune system investigation: Progress, promise and challenges. *Nat Rev Immunol* (2012) 12:786–98. doi: 10.1038/nri3311
8. Hladik F, McElrath MJ. Setting the stage: Host invasion by HIV. *Nat Rev Immunol* (2008) 8:447–57. doi: 10.1038/nri2302
9. Brehm MA, Cuthbert A, Yang C, Miller DM, DiIorio P, Laning J, et al. Parameters for establishing humanized mouse models to study human immunity: Analysis of human hematopoietic stem cell engraftment in three immunodeficient strains of mice bearing the IL2rγnull mutation. *Clin Immunol* (2010) 135:84–98. doi: 10.1016/j.clim.2009.12.008
10. Shultz LD, Lyons BL, Burzenski LM, Gott B, Chen X, Chaleff S, et al. Human Lymphoid and Myeloid Cell Development in NOD/LtSz- scid IL2R γ null Mice Engrafted with Mobilized Human Hemopoietic Stem Cells. *J Immunol* (2005) 174:6477–89. doi: 10.4049/jimmunol.174.10.6477
11. McDermott SP, Eppert K, Lechman ER, Doedens M, Dick JE. Comparison of human cord blood engraftment between immunocompromised mouse strains. *Blood* (2010) 116:193–200. doi: 10.1182/blood-2010-02-271841
12. Pearson T, Shultz LD, Miller D, King M, Laning J, Fodor W, et al. Non-obese diabetic-recombination activating gene-1 (NOD-Rag1 null) interleukin (IL)-2 receptor common gamma chain (IL2rγnull) null mice: A radioresistant model for human lymphohaematopoietic engraftment. *Clin Exp Immunol* (2008) 154:270–84. doi: 10.1111/j.1365-2249.2008.03753.x

13. Cao X, Shores EW, Hu-LI J, Ft Anver M, Kelsall BL, SM R, et al. Defective Lymphoid Development in Mice Lacking Expression of the Common Cytokine Receptor γ Chain. *Immunity* (1995) 2:223–8. doi: 10.1016/1074-7613(95)90047-0
14. Pearson T, Greiner DL, Shultz LD. Creation of "humanized" Mice to study human immunity. *Curr Protoc Immunol* (2008) 81:15.21.1–15.21.21. doi: 10.1002/0471142735.im1521s81
15. Hayakawa J, Hsieh MM, Uchida N, Phang O, Tisdale JF. Busulfan Produces Efficient Human Cell Engraftment in NOD/LtSz- Scid IL2Rγ Null Mice. *Stem Cells* (2009) 27:175–82. doi: 10.1634/stemcells.2008-0583
16. Sato K, Nie C, Misawa N, Tanaka Y, Ito M, Koyanagi Y. Dynamics of memory and naïve CD8+ T lymphocytes in humanized NOD/SCID/IL-2Rγnull mice infected with CCR5-tropic HIV-1. *Vaccine* (2010) 28:B32–7. doi: 10.1016/j.vaccine.2009.10.154
17. Karpel ME, Boutwell CL, Allen TM. BLT humanized mice as a small animal model of HIV infection. *Curr Opin Virol* (2015) 13:75–80. doi: 10.1016/j.coviro.2015.05.002
18. Brainard DM, Seung E, Frahm N, Cariappa A, Bailey CC, Hart WK, et al. Induction of Robust Cellular and Humoral Virus-Specific Adaptive Immune Responses in Human Immunodeficiency Virus-Infected Humanized BLT Mice. *J Virol* (2009) 83:7305–21. doi: 10.1128/jvi.02207-08
19. Lan P, Tonomura N, Shimizu A, Wang S, Yang YG. Reconstitution of a functional human immune system in immunodeficient mice through combined human fetal thymus/liver and CD34+ cell transplantation. *Blood* (2006) 108:487–92. doi: 10.1182/blood-2005-11-4388
20. Smith DJ, Lin LJ, Moon H, Pham AT, Wang X, Liu S, et al. Propagating Humanized BLT Mice for the Study of Human Immunology and Immunotherapy. *Stem Cells Dev* (2016) 25:1863–73. doi: 10.1089/scd.2016.0193
21. Cheng L, Ma J, Li G, Su L. Humanized mice engrafted with human HSC only or HSC and thymus support comparable HIV-1 replication, immunopathology, and responses to ART and immune therapy. *Front Immunol* (2018) 9:817–3. doi: 10.3389/fimmu.2018.00817
22. Denton PW, Nochi T, Lim A, Krisko JF, Martinez-Torres F, Choudhary SK, et al. IL-2 receptor γ-chain molecule is critical for intestinal T-cell reconstitution in humanized mice. *Mucosal Immunol* (2012) 5:555–66. doi: 10.1038/mi.2012.31
23. Nochi T, Denton PW, Wahl A, Garcia JV. Cryptopatches Are Essential for the Development of Human GALT. *Cell Rep* (2013) 3:1874–84. doi: 10.1016/j.celrep.2013.05.037
24. Berges BK, Akkina SR, Folkvord JM, Connick E, Akkina R. Mucosal transmission of R5 and X4 tropic HIV-1 via vaginal and rectal routes in humanized Rag2-/-γc-/- (RAG-hu) mice. *Virology* (2008) 373:342–51. doi: 10.1016/j.virol.2007.11.020
25. Sango K, Joseph A, Patel M, Osiecki K, Dutta M, Goldstein H. Highly active antiretroviral therapy potently suppresses HIV infection in humanized Rag2-/-γc-/- mice. *AIDS Res Hum Retroviruses* (2010) 26:735–46. doi: 10.1089/aid.2009.0136
26. Jiang Q, Zhang L, Wang R, Jeffrey J, Washburn ML, Brouwer D, et al. FoxP3 +CD4+ regulatory T cells play an important role in acute HIV-1 infection in humanized Rag2-/-{gamma}C-/-mice in vivo. *Blood* (2008) 112:2858–68. doi: 10.1182/blood-2008-03-145946
27. Traggiai E, Chicha L, Mazzucchelli L, Bronz L, Piffaretti J-C, Lanzavecchia A, et al. Development of a Human Adaptive Immune System in Cord Blood Cell-Transplanted Mice. (2004) 304:104–7. doi: 10.1126/science.10939330
28. Watanabe Y, Takahashi T, Okajima A, Shiokawa M, Ishii N, Katano I, et al. The analysis of the functions of human B and T cells in humanized NOD/shi-scid/γcnull (NOG) mice (hu-HSC NOG mice). *Int Immunol* (2009) 21:843–58. doi: 10.1093/intimm/dxp050
29. Satheesan S, Li H, Burnett JC, Takahashi M, Li S, Wu SX, et al. HIV Replication and Latency in a Humanized NSG Mouse Model during Suppressive Oral Combinational Antiretroviral Therapy. *J Virol* (2018) 92: e02118–17. doi: 10.1128/jvi.02118-17
30. Xu SX, Leontyev D, Kaul R, Gray-Owen SD. Neisseria gonorrhoeae co-infection exacerbates vaginal HIV shedding without affecting systemic viral loads in human CD34+ engrafted mice. *PloS One* (2018) 13:e0191672. doi: 10.1371/journal.pone.0191672
31. Herndler-Brandstetter D, Shan L, Yao Y, Stecher C, Plajer V, Lietzenmayer M, et al. Humanized mouse model supports development, function, and tissue residency of human natural killer cells. *Proc Natl Acad Sci USA* (2017) 114:E9626–34. doi: 10.1073/pnas.1705301114
32. Denton PW, Estes JD, Sun Z, Othieno FA, Wei BL, Wege AK, et al. Antiretroviral Pre-exposure Prophylaxis Prevents Vaginal Transmission of HIV-1 in Humanized BLT Mice. *PloS Med* (2008) 5:e16. doi: 10.1371/journal.pmed.0050016
33. Sun Z, Denton PW, Estes JD, Othieno FA, Wei BL, Wege AK, et al. Intrarectal transmission, systemic infection, and CD4+ T cell depletion in humanized mice infected with HIV-1. *J Exp Med* (2007) 204:705–14. doi: 10.1084/jem.20062411
34. Danner R, Chaudhari SN, Rosenberger J, Surls J, Richie TL, Brumeanu TD, et al. Expression of HLA class II molecules in humanized NOD.Rag1KO.IL2RgcKO mice is critical for development and function of human T and B cells. *PloS One* (2011) 6:e19826. doi: 10.1371/journal.pone.0019826
35. Majji S, Wijayalath W, Shashikumar S, Pow-Sang L, Villasante E, Brumeanu TD, et al. Differential effect of HLA class-I versus class-II transgenes on human T and B cell reconstitution and function in NRG mice. *Sci Rep* (2016) 6:1–13. doi: 10.1038/srep28093
36. Allam A, Majji S, Peachman K, Jagodzinski L, Kim J, Ratto-Kim S, et al. TFH cells accumulate in mucosal tissues of humanized-DRAG mice and are highly permissive to HIV-1. *Sci Rep* (2015) 5:10443–16. doi: 10.1038/srep10443
37. Li Y, Masse-Ranson G, Garcia Z, Bruel T, Kök A, Strick-Marchand H, et al. A human immune system mouse model with robust lymph node development. *Nat Methods* (2018) 15:623–30. doi: 10.1038/s41592-018-0071-6
38. Masse-Ranson G, Dusséaux M, Fiquet O, Darche S, Boussand M, Li Y, et al. Accelerated thymopoiesis and improved T-cell responses in HLA-A2/-DR2 transgenic BRGS-based human immune system mice. *Eur J Immunol* (2019) 49:954–65. doi: 10.1002/eji.201848001
39. Brown ME, Zhou Y, McIntosh BE, Norman IG, Lou HE, Biermann M, et al. A Humanized Mouse Model Generated Using Surplus Neonatal Tissue. *Stem Cell Rep* (2018) 10:1175–83. doi: 10.1016/j.stemcr.2018.02.011
40. Ito R, Takahashi T, Katano I, Kawai K, Kamisako T, Ogura T, et al. Establishment of a Human Allergy Model Using Human IL-3/GM-CSF–Transgenic NOG Mice. *J Immunol* (2013) 191:2890–9. doi: 10.4049/jimmunol.1203543
41. Perdomo-Celis F, Medina-Moreno S, Davis H, Bryant J, Zapata JC. HIV Replication in Humanized IL-3/GM-CSF-Transgenic NOG Mice. *Pathogens* (2019) 8:33–16. doi: 10.3390/pathogens8010033
42. Yoshihara S, Li Y, Xia J, Danzl N, Sykes M, Yang YG. Posttransplant hemophagocytic lymphohistiocytosis driven by myeloid cytokines and vicious cycles of T-cell and macrophage activation in humanized mice. *Front Immunol* (2019) 10:186. doi: 10.3389/fimmu.2019.00186
43. Billerbeck E, Barry WT, Mu K, Dorner M, Rice CM, Ploss A. Development of human CD4+FoxP3+ regulatory T cells in human stem cell factor-, granulocyte-macrophage colony-stimulating factor-, and interleukin-3-expressing NOD-SCID IL2Rγnull humanized mice. *Blood* (2011) 117:3076–86. doi: 10.1182/blood-2010-08-301507
44. Wunderlichid M, Chouid F-S, Sexton C, Presicceid P, Chougnet CA, Aliberti J, et al. Improved multilineage human hematopoietic reconstitution and function in NSGS mice. *PLoS One* (2018) 13:e0209034. doi: 10.1371/journal.pone.0209034
45. Matsuda M, Ono R, Iyoda T, Endo T, Iwasaki M, Tomizawa-Murasawa M, et al. Human NK cell development in hIL-7 and hIL-15 knockin NOD/SCID/IL2rgKO mice. *Life Sci Alliance* (2019) 2:e201800195. doi: 10.26508/lsa.201800195
46. Rongvaux A, Willinger T, Martinek J, Strowig T, Gearty SV, Teichmann LL, et al. Development and function of human innate immune cells in a humanized mouse model HHS Public Access Author manuscript. *Nat Biotechnol* (2014) 32:364–72. doi: 10.1038/nbt.2858
47. Ivic S, Rochat M-A, Li D, Audigé A, Schlaepfer E, Münz C, et al. Differential Dynamics of HIV Infection in Humanized MISTRG versus MITRG Mice. *ImmunoHorizons* (2017) 1:162–75. doi: 10.4049/immunohorizons.1700042
48. Tonomura N, Habiro K, Shimizu A, Sykes M, Yang YG. Antigen-specific human T-cell responses and T cell-dependent production of human antibodies in a humanized mouse model. *Blood* (2008) 111:4293–6. doi: 10.1182/blood-2007-11-121319
49. Denton PW, García JV. Humanized mouse models of HIV infection. *AIDS Rev* (2011) 13:135–48.
50. Garcia V. Humanized mice for HIV and AIDS research. *Curr Opin Virol* (2016) 19:56–64. doi: 10.1016/j.coviro.2016.06.010

51. Watanabe S, Ohta S, Yajima M, Terashima K, Ito M, Mugishima H, et al. Humanized NOD/SCID/IL2R null Mice Transplanted with Hematopoietic Stem Cells under Nonmyeloablative Conditions Show Prolonged Life Spans and Allow Detailed Analysis of Human Immunodeficiency Virus Type 1 Pathogenesis. *J Virol* (2007) 81:13259–64. doi: 10.1128/jvi.01353-07
52. Nie C, Sato K, Misawa N, Kitayama H, Fujino H, Hiramatsu H, et al. Selective infection of CD4+ effector memory T lymphocytes leads to preferential depletion of memory T lymphocytes in R5 HIV-1-infected humanized NOD/SCID/IL-2Rγnull mice. *Virology* (2009) 394:64–72. doi: 10.1016/j.virol.2009.08.011
53. Gorantla S, Makarov E, Finke-Dwyer J, Gebhart CL, Domm W, Dewhurst S, et al. CD8 + Cell Depletion Accelerates HIV-1 Immunopathology in Humanized Mice. *J Immunol* (2010) 184:7082–91. doi: 10.4049/jimmunol.1000438
54. Kim KC, Choi BS, Kim KC, Park KH, Lee HJ, Cho YK, et al. A Simple Mouse Model for the Study of Human Immunodeficiency Virus. *AIDS Res Hum Retroviruses* (2016) 32:194–202. doi: 10.1089/aid.2015.0211
55. Nakano Y, Misawa N, Juarez-Fernandez G, Moriwaki M, Nakaoka S, Funo T, et al. HIV-1 competition experiments in humanized mice show that APOBEC3H imposes selective pressure and promotes virus adaptation. *PloS Pathog* (2017) 13:e1006348. doi: 10.1371/journal.ppat.1006348
56. Perez EE, Wang J, Miller JC, Jouvenot Y, Kim KA, Liu O, et al. Establishment of HIV-1 resistance in CD4+ T cells by genome editing using zinc-finger nucleases. *Nat Biotechnol* (2008) 26:808–16. doi: 10.1038/nbt1410
57. Sato K, Misawa N, Takeuchi JS, Kobayashi T, Izumi T, Aso H, et al. Experimental adaptive evolution of SIVcpz to pandemic HIV-1 using a humanized mouse model. *J Virol* (2017) 92:JVI.01905–17. doi: 10.1128/jvi.01905-17
58. Nischang M, Sutmuller R, Gers-Huber G, Audigé A, Li D, Rochat MA, et al. Humanized mice recapitulate key features of HIV-1 infection: A novel concept using long-acting anti-retroviral drugs for treating HIV-1. *PloS One* (2012) 7:e38853. doi: 10.1371/journal.pone.0038853
59. Rochat MA, Schlaepfer E, Kuster SP, Li D, Audige A, Ivic S, et al. Monitoring HIV DNA and cellular activation markers in HIV-infected humanized mice under cART. *Virol J* (2018) 15:191–8. doi: 10.1186/s12985-018-1101-9
60. Khamaikawin W, Shimizu S, Kamata M, Cortado R, Jung Y, Lam J, et al. Modeling Anti-HIV-1 HSPC-Based Gene Therapy in Humanized Mice Previously Infected with HIV-1. *Mol Ther - Methods Clin Dev* (2018) 9:23–32. doi: 10.1016/j.omtm.2017.11.008
61. Dash PK, Kaminski R, Bella R, Su H, Mathews S, Ahooyi TM, et al. Sequential LASER ART and CRISPR Treatments Eliminate HIV-1 in a Subset of Infected Humanized Mice. *Nat Commun* (2019) 10:2753–20. doi: 10.1038/s41467-019-10366-y
62. Law KM, Komarova NL, Yewdall AW, Lee RK, Herrera OL, Wodarz D, et al. In Vivo HIV-1 Cell-to-Cell Transmission Promotes Multicopy Micro-compartmentalized Infection. *Cell Rep* (2016) 15:2771–83. doi: 10.1016/j.celrep.2016.05.059
63. Su H, Cheng Y, Sravanam S, Mathews S, Gorantla S, Poluektova LY, et al. Immune Activations and Viral Tissue Compartmentalization During Progressive HIV-1 Infection of Humanized Mice. *Front Immunol* (2019) 10:340–17. doi: 10.3389/fimmu.2019.00340
64. Nguyen PV, Wessels JM, Mueller K, Vahedi F, Anipindi V, Verschoor CP, et al. Frequency of Human CD45+ Target Cells is a Key Determinant of Intravaginal HIV-1 Infection in Humanized Mice. *Sci Rep* (2017) 7:15263–15. doi: 10.1038/s41598-017-15630-z
65. Wessels JM, Lajoie J, Hay Cooper MIJ, Omollo K, Felker AM, Vitali D, et al. Medroxyprogesterone acetate alters the vaginal microbiota and microenvironment in women and increases susceptibility to HIV-1 in humanized mice. *DMM Dis Model Mech* (2019) 12:dmm039669. doi: 10.1242/dmm.039669
66. Goldman JP, Blundell MP, Lopes L, Kinnon C, DI Santo JP, Thrasher AJ. Enhanced human cell engraftment in mice deficient in RAG2 and the common cytokine receptor gamma chain. *Br J Haematol* (1998) 103:335–42. doi: 10.1046/j.1365-2141.1998.00980.x
67. Neff CP, Ndolo T, Tandon A, Habu Y, Akkina R. Oral Pre-Exposure Prophylaxis by Anti-Retrovirals Raltegravir and Maraviroc Protects against HIV-1 Vaginal Transmission in a Humanized Mouse Model. *PloS One* (2010) 5:e15257. doi: 10.1371/journal.pone.0015257
68. Choudhary SK, Rezk NL, Ince WL, Cheema M, Zhang L, Su L, et al. Suppression of Human Immunodeficiency Virus Type 1 (HIV-1) Viremia with Reverse Transcriptase and Integrase Inhibitors, CD4+ T-Cell Recovery, and Viral Rebound upon Interruption of Therapy in a New Model for HIV Treatment in the Humanized Rag2-/- c-/- Mouse. *J Virol* (2009) 83:8254–8. doi: 10.1128/jvi.00580-09
69. Schmitt K, Mohan Kumar D, Curlin J, Remling-Mulder L, Stenglein M, O'Connor S, et al. Modeling the evolution of SIV sooty mangabey progenitor virus towards HIV-2 using humanized mice. *Virology* (2017) 510:175–84. doi: 10.1016/j.virol.2017.07.005
70. Schmitt K, Curlin J, Remling-Mulder L, Moriarty R, Goff K, O'Connor S, et al. Cross-Species Transmission and Evolution of SIV Chimpanzee Progenitor Viruses Toward HIV-1 in Humanized Mice. *Front Microbiol* (2020) 11:1889:1889. doi: 10.3389/fmicb.2020.01889
71. Charlins P, Schmitt K, Remling-Mulder L, Hogan LE, Hanhauser E, Hobbs KS, et al. A humanized mouse-based HIV-1 viral outgrowth assay with higher sensitivity than in vitro qVOA in detecting latently infected cells from individuals on ART with undetectable viral loads. *Virology* (2017) 507:135–9. doi: 10.1016/j.virol.2017.04.011
72. Schmitt K, Akkina R. Ultra-sensitive HIV-1 latency viral outgrowth assays using humanized mice. *Front Immunol* (2018) 9:344. doi: 10.3389/fimmu.2018.00344
73. Veselinovic M, Yang KH, LeCureux J, Sykes C, Remling-Mulder L, Kashuba ADM, et al. HIV pre-exposure prophylaxis: Mucosal tissue drug distribution of RT inhibitor Tenofovir and entry inhibitor Maraviroc in a humanized mouse model. *Virology* (2014) 464–465:253–63. doi: 10.1016/j.virol.2014.07.008
74. Veselinovic M, Yang KH, Sykes C, Remling-Mulder L, Kashuba ADM, Akkina R. Mucosal tissue pharmacokinetics of the integrase inhibitor raltegravir in a humanized mouse model: Implications for HIV pre-exposure prophylaxis. *Virology* (2016) 489:173–8. doi: 10.1016/j.virol.2015.12.014
75. Neff CP, Kurisu T, Ndolo T, Fox K, Akkina R. A Topical Microbicide Gel Formulation of CCR5 Antagonist Maraviroc Prevents HIV-1 Vaginal Transmission in Humanized RAG-hu Mice. *PloS One* (2011) 6:e20209. doi: 10.1371/journal.pone.0020209
76. Veselinovic M, Preston Neff C, Mulder LR, Akkina R. Topical gel formulation of broadly neutralizing anti-HIV-1 monoclonal antibody VRC01 confers protection against HIV-1 vaginal challenge in a humanized mouse model. *Virology* (2012) 432:505–10. doi: 10.1016/j.virol.2012.06.025
77. Li G, Cheng M, Nunoya JI, Cheng L, Guo H, Yu H, et al. Plasmacytoid Dendritic Cells Suppress HIV-1 Replication but Contribute to HIV-1 Induced Immunopathogenesis in Humanized Mice. *PloS Pathog* (2014) 10:e1004291. doi: 10.1371/journal.ppat.1004291
78. Cheng L, Ma J, Li J, Li D, Li G, Li F, et al. Blocking type I interferon signaling enhances T cell recovery and reduces HIV-1 reservoirs. *J Clin Invest* (2017) 127:269–79. doi: 10.1172/JCI90745
79. Lu CL, Murakowski DK, Bournazos S, Schoofs T, Sarkar D, Halper-Stromberg A, et al. Enhanced clearance of HIV-1-infected cells by broadly neutralizing antibodies against HIV-1 in vivo. *Sci (80-)* (2016) 352:1001–4. doi: 10.1126/science.aaf1279
80. Abela IA, Berlinger L, Schanz M, Reynell L, Günthard HF, Rusert P, et al. Cell-cell transmission enables HIV-1 to evade inhibition by potent CD4bs directed antibodies. *PloS Pathog* (2012) 8:e1002634. doi: 10.1371/journal.ppat.1002634
81. Klein F, Halper-Stromberg A, Horwitz JA, Gruell H, Scheid JF, Bournazos S, et al. HIV therapy by a combination of broadly neutralizing antibodies in humanized mice. *Nature* (2012) 492:118–22. doi: 10.1038/nature11604
82. Bella R, Kaminski R, Mancuso P, Young WB, Chen C, Sariyer R, et al. Removal of HIV DNA by CRISPR from Patient Blood Engrafts in Humanized Mice. *Mol Ther - Nucleic Acids* (2018) 12:275–82. doi: 10.1016/j.omtn.2018.05.021
83. Cheng L, Yu H, Wrobel JA, Li G, Liu P, Hu Z, et al. Identification of pathogenic TRAIL-expressing innate immune cells during HIV-1 infection in humanized mice by scRNA-Seq. *JCI Insight* (2020) 5:e135344. doi: 10.1172/jci.insight.135344
84. Godot V, Tcherakian C, Gil L, Cervera-Marzal I, Li G, Cheng L, et al. TLR-9 agonist and CD40-targeting vaccination induces HIV-1 envelope-specific B cells with a diversified immunoglobulin repertoire in humanized mice. *PloS Pathog* (2020) 16:e1009025. doi: 10.1371/journal.ppat.1009025
85. Wahl A, Garcia V. The use of BLT humanized mice to investigate the immune reconstitution of the gastrointestinal tract. *J Immunol Methods* (2014) 410:28–33. doi: 10.1016/j.jim.2014.06.009

86. Skelton JK, Ortega-Prieto AM. Dorner M. A Hitchhiker's guide to humanized mice: new pathways to studying viral infections. *Immunology* (2018) 154:50–61. doi: 10.1111/imm.12906
87. Denton PW, Krisko JF, Powell DA, Mathias M, Kwak YT, Martinez-Torres F, et al. Systemic Administration of Antiretrovirals Prior to Exposure Prevents Rectal and Intravenous HIV-1 Transmission in Humanized BLT Mice. *PloS One* (2010) 5:e8829. doi: 10.1371/journal.pone.0008829
88. Kovarova M, Swanson MD, Sanchez RI, Baker CE, Steve J, Spagnuolo RA, et al. Victor Garcia J. A long-acting formulation of the integrase inhibitor raltegravir protects humanized BLT mice from repeated high-dose vaginal HIV challenges. *J Antimicrob Chemother* (2016) 71:1586–96. doi: 10.1093/jac/dkw042
89. Kovarova M, Benhabbour SR, Massud I, Spagnuolo RA, Skinner B, Baker CE, et al. Ultra-long-acting removable drug delivery system for HIV treatment and prevention. *Nat Commun* (2018) 9:4156–11. doi: 10.1038/s41467-018-06490-w
90. Shanmugasundaram U, Kovarova M, Ho PT, Schramm N, Wahl A, Parniak MA, et al. Efficient inhibition of HIV replication in the gastrointestinal and female reproductive tracts of humanized BLT mice by EFdA. *PloS One* (2016) 11:e0159517. doi: 10.1371/journal.pone.0159517
91. Chateau ML, Denton PW, Swanson MD, McGowan I, Garcia JV. Rectal Transmission of Transmitted/Founder HIV-1 Is Efficiently Prevented by Topical 1% Tenofovir in BLT Humanized Mice. *PloS One* (2013) 8:e60024. doi: 10.1371/journal.pone.0060024
92. Council OD, Swanson MD, Spagnuolo RA, Wahl A, Garcia JV. Role of semen on vaginal HIV-1 transmission and maraviroc protection. *Antimicrob Agents Chemother* (2015) 59:7847–51. doi: 10.1128/AAC.01496-15
93. Sun M, Li Y, Yuan Z, Lu W, Kang G, Fan W, et al. VRC01 antibody protects against vaginal and rectal transmission of human immunodeficiency virus 1 in hu-BLT mice. *Arch Virol* (2016) 161:2449–55. doi: 10.1007/s00705-016-2942-4
94. Balazs AB, Ouyang Y, Hong CM, Chen J, Nguyen SM, Rao DS, et al. Vectored immunoprophylaxis protects humanized mice from mucosal HIV transmission. *Nat Med* (2014) 20:296–300. doi: 10.1038/nm.3471
95. Yuan Z, Kang G, Ma F, Lu W, Fan W, Fennessey CM, et al. Recapitulating Cross-Species Transmission of Simian Immunodeficiency Virus SIVcpz to Humans by Using Humanized BLT Mice. *J Virol* (2016) 90:7728–39. doi: 10.1128/jvi.00860-16
96. Zhen A, Rezek V, Youn C, Lam B, Chang N, Rick J, et al. Targeting type I interferon-mediated activation restores immune function in chronic HIV infection. *J Clin Invest* (2017) 127:260–8. doi: 10.1172/JCI89488
97. Zhen A, Kamata M, Rezek V, Rick J, Levin B, Kasparian S, et al. HIV-specific Immunity Derived from Chimeric Antigen Receptor-engineered Stem Cells. *Mol Ther* (2015) 23:1358–67. doi: 10.1038/mt.2015.102
98. Maidji E, Moreno ME, Rivera JM, Joshi P, Galkina SA, Kosikova G, et al. Cellular HIV reservoirs and viral rebound from the lymphoid compartments of 40-Ethynyl-2-Fluoro-20-Deoxyadenosine (EFdA)-suppressed humanized mice. *Viruses* (2019) 11:256–27. doi: 10.3390/v11030256
99. Tsai P, Wu G, Baker CE, Thayer WO, Spagnuolo RA, Sanchez R, et al. In vivo analysis of the effect of panobinostat on cell-associated HIV RNA and DNA levels and latent HIV infection. *Retrovirology* (2016) 13:36–12. doi: 10.1186/s12977-016-0268-7
100. Claiborne DT, Dudek TE, Maldini CR, Power KA, Ghebremichael M, Seung E, et al. Immunization of BLT Humanized Mice Redirects T Cell Responses to Gag and Reduces Acute HIV-1 Viremia. *J Virol* (2019) 93:e00814–19. doi: 10.1128/jvi.00814-19
101. Norton TD, Zhen A, Tada T, Kim J, Kitchen S, Landau NR. Lentiviral Vector-Based Dendritic Cell Vaccine Suppresses HIV Replication in Humanized Mice. *Mol Ther* (2019) 27:960–73. doi: 10.1016/j.ymthe.2019.03.008
102. Cheng L, Wang Q, Li G, Banga R, Ma J, Yu H, et al. TLR3 agonist and CD40-targeting vaccination induces immune responses and reduces HIV-1 reservoirs. *J Clin Invest* (2018) 128:4387–96. doi: 10.1172/JCI99005
103. Haase AT. Targeting early infection to prevent HIV-1 mucosal transmission. *Nature* (2010) 464:217–23. doi: 10.1038/nature08757
104. Estes JD, Wong SW, Brenchley JM. Nonhuman primate models of human viral infections. *Nat Rev Immunol* (2018) 18:390–404. doi: 10.1038/s41577-018-0005-7
105. Brenchley JM, Douek DC. The mucosal barrier and immune activation in HIV pathogenesis. *Curr Opin HIV AIDS* (2008) 3:356–61. doi: 10.1097/COH.0b013e3282f9ae9c
106. Denton PW, Garcia JV. Mucosal HIV-1 transmission and prevention strategies in BLT humanized mice. *Trends Microbiol* (2012) 20:268–74. doi: 10.1016/j.tim.2012.03.007
107. Gallay PA, Chatterji U, Kirchhoff A, Gandarilla A, Pyles RB, Baum MM, et al. Protection Efficacy of C5A Against Vaginal and Rectal HIV Challenges in Humanized Mice. *Open Virol J* (2018) 12:1–13. doi: 10.2174/1874357901812010001
108. Gallay PA, Chatterji U, Kirchhoff A, Gandarilla A, Gunawardana M, Pyles RB, et al. Prevention of vaginal and rectal HIV transmission by antiretroviral combinations in humanized mice. *PloS One* (2017) 12:e0184303. doi: 10.1371/journal.pone.0184303
109. Wheeler LA, Vrbanac V, Trifonova R, Brehm MA, Gilboa-Geffen A, Tanno S, et al. Durable knockdown and protection from HIV transmission in humanized mice treated with gel-formulated CD4 aptamer-siRNA chimeras. *Mol Ther* (2013) 21:1378–89. doi: 10.1038/mt.2013.77
110. Denton PW, Othieno F, Martinez-Torres F, Zou W, Krisko JF, Fleming E, et al. One Percent Tenofovir Applied Topically to Humanized BLT Mice and Used According to the CAPRISA 004 Experimental Design Demonstrates Partial Protection from Vaginal HIV Infection, Validating the BLT Model for Evaluation of New Microbicide Candidates. *J Virol* (2011) 85:7582–93. doi: 10.1128/jvi.00537-11
111. Wheeler LA, Trifonova R, Vrbanac V, Basar E, McKernan S, Xu Z, et al. Inhibition of HIV transmission in human cervicovaginal explants and humanized mice using CD4 aptamer-siRNA chimeras. *J Clin Invest* (2011) 121:2401–12. doi: 10.1172/JCI45876
112. Destache CJ, Mandal S, Yuan Z, Kang G, Date AA, Lu W, et al. Topical tenofovir disoproxil fumarate nanoparticles prevent HIV-1 vaginal transmission in a humanized mouse model. *Antimicrob Agents Chemother* (2016) 60:3633–9. doi: 10.1128/AAC.00450-16
113. Farr Zuend C, Nomellini JF, Smit J, Horwitz MS. A Caulobacter crescentus Microbicide Protects from Vaginal Infection with HIV-1 JR-CSF in Humanized Bone Marrow-Liver-Thymus Mice. *J Virol* (2019) 93:e00614–19. doi: 10.1128/jvi.00614-19
114. Kovarova M, Council OD, Date AA, Long JM, Nochii T, Belshan M, et al. Nanoformulations of Rilpivirine for Topical Pericoital and Systemic Coitus-Independent Administration Efficiently Prevent HIV Transmission. *PloS Pathog* (2015) 11:e1005075–e1005075. doi: 10.1371/journal.ppat.1005075
115. Melody K, Roy CN, Kline C, Cottrell ML, Evans D, Shutt K, et al. Long-Acting Rilpivirine (RPV) Preexposure Prophylaxis Does Not Inhibit Vaginal Transmission of RPV-Resistant HIV-1 or Select for High-Frequency Drug Resistance in Humanized Mice. *J Virol* (2020) 94:1912–31. doi: 10.1128/jvi.01912-19
116. Sepúlveda-Crespo D, Serramía MJ, Tager AM, Vrbanac V, Gómez R, De La Mata FJ, et al. Prevention vaginally of HIV-1 transmission in humanized BLT mice and mode of antiviral action of polyanionic carbosilane dendrimer G2-S16. *Nanomed Nanotechnol Biol Med* (2015) 11:1299–308. doi: 10.1016/j.nano.2015.04.013
117. Mandal S, Prathipati PK, Kang G, Zhou Y, Yuan Z, Fan W, et al. Tenofovir alafenamide and elvitegravir loaded nanoparticles for long-acting prevention of HIV-1 vaginal transmission. *AIDS* (2017) 31:469–76. doi: 10.1097/QAD.0000000000001349
118. Ferreira VH, Kafka JK, Kaushic C. Influence of Common Mucosal Co-Factors on HIV Infection in the Female Genital Tract. *Am J Reprod Immunol* (2014) 71:543–54. doi: 10.1111/aji.12221
119. Gosmann C, Anahtar MN, Handley SA, Farcasanu M, Abu-Ali G, Bowman BA, et al. Lactobacillus-Deficient Cervicovaginal Bacterial Communities Are Associated with Increased HIV Acquisition in Young South African Women. *Immunity* (2017) 46:29–37. doi: 10.1016/j.immuni.2016.12.013
120. Daharsh L, Zhang J, Ramer-Tait A, Li Q. A double humanized blt-mice model featuring a stable human-like gut microbiome and human immune system. *J Vis Exp* (2019) 150:e59773. doi: 10.3791/59773
121. Park JC, Im SH. Of men in mice: the development and application of a humanized gnotobiotic mouse model for microbiome therapeutics. *Exp Mol Med* (2020) 52:1383–96. doi: 10.1038/s12276-020-0473-2
122. McHugh D, Myburgh R, Caduff N, Spohn M, Kok YL, Keller CW, et al. EBV renders B cells susceptible to HIV-1 in humanized mice. *Life Sci Alliance* (2020) 3:e202000640. doi: 10.26508/LSA.202000640
123. Pawlowski A, Jansson M, Sköld M, Rottenberg ME, Källenius G. Tuberculosis and HIV co-infection. *PloS Pathog* (2012) 8:e1002464. doi: 10.1371/journal.ppat.1002464

124. Huante MB, Nusbaum RJ, Endsley JJ. "Co-Infection with TB and HIV: Converging Epidemics, Clinical Challenges, and Microbial Synergy," in *Tuberculosis Host-Pathogen Interactions*, eds. J. D. Cirillo, Y. Kong. (Cham: Springer International Publishing), p. 123–53. doi: 10.1007/978-3-030-25381-3_7
125. Orme IM, Basaraba RJ. The formation of the granuloma in tuberculosis infection. *Semin Immunol* (2014) 26:601–9. doi: 10.1016/j.smim.2014.09.009
126. Smith CM, Proulx MK, Olive AJ, Laddy D, Mishra BB, Moss C, et al. Tuberculosis Susceptibility and Vaccine Protection Are Independently Controlled by Host Genotype. (2016) 7:e01516–16. doi: 10.1128/mBio.01516-16
127. Heuts F, Gavier-Widén D, Carow B, Juarez J, Wigzell H, Rottenberg ME. CD4+ cell-dependent granuloma formation in humanized mice infected with mycobacteria. *Proc Natl Acad Sci USA* (2013) 110:6482–7. doi: 10.1073/pnas.1219985110
128. Arrey F, Löwe D, Kuhlmann S, Kaiser P, Moura-Alves P, Krishnamoorthy G, et al. Humanized Mouse Model Mimicking Pathology of Human Tuberculosis for in vivo Evaluation of Drug Regimens. *Front Immunol* (2019) 10:89–12. doi: 10.3389/fimmu.2019.00089
129. Calderon VE, Valbuena G, Goez Y, Judy BM, Huante MB, Sutjita P, et al. A Humanized Mouse Model of Tuberculosis. *PloS One* (2013) 8:e63331. doi: 10.1371/journal.pone.0063331
130. Nusbaum RJ, Calderon VE, Huante MB, Sutjita P, Vijayakumar S, Lancaster KL, et al. Pulmonary Tuberculosis in Humanized Mice Infected with HIV-1. *Sci Rep* (2016) 6:21522–11. doi: 10.1038/srep21522
131. Huante MB, Saito TB, Nusbaum RJ, Naqvi KF, Chauhan S, Hunter RL, et al. Small Animal Model of Post-chemotherapy Tuberculosis Relapse in the Setting of HIV Co-infection. *Front Cell Infect Microbiol* (2020) 10:150:150. doi: 10.3389/fcimb.2020.00150
132. Greenblatt MB, Vbranac V, Tivey T, Tsang K, Tager AM, Aliprantis AO. Graft versus Host Disease in the Bone Marrow, Liver and Thymus Humanized Mouse Model. *PloS One* (2012) 7:e44664. doi: 10.1371/journal.pone.0044664
133. Lockridge JL, Zhou Y, Becker YA, Ma S, Kenney SC, Hematti P, et al. Mice engrafted with human fetal thymic tissue and hematopoietic stem cells develop pathology resembling chronic graft-versus-host disease. *Biol Blood Marrow Transplant* (2013) 19:1310–22. doi: 10.1016/j.bbmt.2013.06.007
134. Lavender KJ, Pang WW, Messer RJ, Duley AK, Race B, Phillips K, et al. BLT-humanized C57BL/6 Rag2-/-γc-/-CD47-/- mice are resistant to GVHD and develop B- and T-cell immunity to HIV infection. *Blood* (2013) 122:4013–20. doi: 10.1182/blood-2013-06-506949
135. Lavender KJ, Pace C, Sutter K, Messer RJ, Pouncey DL, Cummins NW, et al. An advanced BLT-humanized mouse model for extended HIV-1 cure studies. *AIDS* (2018) 32:1–10. doi: 10.1097/QAD.0000000000001674
136. Villaudy J, Schotte R, Legrand N, Spits H. Critical assessment of human antibody generation in humanized mouse models. *J Immunol Methods* (2014) 410:18–27. doi: 10.1016/j.jim.2014.06.010
137. McCune JM, Weissman IL. The Ban on US Government Funding Research Using Human Fetal Tissues: How Does This Fit with the NIH Mission to Advance Medical Science for the Benefit of the Citizenry? *Stem Cell Rep* (2019) 13:777–86. doi: 10.1016/j.stemcr.2019.10.003
138. McIntosh BE, Brown ME. No irradiation required: The future of humanized immune system modeling in murine hosts. *Chimerism* (2015) 6:40–5. doi: 10.1080/19381956.2016.1162360
139. Cosgun KN, Rahmig S, Mende N, Reinke S, Hauber I, Schäfer C, et al. Kit regulates HSC engraftment across the human-mouse species barrier. *Cell Stem Cell* (2014) 15:227–38. doi: 10.1016/j.stem.2014.06.001
140. Shultz LD, Saito Y, Najima Y, Tanaka S, Ochi T, Tomizawa M, et al. Generation of functional human T-cell subsets with HLA-restricted immune responses in HLA class I expressing NOD/SCID/IL2rγnull humanized mice. *Proc Natl Acad Sci USA* (2010) 107:13022–7. doi: 10.1073/pnas.1000475107
141. Patton J, Vuyyuru R, Siglin A, Root M, Manser T. Evaluation of the efficiency of human immune system reconstitution in NSG mice and NSG mice containing a human HLA.A2 transgene using hematopoietic stem cells purified from different sources. *J Immunol Methods* (2015) 422:13–21. doi: 10.1016/j.jim.2015.02.007
142. Suzuki M, Takahashi T, Katano I, Ito R, Ito M, Harigae H, et al. Induction of human humoral immune responses in a novel HLA-DR-expressing transgenic NOD/Shi-scid/γc null mouse. *Int Immunol* (2012) 24:243–52. doi: 10.1093/intimm/dxs045
143. Covassin L, Laning J, Abdi R, Langevin DL, Phillips NE, Shultz LD, et al. Human peripheral blood CD4 T cell-engrafted non-obese diabetic-scid IL2rγ null H2-Ab1 tm1Gru Tg (human leucocyte antigen D-related 4) mice: A mouse model of human allogeneic graft-versus-host disease. *Clin Exp Immunol* (2011) 166:269–80. doi: 10.1111/j.1365-2249.2011.04462.x
144. Agarwal Y, Beatty C, Biradar S, Castronova I, Ho S, Melody K, et al. Moving beyond the mousetrap: Current and emerging humanized mouse and rat models for investigating prevention and cure strategies against HIV infection and associated pathologies. *Retrovirology* (2020) 17:1–11. doi: 10.1186/s12977-020-00515-3
145. Legrand N, Huntington ND, Nagasawa M, Bakker AQ, Schotte R, Strick-Marchand H, et al. Functional CD47/signal regulatory protein alpha (SIRPα) interaction is required for optimal human T- and natural killer- (NK) cell homeostasis in vivo. *Proc Natl Acad Sci USA* (2011) 108:13224–9. doi: 10.1073/pnas.1101398108
146. Allam A, Peachman KK, Aguilera-Olvera R, Casares S, Rao M. Isolation of human lymphocytes with high yield and viability from the gastrointestinal and female reproductive tract of a humanized DRAG mouse. *J Immunol Methods* (2018) 454:40–7. doi: 10.1016/j.jim.2017.12.004
147. Mendoza M, Ballesteros A, Qiu Q, Pow Sang L, Shashikumar S, Casares S, et al. Generation and testing anti-influenza human monoclonal antibodies in a new humanized mouse model (DRAGA: HLA-A2. HLA-DR4. Rag1 KO. IL-2Rγc KO. NOD). *Hum Vaccines Immunother* (2018) 14:345–60. doi: 10.1080/21645515.2017.1403703
148. Mendoza M, Gunasekera D, Pratt KP, Qiu Q, Casares S, Brumeanu TD. The humanized DRAGA mouse (HLA-A2. HLA-DR4. RAG1 KO. IL-2R g c KO. NOD) establishes inducible and transmissible models for influenza type A infections. *Hum Vaccines Immunother* (2020) 16:2222–37. doi: 10.1080/21645515.2020.1713605
149. Yi G, Xu X, Abraham S, Petersen S, Guo H, Ortega N, et al. Manjunath N. A DNA Vaccine Protects Human Immune Cells against Zika Virus Infection in Humanized Mice. *EBioMedicine* (2017) 25:87–94. doi: 10.1016/j.ebiom.2017.10.006
150. Gille C, Orlikowsky TW, Spring B, Hartwig UF, Wilhelm A, Wirth A, et al. Monocytes derived from humanized neonatal NOD/SCID/IL2Rγ null mice are phenotypically immature and exhibit functional impairments. *Hum Immunol* (2012) 73:346–54. doi: 10.1016/j.humimm.2012.01.006
151. Li Y, Chen Q, Zheng D, Yin L, Chionh YH, Wong LH, et al. Induction of Functional Human Macrophages from Bone Marrow Promonocytes by M-CSF in Humanized Mice. *J Immunol* (2013) 191:3192–9. doi: 10.4049/jimmunol.1300742
152. Audigé A, Rochat MA, Li D, Ivic S, Fahrny A, Muller CKS, et al. Long-term leukocyte reconstitution in NSG mice transplanted with human cord blood hematopoietic stem and progenitor cells. *BMC Immunol* (2017) 18:28. doi: 10.1186/s12865-017-0209-9

Conflict of Interest: The authors declare that the research was conducted in the absence of any commercial or financial relationships that could be construed as a potential conflict of interest.

frontiers in Immunology

ORIGINAL RESEARCH
published: 18 March 2021
doi: 10.3389/fimmu.2021.651515

Humanized Mice Exhibit Exacerbated Abscess Formation and Osteolysis During the Establishment of Implant-Associated *Staphylococcus aureus* Osteomyelitis

Gowrishankar Muthukrishnan[1], Alexandra Wallimann[2,3†], Javier Rangel-Moreno[4†], Karen L. de Mesy Bentley[1,5], Maria Hildebrand[2], Karen Mys[2], H. Mark Kenney[1], Eric T. Sumrall[2], John L. Daiss[1], Stephan Zeiter[2], R. Geoff Richards[2], Edward M. Schwarz[1,4] and T. Fintan Moriarty[2]*

[1] Center for Musculoskeletal Research, Department of Orthopaedics and Rehabilitation, University of Rochester Medical Center, Rochester, NY, United States, [2] AO Research Institute Davos, Davos, Switzerland, [3] Swiss Institute of Allergy and Asthma Research (SIAF), University of Zurich, Davos, Switzerland, [4] Division of Allergy, Immunology and Rheumatology, Department of Medicine, University of Rochester Medical Center, Rochester, NY, United States, [5] Department of Pathology and Laboratory Medicine, University of Rochester Medical Center, Rochester, NY, United States

Staphylococcus aureus is the predominant pathogen causing osteomyelitis. Unfortunately, no immunotherapy exists to treat these very challenging and costly infections despite decades of research, and numerous vaccine failures in clinical trials. This lack of success can partially be attributed to an overreliance on murine models where the immune correlates of protection often diverge from that of humans. Moreover, *S. aureus* secretes numerous immunotoxins with unique tropism to human leukocytes, which compromises the targeting of immune cells in murine models. To study the response of human immune cells during chronic *S. aureus* bone infections, we engrafted non-obese diabetic (NOD)–*scid* IL2Rγ^{null} (NSG) mice with human hematopoietic stem cells (huNSG) and analyzed protection in an established model of implant-associated osteomyelitis. The results showed that huNSG mice have increases in weight loss, osteolysis, bacterial dissemination to internal organs, and numbers of Staphylococcal abscess communities (SACs), during the establishment of implant-associated MRSA osteomyelitis compared to NSG controls ($p < 0.05$). Flow cytometry and immunohistochemistry demonstrated greater human T cell numbers in infected versus uninfected huNSG mice ($p < 0.05$), and that T-bet^{+} human T cells clustered around the SACs, suggesting *S. aureus*-mediated activation and proliferation of human T cells in the infected bone. Collectively, these proof-of-concept studies underscore the

OPEN ACCESS

Edited by:
*Qingfeng Chen, Institute of Molecular and Cell Biology (A*STAR), Singapore*

Reviewed by:
George Liu, University of California, San Diego, United States
Larisa Y. Poluektova, University of Nebraska Medical Center, United States
Lorena Tuchscherr, Jena University Hospital, Germany

***Correspondence:**
Gowrishankar Muthukrishnan
gowri_shankar@urmc.rochester.edu

†These authors have contributed equally to this work

Specialty section:
This article was submitted to Microbial Immunology, a section of the journal Frontiers in Immunology

Received: *10 January 2021*
Accepted: *02 March 2021*
Published: *18 March 2021*

Citation:
Muthukrishnan G, Wallimann A, Rangel-Moreno J, Bentley KLdM, Hildebrand M, Mys K, Kenney HM, Sumrall ET, Daiss JL, Zeiter S, Richards RG, Schwarz EM and Moriarty TF (2021) Humanized Mice Exhibit Exacerbated Abscess Formation and Osteolysis During the Establishment of Implant-Associated Staphylococcus aureus Osteomyelitis. Front. Immunol. 12:651515. doi: 10.3389/fimmu.2021.651515

utility of huNSG mice for studying an aggressive form of *S. aureus* osteomyelitis, which is more akin to that seen in humans. We have also established an experimental system to investigate the contribution of specific human T cells in controlling *S. aureus* infection and dissemination.

Keywords: humanized mice, *Staphylococcus aureus*, bone infection, osteolysis, staphylococcal abscess communities, T cells

INTRODUCTION

Bone infections, a debilitating complication of total joint replacement (TJR) arthroplasties and fracture fixation, have dramatically increased over the past decade in the United States alone (1–3). *Staphylococcus aureus*, a significant human pathogen, remains the leading cause of bone infections in TJR surgeries, causing 30-42% of fracture-related infections (FRI), and 10,000-20,000 peri-prosthetic joint infections (PJI) in patients each year in the US (4–7). Methicillin-resistant *S. aureus* (MRSA) and newly emerging strains with pan-resistance significantly complicate treatment leading to adverse clinical outcomes such as amputation and septic death (8, 9).

There is an urgent need to control these deep bone infections utilizing non-antibiotic interventions. Unfortunately, no preventative *S. aureus* immunotherapies exist, despite almost 20 years of research to identify conceptually promising vaccine targets and significant money spent on clinical trials (10–12). Poor antigen selection and the ability of *S. aureus* to evade the human immune system might contribute to the failure of vaccines. Alternatively, the lack of relevant models that recapitulate human immune responses could explain the failure of these trials.

Murine models have greatly facilitated our understanding of *S. aureus* pathogenesis and identified critical virulence factors such as staphylococcal protein A, iron-scavenging proteins, fibrinogen binding proteins, penicillin-binding proteins, hemolysins, autolysins, etc. (13–23). However, the knowledge acquired using these murine models does not necessarily translate into these targets becoming useful vaccine candidates in humans. A prominent case in point is the murine preclinical data of an immunogenic vaccine candidate from iron-scavenging protein IsdB (IsdB-V710) that demonstrated reduced infection lethality, and protection against bacteremia in mice (24–27). Unfortunately, a large phase IIb/III vaccination clinical trial based on these preclinical studies involving ~8,000 patients failed to provide any protection and elevated the risk of adverse outcomes, including death, among patients who encountered post-immunization *S. aureus* infections (28). Therefore, we are in dire need of small animal models that can better mimic the human immune system. Moreover, *S. aureus* is a significant human pathogen with several virulence proteins and bicomponent toxins with high degrees of tropism to receptors expressed on human leukocytes (29, 30). Due to these human-specific toxins, it is possible that this pathogen does not necessarily exhibit their typical phenotype in murine *S. aureus* infections.

Non-obese diabetic (NOD)–*scid* IL2Rγ^{null} (NSG) mice, reconstituted with human CD34+ hematopoietic immune system (huNSG), have emerged as a powerful model system to investigate human disease (31–33). These mice evoke a human immune response to infection and have been utilized to study bacterial and viral pathogens such as *Salmonella*, *Leishmania*, HIV, and EBV (34–39). The use of humanized mice to study *S. aureus* infections remains relatively limited (40–42), and until now, no studies have described *S. aureus* pathogenesis during osteomyelitis in humanized mice. To this end, we developed a transtibial implant-associated *S. aureus* osteomyelitis model in humanized NSG mice and examined if *S. aureus* induces a human immune response in these mice during bone infection. Additionally, we also assessed infection severity, the extent of bone osteolysis, and Staphylococcal abscess communities (SAC) formation during the establishment of implant-associated MRSA osteomyelitis.

MATERIALS AND METHODS

Ethics Statement

Animal studies were performed according to protocols approved by the ethical committee of the canton of Grisons in Switzerland. Animal surgical procedures were performed according to Swiss animal protection law and regulations in an Association for Assessment and Accreditation of Laboratory Animal Care (AAALAC) International approved facility.

Murine Implant-Associated Osteomyelitis Model

Female C57BL/6J mice (stock 000664), NSG (NOD.Cg-Prkdc^{scid} Il2rg^{tm1Wjl}/SzJ, stock 005557) mice were purchased from the Jackson Laboratories (Bar Harbor, ME, USA), housed five per cage in two-way housing on a 12-h light/dark cycle, and fed a maintenance diet and water *ad libitum*. Humanized NSG (huNSG) mice were generated by Jackson Labs by engrafting NSG mice with CD34+ human hematopoietic cells from three different donors using protocols described previously (31, 32). Briefly, 3-week old NSG mice were subjected to total body irradiation (100 cGy) and injected intravenously with lineage negative human CD34$^+$ hematopoietic stem cells (2 x 10^5 cells/mice) isolated of cord blood. At 12 weeks post engraftment, mice were subjected to submandibular bleeding to isolate peripheral lymphocytes and human immune cell reconstitution was assessed in huNSG mice by flow cytometry (markers: anti-human CD45 - overall reconstitution, anti-human CD3 – T cells,

anti-human CD20 – B cells, anti-human CD33 – myeloid cells). **Supplemental Table 1** describes the percentage of human CD45 + cells, human B cells, T cells, and myeloid cells engrafted in huNSG mice generated from all different donors. Transtibial implant-associated osteomyelitis with MRSA was performed on skeletally mature 20–24-week-old huNSG mice, and age-matched C57BL/J6 and NSG mice utilizing our well-validated protocols described previously (22, 43, 44). Briefly, mice were anesthetized with Sevoflurane in a Plexiglass box (ca. 7% in O2, flow rate 0.6-1 L/min), maintained with Sevoflurane through a face mask (ca. 2-3% in O2, flow rate 0.6-1 L/min). Peri- and postoperative analgesia consisted of Tramal, which was added to the drinking water 24h prior to surgery (25mg/L) and maintained for two days after surgery to minimize skin wounds from injections and at the same time provide adequate analgesia. Before surgery, a flat stainless-steel surgical wire (cross-section, 0.2 mm by 0.5 mm) 4 mm long (MicroDyne Technologies, Plainville, CT, USA) bent at 1mm to form an L-shape was steam sterilized and inoculated with clinical *S. aureus* USA300 LAC strain grown overnight. After anesthesia induction, the right leg was clipped, and the skin was aseptically prepared with chlorhexidine scrub (Hibiscrub, 4% Chlorhexidine Digluconate) and 70% ethanol. The implant localization was identified (2 to 3 mm under the tibial plateau in the proximal tibia) using the proximal patella as an anatomical landmark and the jaws of the Mayo-Hegar needle driver as the measure. A hole was pre-drilled in the proximal tibia using a percutaneous approach from the medial to lateral cortex using a 26-gauge needle. Subsequently, a *S. aureus* infected pin (5.0×10^5 colony forming units (CFU)/mL) was surgically implanted in the pre-drilled hole from the medial to the lateral cortex. Osteotomy and implant position were confirmed radiographically in the lateral plane immediately after surgery. At 14 days post-infection, mice were euthanized, and the infected leg containing the transtibial implant was excised out for either CFU quantitation or high-resolution micro-computed tomography (μCT) imaging, followed by histology and transmission electron microscopy (TEM). Additionally, internal organs liver, spleen, kidneys, and heart were harvested sterilely for CFU enumeration. Further, all mice were subjected to submandibular bleeding on days 0, 7, and 14 post-infection to collect serum for assessing anti-*S. aureus* antibodies. Murine infection studies were performed four independent times and the results shown are pooled data from these experiments.

Bacteriology

Tibia, tibial implant, and the soft tissue abscesses surrounding the tibia were removed, weighed, and placed in 1mL of room temperature sterile PBS. The implant was sonicated for 2 min to dislodge attached bacteria, and organ tissues were homogenized (Omni TH, tissue homogenizer TH-02/TH21649, Kennesaw, GA, USA) in 1mL of PBS. Implant sonicate fluid and tissue homogenates were serially diluted, plated on blood agar (BA) plates, and incubated overnight at 37°C. To confirm *S. aureus* on the plates, random colonies from each plate/organ/tissue were picked, and StaphLatex agglutination test (Thermo Fisher Scientific, Waltham, MA, USA) was performed. Bacterial colonies were enumerated, and the generated CFU data were presented as CFUs per gram of tissue.

Micro-Computed Tomography (μCT)

The tibia was dissected from mice post-euthanasia and fixed for 72 hours in 4% neutral buffered formalin. Subsequently, specimens were rinsed in PBS, deionized water, and prepared for μCT scans. High-resolution μCT scans of the mice tibia receiving MRSA-contaminated or sterile pin were imaged ex vivo at 10.5 μm voxel size with the VivaCT40 (Scanco Medical AG, Switzerland), using 100 ms integration time, energy of 70 kV, and intensity of 114 μA. Post-processing and analyses of the resultant DICOM files generated from VivaCT40 were performed on Amira software (FEI Visualization Sciences Group; Burlington, MA, USA). Medial and Lateral hole volume quantification was performed by manual segmentation of the void area followed by a point trap triangulation in Amira. Reactive bone volume was also computed using methods described previously by Mys et al. (45). Briefly, the bone was segmented using adaptive thresholding techniques and masks described previously (45). Then, the thickness of all bone structures was calculated in IPL software (Scanco Medical AG, Switzerland), and all the bone structures thicker than 6 voxels (63.0μm) were assigned to be cortex. The reactive bone was calculated by subtracting the quantified outer mask from the cortex. Thresholding was set at 10 voxels to clean the reactive bone masks. The reactive bone volume calculations were performed only on the distal side of the pin to minimize the influence of the pin's position on the results.

Histology

Following μCT, each mouse tibia was rinsed with ddH2O and decalcified in 14% EDTA tetrasodium solution for 7 days, with radiographical monitoring of the decalcification progress. Following decalcification, samples were paraffin-embedded, cut into 5 μm transverse sections, and mounted on glass slides for histological staining. Slides were deparaffinized and stained with Hematoxylin & Eosin (H&E) and Brown and Brenn (Gram) staining as described previously (43, 46). Digital images of the stained slides were created using VS120 Virtual Slide Microscope (Olympus, Waltham, MA, USA). Numbers SACs were manually enumerated and averaged across two or more histologic sections at least 50 μm apart from 6-7 mice in each experimental group. Quantitative analysis of SAC area within the tibias of C57BL/6J WT, NSG, and huNSG animals was performed on Brown and Brenn (Gram) stained slides using Visiopharm (v.2019.07; Hoersholm, Denmark) colorimetric histomorphometry utilizing a custom Analysis Protocol Package (APP). Manual regions-of-interest (ROIs) were drawn around the tibia and SACs within the tibia on each image prior to batch processing for automated quantification of SAC area normalized to tibial area between the groups.

Multicolor Immunofluorescence

Primary antibodies: The following antibodies were utilized for immunostaining: Goat anti-CD3ε (Clone M-20, Santa Cruz Biotechnology, Dallas, TX, USA, RRID : AB_631128), goat

anti-proliferating cell nuclear antigen (Clone C-20, Santa Cruz Biotechnology) at 1:100 dilution, Rabbit anti-human CD20 at 1:50 dilution (LS-B2605-125, LifeSpan Biosciences, Seattle, WA, USA, RRID : AB_10439766), biotin rat anti-mouse Ly6G at 1:50 dilution (Clone 1A8, BioLegend, Austin, TX, USA, RRID : AB_1186108), rabbit anti-Tbet at 1:50 dilution (clone H-210, Santa Cruz Biotechnology), and monoclonal mouse anti-human RORγT at 1:50 dilution (clone 6F3.1, EMDMilipore, Burlington, MA, USA, RRID : AB_11205416). *Secondary antibodies:* All secondary antibodies were used at 1: 200 dilution. These include Alexa Fluor 568 donkey anti-goat IgG (A-11057, Thermo Fisher Scientific, RRID : AB_2534104), Alexa fluor 488 donkey anti-rabbit IgG (711-546-152, Thermo Fisher Scientific, RRID : AB_2340619), Alexa fluor 647 donkey anti-rat IgG (712-606-153, Jackson ImmunoResearch Laboratories, West Grove, PA, USA, RRID : AB2340865), Alexa fluor 647 donkey anti-mouse IgG (715-606-150, Jackson ImmunoResearch Laboratories, RRID : AB2340865), and Alexa Fluor 680 Streptavidin at 1:200 dilution (S32358, Thermo Fisher Scientific).

The 5 μm formalin-fixed paraffin sections were incubated at 60°C overnight for deparaffinization. Tissue sections were quickly transferred to xylene and gradually hydrated by transferring slides to absolute alcohol, 96% alcohol, 70% alcohol, and then water. Slides were immersed in an antigen retrieval solution, boiled for 30 minutes, and cooled down for 10 minutes at room temperature (RT). Slides were rinsed several times in water and transferred to PBS. Non-specific binding was blocked with 5% normal donkey serum in PBS containing 0.1% Tween 20, 0.1% Triton-X-100 for 30 minutes, at RT in a humid chamber. Primary antibodies were added to slides and incubated in a humid chamber at RT, ON. Slides were quickly washed in PBS, and fluorescently labeled secondary antibodies were incubated for 2 hours at RT overnight in a humid chamber. Finally, slides were rinsed for 1 hour in PBS and mounted with Vectashield antifade mounting media with DAPI (H-1200, Vector Laboratories, Burlingame, CA, USA). Pictures were taken with a Zeiss Axioplan 2 microscope and recorded with a Hamamatsu camera.

Transmission Electron Microscopy (TEM)

Brown and Brenn staining was performed to identify SAC presence within the intramedullary canal of MRSA-infected huNSG mice. Once a SAC was identified, the paraffin block was oriented to match the 5 μm section of the Brown and Brenn slide, in order to excise the precise area from the paraffin block. Once the right area was excised, the block was deparaffinized, post-fixed sequentially in 2.5% glutaraldehyde (24 hours) and 1.0% osmium tetroxide (90 minutes), dehydrated in a graded series of ethanol to 100%, transitioned into propylene oxide, infiltrated with EPON/Araldite epoxy resin and finally embedded block face down into a BEEM capsule lid for 48 hours at 60°C. The block was sectioned at one micron and stained with Toluidine blue to confirm the SAC location, then thin sectioned at 70 nm using a diamond knife and an ultramicrotome. The thin sections were mounted onto formvar carbon coated nickel slot grids, then examined using a Hitachi 7650 transmission electron microscope, and images were captured using Gatan Erlangshen 11-megapixel digital camera and DigitalMicrograph software.

Flow Cytometry

Immunophenotyping of spleen from huNSG mice was performed according to protocols described previously (47). Briefly, single-cell suspension of splenocytes were prepared, and 0.5 X 10^6 cells/mice were initially stained with fixable viability dye eFluor™ 780 (eBioscience™, Thermo Fisher Scientific) for 30 minutes at 4° C to exclude dead cells from the analysis. Following washing, the following fluorochrome-conjugated anti-human antibodies were used for phenotyping huNSG splenocytes: BV510 CD45 (clone 2D1), PerCP CD3 (clone UCHT1), PE-Dazzle 594 CD8a (clone HIT8a), FITC CD4 (clone OKT4), PE-Cy5 CD19 (clone SJ25C1), and PE CD56 (clone HCD56). Single channel compensation controls for these antibodies were created using human polymorphonuclear cells (PMBCs). All antibodies were purchased either from BioLegend or BD Biosciences (San Jose, CA, USA). After staining, the cells were fixed with 2% formaldehyde/PBS prior to running on a BD FACSAria™ III multicolor flow cytometer (BD Biosciences). Flow data were analyzed using FlowJo version 10.6 (BD Biosciences), and the gating strategies are outlined in **Supplemental Figure S1**.

Serum Cytokine and Anti-Human Cytokine and Antibody Measurements

HuNSG mice infected with either a sterile (Sham) or *S. aureus* contaminated tibial implant were bled submandibularly to collect serum samples PreOP, at day 7 and day 14 post infection as allowed under the Swiss animal protection regulations, and the protocols approved by the ethical committee of the canton of Grisons in Switzerland. Serum cytokine analyses was performed using a 25-plex MILLIPLEX® xMAP Human cytokine Magnetic Bead Panel for the following cytokines according to manufacturer's instructions: GM-CSF, IFN-γ, IL-1β, IL-2, IL-4, IL-5, IL-6, IL-9, IL-10, IL-12 (p70), IL-13, IL-15, IL-17A, IL-17F, IL-17E/IL-25, IL-21, IL-22, IL-23, IL-27, IL-28A, IL-31, IL-33, MIP-3α/CCL20, TNF-α, and TNF-β. Only 7 out of the 25 analytes expressed at detectible levels: IFN-γ, CCL20, IL-13, IL-9, IL-21, IL-17E/IL-25, and TNF-α. The manufacturer defined assay sensitivity or Lower Limits of Detection for these cytokines are as follows: IFN-γ = 2.4 pg/mL, CCL20 = 3.4 pg/mL, IL-13 = 3.5 pg/mL, IL-9 = 8.7 pg/mL, IL-21 = 3.3 pg/mL, IL-17E/IL-25 = 0.186 pg/mL, and TNF-α = 1.7 pg/mL. Additionally, using our previously validated Luminex bead-based immunoassay (48–50), anti-*S. aureus* human antibody responses in serum were assessed 14 days post-infection in huNSG mice with the following *S. aureus* antigens: iron-regulated surface determinant proteins (IsdA, IsdB, and IsdH), the staphylococcal complement inhibitor (SCIN), the chemotaxis inhibitory protein from *S. aureus* (CHIPS), α-hemolysin (Hla), autolysin (Atl) functional domains amidase (Amd) and glucosaminidase (Gmd), and Leukocidin LukSF-PV/PVL (LukS-PV, LukF-PV).

Statistical Analyses

Unpaired student's t-test was used for statistical comparison of the flow cytometry data. Two-way ANOVA with Sidak's post-hoc tests was performed to compare body weight change over time. One-way ANOVA analyses with Tukey's post-hoc tests were utilized for comparing osteolysis area, number of SACs, SAC area, log-transformed CFUs, and the number of immune cells revealed by immunostaining. All analyses were conducted using GraphPad Prism (version 9.0), and $p < 0.05$ was considered significant.

RESULTS

Humanized NSG Mice Elicit Human T Cell Responses During the Establishment of *S. aureus* Osteomyelitis

Because NSG mice allow the engraftment of human immune cells, we hypothesized that MRSA infection would elicit a human immune response in huNSG mice (**Supplemental Table S1**). To test this, huNSG mice received a sterile (Sham) or MRSA contaminated tibial implant, and the spleens were harvested for analyses on day 14 post-op. Immunophenotyping by flow cytometry revealed that *S. aureus* infection induced significant upregulation of human CD3+ T cells ($p = 0.029$) and its subsets CD4+ T helper cells ($p = 0.007$), CD8+ cytotoxic T cells ($p = 0.019$) in huNSG compared to the control group (**Figure 1A**). No such induction of human CD19+ B cells or CD56+ natural killer (NK) cells were observed in infected huNSG. Additionally, immunofluorescent histochemistry revealed distinctive B and T cell areas in the spleen of infected huNSG mice (**Figure 1B**). Additionally, immunostaining with human cell proliferation marker PCNA revealed expanding human T and B cells in huNSG mice in response to *S. aureus* (**Figure 1C**). However, anti-*S. aureus* human antibody responses in huNSG serum using our custom Luminex assay were undetectable 14 days post infection (data not shown), and serum cytokine levels analyzed over time revealed modest induction of human cytokines including IFN-γ, TNF-α, and IL-13 (**Supplemental Figure S2**). Nonetheless, our results indicate that *S. aureus* infection induces a human immune response in the spleen of huNSG mice.

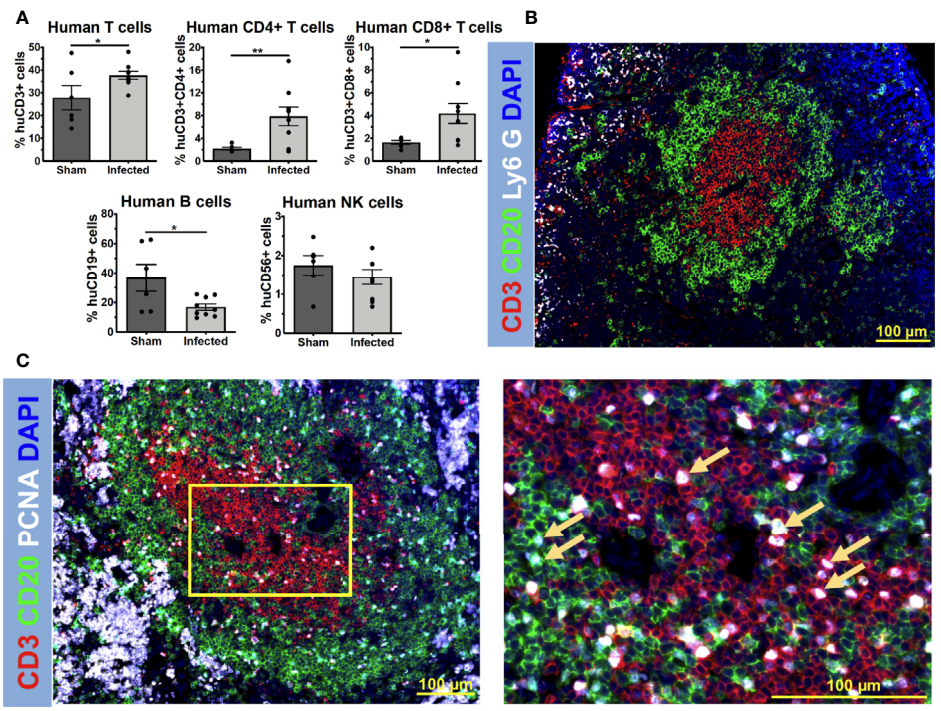

FIGURE 1 | *S. aureus* elicits a human immune response in humanized NSG mice. HuNSG mice received a sterile (Sham) or MRSA contaminated transtibial implant, and 14 days post infection, mice were euthanized, and spleens were harvested for analyses. Single-cell suspensions of splenocytes were prepared and subjected to immunophenotyping analyses by flow cytometry with anti-human mAbs to assess human T cells (CD3+), T helper cells (CD3+CD4+), cytotoxic T cells (CD3+CD8+), B cells (CD19+), and NK cells (CD56+). The sequential gating strategy is depicted in **Supplemental Figure S1**. **(A)** The percentage of each lymphocyte subset of the live/human CD45+ cells analyzed is presented for each mouse with the mean +/- SD for the group (n = 15, $^{*}p < 0.05$, $^{**}p < 0.01$, t-test). **(B)** Paraffin-embedded 5 µm spleen sections from infected humanized NSG mice were stained to visualize the spatial distribution of human $CD3^{+}$ T cells (red), human $CD20^{+}$ B cells (green), and murine $Ly6G^{+}$ neutrophils (white). Representative 3x3 200x mosaic immunofluorescent images are shown highlighting the compartmentalization of interacting human T and B cells in spleens of infected huNSG mice. **(C)** Adjacent 5 µm spleen sections were also stained for examining cell proliferation in response to *S. aureus* infections using proliferating cell nuclear antigen (PCNA) (white). Yellow squares show higher magnification images of proliferating $CD3^{+}$ T cells (red), $CD20^{+}$ B cells (green) (PCNA+ cells, yellow arrows), in the sections of the 3x3 mosaic immunofluorescent micrographs.

Humanized NSG Mice Exhibit Exacerbated Susceptibility to *S. aureus* Osteomyelitis

Given the potential negative impact of *S. aureus* immunotoxins on human immune cells, we hypothesized that the huNSG mice would develop a more severe MRSA infection due to the presence and induction of human immune system. To test this, we examined implant-associated osteomyelitis in huNSG mice and its age-matched NSG, C57BL/6J WT counterparts. In general, huNSG mice appeared sicker, failed to recover their body weight after implant surgery, and exhibited significantly increased weight loss throughout the 14-day study period (**Figure 2A**, $p < 0.05$). High-resolution μCT analyses of the tibiae revealed that *S. aureus*-infected huNSG mice displayed significantly greater peri-implant osteolysis at the insertion site compared to age-matched NSG and C57BL/6J WT controls (**Figures 2B, C**, $p < 0.05$). Interestingly, no differences in reactive bone volume were observed between these groups, suggesting that the human engrafted cells do not affect osteoblast activity (**Supplemental Figure S3**). No difference in osteolysis was observed in animals that underwent sterile-implant surgery, suggesting that the observed bone phenotype is due to *S. aureus* infection.

To assess effects of human engrafted cells on bacterial load, ex vivo CFU quantification was performed on the implants, which revealed higher bacterial loads in huNSG (13-fold, $p = 0.012$) and NSG (4.2-fold, $p = 0.025$) mice compared to C57BL/6J WT (**Figure 3A**). Similarly, an 86.2- to 215.2-fold higher CFU on the tibia ($p < 0.01$) and a 79.7- to 310.9-fold higher CFU load on infected soft tissue ($p < 0.01$) surrounding the bone were observed in huNSG and NSG mice (**Figure 3B**). Interestingly, significantly increased MRSA dissemination from the implant to internal organs (kidney, liver, heart, and spleen) was observed in huNSG compared to control groups (**Figure 3C**). 14/17 huNSG mice were *S. aureus* culture-positive from at least one organ, while only 6/14 and 3/14 mice in the NSG and WT groups were culture-positive in at least one organ (**Figure 3C**). Remarkably, some huNSG mice were highly septic due to MRSA bone infection, while some huNSG mice showed no dissemination (**Figure 3C**).

Next, histopathology of the infected tibia was performed to further assess the extent of bone osteolysis in huNSG mice. H&E staining of the infected tibia confirmed the extensive osteolysis revealed in huNSG mice (**Figure 4E**) compared to C57BL/6 WT (**Figure 4A**) and NSG (**Figure 4C**) controls. In addition, Brown and Brenn staining of the infected tibia revealed extensive Staphylococcal abscess communities (SAC) formation in huNSG mice (**Figure 4F**) compared to control groups (**Figures 4B, D**). The number of SACs formed per infected tibia was significantly higher in huNSG than in control groups (**Figure 4I**, $p < 0.05$). Histomorphometry quantification revealed a marked increase in the SAC area in huNSG, suggesting heightened severity of MRSA bone infection in these animals (**Figures 4G–J**, $p < 0.05$). TEM interrogation of mature SACs in huNSG mice confirmed the formation of a fibrin-like pseudocapsule (51, 52), which sequesters and protects *S. aureus* from host immune cells (**Figure 5**).

Induction of Human T Cell Response in huNSG Tibiae Due to *S. aureus* Osteomyelitis

We next investigated the repertoire and spatial distribution of human T and B cells proximal to SACs *via* multicolor immunofluorescent histochemistry (**Figure 6**). The tibia sections from infected huNSG mice revealed significant induction and trafficking of human T cells clustered adjacent to SACs (**Figures 6B, E, H, J**, $p < 0.0001$). Human B cells were observed in sham treated huNSG mice, but only small amounts of these cells were induced and trafficked in response to *S. aureus* infections (**Figure 6J**). Expectedly, no human B or T cells were identified in nonengrafted NSG control mice (**Figures 6A, D, G**), though *S. aureus* induced production of mouse $Ly6G^+$ neutrophils in the infected tibia of huNSG and NSG animals (**Figure 6K**, $p < 0.05$). Interestingly, the levels of murine $Ly6G^+$ neutrophils in these animals were similar to the levels observed in C57BL/6 WT animals in response to *S. aureus* (**Figure 6K**). Besides, the presence of mouse $Ly6G^+$ neutrophils in huNSG suggests recovery of innate cells post γ-irradiation-induced myeloablation in NSG mice before HSC engraftment. Subsequent immunofluorescent staining of infected huNSG tibiae revealed CD3+ T-bet+ Type 1 human T cells adjacent to the SACs (**Figures 6L, M**). In addition, examination of huNSG tibia sections using proliferating cell nuclear antigen (PCNA) revealed that both human T and B cells are proliferating near the SACs and that the percentage of proliferating human T cells (CD3+PCNA+ cells) is significantly higher than that of B cells (CD20+PCNA+ cells) (**Supplemental Figure S4**). Collectively, these results suggest *S. aureus*-mediated activation and proliferation of type 1 human T cells.

DISCUSSION

Development of effective immunotherapies against *S. aureus* remains among the greatest priorities in orthopedics as bone infections caused by this pathogen continue to be a significant public health problem (1). The failure of several anti-*S. aureus* vaccine trials can be attributed to overreliance on preclinical murine studies, where *S. aureus* does not entirely display their typical phenotype (10, 53). Humanized mice have emerged as an attractive small animal model to investigate human disease (54). In the current study, we assessed its utility to study *S. aureus* pathogenesis during implant-associated osteomyelitis. In this proof-of-concept study involving *S. aureus* transtibial implant-associated osteomyelitis in huNSG mice, we observed that these mice displayed increased susceptibility to *S. aureus* as evidenced by increased weight loss and extensive peri-implant osteolysis compared to C57BL/6 mice. Others have shown that huNSG mice also display increased susceptibility to *S. aureus* infection in peritoneum, skin, and lung infection models (40–42), though these studies were acute infection studies unlike the one described here. Importantly, the authors noted that huNSG mice required 10-100-fold fewer bacteria to have analogous pathology in the non-humanized mice (41). In our model, it is

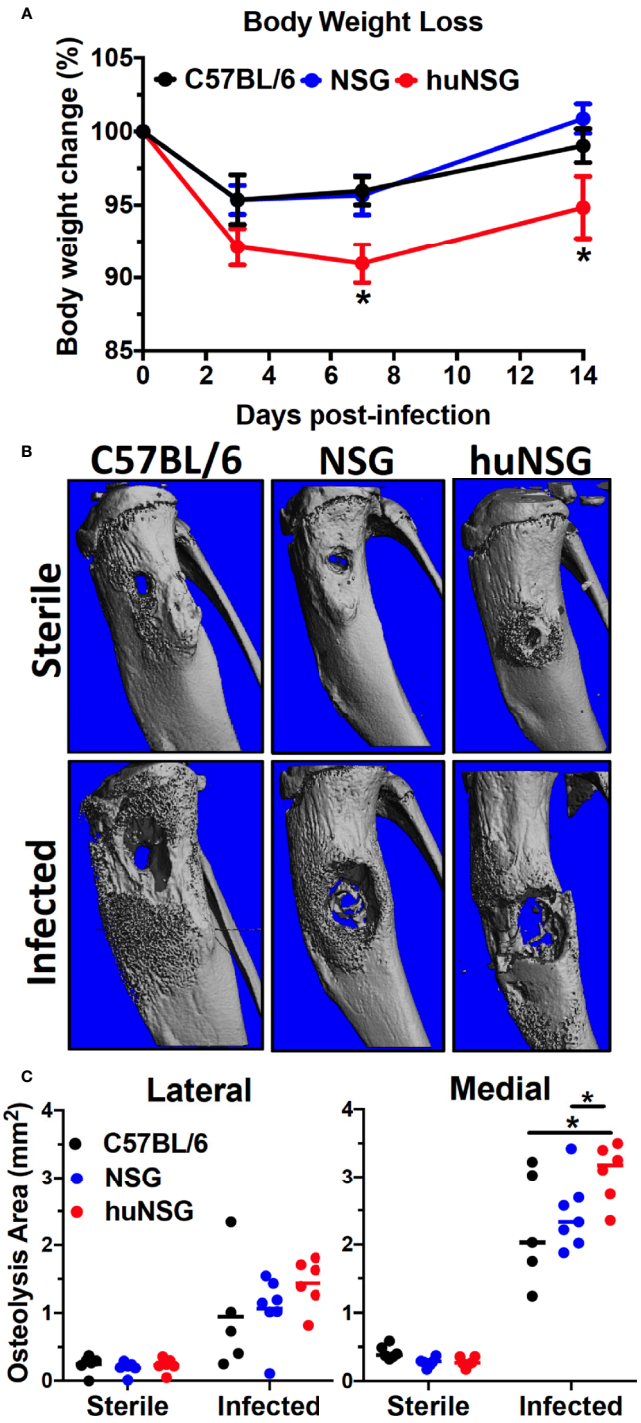

FIGURE 2 | Humanized mice exhibit increased body weight loss and osteolysis during *S. aureus* implant-associated osteomyelitis. **(A)** HuNSG mice and age-matched C57BL/6 WT, NSG controls underwent transtibial implantation of MRSA (USA300 LAC) contaminated stainless steel wire, and total body weight was assessed over the 2-week infection period. The % of baseline body weight on days 0, 3, 7 and 14 is presented for each group with the mean +/- SD (n = 14-17, *$p < 0.05$, two-way ANOVA). **(B)** Tibiae implanted with sterile and MRSA contaminated wires were harvested on day 14 post-op, processed for μCT, and representative 3D renderings are shown to illustrate the levels of reactive bone formation and osteolysis around the implants. Note the extensive osteolysis in the infected huNSG tibia. **(C)** The osteolysis area on the lateral and medial sides of the tibiae were quantified, and the data for each is presented with the mean +/- SD for the group (n = 6, *$p < 0$ .05, one-way ANOVA). Note that osteolysis is greater on the medial side in this model due to the directionality of wire implantation from the medial to the lateral side.

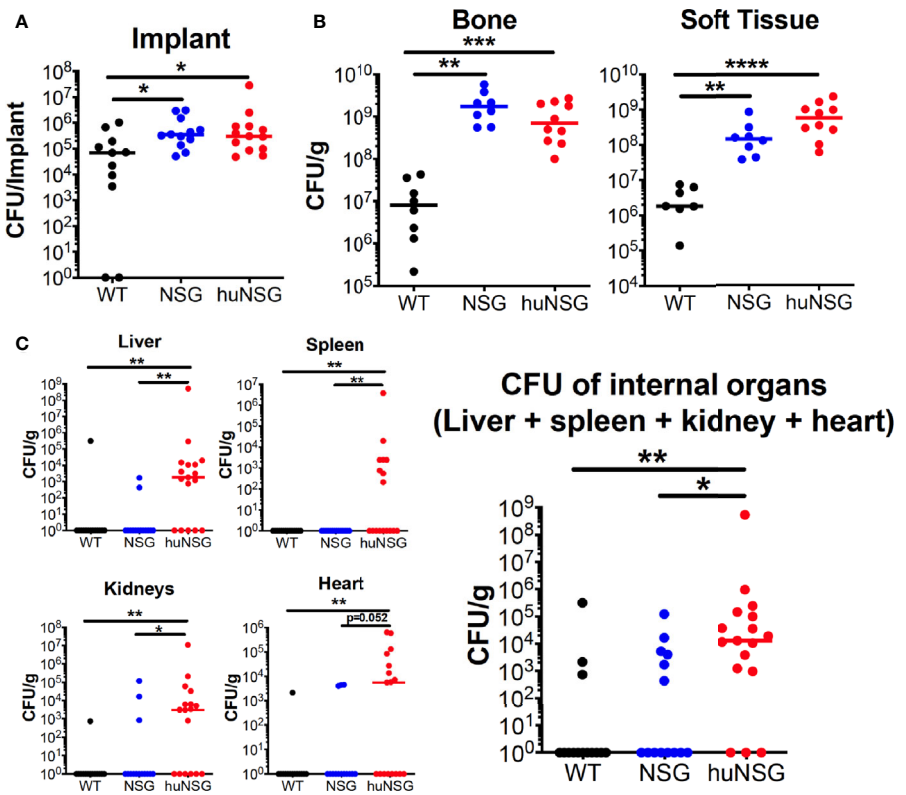

FIGURE 3 | Humanized mice exhibit increased bacterial load at the surgical site and sepsis during *S. aureus* implant-associated osteomyelitis. WT, NSG, and huNSG mice received MRSA infected trans-tibial implants and were euthanized on day 14 post-op to quantify CFUs from the **(A)** implant, **(B)** tibia and adjacent soft tissue, and **(C)** internal organs. The data are presented for each mouse with mean +/- SD for the Group (n = 14-17, $*p < 0.05$, $**p < 0.01$, $***p < 0.001$, one-way ANOVA).

conceivable that the more severe infection phenotype in huNSG mice could be the result of higher bacterial inoculum that we routinely use for achieving reproducible implant-associated osteomyelitis in C57BL/6 mice (22, 23, 43, 44, 55). Nonetheless, this critical finding needs to be carefully examined in our humanized mouse model of implant-associated osteomyelitis.

In vivo MRSA infection in huNSG mice revealed markedly higher CFUs on tibial bone and soft tissue in both huNSG and NSG than C57BL/6J WT mice. Increased MRSA dissemination from the implant to distal organs was also observed in huNSG compared to the control groups confirming their increased susceptibility to *S. aureus*. We found these observations remarkable as several groups have observed no such bacterial dissemination in wild type mouse models of *S. aureus* osteomyelitis (56, 57). The increased tibial bacterial load in the bone and MRSA dissemination in humanized mice could be attributed to induction of human immune response due to *S. aureus*, and the presence of staphylococcal immunotoxins that exhibit high tropism to human leukocyte receptors (29, 30). This idea is consistent with the exacerbated lung pathology reported by Prince et al. and the decreased severity in huNSG mice infected with an MRSA strain deficient in the human-specific PVL toxin (42). Another example is the increased susceptibility to MRSA bacteremia in a humanized C57BL/6J mouse containing human CD11b receptor due to strong tropism of immunotoxin LukAB for human CD11b (58). These studies, including ours, highlight the adaptation processes that this pathogen has evolved to survive in the human host.

Analysis of the MRSA-infected tibia in huNSG mice revealed increased bone osteolysis compared to C57BL/6J WT mice. Perhaps the presence of human immune cells in the bone marrow of huNSG, and the ability of *S. aureus* to target human leukocytes are causing increased osteoclastogenesis and infection-associated trabecular bone loss during MRSA osteomyelitis (59). Nonetheless, the increased dysregulation of bone homeostasis during osteomyelitis in huNSG mice warrants further investigation.

An important finding of the current study is the extensive MRSA-induced SAC formation in huNSG mice. Quantitative analyses of the SACs show that the number of SACs per bone area was significantly higher in huNSG mice suggesting increased interaction between *S. aureus* and human leukocytes in the bone. The formation of a multilayered SAC structure during osteomyelitis is a host-induced mechanism of infection control, which is manipulated by *S. aureus* with the deployment

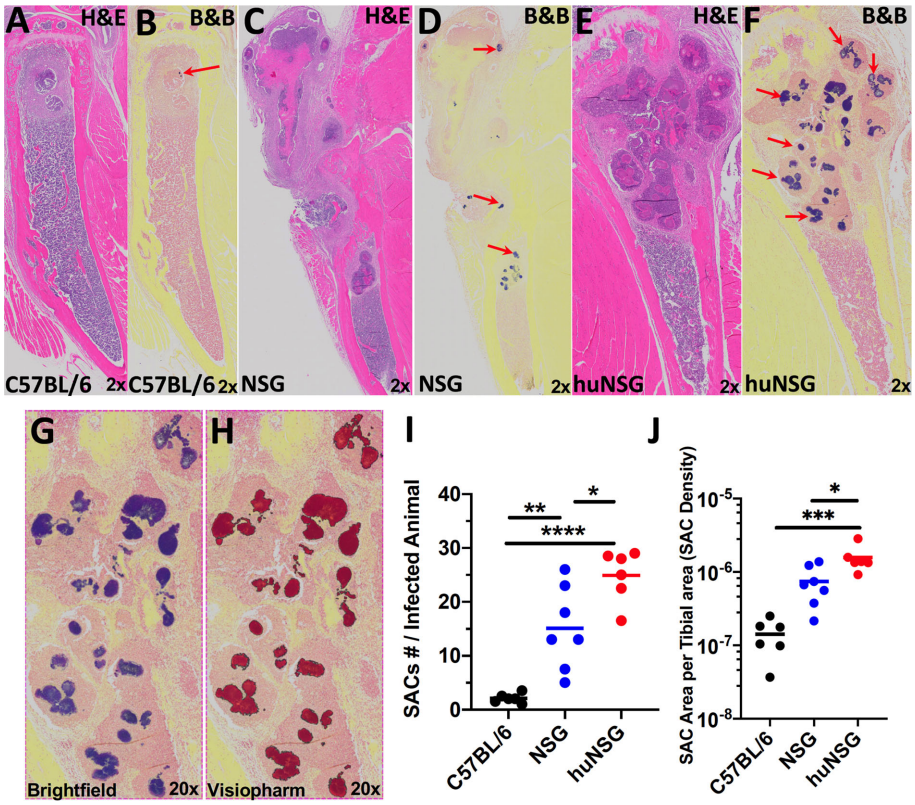

FIGURE 4 | Humanized mice exhibit increased Staphylococcal abscess community (SAC) formation. WT, NSG, and huNSG mice received MRSA infected transtibial implants, and the tibiae were harvested on day 14 post-op for histology and assessment of SACs. Representative micrographs of H&E **(A, C, E)** and Brown & Brenn Gram **(B, D, F)** stained sections are presented to illustrate the abscesses and Gram-positive bacteria (red arrows). **(G, H)** Digital scans of the histology were processed by Visiopharm software, which recognized the Gram-stained bacteria, and scored the positive pixels (purple to red color conversion) for automated histomorphometry of SAC numbers per tibia **(I)** and SAC area per tibia **(J)**. The data are presented for each mouse with the mean for each Group (n = 6-7, $^{*}p < 0.05$, $^{**}p < 0.01$, $^{***}p < 0.001$ one-way ANOVA).

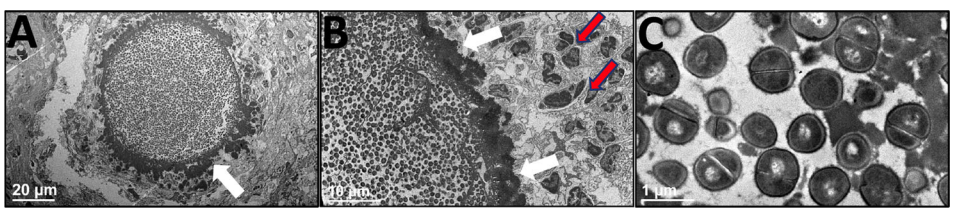

FIGURE 5 | Ultrastructural assessment of Staphylococcal abscess communities (SACs) in humanized mice. HuNSG mice were subjected to MRSA transtibial infection and tibiae were harvested 14 days post-op, formalin-fixed, and decalcified for TEM processing. These paraffin-embedded tibiae samples were reprocessed into epoxy resin for transmission electron microscopy. A representative SAC in the bone marrow cavity is shown in **(A)** x1200 and **(B)** x3000 to illustrate the bacteria within the electron dense pseudocapsule (white arrows), and adjacent immune cells (red arrows) that are unable to penetrate the SAC. **(C)** High magnification of *S. aureus* bacteria within the SAC (x 30,000).

of several virulence genes including clumping factor A (ClfA), chemotaxis inhibitory protein of staphylococci (CHIPS), and staphylococcal complement inhibitor (SCIN) (51, 52, 60–62). In clinical studies, the lack of humoral immunity against SCIN and CHIPS correlated with adverse clinical outcomes in patients with *S. aureus* osteomyelitis (49). Assessing the expression of these genes in a huNSG SAC or a 3D *in vitro* model of SAC (63) using bone marrow cells from these animals could shed light on

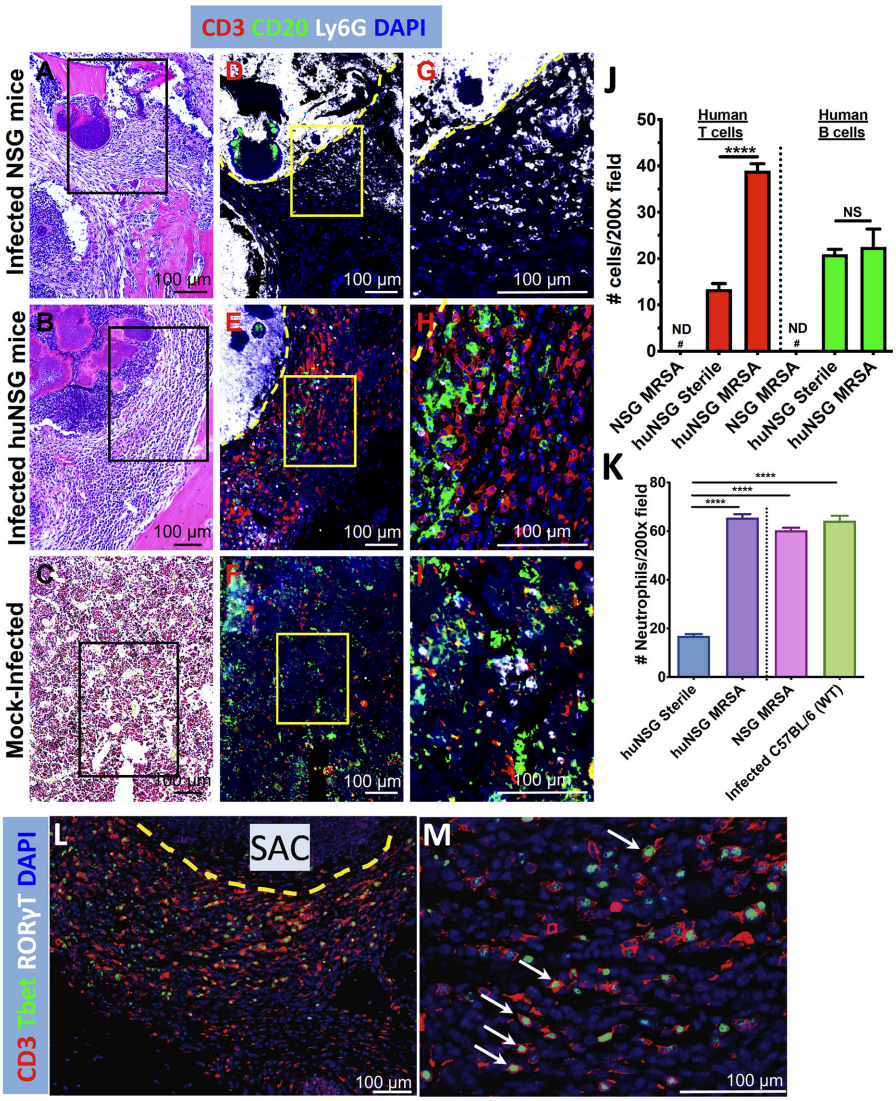

FIGURE 6 | Evidence of human T cell immune responses against *S. aureus* in huNSG mice with implant-associated osteomyelitis. The histology sections (n = 3-5 per Group) described in **Figure 4** were stained with fluorescently labeled antibodies specific for anti-mouse Ly6G, anti-human CD3, anti-human CD20, anti-human Tbet, and anti-human RORγT. Light microscopy of the H&E stained sections **(A–C)**, and fluorescent microscopy of adjacent 5 µm sections **(D–I)** were performed on the SACs in tibiae from infected NSG, infected huNSG mice, and sham-control huNSG mice. Black squares in H&E images show the area depicted in 3x3 mosaic immunofluorescent micrograph. Yellow squares show higher magnification images of the $CD3^+$ T cells (red), $CD20^+$ B cells (green), and $Ly6G^+$ neutrophils (white), in the sections of the 3x3 mosaic immunofluorescent micrographs. The dotted yellow line separates the SAC border from the rest of the bone marrow. Note that mouse $Ly6G^+$ neutrophils accumulated inside and in close proximity to SACs, and the absence of human lymphocytes in infected NSG mice **(D, G)**. In contrast, large numbers of human T and B cells accumulate around the SACs in the infected huNSG mice **(E, H)**, while human lymphocytes are scant in uninfected huNSG mice **(F, I)**. Histomorphometry was performed on 5 randomly chosen fields at 200X magnification in each condition **(J, K)**, and aggregated data is presented as the mean+/- SEM for each Group (n = 3-5 mice, ND, not detected, NS, not significant, $^{****}p < 0.0001$, one-way ANOVA). **(L, M)** Evidence of Type 1 human T cell induction (CD3+T-bet+, white arrows) adjacent to the SACs.

virulence mechanisms associated with increased abscess formation in humanized mice.

T cells are essential for orchestrating anti-*S. aureus* adaptive immunity, and studies have demonstrated their dichotomous roles in protection vs. pathogenesis during infections (64–69). Analysis of human tissue samples in patients with implant-related bacterial biofilm infections indicate the presence of CD4 and CD8 T cells (70, 71), and these T cells were terminally differentiated effector cells (72, 73). However, these observations were not *S. aureus*-specific, and the exact role of T cells in the context of chronic *S aureus* osteomyelitis remains poorly understood. Immunohistopathology of infected huNSG tibia revealed increased numbers of clustered human T cells adjacent to abscesses, suggesting *S. aureus*-mediated human T

cell activation and proliferation. Other studies using intraperitoneal infection model in huNSG mice showed increased human T-cell activation and apoptosis due to *S. aureus*, which led to increased bacterial counts and higher mortality rates in mice (40). Conceivably, exacerbated T cell activation could be due to increased expression of T cell targeting superantigens and immunotoxins in huNSG mice.

The current study is limited by inherent deficiencies in the NSG mouse, including limited myeloid lineage development and insufficient functional T cell development (35, 74). Indeed, *S. aureus* infection was more severe in a humanized NSG mice variant that allowed for enhanced human myeloid lineage reconstitution (42, 75, 76). Additionally, we cannot exclude the effects of sublethal γ-irradiation-induced myeloablation in NSG mice before HSC engraftment. This can be examined in NSG mice with engrafted murine bone marrow cells. A pulmonary infection model utilizing NSG mice engrafted with cells of C57BL/6J mice, reported MRSA levels comparable to those in NSG and C57BL/6J control groups (42), ruling the detrimental impact of radiation on the control of the bacterial infection in the lungs. However, radiation could have a different effect on bone immunity. Nevertheless, further studies are warranted to improve this mouse model to make it highly relevant to human musculoskeletal infections, in addition to validating its usefulness to study fracture-related infections, prosthetic joint infections, and evaluating novel experimental immunotherapies.

DATA AVAILABILITY STATEMENT

The raw data supporting the conclusions of this article will be made available by the authors, without undue reservation.

ETHICS STATEMENT

The animal study was reviewed and approved by Ethical committee of the canton of Grisons in Switzerland.

AUTHOR CONTRIBUTIONS

GM: study conception, experimental design, data acquisition and analysis, funding acquisition, and drafting the manuscript. TM, EMS, JD, RR, and SZ: experimental design, data analysis, funding acquisition, and drafting the manuscript. AW, JR-M, MH, KD, KM, MK, and ETS: experimental design, data acquisition, and analysis. All authors contributed to the article and approved the submitted version.

FUNDING

This work was supported by AO Trauma Clinical Priority Program Fellowship (GM) with additional support from AO Trauma Clinical Priority Program (EMS, TM), NIH NIAMS P30 AR069655 (EMS), P50 AR072000 (EMS), internal funds from the Department of Medicine in the University of Rochester, and R01AI111914 (JR-M).

ACKNOWLEDGMENTS

The authors would like to thank Drs. Aron Keshishian, Marc Antoine Burch, and Caroline Constant for their technical assistance with the *in vivo* studies. The authors would like to thank members of the Moriarty Lab Iris Keller, Pamela Furlong, and Dr. Virginia Post for their technical assistance. The authors would also like to acknowledge the technical support from the members of the Histology, Biochemistry & Molecular Imaging Core and the Biomechanics, Biomaterials, and Multimodal Tissue Imaging Core in the Center for Musculoskeletal Research at the University of Rochester. The authors also wish to thank Dr. Chad Galloway for technical assistance in the University of Rochester's Electron Microscope Shared Resource.

SUPPLEMENTARY MATERIAL

The Supplementary Material for this article can be found online at: https://www.frontiersin.org/articles/10.3389/fimmu.2021.651515/full#supplementary-material

Supplementary Figure 1 | Flow cytometry gating strategy for analyzing human immune cells in huNSG mice spleen. The sequential gating strategy and representative contour plots for identifying live splenocytes (Live/Dead eF780) and their subpopulations of human T cells (CD3+), T helper cells (CD3+CD4+), cytotoxic T cells (CD3+CD8+), B cells (CD19+), and NK cells (CD56+) their subpopulations of human T, B, and NK cells is depicted here.

Supplementary Figure 2 | Serum human cytokine and chemokine expression analyses in humanized mice. Serum samples were collected over time ((PreOP, day 7, day 14 post-op) from huNSG mice infected with either a sterile (Sham) or *S. aureus* contaminated tibial implant. The dotted line indicates the lower limit of detection for each cytokine (n = 20, $*p < 0.05$, $**p < 0.01$, two-way ANOVA).

Supplementary Figure 3 | μCT analyses of new reactive bone formation. Longitudinal μCT analyses for new reactive bone formation were performed on MRSA-infected or sterile-pin infected huNSG, NSG, and C57BL/6 WT mice to reveal **(A)** Bone Volume, **(B)** Total Volume, and **(C)** Bone Volume Density (BV/TV) (N = 4-6 in each cohort, $*p < 0.05$, $**p < 0.01$, $***p < 0.001$, one-way ANOVA).

Supplementary Figure 4 | Evidence of human immune cell proliferation in the huNSG tibia due to *S. aureus* implant-associated osteomyelitis. The histology sections described in **Figure 4** were stained with fluorescently labeled antibodies specific for goat anti-proliferating cell nuclear antigen (PCNA), anti-human CD3, and anti-human CD20. Light microscopy of the H&E stained sections **(A,C)**, and fluorescent microscopy of adjacent 5 μm sections **(B,C,E,F)** were performed on the SACs in tibiae from infected huNSG mice, and sham-control huNSG mice. White squares show higher magnification images of the $CD3^+$ T cells (red), $CD20^+$ B cells (green), and $PCNA^+$ cells (white), in the sections of the 3x3 mosaic immunofluorescent micrographs. Note that proliferating PCNA+ human T cell and B cells accumulate around the SACs only in the infected huNSG mice **(E, F)**. Histomorphometry was performed on 5 randomly chosen fields at 200X magnification in each condition **(G-H)**, and aggregated data is presented as the mean+/- SEM for each group (n = 3 mice/group, $**p < 0.01$, $***p < 0.001$, one-way ANOVA). Note that the percentage of proliferating human T cells (CD3+PCNA+ cells) is significantly higher than proliferating B cells (CD20+PCNA+ cells).

REFERENCES

1. Schwarz EM, Parvizi J, Gehrke T, Aiyer A, Battenberg A, Brown SA, et al. International Consensus Meeting on Musculoskeletal Infection: Research Priorities from the General Assembly Questions. *J Orthop Res* (2019) 37 (5):997–1006. doi: 10.1002/jor.24293
2. Tande AJ, Patel R. Prosthetic joint infection. *Clin Microbiol Rev* (2014) 27 (2):302–45. doi: 10.1128/CMR.00111-13
3. Kurtz SM, Ong KL, Schmier J, Mowat F, Saleh K, Dybvik E, et al. Future clinical and economic impact of revision total hip and knee arthroplasty. *J Bone Joint Surg Am* (2007) 89(Suppl 3):144–51. doi: 10.2106/JBJS.G.00587
4. Depypere M, Morgenstern M, Kuehl R, Senneville E, Moriarty TF, Obremskey WT, et al. Pathogenesis and management of fracture-related infection. *Clin Microbiol Infect* (2020) 26(5):572–8. doi: 10.1016/j.cmi.2019.08.006
5. Govaert GAM, Kuehl R, Atkins BL, Trampuz A, Morgenstern M, Obremskey WT, et al. Diagnosing Fracture-Related Infection: Current Concepts and Recommendations. *J Orthop Trauma* (2020) 34(1):8–17. doi: 10.1097/BOT.0000000000001614
6. Kates SL, Tornetta P, 3. Commentary on Secondary Fracture Prevention: Consensus Clinical Recommendations From a Multistakeholder Coalition Originally Published in the Journal of Bone and Mineral Research. *J Orthop Trauma* (2020) 34(4):221. doi: 10.1097/BOT.0000000000001742
7. Goodson KM, Kee JR, Edwards PK, Novack AJ, Stambough JB, Siegel ER, et al. Streamlining Hospital Treatment of Prosthetic Joint Infection. *J Arthroplasty* (2020) 35(3S):S63–S8. doi: 10.1016/j.arth.2019.10.056
8. Kaplan SL. Recent lessons for the management of bone and joint infections. *J Infect* (2014) 68(Suppl 1):S51–6. doi: 10.1016/j.jinf.2013.09.014
9. Assis LM, Nedeljkovic M, Dessen A. New strategies for targeting and treatment of multi-drug resistant Staphylococcus aureus. *Drug Resist Update* (2017) 31:1–14. doi: 10.1016/j.drup.2017.03.001
10. Fowler VG Jr., Proctor RA. Where does a Staphylococcus aureus vaccine stand? *Clin Microbiol Infect* (2014) 20(Suppl 5):66–75. doi: 10.1111/1469-0691.12570
11. Proctor RA. Immunity to Staphylococcus aureus: Implications for Vaccine Development. *Microbiol Spectr* (2019) 7(4). doi: 10.1128/microbiolspec.GPP3-0037-2018
12. Miller LS, Fowler VG, Shukla SK, Rose WE, Proctor RA. Development of a vaccine against Staphylococcus aureus invasive infections: Evidence-based on human immunity, genetics, and bacterial evasion mechanisms. *FEMS Microbiol Rev* (2019) 44(1):123–53. doi: 10.1093/femsre/fuz030
13. Gomez MI, Lee A, Reddy B, Muir A, Soong G, Pitt A, et al. Staphylococcus aureus protein A induces airway epithelial inflammatory responses by activating TNFR1. *Nat Med* (2004) 10(8):842–8. doi: 10.1038/nm1079
14. Soong G, Paulino F, Wachtel S, Parker D, Wickersham M, Zhang D, et al. Methicillin-resistant Staphylococcus aureus adaptation to human keratinocytes. *mBio* (2015) 6(2). doi: 10.1128/mBio.00289-15
15. Kitur K, Wachtel S, Brown A, Wickersham M, Paulino F, Penaloza HF, et al. Necroptosis Promotes Staphylococcus aureus Clearance by Inhibiting Excessive Inflammatory Signaling. *Cell Rep* (2016) 16(8):2219–30. doi: 10.1016/j.celrep.2016.07.039
16. Powers ME, Bubeck Wardenburg J. Igniting the fire: Staphylococcus aureus virulence factors in the pathogenesis of sepsis. *PloS Pathog* (2014) 10(2): e1003871. doi: 10.1371/journal.ppat.1003871
17. Panizzi P, Nahrendorf M, Figueiredo JL, Panizzi J, Marinelli B, Iwamoto Y, et al. In vivo detection of Staphylococcus aureus endocarditis by targeting pathogen-specific prothrombin activation. *Nat Med* (2011) 17(9):1142–6. doi: 10.1038/nm.2423
18. Gibson GW, Kreuser SC, Riley JM, Rosebury-Smith WS, Courtney CL, Juneau PL, et al. Development of a mouse model of induced Staphylococcus aureus infective endocarditis. *Comp Med* (2007) 57(6):563–9.
19. Gomez MI, O'Seaghdha M, Magargee M, Foster TJ, Prince AS. Staphylococcus aureus protein A activates TNFR1 signaling through conserved IgG binding domains. *J Biol Chem* (2006) 281(29):20190–6. doi: 10.1074/jbc.M601956200
20. Wright JA, Nair SP. Interaction of staphylococci with bone. *Int J Med Microbiol* (2010) 300(2-3):193–204. doi: 10.1016/j.ijmm.2009.10.003
21. Ricciardi BF, Muthukrishnan G, Masters E, Ninomiya M, Lee CC, Schwarz EM. Staphylococcus aureus Evasion of Host Immunity in the Setting of Prosthetic Joint Infection: Biofilm and Beyond. *Curr Rev Musculoskelet Med* (2018) 11(3):389–400. doi: 10.1007/s12178-018-9501-4
22. Masters EA, de Mesy Bentley KL, Gill AL, Hao SP, Galloway CA, Salminen AT, et al. Identification of Penicillin Binding Protein 4 (PBP4) as a critical factor for Staphylococcus aureus bone invasion during osteomyelitis in mice. *PloS Pathog* (2020) 16(10):e1008988. doi: 10.1371/journal.ppat.1008988
23. Nishitani K, Ishikawa M, Morita Y, Yokogawa N, Xie C, de Mesy Bentley KL, et al. IsdB antibody-mediated sepsis following S. aureus surgical site infection. *JCI Insight* (2020) 5(19). doi: 10.1172/jci.insight.141164
24. Torres VJ, Pishchany G, Humayun M, Schneewind O, Skaar EP. Staphylococcus aureus IsdB is a hemoglobin receptor required for heme iron utilization. *J Bacteriol* (2006) 188(24):8421–9. doi: 10.1128/JB.01335-06
25. Kim HK, DeDent A, Cheng AG, McAdow M, Bagnoli F, Missiakas DM, et al. IsdA and IsdB antibodies protect mice against Staphylococcus aureus abscess formation and lethal challenge. *Vaccine* (2010) 28(38):6382–92. doi: 10.1016/j.vaccine.2010.02.097
26. Brown M, Kowalski R, Zorman J, Wang XM, Towne V, Zhao Q, et al. Selection and characterization of murine monoclonal antibodies to Staphylococcus aureus iron-regulated surface determinant B with functional activity in vitro and in vivo. *Clin Vaccine Immunol* (2009) 16(8):1095–104. doi: 10.1128/CVI.00085-09
27. Kuklin NA, Clark DJ, Secore S, Cook J, Cope LD, McNeely T, et al. A novel Staphylococcus aureus vaccine: iron surface determinant B induces rapid antibody responses in rhesus macaques and specific increased survival in a murine S. aureus sepsis model. *Infect Immun* (2006) 74(4):2215–23. doi: 10.1128/IAI.74.4.2215-2223.2006
28. Fowler VG, Allen KB, Moreira ED, Moustafa M, Isgro F, Boucher HW, et al. Effect of an investigational vaccine for preventing Staphylococcus aureus infections after cardiothoracic surgery: a randomized trial. *Jama* (2013) 309 (13):1368–78. doi: 10.1001/jama.2013.3010
29. Alonzo F, 3, Torres VJ. Bacterial survival amidst an immune onslaught: the contribution of the Staphylococcus aureus leukotoxins. *PloS Pathog* (2013) 9 (2):e1003143. doi: 10.1371/journal.ppat.1003143
30. Alonzo F, 3, Torres VJ. The bicomponent pore-forming leucocidins of Staphylococcus aureus. *Microbiol Mol Biol Rev* (2014) 78(2):199–230. doi: 10.1128/MMBR.00055-13
31. Ishikawa F, Yasukawa M, Lyons B, Yoshida S, Miyamoto T, Yoshimoto G, et al. Development of functional human blood and immune systems in NOD/SCID/IL2 receptor {gamma} chain(null) mice. *Blood* (2005) 106(5):1565–73. doi: 10.1182/blood-2005-02-0516
32. Shultz LD, Lyons BL, Burzenski LM, Gott B, Chen X, Chaleff S, et al. Human lymphoid and myeloid cell development in NOD/LtSz-scid IL2R gamma null mice engrafted with mobilized human hemopoietic stem cells. *J Immunol* (2005) 174(10):6477–89. doi: 10.4049/jimmunol.174.10.6477
33. Lan P, Tonomura N, Shimizu A, Wang S, Yang YG. Reconstitution of a functional human immune system in immunodeficient mice through combined human fetal thymus/liver and CD34+ cell transplantation. *Blood* (2006) 108(2):487–92. doi: 10.1182/blood-2005-11-4388
34. Brehm MA, Wiles MV, Greiner DL, Shultz LD. Generation of improved humanized mouse models for human infectious diseases. *J Immunol Methods* (2014) 410:3–17. doi: 10.1016/j.jim.2014.02.011
35. Shultz LD, Brehm MA, Garcia-Martinez JV, Greiner DL. Humanized mice for immune system investigation: progress, promise and challenges. *Nat Rev Immunol* (2012) 12(11):786–98. doi: 10.1038/nri3311
36. Munz C. Humanized mouse models for Epstein Barr virus infection. *Curr Opin Virol* (2017) 25:113–8. doi: 10.1016/j.coviro.2017.07.026
37. Marsden MD, Zack JA. Humanized Mouse Models for Human Immunodeficiency Virus Infection. *Annu Rev Virol* (2017) 4(1):393–412. doi: 10.1146/annurev-virology-101416-041703
38. Mian MF, Pek EA, Chenoweth MJ, Coombes BK, Ashkar AA. Humanized mice for Salmonella typhi infection: new tools for an old problem. *Virulence* (2011) 2(3):248–52. doi: 10.4161/viru.2.3.16133
39. Wege AK, Florian C, Ernst W, Zimara N, Schleicher U, Hanses F, et al. Leishmania major infection in humanized mice induces systemic infection and provokes a nonprotective human immune response. *PloS Negl Trop Dis* (2012) 6(7):e1741. doi: 10.1371/journal.pntd.0001741
40. Knop J, Hanses F, Leist T, Archin NM, Buchholz S, Glasner J, et al. Staphylococcus aureus Infection in Humanized Mice: A New Model to

Study Pathogenicity Associated With Human Immune Response. *J Infect Dis* (2015) 212(3):435–44. doi: 10.1093/infdis/jiv073
41. Tseng CW, Biancotti JC, Berg BL, Gate D, Kolar SL, Muller S, et al. Increased Susceptibility of Humanized NSG Mice to Panton-Valentine Leukocidin and Staphylococcus aureus Skin Infection. *PloS Pathog* (2015) 11(11):e1005292. doi: 10.1371/journal.ppat.1005292
42. Prince A, Wang H, Kitur K, Parker D. Humanized mice exhibit increased susceptibility to Staphylococcus aureus pneumonia. *J Infect Dis* (2016) 215 (9):1386–95. doi: 10.1093/infdis/jiw425
43. Li D, Gromov K, Soballe K, Puzas JE, O'Keefe RJ, Awad H, et al. Quantitative mouse model of implant-associated osteomyelitis and the kinetics of microbial growth, osteolysis, and humoral immunity. *J Orthop Res* (2008) 26(1):96–105. doi: 10.1002/jor.20452
44. Nishitani K, Sutipornpalangkul W, de Mesy Bentley KL, Varrone JJ, Bello-Irizarry SN, Ito H, et al. Quantifying the natural history of biofilm formation in vivo during the establishment of chronic implant-associated Staphylococcus aureus osteomyelitis in mice to identify critical pathogen and host factors. *J Orthop Res* (2015) 33(9):1311–9. doi: 10.1002/jor.22907
45. Mys K, Stockmans F, Vereecke E, van Lenthe GH. Quantification of bone microstructure in the wrist using cone-beam computed tomography. *Bone* (2018) 114:206–14. doi: 10.1016/j.bone.2018.06.006
46. Varrone JJ, Li D, Daiss JL, Schwarz EM. Anti-Glucosaminidase Monoclonal Antibodies as a Passive Immunization for Methicillin-Resistant Staphylococcus aureus (MRSA) Orthopaedic Infections. *Bonekey Osteovision* (2011) 8:187–94. doi: 10.1138/20110506
47. Rochford ETJ, Sabate Bresco M, Zeiter S, Kluge K, Poulsson A, Ziegler M, et al. Monitoring immune responses in a mouse model of fracture fixation with and without Staphylococcus aureus osteomyelitis. *Bone* (2016) 83:82–92. doi: 10.1016/j.bone.2015.10.014
48. Nishitani K, Beck CA, Rosenberg AF, Kates SL, Schwarz EM, Daiss JL. A Diagnostic Serum Antibody Test for Patients With Staphylococcus aureus Osteomyelitis. *Clin Orthop Relat Res* (2015) 473(9):2735–49. doi: 10.1007/s11999-015-4354-2
49. Muthukrishnan G, Beck CA, Owen JR, Xie C, Kates SL, Daiss JL. Serum antibodies against Staphylococcus aureus can prognose treatment success in patients with bone infections. *J Orthop Res* (2020). doi: 10.1002/jor.24955
50. Muthukrishnan G, Soin S, Beck CA, Grier A, Brodell JD, Jr, Lee CC, et al. A Bioinformatic Approach to Utilize a Patient's Antibody-Secreting Cells against Staphylococcus aureus to Detect Challenging Musculoskeletal Infections. *Immunohorizons* (2020) 4(6):339–51. doi: 10.4049/immunohorizons.2000024
51. Cheng AG, DeDent AC, Schneewind O, Missiakas D. A play in four acts: Staphylococcus aureus abscess formation. *Trends Microbiol* (2011) 19(5):225–32. doi: 10.1016/j.tim.2011.01.007
52. Muthukrishnan G, Masters EA, Daiss JL, Schwarz EM. Mechanisms of Immune Evasion and Bone Tissue Colonization That Make Staphylococcus aureus the Primary Pathogen in Osteomyelitis. *Curr Osteoporos Rep* (2019) 17 (6):395–404. doi: 10.1007/s11914-019-00548-4
53. Salgado-Pabon W, Schlievert PM. Models matter: the search for an effective Staphylococcus aureus vaccine. *Nat Rev Microbiol* (2014) 12(8):585–91. doi: 10.1038/nrmicro3308
54. Allen TM, Brehm MA, Bridges S, Ferguson S, Kumar P, Mirochnitchenko O, et al. Humanized immune system mouse models: progress, challenges and opportunities. *Nat Immunol* (2019) 20(7):770–4. doi: 10.1038/s41590-019-0416-z
55. Varrone JJ, de Mesy Bentley KL, Bello-Irizarry SN, Nishitani K, Mack S, Hunter JG, et al. Passive immunization with anti-glucosaminidase monoclonal antibodies protects mice from implant-associated osteomyelitis by mediating opsonophagocytosis of Staphylococcus aureus megaclusters. *J Orthop Res* (2014) 32(10):1389–96. doi: 10.1002/jor.22672
56. Reizner W, Hunter JG, O'Malley NT, Southgate RD, Schwarz EM, Kates SL. A systematic review of animal models for Staphylococcus aureus osteomyelitis. *Eur Cell Mater* (2014) 27:196–212. doi: 10.22203/ecm.v027a15
57. Archer NK, Wang Y, Ortines RV, Liu H, Nolan SJ, Liu Q, et al. Preclinical Models and Methodologies for Monitoring Staphylococcus aureus Infections Using Noninvasive Optical Imaging. *Methods Mol Biol* (2020) 2069:197–228. doi: 10.1007/978-1-4939-9849-4_15
58. Boguslawski KM, McKeown AN, Day CJ, Lacey KA, Tam K, Vozhilla N, et al. Exploiting species specificity to understand the tropism of a human-specific toxin. *Sci Adv* (2020) 6(11):eaax7515. doi: 10.1126/sciadv.aax7515
59. Mbalaviele G, Novack DV, Schett G, Teitelbaum SL. Inflammatory osteolysis: a conspiracy against bone. *J Clin Invest* (2017) 127(6):2030–9. doi: 10.1172/JCI93356
60. McDevitt D, Francois P, Vaudaux P, Foster T. Molecular characterization of the clumping factor (fibrinogen receptor) of Staphylococcus aureus. *Mol Microbiol* (1994) 11(2):237–48. doi: 10.1111/j.1365-2958.1994.tb00304.x
61. Postma B, Poppelier MJ, Van Galen JC, Prossnitz ER, Van Strijp JA, De Haas CJ, et al. Chemotaxis inhibitory protein of Staphylococcus aureus binds specifically to the C5a and formylated peptide receptor. *J Immunol* (2004) 172(11):6994–7001. doi: 10.4049/jimmunol.172.11.6994
62. Rooijakkers SH, Ruyken M, Van Roon J, Van Kessel KP, Van Strijp JA, Van Wamel WJ. Early expression of SCIN and CHIPS drives instant immune evasion by Staphylococcus aureus. *Cell Microbiol* (2006) 8(8):1282–93. doi: 10.1111/j.1462-5822.2006.00709.x
63. Hofstee MI, Riool M, Terjajevs I, Thompson K, Stoddart MJ, Richards RG, et al. Three-Dimensional In Vitro Staphylococcus aureus Abscess Communities Display Antibiotic Tolerance and Protection from Neutrophil Clearance. *Infect Immun* (2020) 88(11). doi: 10.1128/IAI.00293-20
64. Broker BM, Mrochen D, Peton V. The T Cell Response to Staphylococcus aureus. *Pathogens* (2016) 5(1). doi: 10.3390/pathogens5010031
65. Brown AF, Murphy AG, Lalor SJ, Leech JM, O'Keeffe KM, Mac Aogain M, et al. Memory Th1 Cells Are Protective in Invasive Staphylococcus aureus Infection. *PloS Pathog* (2015) 11(11):e1005226. doi: 10.1371/journal.ppat.1005226
66. Parker D, Ryan CL, Alonzo F,3, Torres VJ, Planet PJ, Prince AS. CD4+ T cells promote the pathogenesis of Staphylococcus aureus pneumonia. *J Infect Dis* (2015) 211(5):835–45. doi: 10.1093/infdis/jiu525
67. Liu H, Archer NK, Dillen CA, Wang Y, Ashbaugh AG, Ortines RV, et al. Staphylococcus aureus Epicutaneous Exposure Drives Skin Inflammation via IL-36-Mediated T Cell Responses. *Cell Host Microbe* (2017) 22(5):653–66 e5. doi: 10.1016/j.chom.2017.10.006
68. Kolata JB, Kuhbandner I, Link C, Normann N, Vu CH, Steil L, et al. The Fall of a Dogma? Unexpected High T-Cell Memory Response to Staphylococcus aureus in Humans. *J Infect Dis* (2015) 212(5):830–8. doi: 10.1093/infdis/jiv128
69. Lee B, Olaniyi R, Kwiecinski J, Bubeck Wardenburg J. Staphylococcus aureus alpha-toxin suppresses antigen-specific T cell responses. *J Clin Invest* (2019) 130(3):1122–7. doi: 10.1172/JCI130728
70. Dapunt U, Giese T, Prior B, Gaida MM, Hansch GM. Infectious versus non-infectious loosening of implants: activation of T lymphocytes differentiates between the two entities. *Int Orthop* (2014) 38(6):1291–6. doi: 10.1007/s00264-014-2310-5
71. Kumar G, Roger PM, Ticchioni M, Trojani C, Bernard de Dompsur R, Bronsard N, et al. T cells from chronic bone infection show reduced proliferation and a high proportion of CD28(-) CD4 T cells. *Clin Exp Immunol* (2014) 176(1):49–57. doi: 10.1111/cei.12245
72. Wagner C, Heck D, Lautenschlager K, Iking-Konert C, Heppert V, Wentzensen A, et al. T lymphocytes in implant-associated posttraumatic osteomyelitis: Identification of cytotoxic T effector cells at the site of infection. *Shock* (2006) 25(3):241–6. doi: 10.1097/01.shk.0000192119.68295.14
73. Kotsougiani D, Pioch M, Prior B, Heppert V, Hansch GM, Wagner C. Activation of T Lymphocytes in Response to Persistent Bacterial Infection: Induction of CD11b and of Toll-Like Receptors on T Cells. *Int J Inflam* (2010) 2010:526740. doi: 10.4061/2010/526740
74. Lee JY, Han AR, Lee DR. T Lymphocyte Development and Activation in Humanized Mouse Model. *Dev Reprod* (2019) 23(2):79–92. doi: 10.12717/DR.2019.23.2.079
75. Billerbeck E, Barry WT, Mu K, Dorner M, Rice CM, Ploss A. Development of human CD4+FoxP3+ regulatory T cells in human stem cell factor-, granulocyte-macrophage colony-stimulating factor-, and interleukin-3-expressing NOD-SCID IL2Rgamma(null) humanized mice. *Blood* (2011) 117(11):3076–86. doi: 10.1182/blood-2010-08-301507
76. Wunderlich M, Chou FS, Link KA, Mizukawa B, Perry RL, Carroll M, et al. AML xenograft efficiency is significantly improved in NOD/SCID-IL2RG mice constitutively expressing human SCF, GM-CSF and IL-3. *Leukemia* (2010) 24(10):1785–8. doi: 10.1038/leu.2010.158

Conflict of Interest: The authors declare that the research was conducted in the absence of any commercial or financial relationships that could be construed as a potential conflict of interest.

frontiers in Immunology

MINI REVIEW
published: 23 March 2021
doi: 10.3389/fimmu.2021.640918

Modification of EBV Associated Lymphomagenesis and Its Immune Control by Co-Infections and Genetics in Humanized Mice

*Patrick Schuhmachers and Christian Münz**

Viral Immunobiology, Institute of Experimental Immunology, University of Zürich, Zürich, Switzerland

Epstein Barr virus (EBV) is one of the most successful pathogens in humans with more than 95% of the human adult population persistently infected. EBV infects only humans and threatens these with its potent growth transforming ability that readily allows for immortalization of human B cells in culture. Accordingly, it is also found in around 1-2% of human tumors, primarily lymphomas and epithelial cell carcinomas. Fortunately, however, our immune system has learned to control this most transforming human tumor virus in most EBV carriers, and it requires modification of EBV associated lymphomagenesis and its immune control by either co-infections, such as malaria, Kaposi sarcoma associated herpesvirus (KSHV) and human immunodeficiency virus (HIV), or genetic predispositions for EBV positive tumors to emerge. Some of these can be modelled in humanized mice that, therefore, provide a valuable platform to test curative immunotherapies and prophylactic vaccines against these EBV associated pathologies.

Keywords: cytotoxic lymphocytes, human immunodeficiency virus (HIV), Kaposi sarcoma associated herpesvirus (KSHV), HLA-DRB1*1501, mutant Epstein Barr viruses (EBVs)

OPEN ACCESS

Edited by:
Yan Li,
Nanjing University, China

Reviewed by:
Benjamin E. Gewurz,
Brigham and Women's Hospital and Harvard Medical School, United States
Masakazu Kamata,
University of Alabama at Birmingham, United States
Shannon Kenney,
University of Wisconsin–Milwaukee, United States

***Correspondence:**
Christian Münz
christian.muenz@uzh.ch

Specialty section:
This article was submitted to Viral Immunology, a section of the journal Frontiers in Immunology

Received: *12 December 2020*
Accepted: *08 March 2021*
Published: *23 March 2021*

Citation:
Schuhmachers P and Münz C (2021) Modification of EBV Associated Lymphomagenesis and Its Immune Control by Co-Infections and Genetics in Humanized Mice. Front. Immunol. 12:640918. doi: 10.3389/fimmu.2021.640918

INTRODUCTION ON EBV

The Epstein Barr virus (EBV) or human herpesvirus 4 (HHV4) is a ubiquitous human γ-herpesvirus that persistently infects more than 95% of the human population (1). In Sub-Saharan Africa, this percentage is already reached at 2 years of age, while in Europe and the US one third of the population acquires EBV at a later age (2). This delayed primary EBV infection bears the risk to develop into infectious mononucleosis (IM), an immunopathology due to massive anti-viral $CD8^+$ T cell expansion and the accompanying cytokine release (3). Especially $CD8^+$ T cells that recognize lytic EBV antigens, expressed during the viral infection program that produces viral particles, are increased to high frequencies during IM (4). Even so IM resolves in most cases, alterations in the resulting EBV specific immune response might be the reason for elevated risks for EBV associated Hodgkin's lymphoma and multiple sclerosis (MS) (5, 6).

In addition to immunopathologies due to altered or increased immune responses to EBV infection, this virus is primarily known for its oncogenic potential (7). It was originally discovered in endemic Burkitt's lymphoma (BL) of Sub-Saharan African children (8, 9). Furthermore, EBV can be found in a subset of Hodgkin's lymphoma (HL), diffuse large B cell lymphoma (DLBCL) and immunoblastic lymphomas during immune suppression after transplantation, such as post-

transplantation lymphoproliferative disease (PTLD), or during HIV co-infection (10). These are mostly B cell lymphomas, but also EBV associated natural killer (NK)/T cell lymphomas can occur, often after prolonged uncontrolled EBV infection (11). In addition, EBV is associated with epithelial cell derived nasopharyngeal carcinoma (NPC) and 10% of gastric carcinomas. These EBV associated malignancies mainly express latent EBV antigens that are not involved in infectious virus production but contain at least one of the main two EBV oncogenes, nuclear antigen 2 (EBNA2) and latent membrane protein 1 (LMP1) (12, 13). Latent EBV infection follows a pre-latent phase upon B cell entry during which a set of both lytic and latent antigens are expressed in order to support B cell activation, proliferation and survival [as reviewed in (14)]. During latent infection, which is the default gene expression program upon B cell infection by EBV, up to 6 EBNAs, two LMPs as well as non-translated Epstein–Barr virus-encoded small RNAs (EBERs) and miRNAs are expressed. This gene expression program is thought to drive EBV infected B cells after viral transmission *via* saliva in sub-mucosal secondary lymphoid tissues like tonsils into activation and differentiation to memory B cells, in which EBV then persists for life (15). From this memory B cell compartment, in which EBV only expresses non-translated RNAs, lytic reactivation and infectious virus production occurs after plasma cell differentiation, presumably after encountering the cognate antigen of the B cell receptor of the infected cell (16). At submucosal secondary lymphoid tissues this might lead to viral shedding into saliva for transmission. The distinct B cell differentiation stages and their respective EBV gene expression patterns can also be found in the EBV associated malignancies, and the respective B cell lymphomas (BL, HL and DLBCL) increase in frequency during iatrogenic or HIV induced immune suppression (10, 17). This suggests that immune responses prevent transition from premalignant latent EBV infections to overt tumors. Indeed, primary immunodeficiencies that affect individual genes map to cytotoxic lymphocytes and their ability to kill EBV infected B cells as the most important component of EBV specific immune control (18–20). In order to interrogate the function of the in patients identified genes, dissect the contribution of viral genes with EBV mutants and characterize the influence of co-infections *in vivo*, preclinical mouse models with reconstituted human immune cells (humanized mice) have been developed and their contribution to a better understanding of EBV infection, oncogenesis and immune control will be summarized in this review.

EBV INFECTION, IMMUNE CONTROL, AND LYMPHOMAGENESIS IN HUMANIZED MICE

To date humanized mice serve as a reliable model to study pathogens that exclusively target humans. In the past decades, several humanized mouse models were established that responded to infection with EBV and allowed for assessing the importance of host immune factors as well as viral proteins during an infection. In this review, we will primarily focus on NOD/Shi-scid/IL-2Rγ^{null} (NOG) and NOD/LtSz-scid IL2Rγ^{null} (NSG) mice with and without HLA-A2 transgenes as well as NSG or NOD/LtSz-scid mice implanted with human fetal liver and thymus tissue (BLT) that were all either neonatally or as adult mice reconstituted with human immune system components by transfer of human CD34$^+$ hematopoietic progenitor cells (HPCs) or of cord blood often after CD34$^+$ HPC depletion. Most studies with EBV infection have been performed in these particular humanized mouse models and these were consistently permissive for multiple EBV strains (21–25), mirroring acute infection as well as EBV associated lymphomagenesis of humans. A more complete overview of humanized mouse models was recently published (26). As is the case for humans, human B cells constitute the main reservoir for EBV in humanized mice, enabling viral replication and lymphoproliferation. EBV infection of humanized mice was therefore marked by viral loads in blood and secondary lymphoid organs (22, 24, 27, 28).

Analogously to acute symptomatic primary infection in humans (29–31), the number of NK cells in peripheral blood and spleen of humanized NSG mice increases starting at three weeks of EBV infection and peaks at week four. The NK cell response constitutes an important measure to prevent uncontrolled lytic EBV infection and to bridge the time until adaptive T cell responses are primed. Indicative of this is that depletion of NK populations in humanized NSG mice resulted in higher viral loads and tumor incidence (32, 33).

Initial control by NK cells is succeeded by priming and expansion of cytotoxic CD8$^+$ T lymphocytes (CTLs) in peripheral blood. Those CTLs are mainly specific for lytic antigens (22, 25, 34, 35) and exhibit a cytolytic effector profile determined by high expression of activation molecules like HLA-DR or 2B4 and cytotoxic effector molecules such as Granzyme B (22, 25, 35). Consequently, expression of HLA-DR positively correlates with increasing viral loads in infected humanized NSG mice (36). In contrast to CTL expansion, CD4$^+$ helper T cells do not expand to a similar degree which is why an inversion of the CD8 to CD4 T cell ratio is one of the hallmarks of EBV infection in humanized mice as is in humans suffering from IM (25, 34). Despite lower expansion rates and total numbers, CD4$^+$ T cell help seems to be required to tackle the infection in humanized mice since CD4$^+$ T cell depletion prior to infection results in higher viral loads (22). This corresponds to human data depicting a cytolytic effector function of EBV specific CD4$^+$ T cells during infection (37, 38).

In contrast to T cell responses, antibody mediated responses to EBV are not yet as well characterized in humanized mice. In humanized NOG and NSG mice, IgM responses to BFRF3 and EBNA1, respectively, were observed. Detection of EBV specific IgG antibodies, however, has proven to be more difficult. This drawback might arise from deficiencies in germinal center formation and therefore difficulties in antibody isotype class switching as well as inefficient B cell development in several humanized mouse systems (22, 39–43). There are, however, promising developments in the generation of humanized mice capable of mounting IgG responses to pathogens (44, 45).

Despite active immune control of EBV infection, lymphoma formation can be observed in humanized mice. The degree of lymphomagenesis is thereby dependent on the amount of viral particles with which the animal is challenged. Humanized NSG mice, for example, present in 20 – 30% of cases with disseminated lymphomas in spleen, liver, lymph nodes or kidney when challenged intraperitoneally with high dose EBV (10^5 infectious particles) for four to five weeks (46, 47). Other mouse models, as for example humanized BALB/c $Rag2^{null}IL2r\gamma^{null}$ $Sirpa^{NOD}$ (BRGS) mice, present with higher lymphoma incidences of up to 75% while surviving four weeks of infection (48). Besides that, lymphomagenesis may be dependent on genomic or host immunologic alterations which will be discussed in the following sections.

ALTERED EBV PATHOLOGY DUE TO GENETIC ALTERATIONS IN THE VIRAL GENOME

Since the discovery that humanized mice are susceptible to EBV infection and allow for the identification of host immune factors in response to the pathogen, several groups started assessing the importance of viral genes during infection. For example, infection of a humanized BRGS mouse with type 1 or 2 EBV strains was examined. The two EBV strains differ mainly in their genetic sequence of the latent genes EBNA2, EBNA3A and EBNA3C (49–51) and, consequently, in their ability to transform infected cells *in vitro*. More importantly, in contrast to EBV type 1, EBV type 2 was additionally observed to be human T cell tropic which could explain findings of EBV related human T cell lymphomas (48). *Coleman and colleagues* were able to reproduce T cell tropism of EBV type 2 *in vivo*. However, the infection of humanized mice with either strain resulted in comparable degrees of viral replication and lymphomagenesis contrasting the *in vitro* findings. Lymphomas caused by both strains exhibited similar features, resembling diffuse large B cell lymphomas (DLBCL) and expressing all latent EBV gene products (48, 52). The strain specific differences that underlie *in vivo* infection seem, for now, to be limited to lower LMP1 expression levels and higher lytic activity in EBV type 2 infected animals (52). Still, the reason why the two EBV strains developed different strategies, remains elusive. In addition to EBV type 2 that is primarily found in Sub-Saharan Africa (53), also Asian EBV strains present with higher lytic EBV replication, and this also extends to infections of humanized mice (21, 54, 55).

Apart from defining differences between the virus strains, various gene loci of EBV type 1 were extensively studied in the past decades using humanized mice (**Figure 1**). *White and colleagues* investigated the contribution of EBNA3B to infection. In their study, they infected humanized NSG mice with the B95-8 (EBV type 1) strain of EBV which lacked the EBNA3B gene locus. Interestingly, the absence of EBNA3B led to higher tumor incidences in those mice which *White and colleagues* assigned to higher replicative activity of infected cells and a lower level of T cell infiltration into tumors due to decreased expression of chemoattractants as for example CXCL9 and CXCL10 (56). A lower degree of T cell infiltration is thereby in line with EBNA3B being often targeted by T cells (57).

In addition to T cell infiltration, the importance of MHC class I restricted antigen presentation for EBV specific immune control by $CD8^+$ T cells in humanized mice was demonstrated with a B95-8 virus that lacks the viral miRNAs (36). These compromise antigen processing for MHC class I presentation (58). In their absence EBV is more efficiently immune controlled in humanized mice in a $CD8^+$ T cell dependent manner. In contrast to miRNA deficiency, EBER knock-out EBV infects humanized mice similarly to wild-type virus (59), except for the increased inflammation promoting potential of EBER2 of some Asian EBV strains (55).

Other studies on B95-8 viruses lacking the EBNA3A or EBNA3C gene locus highlighted that these genes are dispensable for establishment of persistent infection *in vivo*. Despite findings suggesting that EBNA3A or 3C knockout viruses are hardly able to transform B cells *in vitro*, persistence was established in secondary lymphoid organs and blood over a period of three months and T cell responses were mounted against the virus. Lack of EBNA3A or 3C, however, seems to result in decreased aggressiveness of EBV infection as viral loads were lower and the tumorigenic potential was presumably lost (60). Studies in cord blood reconstituted humanized NSG mice in which T cells might exert less immune control due to efficient inhibitory receptor engagement and in which higher frequencies of EBV associated lymphomas are observed (61), came to similar conclusions regarding a decreased aggressiveness in the absence of EBNA3A and 3C. However, EBNA3A mutants could not only establish persistent infection in this model, but tumorigenic potential was delayed and not lost. Still, both studies observed decreased LMP1 expression levels in infected cells in spleen and tumor tissue (60, 62). In addition, the use of a complete EBNA3A knockout virus (60) compared to an EBV mutant with only decreased EBNA3A expression (62) might explain differences in the viruses' tumorigenic potential. In the same cord blood reconstituted humanized NSG mouse model, EBNA3C knockout EBV was able to cause lymphomas with lower frequency. Similar to EBNA3A hypomorphic EBV, lymphoma formation seemed to be delayed (52). Therefore, in humanized mice with diminished immune control, decreased EBNA3A or absent EBNA3C expression might still allow for the delayed development of EBV associated diffuse large B cell lymphomas.

Furthermore, LMP1 and 2 might also be dispensable for EBV infection in humanized mice (63, 64), but their absence delays lymphomagenesis. In the case of LMP1 deficiency the observed lymphoma formation required $CD4^+$ T cell help (63).

Surprisingly also lytic EBV reactivation, at least early lytic gene expression, seems to promote lymphomagenesis in humanized mice. B95-8 EBV infection caused less tumors in the absence of the immediate early transactivation factor BZLF1 that induces lytic reactivation (23, 46). Vice versa, BZLF1 promotors that enhance lytic EBV infection are associated with increased lymphoma formation (65, 66). Infection of humanized mice with mutant EBV viruses can therefore reveal the function

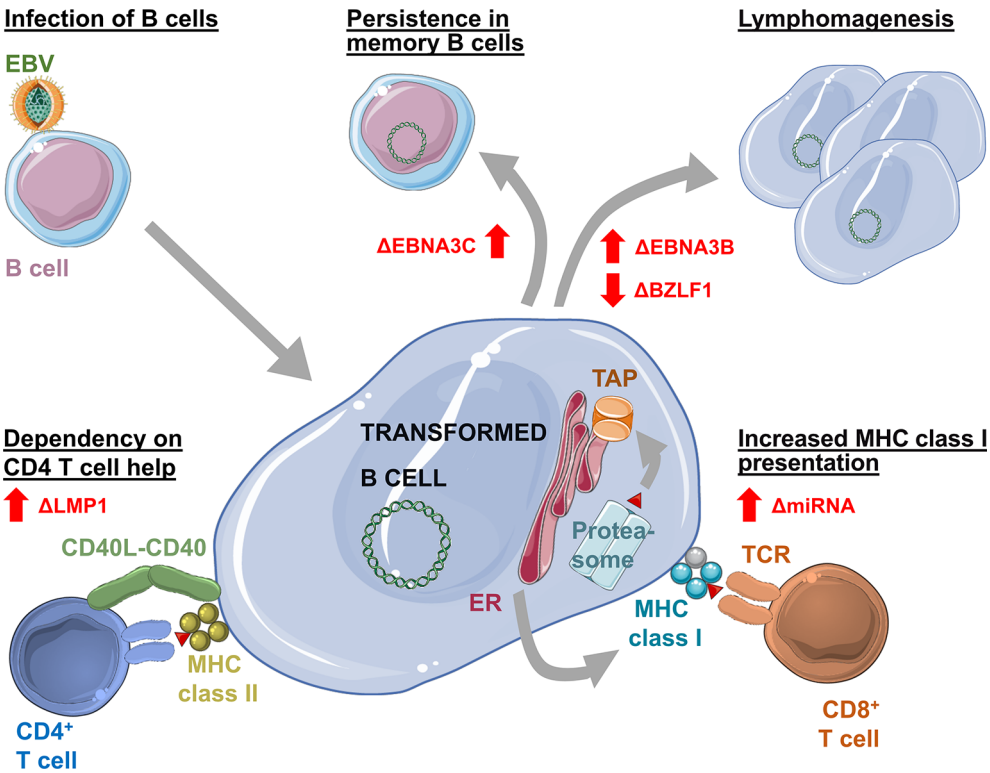

FIGURE 1 | Changes in Epstein Barr virus (EBV) infection, pathogenesis and immune control as revealed by infection of humanized mice with mutant viruses. Elimination of EBNA3C (ΔEBNA3C) allows establishment of persistent EBV infection without transformation. Loss of EBNA3B (ΔEBNA3B) increases and loss of BZLF1 (ΔBZLF1) decreases EBV associated lymphomagenesis. Loss of viral miRNAs (ΔmiRNA) leads to increased expression of the antigen processing machinery for MHC class I presentation, allowing for improved immune control by $CD8^+$ T cells. Deficiency in LMP1 (ΔLMP1) causes dependency on $CD4^+$ T cell help for EBV induced B cell transformation.

of genetic variability or viral gene products, enabling further insights into the life cycle of EBV *in vivo*.

MODIFICATION OF EBV SPECIFIC IMMUNE CONTROL BY HOST GENETICS AND MANIPULATION OF HUMAN IMMUNE COMPARTMENTS

In addition to testing mutant EBV viruses and different viral isolates *in vivo*, humanized mice also allow interrogation of human genetic variation, gene products and leucocyte compartments during EBV infection, oncogenesis and immune control. With regards to genetic variation IM and elevated antibody responses against EBV nuclear antigen 1 (EBNA1) have been found to synergize with the MHC class II molecule HLA-DRB1*1501 to increase risk for the development of MS (5). Indeed, HLA-DRB1*1501 restricted EBNA1 specific $CD4^+$ T cell responses are also elevated in MS patients (67–69). However, despite elevated T cell responses to EBV infection in humanized mice that have been reconstituted from HLA-DRB1*1501 donors, these animals experience higher viral loads (70). Furthermore, the respective HLA-DRB1*1501 restricted $CD4^+$ T cells that recognize EBV transformed B cells (lymphoblastoid cell lines or LCL) cross-react with myelin basic protein (MBP), an autoantigen in MS. These findings suggest that EBV is inefficiently immune controlled in the context of HLA-DRB1*1501 and that the resulting increased numbers of EBV infected B cells might stimulate in turn myelin antigen specific autoreactive T cell responses to cause MS.

Indeed $CD4^+$ T cell responses seem essential to maintain efficient immune control of EBV in humanized mice. Both, iatrogenic immune suppression with tacrolimus (FK506) that mainly affects $CD4^+$ T cell activation and expansion after EBV infection of humanized mice, and $CD4^+$ T cell depletion by HIV co-infection leads to elevated viral loads and increased EBV associated B cell lymphoma formation (71, 72). During HIV co-infection $CD8^+$ T cell depletion does not further increase EBV viral loads or lymphoma formation (72). This suggests that HIV induced $CD4^+$ T cell depletion compromises T cell help to maintain protective $CD8^+$ T cell function because $CD8^+$ T cell depletion during only EBV infection of humanized mice significantly affects immune control (22, 36, 72, 73). Moreover, antibody mediated depletion of both $CD4^+$ and $CD8^+$ T cells increases viral loads and associated tumors in EBV infected humanized mice (22, 43). In addition, antibody blocking of 2B4, a co-stimulatory molecule on cytotoxic lymphocytes that uses SLAM-associated protein (SAP), and SAP is mutated in X-linked

lymphoproliferative disease 1 (XLP1) thereby predisposing for EBV associated pathology, increases EBV viral loads and lymphomagenesis in humanized mice (73). 2B4 blocking on top of $CD8^+$ T cell depletion does not lower EBV specific immune control further, suggesting that 2B4 is mainly required on $CD8^+$ T cells to suppress EBV infection. SAP deficiency is, however, also associated with loss of invariant NKT cells (74) which have been shown to restrict EBV transformed B cells in humanized mice (75, 76). This could also contribute to compromised immune control of EBV in XLP1. Moreover, antibody blocking of PD-1, an inhibitory receptor on both effector and regulatory T cells, increases EBV loads and lymphomagenesis in infected humanized NSG mice engrafted with human $CD34^+$ HPCs (26, 35). This loss of immune control correlates with immune suppressive cytokine and regulatory T cell amounts in anti-PD-1 treated and EBV infected humanized mice. Strikingly, blocking PD-1 and/or CTLA-4 in cord blood reconstituted humanized NSG mice resulted in decreased tumor formation (61). As cord blood reconstituted humanized NSG mice seem to develop weaker T cell mediated immune control after EBV infection and allow for higher frequencies of EBV associated lymphomas, especially after infection with the lytic M81 EBV strain, PD-1 and CTLA-4 blockade might be required to strengthen this immune control (61) which seems to be in part based on Vγ9Vδ2 T cells (77). Thus, composition of the T cell compartment and balance between regulatory and anti-viral T cells might determine the outcome of PD-1 and CTLA-4 blockade. However, genetic loss of CTLA-4 seems to be associated with EBV associate pathologies in some of the affected individuals (78). Similarly, PD-1 blockade seems to cause loss of EBV specific immune control and brain homing of EBV infected B cells in a subgroup of treated patients (79).

In addition to T cells, innate lymphocytes contribute to EBV specific immune control. Protection against EBV infection of humanized mice has been shown for NK, NKT and Vγ9Vδ2 T cells (32, 33, 75, 77, 80). Early differentiated $NKG2A^+KIR^-$ NK cells restrict primarily lytic EBV replication and degranulate their cytotoxic machinery toward lytically EBV replicating BL cells (29, 32). In contrast, depletion of plasmacytoid dendritic cells, the main hematopoietic source of type I interferon (IFN) during viral infections, does not significantly influence EBV infection of humanized mice (81). Accordingly, type I IFN signaling deficiencies do not predispose for EBV associated pathologies (19). These studies demonstrate that humanized mice can be used to interrogate the role of genetic variations, of leucocyte compartments and of their receptors in EBV specific immune control.

ALTERATION OF EBV ASSOCIATED PATHOGENESIS BY CO-INFECTION

In addition to HIV infection, some EBV associated malignancies are also observed during additional co-infections. Endemic BL can be primarily observed in geographic areas of holoendemic exposure to the malaria parasite *Plasmodium falciparum* (82, 83). In Sub-Saharan Africa, where Denis Burkitt described this tumor for the first time (84), Kaposi sarcoma associated herpesvirus (KSHV) or human herpesvirus 8 (HHV8) a another pathogen with which EBV interacts during co-infections is also highly prevalent (85). Both EBV and KSHV are found in the tumor cells of 90% of primary effusion lymphomas (PELs) (10). Moreover, KSHV infection seems to benefit from EBV co-infection for persistence (47, 86–88). Humanized mice that are infected with both KSHV and EBV develop B cell lymphomas with higher incidence (47). The developing lymphomas harbor both EBV and KSHV (**Figure 2**). They present with hallmarks of plasma cell differentiation that is characteristic for PELs (89). Interestingly, this plasma cell differentiation that is also in healthy EBV carriers associated with lytic EBV replication (16), causes elevated induction of at least early lytic EBV reactivation in PEL-like tumors of double-infected humanized mice (47). Co-infection with an EBV mutant that can no longer activate lytic infection (BZLF1 deficient EBV), reduces lymphomagenesis during EBV and KSHV co-infection of humanized mice, suggesting that the transactivated lytic EBV gene expression might contribute to conditioning of the tumor microenvironment for efficient growth (7).

HIV co-infection also does more than just suppress EBV specific immune control. It was noted that anti-retroviral therapy (ART) reduced immunoblastic EBV associated lymphomas in HIV infected individuals, while BL and HL frequencies did not decline (17). Similarly, in humanized mice HIV co-infection influences EBV infected B cells directly (72). It was found that HIV is capable to infect EBV transformed B cells due to CD4 up-regulation during EBV infection and maintained CXCR4 expression on human B cells (**Figure 2**). HIV also integrates and replicates in EBV infected B cells but alters their gene expression pattern for enhanced antigen processing toward MHC class I restricted antigen presentation. Accordingly, HIV and EBV infected B cells are efficiently recognized by both EBV and HIV specific $CD8^+$ T cells and mainly accumulate in double-infected humanized mice after $CD8^+$ T cell depletion. Future studies will need to show if double-infected B cells alter EBV associated lymphoma formation over a longer observation period, independent of HIV induced immune suppression.

CONCLUSIONS AND OUTLOOK

In summary, the development of humanized mice revolutionized the study of pathogens exclusive to humans such as EBV. The possibility to use small rodents instead of endangered New World monkeys (90, 91) greatly facilitated the research on host immune factors and viral genes during infection. Various humanized mouse models are consistently permissive for infection with and allow replication of EBV. Even more promising, these models mimic human lymphoproliferative diseases and the reaction of human immune system components to infection. In addition, host and virus genetic alterations and their implications in disease outcome may be more extensively studied in humanized mice which may not be comparably easy in humans. Further studies on host susceptibility factors like HLA-DRB1*1501 are needed to

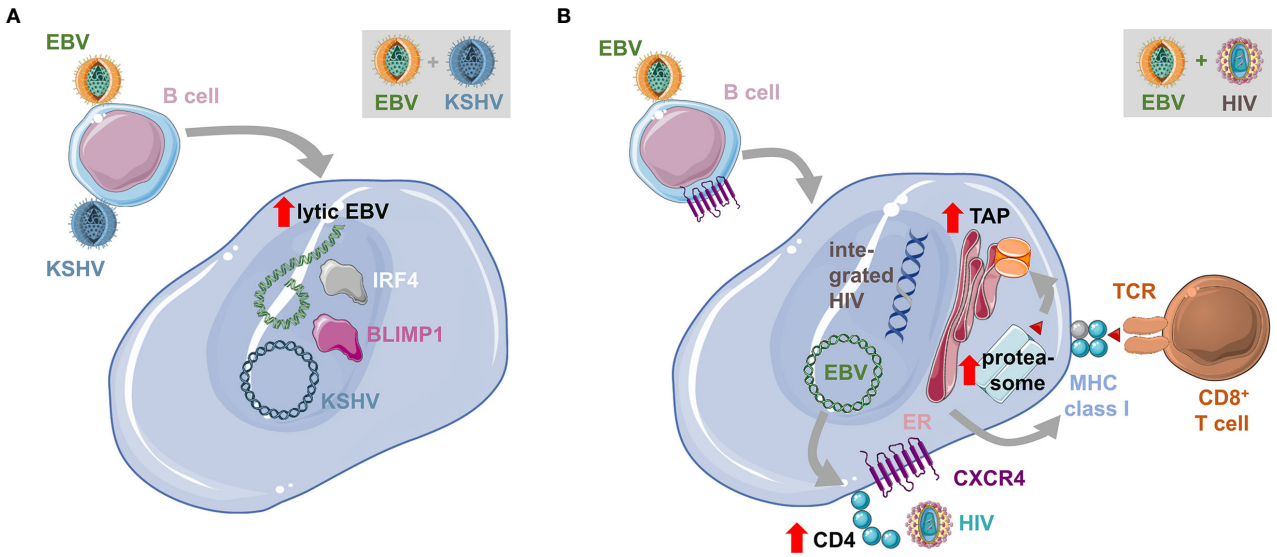

FIGURE 2 | Influence of co-infections on EBV transformed B cells. **(A)** Co-infection with the Kaposi sarcoma associated herpesvirus (KSHV) transactivates lytic EBV replication and is associated with plasma cell differentiation, characterized for example by BLIMP1 and IRF4 expression. This leads to enhanced lymphomagenesis and the resulting tumors have characteristics of primary effusion lymphomas (PELs). **(B)** EBV infection of B cells up-regulates CD4 and with the sustained expression of CXCR4 renders EBV transformed B cells susceptible to infection with the human immunodeficiency virus (HIV). This leads to the integration of the reverse transcribed HIV genome into the host cell genome. Double-infected B cells up-regulate the antigen processing machinery for MHC class I presentation and are therefore efficiently immune controlled by $CD8^+$ T cells.

assess additional groups at risk of developing EBV associated diseases and to develop personalized treatments in the future. Similarly, the interplay between EBV and other co-infecting pathogens is difficult to assess in humans but may be elucidated in humanized mice. Thus, with humanized mice it became feasible to study not only contributions of single immune cell types or single molecules to infection outcome but also to investigate the importance of virus and host genetics. The findings resulting from infection models in humanized mice thereby enable applied research on EBV vaccines, or the development of new treatments against EBV induced lymphomas.

Despite these advantages there are still limitations to each of the humanized mouse models employed. The biggest limitation with respect to EBV infection is that humanized mice do not support infection of oropharyngeal epithelia. In humans the infection starts in the oropharynx with a complex interplay between submucosal B cells and polarized epithelia. Therefore, EBV's complete life cycle cannot be mimicked thus far. Furthermore, most models failed to mount proper antibody responses to EBV which is why their contribution to infection could not yet be well studied using a mouse model. Reports on new humanized mouse models with improved seroconversion to IgG, however, seem promising in solving this problem (44, 92). A further limitation of the presented EBV infection models is that in most cases lymphomas with expression of all latent EBV genes develop. As a result, the in humans more prominent HL or BL with restricted latent gene expression cannot currently be modelled in humanized mice and therefore such models still have to be developed. Along these lines infection with EBNA2 deficient EBV has recently been reported to cause lymphomas with some HL characteristics and might be further explored to gain insights into this EBV associated malignancy (93). With further developments of humanized mice in the upcoming years we may be able to reveal even minor host and viral genetic as well as host immune factors that contribute to control of EBV infection. Thus, we may be able to use the gained knowledge to design vaccines or therapies against this most transforming human tumor virus.

AUTHOR CONTRIBUTIONS

PS and CM wrote the manuscript. All authors contributed to the article and approved the submitted version.

FUNDING

Our research is supported by Cancer Research Switzerland (KFS-4962-02-2020), CRPP-Precision^{MS} and HMZ ImmunoTargET of the University of Zurich, the Cancer Research Center Zurich, the Baugarten Foundation, the Sobek Foundation, the Swiss Vaccine Research Institute, Roche, Novartis, Novartis Foundation (20B099), and the Swiss National Science Foundation (310030B_182827, 310030L_197952/1 and CRSII5_180323).

REFERENCES

1. Ehlers B, Spiess K, Leendertz F, Peeters M, Boesch C, Gatherer D, et al. Lymphocryptovirus phylogeny and the origins of Epstein-Barr virus. *J Gen Virol* (2010) 91:630–42. doi: 10.1099/vir.0.017251-0
2. Dunmire SK, Verghese PS, Balfour HHJr. Primary Epstein-Barr virus infection. *J Clin Virol* (2018) 102:84–92. doi: 10.1016/j.jcv.2018.03.001
3. Luzuriaga K, Sullivan JL. Infectious mononucleosis. *N Engl J Med* (2010) 362:1993–2000. doi: 10.1056/NEJMcp1001116
4. Callan MF, Tan L, Annels N, Ogg GS, Wilson JD, O'Callaghan CA, et al. Direct visualization of antigen-specific $CD8^+$ T cells during the primary immune response to Epstein-Barr virus In vivo. *J Exp Med* (1998) 187:1395–402. doi: 10.1084/jem.187.9.1395
5. Olsson T, Barcellos LF, Alfredsson L. Interactions between genetic, lifestyle and environmental risk factors for multiple sclerosis. *Nat Rev Neurol* (2017) 13:25–36. doi: 10.1038/nrneurol.2016.187
6. Hjalgrim H, Askling J, Rostgaard K, Hamilton-Dutoit S, Frisch M, Zhang JS, et al. Characteristics of Hodgkin's lymphoma after infectious mononucleosis. *N Engl J Med* (2003) 349:1324–32. doi: 10.1056/NEJMoa023141
7. Münz C. Latency and lytic replication in the oncogenesis of the Epstein Barr virus. *Nat Rev Micobiol* (2019) 17:691–700. doi: 10.1038/s41579-019-0249-7
8. Epstein MA, Achong BG, Barr YM. Virus particles in cultured lymphoblasts from Burkitt's lymphoma. *Lancet* (1964) 1:702–3. doi: 10.1016/S0140-6736(64)91524-7
9. Epstein MA, Henle G, Achong BG, Barr YM. Morphological and biological studies on a virus in cultured lymphoblasts from Burkitt's lymphoma. *J Exp Med* (1964) 121:761–70. doi: 10.1084/jem.121.5.761
10. Shannon-Lowe C, Rickinson A. The Global Landscape of EBV-Associated Tumors. *Front Oncol* (2019) 9:713. doi: 10.3389/fonc.2019.00713
11. Fournier B, Boutboul D, Bruneau J, Miot C, Boulanger C, Malphettes M, et al. Rapid identification and characterization of infected cells in blood during chronic active Epstein-Barr virus infection. *J Exp Med* (2020) 217:e20192262. doi: 10.1084/jem.20192262
12. Kempkes B, Ling PD. EBNA2 and Its Coactivator EBNA-LP. *Curr Top Microbiol Immunol* (2015) 391:35–59. doi: 10.1007/978-3-319-22834-1_2
13. Kieser A, Sterz KR. The Latent Membrane Protein 1 (LMP1). *Curr Top Microbiol Immunol* (2015) 391:119–49. doi: 10.1007/978-3-319-22834-1_4
14. Kalla M, Hammerschmidt W. Human B cells on their route to latent infection-early but transient expression of lytic genes of Epstein-Barr virus. *Eur J Cell Biol* (2012) 91:65–9. doi: 10.1016/j.ejcb.2011.01.014
15. Babcock JG, Hochberg D, Thorley-Lawson AD. The expression pattern of Epstein-Barr virus latent genes in vivo is dependent upon the differentiation stage of the infected B cell. *Immunity* (2000) 13:497–506. doi: 10.1016/S1074-7613(00)00049-2
16. Laichalk LL, Thorley-Lawson DA. Terminal differentiation into plasma cells initiates the replicative cycle of Epstein-Barr virus in vivo. *J Virol* (2005) 79:1296–307. doi: 10.1128/JVI.79.2.1296-1307.2005
17. Totonchy J, Cesarman E. Does persistent HIV replication explain continued lymphoma incidence in the era of effective antiretroviral therapy? *Curr Opin Virol* (2016) 20:71–7. doi: 10.1016/j.coviro.2016.09.001
18. Damania B, Münz C. Immunodeficiencies that predispose to pathologies by human oncogenic gamma-herpesviruses. *FEMS Microbiol Rev* (2019) 43:181–92. doi: 10.1093/femsre/fuy044
19. Latour S, Fischer A. Signaling pathways involved in the T-cell-mediated immunity against Epstein-Barr virus: Lessons from genetic diseases. *Immunol Rev* (2019) 291:174–89. doi: 10.1111/imr.12791
20. Tangye SG, Latour S. Primary immunodeficiencies reveal the molecular requirements for effective host defense against EBV infection. *Blood* (2020) 135:644–55. doi: 10.1182/blood.2019000928
21. Tsai MH, Lin X, Shumilov A, Bernhardt K, Feederle R, Poirey R, et al. The biological properties of different Epstein-Barr virus strains explain their association with various types of cancers. *Oncotarget* (2017) 8:10238–54. doi: 10.18632/oncotarget.14380
22. Strowig T, Gurer C, Ploss A, Liu YF, Arrey F, Sashihara J, et al. Priming of protective T cell responses against virus-induced tumors in mice with human immune system components. *J Exp Med* (2009) 206:1423–34. doi: 10.1084/jem.20081720
23. Ma SD, Hegde S, Young KH, Sullivan R, Rajesh D, Zhou Y, et al. A new model of Epstein-Barr virus infection reveals an important role for early lytic viral protein expression in the development of lymphomas. *J Virol* (2011) 85:165–77. doi: 10.1128/JVI.01512-10
24. Yajima M, Imadome K, Nakagawa A, Watanabe S, Terashima K, Nakamura H, et al. A new humanized mouse model of Epstein-Barr virus infection that reproduces persistent infection, lymphoproliferative disorder, and cell-mediated and humoral immune responses. *J Infect Dis* (2008) 198:673–82. doi: 10.1086/590502
25. Shultz LD, Saito Y, Najima Y, Tanaka S, Ochi T, Tomizawa M, et al. Generation of functional human T-cell subsets with HLA-restricted immune responses in HLA class I expressing NOD/SCID/IL2r gamma(null) humanized mice. *Proc Natl Acad Sci U S A* (2010) 107:13022–7. doi: 10.1073/pnas.1000475107
26. Stripecke R, Münz C, Schuringa JJ, Bissig KD, Soper B, Meeham T, et al. Innovations, challenges, and minimal information for standardization of humanized mice. *EMBO Mol Med* (2020) 12:e8662. doi: 10.15252/emmm.201708662
27. Islas-Ohlmayer M, Padgett-Thomas A, Domiati-Saad R, Melkus MW, Cravens PD, Martin Mdel P, et al. Experimental infection of NOD/SCID mice reconstituted with human $CD34^+$ cells with Epstein-Barr virus. *J Virol* (2004) 78:13891–900. doi: 10.1128/JVI.78.24.13891-13900.2004
28. Melkus MW, Estes JD, Padgett-Thomas A, Gatlin J, Denton PW, Othieno FA, et al. Humanized mice mount specific adaptive and innate immune responses to EBV and TSST-1. *Nat Med* (2006) 12:1316–22. doi: 10.1038/nm1431
29. Azzi T, Lunemann A, Murer A, Ueda S, Beziat V, Malmberg KJ, et al. Role for early-differentiated natural killer cells in infectious mononucleosis. *Blood* (2014) 124:2533–43. doi: 10.1182/blood-2014-01-553024
30. Williams H, McAulay K, Macsween KF, Gallacher NJ, Higgins CD, Harrison N, et al. The immune response to primary EBV infection: a role for natural killer cells. *Br J Haematol* (2005) 129:266–74. doi: 10.1111/j.1365-2141.2005.05452.x
31. Hendricks DW, Balfour HHJr., Dunmire SK, Schmeling DO, Hogquist KA, Lanier LL. Cutting edge: $NKG2C^{hi}CD57^+$ NK cells respond specifically to acute infection with cytomegalovirus and not Epstein-Barr virus. *J Immunol* (2014) 192:4492–6. doi: 10.4049/jimmunol.1303211
32. Chijioke O, Muller A, Feederle R, Barros MH, Krieg C, Emmel V, et al. Human natural killer cells prevent infectious mononucleosis features by targeting lytic Epstein-Barr virus infection. *Cell Rep* (2013) 5:1489–98. doi: 10.1016/j.celrep.2013.11.041
33. Landtwing V, Raykova A, Pezzino G, Beziat V, Marcenaro E, Graf C, et al. Cognate HLA absence in trans diminishes human NK cell education. *J Clin Invest* (2016) 126:3772–82. doi: 10.1172/JCI86923
34. Balfour HHJr., Odumade OA, Schmeling DO, Mullan BD, Ed JA, Knight JA, et al. Behavioral, virologic, and immunologic factors associated with acquisition and severity of primary epstein-barr virus infection in university students. *J Infect Dis* (2013) 207:80–8. doi: 10.1093/infdis/jis646
35. Chatterjee B, Deng Y, Holler A, Nunez N, Azzi T, Vanoaica LD, et al. $CD8^+$ T cells retain protective functions despite sustained inhibitory receptor expression during Epstein-Barr virus infection in vivo. *PLoS Pathog* (2019) 15:e1007748. doi: 10.1371/journal.ppat.1007748
36. Murer A, Ruhl J, Zbinden A, Capaul R, Hammerschmidt W, Chijioke O, et al. MicroRNAs of Epstein-Barr Virus Attenuate T-Cell-Mediated Immune Control In Vivo. *MBio* (2019) 10:e01941–18. doi: 10.1128/mBio.01482-19
37. Landais E, Saulquin X, Scotet E, Trautmann L, Peyrat MA, Yates JL, et al. Direct killing of Epstein-Barr virus (EBV)-infected B cells by CD4 T cells directed against the EBV lytic protein BHRF1. *Blood* (2004) 103:1408–16. doi: 10.1182/blood-2003-03-0930
38. Meckiff BJ, Ladell K, McLaren JE, Ryan GB, Leese AM, James EA, et al. Primary EBV Infection Induces an Acute Wave of Activated Antigen-Specific Cytotoxic $CD4^+$ T Cells. *J Immunol* (2019) 203:1276–87. doi: 10.4049/jimmunol.1900377
39. Rongvaux A, Willinger T, Martinek J, Strowig T, Gearty SV, Teichmann LL, et al. Development and function of human innate immune cells in a humanized mouse model. *Nat Biotechnol* (2014) 32:364–72. doi: 10.1038/nbt.2858
40. Lang JL, Kelly M, Freed BM, McCarter MD, Kedl RM, Torres RM, et al. Studies of Lymphocyte Reconstitution in a Humanized Mouse Model Reveal a

Requirement of T Cells for Human B Cell Maturation. *J Immunol* (2013) 190:2090–101. doi: 10.4049/jimmunol.1202810
41. Watanabe Y, Takahashi T, Okajima A, Shiokawa M, Ishii N, Katano I, et al. The analysis of the functions of human B and T cells in humanized NOD/shi-scid/gammac(null) (NOG) mice (hu-HSC NOG mice). *Int Immunol* (2009) 21:843–58. doi: 10.1093/intimm/dxp050
42. Gurer C, Strowig T, Brilot F, Pack M, Trumpfheller C, Arrey F, et al. Targeting the nuclear antigen 1 of Epstein-Barr virus to the human endocytic receptor DEC-205 stimulates protective T-cell responses. *Blood* (2008) 112:1231–9. doi: 10.1182/blood-2008-03-148072
43. Yajima M, Imadome K, Nakagawa A, Watanabe S, Terashima K, Nakamura H, et al. T cell-mediated control of Epstein-Barr virus infection in humanized mice. *J Infect Dis* (2009) 200:1611–5. doi: 10.1086/644644
44. Li Y, Masse-Ranson G, Garcia Z, Bruel T, Kok A, Strick-Marchand H, et al. A human immune system mouse model with robust lymph node development. *Nat Methods* (2018) 15:623–30. doi: 10.1038/s41592-018-0071-6
45. Jangalwe S, Shultz LD, Mathew A, Brehm MA. Improved B cell development in humanized NOD-scid IL2Rgamma(null) mice transgenically expressing human stem cell factor, granulocyte-macrophage colony-stimulating factor and interleukin-3. *Immun Inflamm Dis* (2016) 4:427–40. doi: 10.1002/iid3.124
46. Antsiferova O, Müller A, Rämer P, Chijioke O, Chatterjee B, Raykova A, et al. Adoptive transfer of EBV specific $CD8^+$ T cell clones can transiently control EBV infection in humanized mice. *PLoS Pathog* (2014) 10:e1004333. doi: 10.1371/journal.ppat.1004333
47. McHugh D, Caduff N, Barros MHM, Rämer P, Raykova A, Murer A, et al. Persistent KSHV infection increases EBV-associated tumor formation in vivo via enhanced EBV lytic gene expression. *Cell Host Microbe* (2017) 22:61–73. doi: 10.1016/j.chom.2017.06.009
48. Coleman CB, Lang J, Sweet LA, Smith NA, Freed BM, Pan Z, et al. Epstein-Barr Virus Type 2 Infects T Cells and Induces B Cell Lymphomagenesis in Humanized Mice. *J Virol* (2018) 92:e00813-818. doi: 10.1128/JVI.00813-18
49. Adldinger HK, Delius H, Freese UK, Clarke J, Bornkamm GW. A putative transforming gene of Jijoye virus differs from that of Epstein-Barr virus prototypes. *Virology* (1985) 141:221–34. doi: 10.1016/0042-6822(85)90253-3
50. Dambaugh T, Hennessy K, Chamnankit L, Kieff E. U2 region of Epstein-Barr virus DNA may encode Epstein-Barr nuclear antigen 2. *Proc Natl Acad Sci U S A* (1984) 81:7632–6. doi: 10.1073/pnas.81.23.7632
51. Sample J, Young L, Martin B, Chatman T, Kieff E, Rickinson A, et al. Epstein-Barr virus types 1 and 2 differ in their EBNA-3A, EBNA-3B, and EBNA-3C genes. *J Virol* (1990) 64:4084–92. doi: 10.1128/JVI.64.9.4084-4092.1990
52. Romero-Masters JC, Ohashi M, Djavadian R, Eichelberg MR, Hayes M, Bristol JA, et al. An EBNA3C-deleted Epstein-Barr virus (EBV) mutant causes B-cell lymphomas with delayed onset in a cord blood-humanized mouse model. *PLoS Pathog* (2018) 14:e1007221. doi: 10.1371/journal.ppat.1007221
53. Correia S, Bridges R, Wegner F, Venturini C, Palser A, Middeldorp JM, et al. Sequence Variation of Epstein-Barr Virus: Viral Types, Geography, Codon Usage, and Diseases. *J Virol* (2018) 92:e01132-18. doi: 10.1128/JVI.01132-18
54. Tsai MH, Raykova A, Klinke O, Bernhardt K, Gartner K, Leung CS, et al. Spontaneous lytic replication and epitheliotropism define an Epstein-Barr virus strain found in carcinomas. *Cell Rep* (2013) 5:458–70. doi: 10.1016/j.celrep.2013.09.012
55. Li Z, Tsai MH, Shumilov A, Baccianti F, Tsao SW, Poirey R, et al. Epstein-Barr virus ncRNA from a nasopharyngeal carcinoma induces an inflammatory response that promotes virus production. *Nat Microbiol* (2019) 4:2475–86. doi: 10.1038/s41564-019-0546-y
56. White RE, Ramer PC, Naresh KN, Meixlsperger S, Pinaud L, Rooney C, et al. EBNA3B-deficient EBV promotes B cell lymphomagenesis in humanized mice and is found in human tumors. *J Clin Invest* (2012) 122:1487–502. doi: 10.1172/JCI58092
57. Taylor GS, Long HM, Brooks JM, Rickinson AB, Hislop AD. The immunology of Epstein-Barr virus-induced disease. *Annu Rev Immunol* (2015) 33:787–821. doi: 10.1146/annurev-immunol-032414-112326
58. Albanese M, Tagawa T, Bouvet M, Maliqi L, Lutter D, Hoser J, et al. Epstein-Barr virus microRNAs reduce immune surveillance by virus-specific $CD8^+$ T cells. *Proc Natl Acad Sci U S A* (2016) 113:E6467–75. doi: 10.1073/pnas.1605884113
59. Gregorovic G, Boulden EA, Bosshard R, Karstegl CE, Skalsky R, Cullen BR, et al. Epstein-Barr viruses deficient in EBER RNAs give higher LMP2 RNA expression in lymphoblastoid cell lines and efficiently establish persistent infection in humanized mice. *J Virol* (2015) 89:11711–4. doi: 10.1128/JVI.01873-15
60. Murer A, McHugh D, Caduff N, Kalchschmidt JS, Barros MH, Zbinden A, et al. EBV persistence without its EBNA3A and 3C oncogenes in vivo. *PLoS Pathog* (2018) 14:e1007039. doi: 10.1371/journal.ppat.1007039
61. Ma SD, Xu X, Jones R, Delecluse HJ, Zumwalde NA, Sharma A, et al. PD-1/CTLA-4 Blockade Inhibits Epstein-Barr Virus-Induced Lymphoma Growth in a Cord Blood Humanized-Mouse Model. *PLoS Pathog* (2016) 12:e1005642. doi: 10.1371/journal.ppat.1005642
62. Romero-Masters JC, Ohashi M, Djavadian R, Eichelberg MR, Hayes M, Zumwalde NA, et al. An EBNA3A-Mutated Epstein-Barr Virus Retains the Capacity for Lymphomagenesis in a Cord Blood-Humanized Mouse Model. *J Virol* (2020) 94:e02168–19. doi: 10.1128/JVI.02168-19
63. Ma SD, Xu X, Plowshay J, Ranheim EA, Burlingham WJ, Jensen JL, et al. LMP1-deficient Epstein-Barr virus mutant requires T cells for lymphomagenesis. *J Clin Invest* (2015) 125:304–15. doi: 10.1172/JCI76357
64. Ma SD, Tsai MH, Romero-Masters JC, Ranheim EA, Huebner SM, Bristol J, et al. LMP1 and LMP2A collaborate to promote Epstein-Barr virus (EBV)-induced B cell lymphomas in a cord blood-humanized mouse model but are not essential. *J Virol* (2017) 91:e01928-16. doi: 10.1128/JVI.01928-16
65. Ma SD, Yu X, Mertz JE, Gumperz JE, Reinheim E, Zhou Y, et al. An Epstein-Barr Virus (EBV) mutant with enhanced BZLF1 expression causes lymphomas with abortive lytic EBV infection in a humanized mouse model. *J Virol* (2012) 86:7976–87. doi: 10.1128/JVI.00770-12
66. Bristol JA, Djavadian R, Albright ER, Coleman CB, Ohashi M, Hayes M, et al. A cancer-associated Epstein-Barr virus BZLF1 promoter variant enhances lytic infection. *PLoS Pathog* (2018) 14:e1007179. doi: 10.1371/journal.ppat.1007179
67. Lünemann JD, Edwards N, Muraro PA, Hayashi S, Cohen JI, Münz C, et al. Increased frequency and broadened specificity of latent EBV nuclear antigen-1-specific T cells in multiple sclerosis. *Brain* (2006) 129:1493–506. doi: 10.1093/brain/awl067
68. Lünemann JD, Jelcic I, Roberts S, Lutterotti A, Tackenberg B, Martin R, et al. EBNA1-specific T cells from patients with multiple sclerosis cross react with myelin antigens and co-produce IFN-g and IL-2. *J Exp Med* (2008) 205:1763–73. doi: 10.1084/jem.20072397
69. Wang J, Jelcic I, Muhlenbruch L, Haunerdinger V, Toussaint NC, Zhao Y, et al. HLA-DR15 Molecules Jointly Shape an Autoreactive T Cell Repertoire in Multiple Sclerosis. *Cell* (2020) 183:1264–81.e20. doi: 10.1016/j.cell.2020.09.054
70. Zdimerova H, Murer A, Engelmann C, Raykova A, Deng Y, Gujer C, et al. Attenuated immune control of Epstein-Barr virus in humanized mice is associated with the multiple sclerosis risk factor HLA-DR15. *Eur J Immunol* (2021) 51:64-75. doi: 10.1002/eji.202048655
71. Caduff N, McHugh D, Murer A, Ramer P, Raykova A, Landtwing V, et al. Immunosuppressive FK506 treatment leads to more frequent EBV-associated lymphoproliferative disease in humanized mice. *PLoS Pathog* (2020) 16:e1008477. doi: 10.1371/journal.ppat.1008477
72. McHugh D, Myburgh R, Caduff N, Spohn M, Kok YL, Keller CW, et al. EBV renders B cells susceptible to HIV-1 in humanized mice. *Life Sci Alliance* (2020) 3:e202000640. doi: 10.26508/lsa.202000640
73. Chijioke O, Marcenaro E, Moretta A, Capaul R, Munz C. The SAP-dependent 2B4 receptor mediates $CD8^+$ T cell dependent immune control of Epstein Barr virus infection in mice with reconstituted human immune system components. *J Infect Dis* (2015) 212:803–7. doi: 10.1093/infdis/jiv114
74. Pasquier B, Yin L, Fondaneche MC, Relouzat F, Bloch-Queyrat C, Lambert N, et al. Defective NKT cell development in mice and humans lacking the adapter SAP, the X-linked lymphoproliferative syndrome gene product. *J Exp Med* (2005) 201:695–701. doi: 10.1084/jem.20042432
75. Yuling H, Ruijing X, Li L, Xiang J, Rui Z, Yujuan W, et al. EBV-induced human $CD8^+$ NKT cells suppress tumorigenesis by EBV-associated malignancies. *Cancer Res* (2009) 69:7935–44. doi: 10.1158/0008-5472.CAN-09-0828
76. Chung BK, Tsai K, Allan LL, Zheng DJ, Nie JC, Biggs CM, et al. Innate immune control of EBV-infected B cells by invariant natural killer T cells. *Blood* (2013) 122:2600–8. doi: 10.1182/blood-2013-01-480665

77. Zumwalde NA, Sharma A, Xu X, Ma S, Schneider CL, Romero-Masters JC, et al. Adoptively transferred Vgamma9Vdelta2 T cells show potent antitumor effects in a preclinical B cell lymphomagenesis model. *JCI Insight* (2017) 2: e93179. doi: 10.1172/jci.insight.93179
78. Schwab C, Gabrysch A, Olbrich P, Patino V, Warnatz K, Wolff D, et al. Phenotype, penetrance, and treatment of 133 CTLA-4-insufficient individuals. *J Allergy Clin Immunol* (2018) 142:1932–46. doi: 10.1016/j.jaci.2018.02.055
79. Johnson DB, McDonnell WJ, Gonzalez-Ericsson PI, Al-Rohil RN, Mobley BC, Salem JE, et al. A case report of clonal EBV-like memory $CD4^+$ T cell activation in fatal checkpoint inhibitor-induced encephalitis. *Nat Med* (2019) 25:1243–50. doi: 10.1038/s41591-019-0523-2
80. Xiang Z, Liu Y, Zheng J, Liu M, Lv A, Gao Y, et al. Targeted activation of human Vgamma9Vdelta2-T cells controls epstein-barr virus-induced B cell lymphoproliferative disease. *Cancer Cell* (2014) 26:565–76. doi: 10.1016/j.ccr.2014.07.026
81. Gujer C, Murer A, Muller A, Vanoaica D, Sutter K, Jacque E, et al. Plasmacytoid dendritic cells respond to Epstein-Barr virus infection with a distinct type I interferon subtype profile. *Blood Adv* (2019) 3:1129–44. doi: 10.1182/bloodadvances.2018025536
82. Thorley-Lawson DA, Allday MJ. The curious case of the tumour virus: 50 years of Burkitt's lymphoma. *Nat Rev Microbiol* (2008) 6:913–24. doi: 10.1038/nrmicro2015
83. Rochford R, Cannon MJ, Moormann AM. Endemic Burkitt's lymphoma: a polymicrobial disease? *Nat Rev Microbiol* (2005) 3:182–7. doi: 10.1038/nrmicro1089
84. Burkitt D. A sarcoma involving the jaws in African children. *Br J Surg* (1958) 46:218–23. doi: 10.1002/bjs.18004619704
85. Cesarman E, Damania B, Krown SE, Martin J, Bower M, Whitby D. Kaposi sarcoma. *Nat Rev Dis Primers* (2019) 5:9. doi: 10.1038/s41572-019-0060-9
86. Faure A, Hayes M, Sugden B. How Kaposi's sarcoma-associated herpesvirus stably transforms peripheral B cells towards lymphomagenesis. *Proc Natl Acad Sci U S A* (2019) 116:16519–28. doi: 10.1073/pnas.1905025116
87. Labo N, Marshall V, Miley W, Davis E, McCann B, Stolka KB, et al. Mutual detection of Kaposi's sarcoma-associated herpesvirus and Epstein-Barr virus in blood and saliva of Cameroonians with and without Kaposi's sarcoma. *Int J Cancer* (2019) 145:2468–77. doi: 10.1002/ijc.32546
88. Sallah N, Miley W, Labo N, Carstensen T, Fatumo S, Gurdasani D, et al. Distinct genetic architectures and environmental factors associate with host response to the gamma2-herpesvirus infections. *Nat Commun* (2020) 11:3849. doi: 10.1038/s41467-020-17696-2
89. Klein U, Gloghini A, Gaidano G, Chadburn A, Cesarman E, Dalla-Favera R, et al. Gene expression profile analysis of AIDS-related primary effusion lymphoma (PEL) suggests a plasmablastic derivation and identifies PEL-specific transcripts. *Blood* (2003) 101:4115–21. doi: 10.1182/blood-2002-10-3090
90. Epstein MA, Morgan AJ, Finerty S, Randle BJ, Kirkwood JK. Protection of cottontop tamarins against Epstein-Barr virus-induced malignant lymphoma by a prototype subunit vaccine. *Nature* (1985) 318:287–9. doi: 10.1038/318287a0
91. Cleary ML, Epstein MA, Finerty S, Dorfman RF, Bornkamm GW, Kirkwood JK, et al. Individual tumors of multifocal EB virus-induced malignant lymphomas in tamarins arise from different B-cell clones. *Science* (1985) 228:722–4. doi: 10.1126/science.2986287
92. Yu H, Borsotti C, Schickel JN, Zhu S, Strowig T, Eynon EE, et al. A novel humanized mouse model with significant improvement of class-switched, antigen-specific antibody production. *Blood* (2017) 129:959–69. doi: 10.1182/blood-2016-04-709584
93. Li C, Romero-Masters JC, Huebner S, Ohashi M, Hayes M, Bristol JA, et al. EBNA2-deleted Epstein-Barr virus (EBV) isolate, P3HR1, causes Hodgkin-like lymphomas and diffuse large B cell lymphomas with type II and Wp-restricted latency types in humanized mice. *PLoS Pathog* (2020) 16:e1008590. doi: 10.1371/journal.ppat.1008590

Conflict of Interest: The authors declare that the research was conducted in the absence of any commercial or financial relationships that could be construed as a potential conflict of interest.

frontiers in Immunology

REVIEW
published: 01 April 2021
doi: 10.3389/fimmu.2021.636775

Humanized Mice for the Evaluation of Novel HIV-1 Therapies

Shawn Abeynaike[1,2] *and Silke Paust*[1,2*]

[1] Department of Immunology and Microbiology, The Scripps Research Institute, La Jolla, CA, United States, [2] The Skaggs Graduate Program in Chemical and Biological Sciences, The Scripps Research Institute, La Jolla, CA, United States

With the discovery of antiretroviral therapy, HIV-1 infection has transitioned into a manageable but chronic illness, which requires lifelong treatment. Nevertheless, complete eradication of the virus has still eluded us. This is partly due to the virus's ability to remain in a dormant state in tissue reservoirs, 'hidden' from the host's immune system. Also, the high mutation rate of HIV-1 results in escape mutations in response to many therapeutics. Regardless, the development of novel cures for HIV-1 continues to move forward with a range of approaches from immunotherapy to gene editing. However, to evaluate *in vivo* pathogenesis and the efficacy and safety of therapeutic approaches, a suitable animal model is necessary. To this end, the humanized mouse was developed by McCune in 1988 and has continued to be improved on over the past 30 years. Here, we review the variety of humanized mouse models that have been utilized through the years and describe their specific contribution in translating HIV-1 cure strategies to the clinic.

Keywords: humanized mice, BLT, DRAG, HIV-1 infection, viral latency, latency reversal, immunotherapy, gene therapy

OPEN ACCESS

Edited by:
Qingfeng Chen,
*Institute of Molecular and Cell Biology (A*STAR), Singapore*

Reviewed by:
Mangai Asokan,
Independent Researcher, Bengaluru, India
Namal P. M. Liyanage,
The Ohio State University, United States

***Correspondence:**
Silke Paust
paust@scripps.edu

Specialty section:
This article was submitted to Viral Immunology, a section of the journal Frontiers in Immunology

Received: *02 December 2020*
Accepted: *01 March 2021*
Published: *01 April 2021*

Citation:
Abeynaike S and Paust S (2021) Humanized Mice for the Evaluation of Novel HIV-1 Therapies. Front. Immunol. 12:636775. doi: 10.3389/fimmu.2021.636775

INTRODUCTION

Human immunodeficiency virus-1 (HIV-1) was first discovered in 1983 by the laboratory of Luc Montagniers at the Pasteur Institute, by culturing T cells isolated from the lymph nodes of a patient with early symptoms of AIDS (1). Since its discovery, the battle to control and eradicate HIV-1 has been long and tumultuous. Close to four decades have passed. While great strides have been made in managing HIV and preventing the onset of AIDS in patients *via* daily treatment with combination antiretroviral therapy (ART) (2), a successful vaccine or curative treatment has yet to be developed. The key to research on HIV cure therapy is using a suitable animal model, as a comprehensive analysis of the human immune system is limited due to ethical and practical restrictions. Humans and chimpanzees are the natural hosts for HIV-1 replication. However, due to ethical and practical reasons are not amenable to most methods of experimentation. Mice reconstituted with human immune systems and non-human primates are the two animal models that have received the most attention in investigating HIV-1 pathogenesis. Non-human primate models provide many advantages, such as being a natural host for the closely related Simian Immunodeficiency Virus (SIV) and the chimeric SHIV virus and having similar anatomical and physiological features to

humans. The complete range of advantages and disadvantages of these models have been reviewed elsewhere (3–5). In contrast, humanized mice contain human CD4+ T cells, which are permissible to HIV-1 infection and simultaneously allow in-depth analysis of the human immune response to HIV-1 pathogenesis *in vivo*. Humanized mice have provided important insights into preventative approaches to HIV-1 infection (6–8). These approaches have been reviewed in detail elsewhere (9, 10). Here we review the history and development of humanized mouse models (**Tables 1** and **2**) and describe their applications in a wide range of novel approaches for HIV-1 eradication (**Table 3**).

HUMANIZED MOUSE MODELS

SCID-hu Mouse

Severe combined immunodeficiency (SCID) is a debilitating disease characterized by T and B lymphocyte differentiation impairment. Those affected show high susceptibility to recurring infections from viruses, bacteria, and fungi and leads to death within the first two years of life unless treated by stem cell transplant (68). Bosma, Custer (69) observed mice of ty -65the C.B-17 strain that had impaired lymphopoiesis, caused by an autosomal recessive mutation (*scid*). These mice became the first mouse model of SCID, with mice homozygous for this recessive gene showing hypogammaglobulinemia and deficiency in functional T and B lymphocytes (69).

In 1988, McCune reasoned that if human hematopoietic stem cells (HSCs) and human thymus were introduced together into a mouse unable to reject them, T cell development and maturation could proceed in a fashion mimicking human physiology (11). McCune implanted C.B17 *scid/scid* mice (SCID mice) with human fetal thymus and injected them with human fetal liver cells, either intravenously or intrathymically (11). Mice were sub-lethally irradiated to ensure full reconstitution, as was seen previously in SCID mice implanted with long-term bone marrow cultures (70). These so-called SCID-hu mice showed human T cells in peripheral circulation at 6-7 weeks post-transplantation, but this population was no longer seen by 10-12

TABLE 1 | Summary of humanized mouse models and their tissue-based chimerism.

	SCID-hu	hu-PBL	hu-HSC	BLT	TKO-BLT
Mouse Model					
Genetic Background	C.B17scid/scid (SCID)	SCID NOD-SCID NSG BRG NCG	SCID NOD-SCID NSG BRG NRG DRAG	SCID NOD-SCID NSG NRG	C57BL/6 Rag2 $^{-/-}$ $g_c^{-/-}$
Humanization Method	Subcapsular Coimplantation of human fetal thymus and liver fragments 	Intraperitoneal Injection of human PBMCs 	Injection of CD34+ cells from cord blood/fetal liver 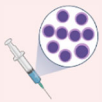	Coimplantation human fetal thy/liv with i.v. injection of CD34+ cells from fetal liver 	Coimplantation human fetal thy/liv with i.v. injection of CD34+ cells from fetal liver 
Immune Reconstitution	T cell engraftment Multilineage hematopoiesis No primary immune response	T cell engraftment No multilineage hematopoiesis No primary immune response	Multilineage hematopoiesis Primary immune response No HLA restriction	Multilineage hematopoiesis Primary immune response Human HLA T cell restriction	Multilineage hematopoiesis Primary immune response Human HLA T cell restriction
References	McCune Namikawa (11), Namikawa Weilbaecher (12)	Moiser, Gulizia (13), Hesselton. Greiner (14), van Rijn, Simonetti (15), Ali, Flutter (16)	Kamei-Reid and Dick (17), Peault, Weissman (18), Hiramatsu, Nishikomori (19), Danner, Chaudhari (20)	Lan, Tonomura (21), Melkus, Estes (22), Brainard, Seung (23), Stoddart, Maidji (24)	Lavender, Messer (25), Lavender, Pang (26), Lavander, Pace (27)

Created with BioRender.com.

TABLE 2 | Summary of known immunophenotypic characteristics of humanized mice.

Humanized mouse model	Immune cells	Phenotypic characteristics	References
Hu-PBL	T cells	Donor immunological memory is conferred High activation due to MHC mismatch and thus high propensity of GVHD	Mosier, Gulizia (13); Hesselton, Greiner (14); van Rijn, Simonetti (15), Ali, Flutter (16)
	B Cells	Present at low levels Donor immunological memory is conferred Limited class switching and SHM	
Hu-HSC	T cells	HLA mismatched T cells Th2 Polarization driven by increased GATA3 expression	Kamel-Reid and Dick (17); Péault, Weissman (18); Lapidot, Pflumio (28); Hiramatsu, Nishikomori (19); Shultz, Saito (29); Danner, Chaudhari (20); Choi, Chun (30); Chen, He (31); Ito, Takahashi (32); Rongvaux, Willinger (33), Billerbeck, Horwitz (34), Billerbeck, Labitt (35); Ding, Wilkinson (36); Majji, Wijayalath (37); Li, Mention (38); Herndler-Brandstetter, Shan (39)
	B cells	Predominantly immature, express CD5+ at higher levels Limited class switching and somatic hypermutation IgG and IgM present at lower levels than in humans	
	NK cells	Present in low numbers	
	Macrophages	Present and intact phagocytic function	
	Dendritic Cells	Both plasmacytoid DCs and Myeloid DCs are present at low frequencies Able to induce the activation of allogeneic human T cells Able to produce IFN-a upon stimulation	
	Mast Cells	Present in low numbers Incomplete development due to lack of species-specific cytokines Poor allergic responses	
BLT	T cells	HLA restricted T cells	Lan, Tonomura (21); Melkus, Estes (22); Brainard, Seung (23); Stoddart, Maidji (24); Biswas, Chang (40); Kalscheuer, Danzl (41); Denton, Nochi (42), Smith, Lin (43); Bryce, Falahati (44), Honeycutt, Wahl (45); Nikzad, Angelo (46)
	CD8+ T cells	Capable of functional, antigen specific effector responses Tend towards a more naïve phenotype expressing high levels of CD45RA, CD27 and CCR7	
	CD4+ T cells	Capable of functional, antigen specific responses Th2 Polarization driven by increased GATA3 expression	
	B cells	Limited class switching and somatic hypermutation Incomplete maturation indicated by CD10+ B cells in Spleen and Bone Marrow and CD5+ B Cells in spleen and peripheral circulation IgG and IgM present at lower levels than in humans	
	NK Cells	Lower numbers but phenotypically similar to human NK cells Maintain cytotoxic activity CD62L expression is higher in spleen and liver potentially caused by underdeveloped lymphoid follicles	
	Dendritic Cells	Both plasmacytoid DCs and Myeloid DCs are present at low frequencies	
	Macrophages	Present and intact phagocytic function Incomplete development due to lack of species-specific cytokines	
	Mast Cells	Present in spleen and lung Absent in skin, heart, stomach, and small intestine Incomplete development due to lack of species-specific cytokines Poor allergic responses	

weeks (11). They also identified that the intravenously injected fetal liver cells could home to the implanted fetal thymus, and after 10 weeks, can be found in the peripheral circulation. If the thymus is engrafted in SCID mice alone, it eventually recedes over time. Therefore, a source of human progenitor cells needs to be provided (11, 71). Human fetal liver, in particular, is used as it is the primary site of hematopoiesis in humans between 8 to 24 weeks of gestation. The human fetal liver also contains progenitors for lymphoid, myeloid, and erythroid lineages (72) but limited numbers of mature CD3+ T cells (73). This reduces the risk of graft-versus-host disease (12) and allows human immune cells to engraft more efficiently than an adult or post-natal tissue (74).

Shortly after, Namikawa, Weilbaecher (12) implanted fetal thymus and liver concurrently. The resulting Thy/Liv mice show prolonged reconstitution with human immune cells with minimal graft-versus-host disease. These mice showed increased longevity in lymphopoiesis, even up to 15 months post-transplantation.

The SCID-hu mouse provided us with the first mouse model that could be used to study HIV-1 pathogenesis (75, 76). The first infection of a humanized mouse model (SCID-hu) with HIV-1_{JRCSF} was in 1988, shortly after McCune had developed the model (76). McCune, Namikawa (77) utilized this model to confirm, for the first time, the efficacy of the nucleoside analog azidothymidine (AZT) as an ART for HIV-1.

While providing a great stride forward in using humanized mice in HIV cure research, SCID-hu mice had some limitations. While the rapid generation of human thymocytes and naïve T cells was possible, mature T cells are primarily restricted to the implanted thy/liver organoid. Furthermore, these mice do not produce functional immune responses that recapitulate the human immune response.

Peripheral Blood Leukocyte (Hu-PBL) Mouse

Mosier and colleagues conducted the first iteration of humanizing SCID mice by transferring human PBMCs in 1988 (13). These mice were susceptible to HIV-1 infection, with 50% of them presenting with detectable viral RNA 16 weeks post-infection (78). Infection of hu-PBL-SCID mice as early as 2 hours

post reconstitution has led to productive HIV-1 infection and a dramatic decrease in CD4+ T cell numbers (79).

The establishment of non-obese diabetic (NOD) mice further progressed the field of humanized mice (80, 81). These NOD mice showed defects in the innate immune system, resulting in better engraftment when crossed with SCID mice. Further development came from crossing these so-called NOD-SCID mice with those who had the IL-2Rγ-chain null mutation (82) or truncation of the intracellular signaling domain (83). This common cytokine receptor gamma chain is required for the signaling of IL-2, IL-4. IL-7, IL-9 IL-15, and IL-21 (84–90) and its deletion completely abrogates murine Natural Killer (NK) cell development and function (82) which has shown to negatively impact engraftment of human lymphoid cells in mice (91). Modern versions of hu-PBL mice utilize NOD/SCID/IL2rγ-null (NSG) or BALB/c-Rag2null IL-2Rγnull (BRG) backgrounds as they provide better reconstitution (14–16). These mice show partial functionality (13, 78, 92, 93) but lack *de novo* multilineage hematopoiesis and therefore are absent of a primary immune response. They are also amenable to HIV-1 infection (14, 94, 95) and are responsive to HAART (95). This model is particularly suited to studying GVHD (16, 96, 97), simultaneously creating a significant limitation in this model's utility for long-term HIV-1 studies.

Hematopoietic Stem Cell (HSC) Mouse

Following the early success of reconstituting human immune systems in SCID mice, Kamel-Reid and Dick (17) intravenously infused hematopoietic stem cells from human bone marrow into the SCID mouse as well as the bg/nu/xid mouse, which are deficient in natural killer responses. They found bg/nu/xid mice show higher levels of human progenitors and, in addition to T and B cells, found that macrophage progenitors can be isolated and cultured *in vitro* (17). It was subsequently identified that by providing these HSC humanized mice with erythropoietin, human mast cell growth factor and human IL-3 stimulated the immature cells from human bone marrow to differentiate into cells of the erythroid, myeloid, and lymphoid lineages (28).

The cell surface sialomucin-like adhesion molecule CD34 is widely accepted as a marker for human HSCs (98, 99), having showing both short-term (98) and long-term (100) colony-forming potential *in vitro* and allowing the differentiation of both myeloid and lymphoid cell lineages in NOD/SCID mice (101). Péault, Weissman (18) isolated CD34+ cells from human bone marrow and human fetal liver and was able to reconstitute human fetal thymus *in vitro* and then implanted them into SCID mice. The third source of HSCs is umbilical cord blood (UCB). High levels of HSCs can be isolated from fetal liver, bone marrow, and UCB, although they produce varying levels of lymphoid, myeloid, and erythroid progeny (102). Hao, Shah (103) showed that CD34+CD38- cells isolated from UCB have a higher cloning efficiency, proliferate more rapidly in response to cytokine stimulation, and generate more progeny than those derived from human bone marrow. Furthermore, as few as 500 CD34+CD38- cells separated from UCB were able to reconstitute NOD/SCID mice (104).

Several mouse backgrounds have been utilized for reconstitution with HSCs, including NOD/SCID (104), NOD/Shi-Scid mice (105). NOD/Shi-*scid/IL2Rγnull* (NOG) (106) and NSG (19, 107). McDermott et al. performed a comparative analysis of each mouse background (108). They used the current optimized methods for each mouse model, which included interfemoral injection of HSCs to all mice and anti-CD122 (IL-2Rβ) treatment for NOD/Lt-*scid* and NOD/Shi-*scid*, to inhibit NK cell activity (109). They identified that NSG and NOG mice had superior engraftment in the thymus and spleen compared to NOD/Lt-*scid* and NOD/Shi-*scid* mice. Also, NSG mice showed 1.5-fold greater engraftment in the bone marrow over NOG, NOD/Lt-*scid*, and NOD/Shi-*scid* mice (108). Finally, at limiting doses of HSCs, female NSGs showed improved engraftment compared to males (108).

Successful infection with HIV-1 through multiple routes have been demonstrated in CD34+ reconstituted NOG (110–114), BRG (115–117), NRG (118) and NSG mice (65, 119–124). They are also responsive to HAART (65, 118, 119) and have significant potential to contribute to our understanding of HIV-1 latency and therapeutic studies.

DRAG Mouse

Impaired T cell development and consequent lack of antibody class switching in HSC humanized mice is mainly attributed to the lack of donor matched HLA molecules in the mouse thymus. Lack of a thymic environment hampers the negative selection of self-reactive T cells by which autoimmunity is prevented. Danner, Chaudhari (20) hypothesized that by expressing human HLA class II molecules in a transgenic mouse model, they could rescue the development of CD4+ T cells and consequently B cell development and antibody class switching. They generated NOD.Rag1KO.IL2RccKO mice expressing HLA-DR4 (0401), abbreviated DRAG, and at 4-6 weeks old intravenously injected them with CD34+ HSCs isolated from HLA-DR*0401 positive UCB (20). When compared against HLA mismatched recipients, higher levels of reconstitution of CD4 + T cells were seen in DRAG mice comparable to human blood levels. However, levels of CD8+ T cells did not show as drastic an increase. These mice showed the presence of dendritic cells (2.9% in spleen) and NK cells (0.05% in spleen), although their development appeared to be unaffected by HLA-DR4 expression. T cells isolated from DRAG mice showed vigorous responses, similar to that of PBMCs from healthy volunteers upon stimulation with either CD3/CD28 or PMA/ionomycin. B cell reconstitution was seen at similar levels to control mice, although IgM levels were significantly higher in DRAG mice. Interestingly, DRAG mice showed substantial IgG reconstitution, confirming that the mechanism of immunoglobulin class switching is rescued in DRAG mice, a feature lacking in most other humanized mouse models. Further, DRAG mice showed reconstituted plasma levels of all human IgG subclasses, with IgG2 being the most prevalent.

Studies have shown that DRAG mice are susceptible to HIV-1 infection, similar to other HSC reconstituted mice (125, 126). The replication-competent virus was isolated from plasma, lymph nodes, bone marrow, spleen, gut, brain, and female

reproductive tissue upon a single intravaginal challenge of purified primary HIV-1 (125). High reconstitution in the gut and female reproductive tract, particularly with CXCR5+PD-1++ Follicular T helper cells, which are highly permissive to HIV-1 infection, are potentially a significant contributor to the above (126). Also, plasma viral loads were stable as far as 18 weeks post-infection, making the DRAG mouse a suitable model system, particularly for long-term vaccination studies.

Bone Marrow-Liver-Thymus (BLT) Mouse

While implantation of Thy/Liv into SCID or NOD/SCID mice results in thymopoiesis and functional T cells, strong *in vivo* immune responses are not observed. In 2006 (21), Lan et al. combined the implantation of fetal Thy/Liv with the simultaneous transplantation of CD34+ fetal liver cells in NOD/SCID mice (21). In the same year, Melkus, Estes (22) performed a similar transplant on the NOD-SCID background, coining the term 'BLT' to describe these bone marrow-liver-thymus humanized mice (22). A significant advantage of the BLT model is that it allows the development of MHC-restricted T cells due to the presence of an autologous human thymic environment (22). This iteration of the humanized mouse showed stronger *in vivo* immune responses and repopulates with multiple lineages of immune cells, including T cells, B cells, NK cells, Dendritic Cells, Neutrophils, and Monocytes distributed through multiple organs, including bone marrow, lymph nodes, spleen, thymus, liver, lung, digestive and reproductive tracts (21–23, 42, 43, 46, 127, 128).

Soon after its development, Sun, Denton (128) identified that BLTs contain CD4+ T cells throughout the gut-associated lymphoid tissue (GALT), including the colon and rectum, and thus hypothesized that they would be ideal for modeling intrarectal transmission, a predominant form of HIV-1 transmission. BLT mice were inoculated intrarectally with a single dose of cell-free HIV-1 (LAI CXCR4 strain), and six out of seven infected BLTs were found positive for viral RNA and the presence of p24 antigen (128). Similarly, Denton, Estes (127) showed that BLTs were susceptible to vaginal transmission of HIV-1 (CCR5-tropic JR-CSF). Infection was prevented in BLTs pre-treated with a daily dose of the ARTs emtricitabine and tenofovir diosoproxil fumarate (FTC/TDF), making the BLT model additionally suited for preclinical testing of pre-exposure prophylactics (PrEP). Subsequent studies of topically administered 1% tenofovir in BLT mice also showed partial protection against vaginal transmission of HIV-1 (129).

Brainard, Seung (23) infected BLT mice made with mice of both NOD/SCID and NSG backgrounds, implanting tissue under both right and left kidney capsules. Stoddart, Maidji (24) also demonstrated that NSG reconstitution was highly superior to NOD/SCID reconstitution (24). However, Denton, Nochi (42) showed higher levels of intraepithelial lymphocytes in the small and large intestines of NOD/SCID BLTs.

The functional human cellular immune response observed in BLTs makes it a particularly valuable model for studying HIV specific immunity. HIV infection in BLT humanized mice is associated with both CD8+ T cell activation (23, 130, 131) as well as HIV-specific IgM and IgG (23, 40). HIV-1 specific CD8+ T cell responses show strong similarities to human cellular immunity and result in rapid viral escape in BLT mice (131). Furthermore, mice created with tissue from elite controllers that express the HLA-B*57 allele exhibited enhanced Gag mediated control of viremia (131).

While substantial reconstitution with B cells is observed in BLT mice, they are considered primarily immature, and antibody class-switching is thought to be defective. Interestingly, it has been speculated that the humoral immunity observed in BLT mice in response to viral infection is driven by extra-follicular or 'innate-like' B cells rather than conventional post-germinal B cells (40, 132, 133). This inadequate antibody response has led to the proposal of the BLT mouse as a model for hypogammaglobulinemia (134).

Crucial to HIV-1 therapeutic studies is the establishment of latency in the BLT mouse model. Denton, Olesen (135) used a commonly used combination ART regimen, a combination of tenofovir, emtricitabine, and raltegravir, to suppress viral replication in BLT humanized mice, and thereafter isolated CD4+ T cells and cultured them ex vivo. Stimulation of these CD4+ T cells with Phytohemagglutinin and IL-2 led to a rebound in viral load (135).

Triple Knockout (TKO)-BLT

While modern BLT and humanized mouse models primarily use NOD/SCID backgrounds, there is the potential benefit of developing a BLT model on the C57BL/6 background due to the wide availability of transgenes and genes inactivation as well as its relative resistance to radiation. A significant barrier to this is the expression of a different form of the signal recognition protein α (SIRPα) receptor by C57BL/6 mice, which does not recognize the human ligand CD47 (integrin associated protein) unlike in NOD mice (136, 137). Recognition of CD47 on transplanted human cells by SIRPα on mouse macrophages leads to the transmission of inhibitory signals preventing their phagocytosis (138, 139). The Hasenkrug lab demonstrated that creating C57BL/6 Rag2-/-γc-/- (TKO) facilitated a CD47-negative environment, which leads to tolerizing of cells without the need for the SIRPα-CD47 interaction, thereby allowing successful long-term human immune systems in TKO-BLT mice (25, 26).

The TKO-BLT mice showed no clinical signs of graft-versus-host disease (GVHD) up to 29 weeks post-transplantation compared to NSG-BLT mice, of which a third had died from lethal GVHD at the same timepoint (26). Furthermore, TKO-BLT mice developed human GALT, including CD4+ T cells, supporting mucosal HIV infection through intraperitoneal and intrarectal routes (26). HIV-1 infected TKO-BLTs showed HIV $gp120_{JR\text{-}CSF}$ specific IgG antibodies demonstrating both antibody responses and T-cell dependent class switching (26). Furthermore, cells from the spleens of HIV infected TKO-BLTs were assayed by IFN-γ ELISPOT and were shown to be responsive to a broad range of peptide pools spanning the $HIV\text{-}1_{JR\text{-}CSF}$ proteome (26). Similar to NSG-BLT mice, the TKO-BLT can also recapitulate HIV-1 latency upon treatment with ART up to 18 weeks, with viral rebound seen upon removal of therapy (27). GVHD is a limitation in the BLT humanized model (140). Resistance to GVHD makes the TKO-BLT particularly suited to

long-term studies required to study HIV-1 latency and measure the lasting efficacy of current curative approaches.

HUMANIZED MICE IN HIV-1 CURE RESEARCH

The primary barrier to eradicating HIV-1 is its integration into the host genome and continued persistence in a non-replicating or 'latent' state, even under ART (141–143). Furthermore, chronic infection with HIV-1 leads to significant disruptions in the host's immune response (144). Consequently, latently infected cells are difficult to find, and the host immune response is inefficient in killing these cells. Therefore, innovative strategies are required to find, measure, and ultimately eradicate the latent HIV-1 reservoir.

Two definitions exist for a cure for HIV. The complete eradication of the virus from all cells in the body is defined as a sterilizing cure. In contrast, a functional cure would be a treatment that would lead to HIV+ people being able to halt ARV treatment while maintaining long-term viral suppression and preventing transmission of the virus. The humanized mouse models described in this review have played a vital role in pre-clinical testing of many approaches to an HIV-1 cure, with some directly leading to clinical trials.

Latency Reversal

One major strategy in the fight for a sterilizing cure is the "shock" and "kill" approach. This strategy involves utilizing latency reversal agents to 'shock' the latently infected cells into resuming replication of the virus, allowing the immune system to recognize and kill infected cells or for virus-induced cytolysis to occur. Several classes of LRAs have been identified which include histone deacetylase inhibitors (HDACis) (145–147), histone methyltransferase (HMT) inhibitors (148), DNA methyltransferase inhibitors, Protein Kinase C (PKC) activators (149), bromodomain inhibitors (150), Disulfiram (a drug used to treat chronic alcoholism) (151), agonists to Toll-like receptor 7 (152) and cytokines such as IL-15 (153).

One of the most well-studied classes of LRAs, HDACi's work by inhibiting the enzymes that remove acetyl groups from histones, leaving them in an open state, and increasing the ability for transcription to resume. While HDAC inhibitors such as Panobinostat successfully increase levels of histone acetylation *in vivo* (154) and reactivation of latently infected cells *ex vivo* (149, 155), reactivation of HIV-1 replication was not seen in ART-treated HIV-1 infected BLT mice (154).

Other classes of LRAs impact cellular factors such as NF-κB and pTEFB by either increasing their expression or activating them. Protein kinase C (PKC) agonists are one such class that activates the NF-κB pathway leading to reactivation of latent HIV-1 (156, 157). Prostratin, a PKC agonist, was one of the earliest LRAs of this class identified with potency in reactivating latent HIV-1 (158). Additionally, IDB and Bryostatin 1 can effectively reactivate viruses in cells isolated from HIV-infected patients (149, 159). Marsden, Loy (160) identified a synthetic analog of the PKC modulator bryostatin 1, SUW133, which when intraperitoneally injected into ART-treated HIV-1 infected BLT mice, reactivated HIV-1 more potently, was more tolerable than the natural analog, and led to infected cells' death.

Bobardt, Kuo (161) showed that an inhibitor apoptosis protein antagonist (IAPa) reactivates latent HIV-1 by degrading the ubiquitin ligase BIRC2, a repressor of the non-canonical NF-κB pathway. Substantial reactivation was seen *ex vivo* in latently infected CD4+ T cells isolated from ART-treated HIV-1 infected BLT mice at much greater levels than the HDACis panobinostat and vorinostat as well as another IAPa LCL-161 (161). Similar results were seen *in vivo* with AZD5582, which also works as a SMAC mimetic and activates the non-canonical NF-kB pathway (162). Upon a single dose of 3mgkg-1 of AZD5582 HIV-1 RNA was detected in 3 out of 6 and 3 out of 4 ART-treated HIV-1 infected BLT mice, with no signs of general toxicity (162).

Specific cytokines have dual potential to both reactivate HIV-1 replication and simultaneously activate host immune cells such as NK cells to kill infected cells (153, 163, 164). Recently, the IL-15 'super-agonist' N-803 tested in the BLT humanized model showed reactivation of the viral reservoir only upon depletion of CD8+ T cells, showing further nuance in the interactions between LRAs, viral reactivation, and immune cells (165).

Interestingly, Llewellyn, Alvarez-Carbonell (166) found that HSC mice (NSG fetal liver CD34+) reconstitute with human microglial cells in the brain when endogenous microglia are depleted using the chemotherapeutic agent busulfan at much greater levels than mice pretreated with irradiation. These human-derived microglial cells could be infected with HIV-1 and, upon exposure to the MAO inhibitor phenelzine, they could reactivate latent virus *ex vivo* (166). These results further emphasize the potential for humanized mouse models in studying latency reversal in multiple tissue reservoirs of HIV-1.

Unfortunately, while many LRAs have successfully reactivated HIV, the subsequent killing by viral cytopathic effects, killing by host immune cells, or intensifying ART has proven ineffective in the clinic (167). This is partly due to dysfunctional CTLs (168) and NK cells (169–171) and due to the presence of escape mutant viruses in the latent reservoir (172). Therefore, to enhance the 'kill' arm, multiple immunotherapies, gene therapies, and pharmacological interventions have been explored.

Broadly Neutralizing Antibodies (bNAbs)

The HIV-1 envelope protein (env) is a trimeric glycoprotein of gp41 and gp120 heterodimers and is on the virus's surface and consists of multiple sites that can be targeted by host antibodies. The majority of neutralizing antibodies that develop in humans are strain-specific, but a small subset of antibodies can bind to and neutralize a broad range of HIV-1 strains (173–176). Initial attempts to utilized these broadly neutralizing antibodies (bNAbs) in HIV-1 therapy proved unsuccessful in both humanize mice (47) as well as in the clinic (177, 178). However, with the advent of single-cell antibody cloning methods, highly potent bNAbs have been identified (179).

TABLE 3 | Summary of therapeutic approaches and humanized mouse models utilized in their testing.

Therapeutic approach	Model	Genetic background	References
bNAbs	Hu-PBL	SCID	Poignard, Sabbe (47)
	Hu-HSC	NRG	Klein, Halper-Stromberg (48), Horwitz, Halper-Stromberg (49), Halper-Stromberg, Lu (50)
		NSG	Wang, Gajjar (51)
	BLT	NSG	Badamchi-Zadeh, Tartaglia (52)
CAR T Cell Therapy	Hu-HSC	SCID	Kitchen, Bennett (53)
	BLT	NSG	Kitchen, Levin (54), Zhen, Kamata (55)
	Hu-PBL	NSG	Leibman, Richardson (56), Bardhi, Wu (57), Anthony-Gonda, Bardhi (58)
Zinc Finger Nucleases	Hu-PBL	NOG	Perez, Wang (59)
		NSG	Yi, Choi (60), Wilen, Wang (61), Yuan, Wang (62)
TALENs	Hu-HSC	NSG	Llewellyn, Seclén (63)
CRISPR/Cas9	Hu-PBL	NCG	Xiao, Chen (64)
	Hu-HSC	NSG	Dash, Kaminski (65)
	BLT	NSG	Yin, Zhang (66)
Block and Lock	BLT	NSG	Kessing, Nixon (67)

Over the past decade, humanized mice have proved instrumental in developing therapies utilizing bNAbs for viral suppression and eradicating latently infected cells.

Klein, Halper-Stromberg (48) showed that treatment with a combination of bNAbs (45-46^{G54W}, PG16, PGT128, 10-1074, and 3BC176) that target different epitopes could suppress viral replication in HIV-1 infected hu-HSC mice. These humanized mice were then infected with HIV-1_{YU2}, and treated with a penta-mix treatment therapy reducing viral loads to undetectable levels for up to 60 days post removal of therapy compared to only 10 days when treated with ART. Shortly after, Horwitz, Halper-Stromberg (49) showed in the same mouse model that lowering the viral load by ART followed by treatment with bNAb monotherapy (3BNC117, PG16, or 10-1074) can similarly lead to control of viremia until antibody titers dropped to low or undetectable levels. Also, a single injection of adeno-associated virus directing expression of a single bNAb suppressed viral replication after the termination of ART (49). Following these studies, Halper-Stromberg, Lu (50) hypothesized that these capabilities of bNAbs could be harnessed to amplify the "kill" arm with bNAb therapy after reactivation of the latent reservoir. They used three LRAs; the HDACi Vorinostat, the BET protein inhibitor I-BET151, and CTLA, a T cell inhibitory pathway blocker given individually or in combination (50). They discovered that combination treatment with the three LRAs with the trimix bNAb treatment (3BNC117, PG16, or 10-1074) in humanized mice reduced the viral reservoir, evidenced by reduced viral rebound at significantly higher levels than with single LRAs (50). They further showed that bNAbs exert this effect primarily through Fc mediated functions by comparing their bNAbs to those with mutated Fc regions (50).

These results provided the preclinical evidence that combination bNAb therapy is a critical tool that can be utilized in HIV-1 eradication and has since led to the translation of these ideas to the clinic (180). In an open-label clinical trial, Caskey, Klein (181) showed that monotherapy with a single 30mgkg^{-1} infusion of 3BNC117, the antibody targeting the CD4 binding site, was able to suppress viral load in HIV-1 infected individuals for up to 28 days. Also, in the following phase II trial, the same therapy suppressed HIV-1 viral load in infected individuals on average for 10 weeks, upon four doses given two weeks apart (182). Further investigation by adoptive transfer of patient T cells into NRG mice identified that these effects are not limited to preventing new infection of cells, but also aids in the clearance of infected cells by Fcγ receptor-mediated engagement (183). Shortly after, Caskey, Schoofs (184) tested 10-1074, which targets a glycan on the V3 loop of the HIV-1 envelope spike, as monotherapy in HIV-1 infected patients. Similarly, at a dose of 30mgkg$^{-1,}$ 11 out of 13 HIV-1 positive individuals showed suppression of viral loads. The two that failed to respond carried mutations leading to single-amino-acid changes, making them 10-1074 resistant before treatment (184). Unfortunately, while monotherapy with bNAbs was proven to be safe and efficacious, in both cases, it led to viral escape (181, 183, 184).

In contrast to monotherapy, but similar to the results in humanized mice, combination therapy with 3BNC117 and 10-1074 at a dose of 30mgkg^{-} was found to be both safe and more effective at viral suppression in humans (185–187). When administered upon treatment interruption three times at three weeks apart, 11 HIV-1 infected individuals resulted in viral suppression for a median of 21 weeks post final dose of antibody therapy (186). Furthermore, none of the rebounding viruses showed resistance to both therapeutic bNAbs. Similar to data generated in humanized mice, these data demonstrate the enhanced utility of combination bNAb therapy to suppress viral replication (186). Moreover, combination bNAb therapy during treatment interruption led to increases in antigen-specific CD8+ T cells that expressed IFN-γ. TNF-α, MIP1-β, and CD107a in all individuals at 6-7 weeks while plasma bNAb levels were at their peak (188). While latency reversal agents combined with bNAB therapy have yet to be tested in the clinic, the evidence provided so far shows a clear line from preclinical experiments in humanized mice to the successful translation of these therapies into the clinic.

Chimeric Antigen Receptor (CAR) T Cell Immunotherapy

Since the advent of CAR T cell therapies and their successful use in treating B cell malignancies (189–191), several approaches

have been taken to utilize this technology to target HIV-1 infected cells.

Kitchen, Bennett (53) transduced HSCs isolated from human fetal liver with an HLA-A*0201 restricted T cell receptor (TCR) targeted towards the HIV-1 gag SL9 epitope and injected them into human thymic implants in SCID-hu mice, providing them with an optimal environment for development. This led to the development of anti-HIV TCR+ CD8+ T cells, which produced Interferon-γ (IFN- γ) and lyse target cells in response to SL9 peptide stimulation *ex vivo* when biopsied from the thymus after seven weeks (53). In a subsequent study Kitchen, Levin (54) transduced HSCs with the same vector. They tested the ability of these anti-HIV TCR+ CTLs to suppress viral replication in a modified NSG-BLT model, which received a fetal thymus/liver implant along with the transduced HSCs. They found a significant decrease in plasma viremia at two weeks and six weeks and a higher percentage of CD4+ cells in mice transduced with the HIV-1 specific TCR when compared against a non-specific TCR control (54). Similar results were seen upon analyses of other organs of infected mice, with lower HIV-1 DNA at six weeks in the spleen, bone marrow, and human thymus (54). Importantly, their analysis of the viral RNA in the blood showed that within this time, no viral escape had occurred in response to the selective pressure of the SL9 specific TCR (54).

While modification with molecularly cloned anti-HIV TCRs showed to be effective, its application is restricted by HLA type, and several effective HIV CTLs use uncommon HLA alleles (192). A second alternative approach is a CD4ζ CAR, a chimeric molecule consisting of the extracellular and transmembrane domains of the human CD4 molecule fused to the signaling molecule of the CD3 ζ chain. Zhen, Kamata (55) transduced human HSPCs with an HIV-specific CD4ζ CAR and two antiviral genes (Triple CAR vector) and transferred them into NSGs transplanted with fetal thymus and liver (55). The antiviral genes included a small hairpin (sh) RNA molecule specific to human CCR5 and shRNA targeting specific HIV-1 long-terminal repeat (LTR) sequences to prevent the newly CD4 CAR-expressing cells from being infected by HIV-1, an obstacle previously observed with this approach (55). The Triple CAR construct was expressed on T cells, NK cells, B cells, and myeloid cells (55). They found these cells are resistant to HIV infection themselves, suppressed HIV replication *in vivo*, and isolated CD4ζ CAR-expressing cells could produce IFN- γ and tumor necrosis factor (TNF)-α when cultured with virally infected cells (55).

While CD4ζ CARs showed promise *in vitro* and in preclinical studies, clinical trials showed that while they survive for at least 11 years post-transfusion, they could not suppress the viral reservoir in a sustained manner (193). Therefore, Leibman, Richardson (56) decided to identify several components of the CD4ζ CAR construct to be optimized to improve their antiviral function. First, they switched from a murine retroviral vector (MMLV) to a lentiviral vector, as MMLV targets promoter regions while lentiviral vectors preferentially integrate into open reading frames (56). Next, they switched from the PGK promoter to the EF1α promotor, which induces higher expression better sustained as T cells reach a resting state (56). Thirdly, they swapped the CD4 transmembrane domain to a CD8a transmembrane domain to promote CAR dimerization (56). Finally, they assessed the inclusion of different co-stimulatory receptors such as 4-1BB and CD28 (56). While each modification individually produced significant improvements to target cell killing *in vitro*, in combination, they resulted in a 50-fold increase in potency over the original construct (56). To test their optimized CD4ζ CARs *in vivo*, they utilized a modified hu-PBL mouse as an HIV-1 treatment model. Briefly, they transferred CD8+ T cell-depleted PBMCs into NSGs, transfused them with HIV-1 infected CD4+ T cells, treated with 200mg/kg TDF for four days, and after removal of ART, transfused the mice with their CD4ζ CAR transduced CD8+ T cells (56). They found that mice infused with the optimized CD4ζ CARs T cells controlled HIV-1 replication better and expanded to greater levels *in vivo* than their first-generation counterparts (56).

In addition to CD4ζ, CARs with a single-chain variable fragment (scFv) derived from bNabs have been utilized. However recent clinical trials using bNAb monotherapy led to viral rebound upon interruption of ART (181, 184, 194). Bardhi, Wu (57) showed that a hexavalent fusion protein which consisted of m36.4, the scFv heavy chain only domain which targets the gp120 co-receptor binding site and mD1.22 an engineered mutant of the CD4 extracellular domain when intravenously injected into a modified hu-PBL model induced NK cell-mediated killing of HIV-1 infected cells. The model they used involved injecting human PBMCs intrasplenically (hu-spl-PBMC-NSG) into NSG mice followed by intrasplenic inoculation with HIV-1 (57, 58, 164). Subsequently, Anthony-Gonda, Bardhi (58) utilized m36.4, mD1.22, and a fusion inhibitor peptide C46, individually or in combination, to develop novel multi-specific CAR constructs. Using their hu-spl-PBMC-NSG model, they discovered that their duoCAR construct, by which m136.4 and mD1.22 were expressed as individual CARs on the same cell, was able to suppress HIV-1 infection for up to 30 days while mitigating CD4+ T cell depletion, compared to their monoCAR or untransduced counterparts (58). Altogether, these findings clearly show the utility of various humanized mouse models in elucidating CAR-based immunotherapy *in vivo* efficacy in the clearance of HIV-1 infected cells.

Gene Editing With Designer Nucleases

The first patient cured of HIV to date was treated for myeloid leukemia with total body irradiation and two allogeneic hematopoietic stem-cell transplants (HSCT) from donors with the CCR5Δ32/Δ32 mutations (195). While the second patient exhibiting HIV-1 remission reported in 2019 received no radiation and only one HSCT transplant (196). These treatment methods are not feasible for the wide-scale treatment of otherwise healthy HIV-positive people. However, these successes have inspired the gene-editing field to target the CCR5 gene to induce resistance to HIV-1 infection (at least through CCR5 tropic HIV-1).

To date, three major types of nucleases are used for genome editing, namely, zinc finger nucleases (ZFN), transcription activator-like effector nucleases (TALEN), and the Cas9 endonuclease with clustered regularly interspaced short palindromic repeats (CRISPR). All three utilize a similar overall mechanism of binding a target DNA sequence, creating a double-stranded break allowing the DNA to undergo repair through the error-prone non-homologous end joining (NHEJ), resulting in small insertions or deletions disrupting gene expression [reviewed in (197)].

ZFN consist of pairs of zinc finger DNA binding domains that recognize three base pairs of DNA and are covalently linked to complementary halves of a FokI restriction endonuclease. ZFNs have been utilized to confer resistance to HIV-1 infection in resting CD4+ T cells through the disruption of the CCR5 gene in humanized mouse models (59, 60). Similarly, Holt, Wang (123) showed human HSCs in which CCR5 was disrupted by ZFN, were able to engraft in NSG mice successfully and led to the development of CCR5-tropic HIV-1 resistant cells. Also, ZFNs targeting the CXCR4 co-receptor on CD4+ T cells have shown success in protecting from HIV-1 infection in humanized mice, although resistance was eventually lost upon selection for CCR5-tropic mutants (61, 62). Following these promising results in humanized mice, the first phase 1 human clinical trial with ZFN-CCR5 mutated CD4+ T cells was conducted, showing that these genetically modified CD4+ T cells were more resistant to HIV-1 infection and led to decrease viral loads during ART interruption (198).

The gene-editing field was revolutionized by the discovery of CRISPR/Cas9 in prokaryotes (199, 200) and its role in bacterial and archeal adaptive immunity against invading viruses (201). Unlike ZFNs, CRISPR/Cas9 relies on short sequences of guide RNA (gRNA) to target the Cas9 nuclease to the complementary DNA sequence to be edited. This feature of CRISPR/Cas9 makes it more sequence-specific and easier to design and produce, leading to its first use in gene editing by Jinek, Chylinski (202), a landmark discovery leading to a Nobel prize award in chemistry in 2020. Not long after, CRISPR/Cas9 was used to target the HIV-1 LTR in human cell lines resulting in a significant decrease in HIV-1 expression upon stimulation (203). Recently, CRISPR with *Staphylococcus aureus* Cas9 (SaCas9) delivered by a lentiviral vector improved primary CD4+ T cell resistance to HIV-1 infection. Also, transplanting these cells into NCG humanized mice resulted in enhanced survival upon challenge with CCR5 tropic HIV-1_{YU2} (64).

In addition to targeting host factors, another gene-editing approach that has picked up steam is to directly target the integrated HIV-1 provirus for excision (203–205). This approach has been used to remove the entire HIV-1 genome between the 5' and 3 LTRs from latently infected human CD4+ T cells (206). Humanized mice have shown to be invaluable in testing these approaches in a model that accurately recapitulates HIV latency, as is seen in humans. Yin, Zhang (66) discovered that *in vivo* excision of the HIV-1 provirus with a SaCas9 with multiplex single-guide RNAs (sgRNA) was successful in a small cohort of BLT mice. A TALEN targeting the TATA-box of the HIV-1 LTR has also been used successfully to clear HIV-1 *ex vivo* on splenocytes derived from humanized mice (63).

Recently the Gendelmann lab combined long-acting slow-effective release (LASER) ART treatment with consequent CRISPR/Cas9 treatment to excise HIV DNA (65). They showed in 3 donor cohorts of hu-HSC mice, over a third 9/23 of the mice showed no rebound of the infectious virus following combination treatment than LASER ART or CRISPR/Cas9 treatment alone (65). Multiple organs, including the spleen, bone marrow, gut, brain, liver, kidney, and lung of these mice were assessed and showed no viral rebound (65). This data provides a solid foundation for the efficacy of these gene-editing approaches *in vivo* and can pave the way for human clinical trials.

Block and Lock

While the therapeutic approaches discussed so far have focused on the complete eradication of HIV-1 reservoirs, the Valente lab took an alternate approach to lock HIV-1 in its latent state by targeting the HIV-1 Tat protein (67, 207). Tat is transcribed early in the HIV-1 lifecycle and recruits the necessary transcription factors to enhance viral transcription and stabilize elongation (208). Specifically, Tat binds the 5' terminal region of the transactivation response element (TAR) (208) on HIV mRNA and recruits the positive transcription elongation factor B (PTEF-b) (209). PTEFb is composed of cyclin T1 and cyclin-dependent kinase 9 (CDK9), promoting transcription elongation from the viral promoter (210). Also, Tat has shown to recruit chromatin remodeling factors such as SWI/SNF (211, 212) and histone acetyltransferases (213–215) allowing chromatin to remain in an open state and thus allowing easier access to transcription factors such as nuclear factor-kB (NFkB).

Targeting viral factors such as Tat is a major focus of antiretroviral therapy research, mainly due to the absence of a host cellular homolog, resulting in less toxicity. The Valente Lab discovered that didehydro-cortistatin A (dCA), a synthetic analog of the natural product cortistatin A, potently inhibits Tat-dependent transcription activity in both acutely and chronically infected cells (216). dCA was also found to act additively with conventional HAART, inhibiting spontaneous viral particle release from CD4+ T cells in virally suppressed subjects (216). Soon after that, they showed that dCA effectively inhibits viral reactivation by a PKC agonist or by antigenic stimulation of primary latently infected cells isolated from ART-treated individuals (207). Furthermore, they demonstrated that dCA, unlike conventional ART, can reduce the base level cell-associated HIV-1 RNA production by decreasing RNA Polymerase II recruitment to the viral promoter (207). Primary CD4+ T cell cultures alone cannot fully capture the characteristics of latently reservoirs, as these use clonal HIV strains and specific cytokine cocktails to prolong lifespan. These conditions may transform these cells and alter cell-subset representation. Therefore, in a subsequent study, Kessing, Nixon (67) tested the ability of dCA to suppress viral reactivation in a BLT mouse

model. Humanized mice were infected with HIV-1_{JRCSF} and treated with ART for three weeks, at which point dCA was combined with ART for the fourth week (67). Strikingly, upon treatment interruption, viral rebound was delayed up to 19 days in mice treated with dCA compared to the controls, which showed rebound between 3-7 days upon treatment interruption (67). Unfortunately, certain viruses develop resistance to dCA through a combination of mutations in Nef and Vpr that increase NF-κB activity and lead to a higher Tat-independent basal transcription (217). The discovery of additional transcriptional inhibitors that promote deep latency through different mechanisms, used in combination with dCA could be the way forward for the block and lock strategy. In *vivo* analysis in humanized mouse models will be critical in their translation to the clinic.

LIMITATIONS OF HUMANIZED MICE

Despite the fact that they are an advantageous small animal model for HIV-1 cure research, humanized mice have their limitations. Hu-PBL mice and, to a lesser extent, hu-HSC and BLT mice occasionally develop graft-versus-host disease. GvHD is characterized by lymphocytic infiltration, progressive inflammation, and sclerosis in multiple organs, eventually leading to death (140). Moreover, the associated excessive inflammation can confound results from long-term HIV-1 studies. The use of NSG mice over NOD/SCID mice for the construction of BLT humanized mice was found to delay the onset of GVHD, although it did not decrease its incidence (140). Furthermore, even with many advances over the years, here remain deficiencies in the immune response of humanized mice compared to a complete human immune system. First, they lack robust humoral immune responses due to limited class switch recombination and mutation rates, limiting the study of B cell responses, particularly in vaccination studies (23, 134). Also, hu-PBL, and hu-HSC mice lack human HLA restriction of T cells, leading to deficiencies in the development and functionality of T cells, a significant advantage of the BLT model.

On the other hand, the construction of BLT mice requires significant technical expertise to produce, and access to fetal tissue for scientific research continues to become scarce. Moreover, the murine environment lacks human cytokines and poor cross-reactivity with murine cytokines leads to incomplete development of some human myeloid and lymphoid cell subsets. Several solutions for this include treatment with exogenous human cytokines. For instance, periodic intraperitoneal injection of human IL-15/IL-15Rα is used to support the proliferation and survival of NK cells (46, 218). Other strategies involve knock-in and transgenic human cytokine insertions into immunodeficient mice. For example, human IL-2 and IL-15 transgenics (219), IL-15 and SIRPα knock-in (39), and IL-7 and IL-15 knock-in mice (220) promote NK cell development in humanized mice. Also, mice that comprise multiples gene modifications to produce the cytokines macrophage-colony stimulating factor (M-CSF), IL-3, granulocyte-colony stimulating factor (GM-CSF), and thrombopoietin have been established to support monocytes and macrophage development (33). While these modified humanized mouse models show potential in producing a more comprehensive innate immune system, their utility in HIV-1 persistence and therapeutic studies has yet to be evaluated.

Another limitation to long term persistence studies is the limited lifespan of mice (221), making studies lasting several years impractical. In these cases, an NHP model would be more suitable. Even though small animals are easier to house and maintain, they bring the additional constraint of having lower blood volumes and cell numbers for analyses, making *ex vivo* assays technically challenging to perform. Furthermore, the murine basal metabolic rate is different from that of humans and needs to be considered, particularly when dealing with pharmacological approaches (222). Lastly, the murine gut microbiome differs significantly from that of humans. This important topic has been reviewed in detail elsewhere (223, 224). The microbiome has several implications in HIV-1 infection, pathogenesis, and the host immune response [reviewed in (225–228)], and the microbiomes of inbred mice in a controlled environment aren't capable of fully recapitulating these effects. To skew the microbiome to resemble that seen in humans, Daharsh, Zhang (229) treated BLT mice with broad-spectrum antibiotics to deplete the murine gut microbiome, followed by fecal transplants from healthy human donor samples *via* oral gavage. While this approach shifted the murine microbiome towards the corresponding human donors, they didn't wholly resemble a human gut microbiome. Future developments may improve this premise, leading to a more comprehensive mouse model mimicking both a human immune system and the human gut microbiome.

CONCLUSION

Regardless of its limitations, the humanized mouse is currently the only small animal model for HIV-1 and has proved to be an incredible resource in many facets of HIV-1 research in the past four decades. Large cohorts of mice can be generated from tissues derived from a single human donor, resulting in animals with genetically identical human immune cells. This approach allows us to control genetic variables and perform specific experiments such as adoptive transfers of lymphocytes, which would not be possible in most NHPs. Furthermore, humanized mice do not require a surrogate virus for infection and are susceptible to multiple routes of HIV-1 transmission. Moreover, tissue reservoirs harboring latent viruses can be analyzed, allowing a more straightforward comparison of the systemic effects of administered therapeutics, which is exceedingly essential for HIV-1 eradication efforts. Humanized mice have been critical in HIV-1 research, and we expect they will continue to play a significant role in ultimately translating a cure from bench to bedside.

AUTHOR CONTRIBUTIONS

SA and SP conceptualized the content of and wrote the article. All authors contributed to the article and approved the submitted version.

FUNDING

This work was supported by NIH RO1 AI116282 (SP), and unrestricted funds from The Scripps Research Institute, La Jolla, CA (SP).

REFERENCES

1. Barre-Sinoussi F, Chermann JC, Rey F, Nugeyre MT, Chamaret S, Gruest J, et al. Isolation of a T-lymphotropic retrovirus from a patient at risk for acquired immune deficiency syndrome (AIDS). *Sci (N Y NY)* (1983) 220 (4599):868–71. doi: 10.1126/science.6189183
2. Arts EJ, Hazuda DJ. HIV-1 antiretroviral drug therapy. *Cold Spring Harb Perspect Med* (2012) 2(4):a007161–a. doi: 10.1101/cshperspect.a007161
3. Apetrei C, Pandrea I, Mellors JW. Nonhuman primate models for HIV cure research. *PloS Pathog* (2012) 8(8):e1002892–e. doi: 10.1371/journal.ppat.1002892
4. Evans DT, Silvestri G. Nonhuman primate models in AIDS research. *Curr Opin HIV AIDS* (2013) 8(4):255–61. doi: 10.1097/COH.0b013e328361cee8
5. Van Rompay KKA, Tackling HIV. and AIDS: contributions by non-human primate models. *Lab Anim* (2017) 46(6):259–70. doi: 10.1038/laban.1279
6. Sun M, Li Y, Yuan Z, Lu W, Kang G, Fan W, et al. VRC01 antibody protects against vaginal and rectal transmission of human immunodeficiency virus 1 in hu-BLT mice. *Arch Virol* (2016) 161(9):2449–55. doi: 10.1007/s00705-016-2942-4
7. Pardi N, Secreto AJ, Shan X, Debonera F, Glover J, Yi Y, et al. Administration of nucleoside-modified mRNA encoding broadly neutralizing antibody protects humanized mice from HIV-1 challenge. *Nat Commun* (2017) 8:14630. doi: 10.1038/ncomms14630
8. Baum MM, Ramirez CM, Moss JA, Gunawardana M, Bobardt M, Gallay PA. Highly synergistic drug combination prevents vaginal HIV infection in humanized mice. *Sci Rep* (2020) 10(1):12995. doi: 10.1038/s41598-020-69937-5
9. Denton PW, Garcia JV. Mucosal HIV-1 transmission and prevention strategies in BLT humanized mice. *Trends Microbiol* (2012) 20(6):268–74. doi: 10.1016/j.tim.2012.03.007
10. Tager AM, Pensiero M, Allen TM. Recent advances in humanized mice: accelerating the development of an HIV vaccine. *J Infect Dis* (2013) 208Suppl 2(Suppl 2):S121–S4. doi: 10.1093/infdis/jit451
11. McCune JM, Namikawa R, Kaneshima H, Shultz LD, Lieberman M, Weissman IL. The SCID-hu mouse: murine model for the analysis of human hematolymphoid differentiation and function. *Sci (N Y NY)* (1988) 241(4873):1632–9. doi: 10.1126/science.2971269
12. Namikawa R, Weilbaecher KN, Kaneshima H, Yee EJ, McCune JM. Long-term human hematopoiesis in the SCID-hu mouse. *J Exp Med* (1990) 172 (4):1055–63. doi: 10.1084/jem.172.4.1055
13. Mosier DE, Gulizia RJ, Baird SM, Wilson DB. Transfer of a functional human immune system to mice with severe combined immunodeficiency. *Nature* (1988) 335(6187):256–9. doi: 10.1038/335256a0
14. Hesselton RM, Greiner DL, Mordes JP, Rajan TV, Sullivan JL, Shultz LD. High levels of human peripheral blood mononuclear cell engraftment and enhanced susceptibility to human immunodeficiency virus type 1 infection in NOD/LtSz-scid/scid mice. *J Infect Dis* (1995) 172(4):974–82. doi: 10.1093/infdis/172.4.974
15. van Rijn RS, Simonetti ER, Hagenbeek A, Hogenes MCH, de Weger RA, Canninga-van Dijk MR, et al. A new xenograft model for graft-versus-host disease by intravenous transfer of human peripheral blood mononuclear cells in RAG2-/- γc-/- double-mutant mice. *Blood* (2003) 102(7):2522–31. doi: 10.1182/blood-2002-10-3241
16. Ali N, Flutter B, Sanchez Rodriguez R, Sharif-Paghaleh E, Barber LD, Lombardi G, et al. Xenogeneic graft-versus-host-disease in NOD-scid IL-2Rγnull mice display a T-effector memory phenotype. *PloS One* (2012) 7(8): e44219. doi: 10.1371/journal.pone.0044219
17. Kamel-Reid S, Dick J. Engraftment of immune-deficient mice with human hematopoietic stem cells. *Sci (N Y NY)* (1988) 242(4886):1706–9. doi: 10.1126/science.2904703
18. Péault B, Weissman IL, Baum C, McCune JM, Tsukamoto A. Lymphoid reconstitution of the human fetal thymus in SCID mice with CD34+ precursor cells. *J Exp Med* (1991) 174(5):1283–6. doi: 10.1084/jem.174.5.1283
19. Hiramatsu H, Nishikomori R, Heike T, Ito M, Kobayashi K, Katamura K, et al. Complete reconstitution of human lymphocytes from cord blood CD34 + cells using the NOD/SCID/gammacnull mice model. *Blood* (2003) 102 (3):873–80. doi: 10.1182/blood-2002-09-2755
20. Danner R, Chaudhari SN, Rosenberger J, Surls J, Richie TL, Brumeanu TD, et al. Expression of HLA class II molecules in humanized NOD.Rag1KO.IL2RgcKO mice is critical for development and function of human T and B cells. *PloS One* (2011) 6(5):e19826. doi: 10.1371/journal.pone.0019826
21. Lan P, Tonomura N, Shimizu A, Wang S, Yang Y-G. Reconstitution of a functional human immune system in immunodeficient mice through combined human fetal thymus/liver and CD34+ cell transplantation. *Blood* (2006) 108(2):487–92. doi: 10.1182/blood-2005-11-4388
22. Melkus MW, Estes JD, Padgett-Thomas A, Gatlin J, Denton PW, Othieno FA, et al. Humanized mice mount specific adaptive and innate immune responses to EBV and TSST-1. *Nat Med* (2006) 12(11):1316–22. doi: 10.1038/nm1431
23. Brainard DM, Seung E, Frahm N, Cariappa A, Bailey CC, Hart WK, et al. Induction of robust cellular and humoral virus-specific adaptive immune responses in human immunodeficiency virus-infected humanized BLT mice. *J Virol* (2009) 83(14):7305–21. doi: 10.1128/JVI.02207-08
24. Stoddart CA, Maidji E, Galkina SA, Kosikova G, Rivera JM, Moreno ME, et al. Superior human leukocyte reconstitution and susceptibility to vaginal HIV transmission in humanized NOD-scid IL-2Rγ(-/-) (NSG) BLT mice. *Virology* (2011) 417(1):154–60. doi: 10.1016/j.virol.2011.05.013
25. Lavender KJ, Messer RJ, Race B, Hasenkrug KJ. Production of bone marrow, liver, thymus (BLT) humanized mice on the C57BL/6 Rag2(-/-)γc(-/-)CD47 (-/-) background. *J Immunol Methods* (2014) 407:127–34. doi: 10.1016/j.jim.2014.04.008
26. Lavender KJ, Pang WW, Messer RJ, Duley AK, Race B, Phillips K, et al. BLT-humanized C57BL/6 Rag2-/-γc-/-CD47-/- mice are resistant to GVHD and develop B- and T-cell immunity to HIV infection. *Blood* (2013) 122 (25):4013–20. doi: 10.1182/blood-2013-06-506949
27. Lavender KJ, Pace C, Sutter K, Messer RJ, Pouncey DL, Cummins NW, et al. An advanced BLT-humanized mouse model for extended HIV-1 cure studies. *AIDS* (2018) 32(1):1–10. doi: 10.1097/QAD.0000000000001674
28. Lapidot T, Pflumio F, Doedens M, Murdoch B, Williams DE, Dick JE. Cytokine stimulation of multilineage hematopoiesis from immature human cells engrafted in SCID mice. *Sci (N Y NY)* (1992) 255(5048):1137–41. doi: 10.1126/science.1372131
29. Shultz LD, Saito Y, Najima Y, Tanaka S, Ochi T, Tomizawa M, et al. Generation of functional human T-cell subsets with HLA-restricted immune responses in HLA class I expressing NOD/SCID/IL2r gamma(null) humanized mice. *Proc Natl Acad Sci USA* (2010) 107(29):13022–7. doi: 10.1073/pnas.1000475107
30. Choi B, Chun E, Kim M, Kim ST, Yoon K, Lee KY, et al. Human B cell development and antibody production in humanized NOD/SCID/IL-2Rγ(null) (NSG) mice conditioned by busulfan. *J Clin Immunol* (2011) 31 (2):253–64. doi: 10.1007/s10875-010-9478-2
31. Chen Q, He F, Kwang J, Chan JKY, Chen J. GM-CSF and IL-4 Stimulate Antibody Responses in Humanized Mice by Promoting T, B, and Dendritic Cell Maturation. *J Immunol* (2012) 189(11):5223–9. doi: 10.4049/jimmunol.1201789
32. Ito R, Takahashi T, Katano I, Kawai K, Kamisako T, Ogura T, et al. Establishment of a Human Allergy Model Using Human IL-3/GM-CSF–Transgenic NOG Mice. *J Immunol* (2013) 191(6):2890–9. doi: 10.4049/jimmunol.1203543

33. Rongvaux A, Willinger T, Martinek J, Strowig T, Gearty SV, Teichmann LL, et al. Development and function of human innate immune cells in a humanized mouse model. *Nat Biotechnol* (2014) 32(4):364–72. doi: 10.1038/nbt.2858
34. Billerbeck E, Horwitz JA, Labitt RN, Donovan BM, Vega K, Budell WC, et al. Characterization of human antiviral adaptive immune responses during hepatotropic virus infection in HLA-transgenic human immune system mice. *J Immunol (Baltimore Md 1950)* (2013) 191(4):1753–64. doi: 10.4049/jimmunol.1201518
35. Billerbeck E, Labitt RN, Vega K, Frias-Staheli N, Dorner M, Xiao JW, et al. Insufficient interleukin-12 signalling favours differentiation of human CD4+ and CD8+ T cells into GATA-3+ and GATA-3+ T-bet+ subsets in humanized mice. *Immunology* (2014) 143(2):202–18. doi: 10.1111/imm.12304
36. Ding Y, Wilkinson A, Idris A, Fancke B, O'Keeffe M, Khalil D, et al. FLT3-Ligand Treatment of Humanized Mice Results in the Generation of Large Numbers of CD141+ and CD1c+ Dendritic Cells In Vivo. *J Immunol* (2014) 192(4):1982–9. doi: 10.4049/jimmunol.1302391
37. Majji S, Wijayalath W, Shashikumar S, Pow-Sang L, Villasante E, Brumeanu TD, et al. Differential effect of HLA class-I versus class-II transgenes on human T and B cell reconstitution and function in NRG mice. *Sci Rep* (2016) 6:28093. doi: 10.1038/srep28093
38. Li Y, Mention JJ, Court N, Masse-Ranson G, Toubert A, Spits H, et al. A novel Flt3-deficient HIS mouse model with selective enhancement of human DC development. *Eur J Immunol* (2016) 46(5):1291–9. doi: 10.1002/eji.201546132
39. Herndler-Brandstetter D, Shan L, Yao Y, Stecher C, Plajer V, Lietzenmayer M, et al. Humanized mouse model supports development, function, and tissue residency of human natural killer cells. *Proc Natl Acad Sci* (2017) 114(45):E9626–E34. doi: 10.1073/pnas.1705301114
40. Biswas S, Chang H, Sarkis PT, Fikrig E, Zhu Q, Marasco WA. Humoral immune responses in humanized BLT mice immunized with West Nile virus and HIV-1 envelope proteins are largely mediated via human CD5+ B cells. *Immunology* (2011) 134(4):419–33. doi: 10.1111/j.1365-2567.2011.03501.x
41. Kalscheuer H, Danzl N, Onoe T, Faust T, Winchester R, Goland R, et al. A model for personalized in vivo analysis of human immune responsiveness. *Sci Transl Med* (2012) 4(125):125ra30. doi: 10.1126/scitranslmed.3003481
42. Denton PW, Nochi T, Lim A, Krisko JF, Martinez-Torres F, Choudhary SK, et al. IL-2 receptor γ-chain molecule is critical for intestinal T-cell reconstitution in humanized mice. *Mucosal Immunol* (2012) 5(5):555–66. doi: 10.1038/mi.2012.31
43. Smith DJ, Lin LJ, Moon H, Pham AT, Wang X, Liu S, et al. Propagating Humanized BLT Mice for the Study of Human Immunology and Immunotherapy. *Stem Cells Dev* (2016) 25(24):1863–73. doi: 10.1089/scd.2016.0193
44. Bryce PJ, Falahati R, Kenney LL, Leung J, Bebbington C, Tomasevic N, et al. Humanized mouse model of mast cell-mediated passive cutaneous anaphylaxis and passive systemic anaphylaxis. *J Allergy Clin Immunol* (2016) 138(3):769–79. doi: 10.1016/j.jaci.2016.01.049
45. Honeycutt JB, Wahl A, Baker C, Spagnuolo RA, Foster J, Zakharova O, et al. Macrophages sustain HIV replication in vivo independently of T cells. *J Clin Invest* (2016) 126(4):1353–66. doi: 10.1172/JCI84456
46. Nikzad R, Angelo LS, Aviles-Padilla K, Le DT, Singh VK, Bimler L, et al. Human natural killer cells mediate adaptive immunity to viral antigens. *Sci Immunol* (2019) 4(35):eaat8116. doi: 10.1126/sciimmunol.aat8116
47. Poignard P, Sabbe R, Picchio GR, Wang M, Gulizia RJ, Katinger H, et al. Neutralizing antibodies have limited effects on the control of established HIV-1 infection in vivo. *Immunity* (1999) 10(4):431–8. doi: 10.1016/S1074-7613(00)80043-6
48. Klein F, Halper-Stromberg A, Horwitz JA, Gruell H, Scheid JF, Bournazos S, et al. HIV therapy by a combination of broadly neutralizing antibodies in humanized mice. *Nature* (2012) 492(7427):118–22. doi: 10.1038/nature11604
49. Horwitz JA, Halper-Stromberg A, Mouquet H, Gitlin AD, Tretiakova A, Eisenreich TR, et al. HIV-1 suppression and durable control by combining single broadly neutralizing antibodies and antiretroviral drugs in humanized mice. *Proc Natl Acad Sci* (2013) 110(41):16538–43. doi: 10.1073/pnas.1315295110
50. Halper-Stromberg A, Lu C-L, Klein F, Horwitz Joshua A, Bournazos S, Nogueira L, et al. Broadly Neutralizing Antibodies and Viral Inducers Decrease Rebound from HIV-1 Latent Reservoirs in Humanized Mice. *Cell* (2014) 158(5):989–99. doi: 10.1016/j.cell.2014.07.043
51. Wang P, Gajjar MR, Yu J, Padte NN, Gettie A, Blanchard JL, et al. Quantifying the contribution of Fc-mediated effector functions to the antiviral activity of anti-HIV-1 IgG1 antibodies in vivo. *Proc Natl Acad Sci U S A* (2020) 117(30):18002–9. doi: 10.1073/pnas.2008190117
52. Badamchi-Zadeh A, Tartaglia LJ, Abbink P, Bricault CA, Liu P-T, Boyd M, et al. Therapeutic Efficacy of Vectored PGT121 Gene Delivery in HIV-1-Infected Humanized Mice. *J Virol* (2018) 92(7):e01925–17. doi: 10.1128/JVI.01925-17
53. Kitchen SG, Bennett M, Galić Z, Kim J, Xu Q, Young A, et al. Engineering antigen-specific T cells from genetically modified human hematopoietic stem cells in immunodeficient mice. *PloS One* (2009) 4(12):e8208. doi: 10.1371/journal.pone.0008208
54. Kitchen SG, Levin BR, Bristol G, Rezek V, Kim S, Aguilera-Sandoval C, et al. In vivo suppression of HIV by antigen specific T cells derived from engineered hematopoietic stem cells. *PloS Pathog* (2012) 8(4):e1002649. doi: 10.1371/journal.ppat.1002649
55. Zhen A, Kamata M, Rezek V, Rick J, Levin B, Kasparian S, et al. HIV-specific Immunity Derived From Chimeric Antigen Receptor-engineered Stem Cells. *Mol Ther J Am Soc Gene Ther* (2015) 23(8):1358–67. doi: 10.1038/mt.2015.102
56. Leibman RS, Richardson MW, Ellebrecht CT, Maldini CR, Glover JA, Secreto AJ, et al. Supraphysiologic control over HIV-1 replication mediated by CD8 T cells expressing a re-engineered CD4-based chimeric antigen receptor. *PloS Pathog* (2017) 13(10):e1006613. doi: 10.1371/journal.ppat.1006613
57. Bardhi A, Wu Y, Chen W, Li W, Zhu Z, Zheng JH, et al. Potent In Vivo NK Cell-Mediated Elimination of HIV-1-Infected Cells Mobilized by a gp120-Bispecific and Hexavalent Broadly Neutralizing Fusion Protein. *J Virol* (2017) 91(20):e00937–17. doi: 10.1128/JVI.00937-17
58. Anthony-Gonda K, Bardhi A, Ray A, Flerin N, Li M, Chen W, et al. Multispecific anti-HIV duoCAR-T cells display broad in vitro antiviral activity and potent in vivo elimination of HIV-infected cells in a humanized mouse model. *Sci Trans Med* (2019) 11(504):eaav5685. doi: 10.1126/scitranslmed.aav5685
59. Perez EE, Wang J, Miller JC, Jouvenot Y, Kim KA, Liu O, et al. Establishment of HIV-1 resistance in CD4+ T cells by genome editing using zinc-finger nucleases. *Nat Biotechnol* (2008) 26(7):808–16. doi: 10.1038/nbt1410
60. Yi G, Choi JG, Bharaj P, Abraham S, Dang Y, Kafri T, et al. CCR5 Gene Editing of Resting CD4(+) T Cells by Transient ZFN Expression From HIV Envelope Pseudotyped Nonintegrating Lentivirus Confers HIV-1 Resistance in Humanized Mice. *Mol Ther Nucleic Acids* (2014) 3:e198. doi: 10.1038/mtna.2014.52
61. Wilen CB, Wang J, Tilton JC, Miller JC, Kim KA, Rebar EJ, et al. Engineering HIV-Resistant Human CD4+ T Cells with CXCR4-Specific Zinc-Finger Nucleases. *PloS Pathog* (2011) 7(4):e1002020. doi: 10.1371/journal.ppat.1002020
62. Yuan J, Wang J, Crain K, Fearns C, Kim KA, Hua KL, et al. Zinc-finger Nuclease Editing of Human cxcr4 Promotes HIV-1 CD4+ T Cell Resistance and Enrichment. *Mol Ther* (2012) 20(4):849–59. doi: 10.1038/mt.2011.310
63. Llewellyn GN, Seclén E, Wietgrefe S, Liu S, Chateau M, Pei H, et al. Humanized Mouse Model of HIV-1 Latency with Enrichment of Latent Virus in PD-1(+) and TIGIT(+) CD4 T Cells. *J Virol* (2019) 93(10):e02086–18. doi: 10.1128/JVI.02086-18
64. Xiao Q, Chen S, Wang Q, Liu Z, Liu S, Deng H, et al. CCR5 editing by Staphylococcus aureus Cas9 in human primary CD4+ T cells and hematopoietic stem/progenitor cells promotes HIV-1 resistance and CD4+ T cell enrichment in humanized mice. *Retrovirology* (2019) 16(1):15. doi: 10.1186/s12977-019-0477-y
65. Dash PK, Kaminski R, Bella R, Su H, Mathews S, Ahooyi TM, et al. and CRISPR Treatments Eliminate HIV-1 in a Subset of Infected Humanized Mice. *Nat Commun* (2019) 10(1):2753. doi: 10.1038/s41467-019-10366-y
66. Yin C, Zhang T, Qu X, Zhang Y, Putatunda R, Xiao X, et al. In Vivo Excision of HIV-1 Provirus by saCas9 and Multiplex Single-Guide RNAs in Animal

Models. *Mol Ther J Am Soc Gene Ther* (2017) 25(5):1168–86. doi: 10.1016/j.ymthe.2017.03.012
67. Kessing CF, Nixon CC, Li C, Tsai P, Takata H, Mousseau G, et al. In Vivo Suppression of HIV Rebound by Didehydro-Cortistatin A, a "Block-and-Lock" Strategy for HIV-1 Treatment. *Cell Rep* (2017) 21(3):600–11. doi: 10.1016/j.celrep.2017.09.080
68. Gatti RA, Meuwissen HJ, Allen HD, Hong R, Good RA. Immunological reconstitution of sex-linked lymphopenic immunological deficiency. *Lancet (London England)* (1968) 2(7583):1366–9. doi: 10.1016/S0140-6736(68)92673-1
69. Bosma GC, Custer RP, Bosma MJ. A severe combined immunodeficiency mutation in the mouse. *Nature* (1983) 301(5900):527–30. doi: 10.1038/301527a0
70. Fulop GM, Phillips RA. Full reconstitution of the immune deficiency in scid mice with normal stem cells requires low-dose irradiation of the recipients. *J Immunol (Baltimore Md 1950)* (1986) 136(12):4438–43.
71. McCune J, Kaneshima H, Krowka J, Namikawa R, Outzen H, Peault B, et al. The SCID-hu mouse: a small animal model for HIV infection and pathogenesis. *Annu Rev Immunol* (1991) 9:399–429. doi: 10.1146/annurev.iy.09.040191.002151
72. Moore MAS, Owen JJT. STEM-CELL MIGRATION IN DEVELOPING MYELOID AND LYMPHOID SYSTEMS. *Lancet* (1967) 290(7517):658–9. doi: 10.1016/S0140-6736(67)90693-9
73. Namikawa R, Mizuno T, Matsuoka H, Fukami H, Ueda R, Itoh G, et al. Ontogenic development of T and B cells and non-lymphoid cells in the white pulp of human spleen. *Immunology* (1986) 57(1):61–9.
74. Barry TS, Jones DM, Richter CB, Haynes BF. Successful engraftment of human postnatal thymus in severe combined immune deficient (SCID) mice: differential engraftment of thymic components with irradiation versus anti-asialo GM-1 immunosuppressive regimens. *J Exp Med* (1991) 173 (1):167–80. doi: 10.1084/jem.173.1.167
75. Aldrovandi GM, Feuer G, Gao L, Jamieson B, Kristeva M, Chen IS, et al. The SCID-hu mouse as a model for HIV-1 infection. *Nature* (1993) 363 (6431):732–6. doi: 10.1038/363732a0
76. Namikawa R, Kaneshima H, Lieberman M, Weissman IL, McCune JM. Infection of the SCID-hu mouse by HIV-1. *Sci (N Y NY)* (1988) 242 (4886):1684–6. doi: 10.1126/science.3201256
77. McCune J, Namikawa R, Shih C, Rabin L, Kaneshima H. Suppression of HIV infection in AZT-treated SCID-hu mice. *Sci (N Y NY)* (1990) 247 (4942):564–6. doi: 10.1126/science.2300816
78. Torbett BE, Picchio G, Mosier DE. hu-PBL-SCID Mice: A Model for Human Immune Function, AIDS, and Lymphomagenesis. *Immunol Rev* (1991) 124 (1):139–64. doi: 10.1111/j.1600-065X.1991.tb00620.x
79. Rizza P, Santini SM, Logozzi MA, Lapenta C, Sestili P, Gherardi G, et al. T-cell dysfunctions in hu-PBL-SCID mice infected with human immunodeficiency virus (HIV) shortly after reconstitution: in vivo effects of HIV on highly activated human immune cells.s. *J Virol* (1996) 70 (11):7958–64. doi: 10.1128/JVI.70.11.7958-7964.1996
80. Makino S, Kunimoto K, Muraoka Y, Mizushima Y, Katagiri K, Tochino Y. Breeding of a non-obese, diabetic strain of mice. *Jikken Dobutsu* (1980) 29 (1):1–13. doi: 10.1538/expanim1978.29.1_1
81. Leiter EH, Serreze DV, Prochazka M. The genetics and epidemiology of diabetes in NOD mice. *Immunol Today* (1990) 11(5):147–9. doi: 10.1016/0167-5699(90)90057-G
82. Cao X, Shores EW, Hu-Li J, Anver MR, Kelsall BL, Russell SM, et al. Defective lymphoid development in mice lacking expression of the common cytokine receptor gamma chain. *Immunity* (1995) 2(3):223–38. doi: 10.1016/1074-7613(95)90047-0
83. Ohbo K, Suda T, Hashiyama M, Mantani A, Ikebe M, Miyakawa K, et al. Modulation of hematopoiesis in mice with a truncated mutant of the interleukin-2 receptor gamma chain. *Blood* (1996) 87(3):956–67. doi: 10.1182/blood.V87.3.956.bloodjournal873956
84. Russell S, Keegan A, Harada N, Nakamura Y, Noguchi M, Leland P, et al. Interleukin-2 receptor gamma chain: a functional component of the interleukin-4 receptor. *Sci (N Y NY)* (1993) 262(5141):1880–3. doi: 10.1126/science.8266078
85. Kondo M, Takeshita T, Ishii N, Nakamura M, Watanabe S, K-i A, et al. Sharing of the Interleukin-2 (IL-2) receptor ?? chain between receptors for IL-2 and IL-4. *Sci (N Y NY)* (1994) 262:1874–7. doi: 10.1126/science.8266076
86. Noguchi M, Nakamura Y, Russell S, Ziegler S, Tsang M, Cao X, et al. Interleukin-2 receptor gamma chain: a functional component of the interleukin-7 receptor. *Sci (N Y NY)* (1993) 262(5141):1877–80. doi: 10.1126/science.8266077
87. Kondo M, Takeshita T, Higuchi M, Nakamura M, Sudo T, Nishikawa S, et al. Functional participation of the IL-2 receptor gamma chain in IL-7 receptor complexes. *Sci (N Y NY)* (1994) 263(5152):1453–4. doi: 10.1126/science.8128231
88. Kimura Y, Takeshita T, Kondo M, Ishii N, Nakamura M, Van Snick J, et al. Sharing of the IL-2 receptor gamma chain with the functional IL-9 receptor complex. *Int Immunol* (1995) 7(1):115–20. doi: 10.1093/intimm/7.1.115
89. Giri JG, Ahdieh M, Eisenman J, Shanebeck K, Grabstein K, Kumaki S, et al. Utilization of the beta and gamma chains of the IL-2 receptor by the novel cytokine IL-15. *EMBO J* (1994) 13(12):2822–30. doi: 10.1002/j.1460-2075.1994.tb06576.x
90. Habib T, Senadheera S, Weinberg K, Kaushansky K. The common gamma chain (gamma c) is a required signaling component of the IL-21 receptor and supports IL-21-induced cell proliferation via JAK3. *Biochemistry* (2002) 41(27):8725–31. doi: 10.1021/bi0202023
91. Christianson SW, Greiner DL, Schweitzer IB, Gott B, Beamer GL, Schweitzer PA, et al. Role of natural killer cells on engraftment of human lymphoid cells and on metastasis of human T-lymphoblastoid leukemia cells in C57BL/6J-scid mice and in C57BL/6J-scid bg mice. *Cell Immunol* (1996) 171(2):186–99. doi: 10.1006/cimm.1996.0193
92. Ifversen P, Borrebaeck CA. SCID-hu-PBL: a model for making human antibodies? *Semin Immunol* (1996) 8(4):243–8. doi: 10.1006/smim.1996.0030
93. Murphy WJ, Taub DD, Longo DL. The huPBL-SCID mouse as a means to examine human immune function in vivo. *Semin Immunol* (1996) 8(4):233–41. doi: 10.1006/smim.1996.0029
94. Koyanagi Y, Tanaka Y, Kira J, Ito M, Hioki K, Misawa N, et al. Primary human immunodeficiency virus type 1 viremia and central nervous system invasion in a novel hu-PBL-immunodeficient mouse strain. *J Virol* (1997) 71 (3):2417–24. doi: 10.1128/JVI.71.3.2417-2424.1997
95. Kim KC, Choi BS, Kim KC, Park KH, Lee HJ, Cho YK, et al. A Simple Mouse Model for the Study of Human Immunodeficiency Virus. *AIDS Res Hum Retroviruses* (2016) 32(2):194–202. doi: 10.1089/aid.2015.0211
96. Mutis T, van Rijn RS, Simonetti ER, Aarts-Riemens T, Emmelot ME, van Bloois L, et al. Human Regulatory T Cells Control Xenogeneic Graft-versus-Host Disease Induced by Autologous T Cells in RAG2−/−γc−/− Immunodeficient Mice. *Clin Cancer Res* (2006) 12(18):5520–5. doi: 10.1158/1078-0432.CCR-06-0035
97. Gregoire-Gauthier J, Durrieu L, Duval A, Fontaine F, Dieng MM, Bourgey M, et al. Use of immunoglobulins in the prevention of GvHD in a xenogeneic NOD/SCID/γc− mouse model. *Bone Marrow Transplant* (2012) 47(3):439–50. doi: 10.1038/bmt.2011.93
98. Civin CI, Strauss LC, Brovall C, Fackler MJ, Schwartz JF, Shaper JH. Antigenic analysis of hematopoiesis. III. A hematopoietic progenitor cell surface antigen defined by a monoclonal antibody raised against KG-1a cells. *J Immunol (Baltimore Md 1950)* (1984) 133(1):157–65.
99. Andrews RG, Singer JW, Bernstein ID. Precursors of colony-forming cells in humans can be distinguished from colony-forming cells by expression of the CD33 and CD34 antigens and light scatter properties. *J Exp Med* (1989) 169 (5):1721–31. doi: 10.1084/jem.169.5.1721
100. Sutherland HJ, Eaves CJ, Eaves AC, Dragowska W, Lansdorp PM. Characterization and partial purification of human marrow cells capable of initiating long-term hematopoiesis in vitro. *Blood* (1989) 74(5):1563–70. doi: 10.1182/blood.V74.5.1563.1563
101. Bhatia M, Wang JC, Kapp U, Bonnet D, Dick JE. Purification of primitive human hematopoietic cells capable of repopulating immune-deficient mice. *Proc Natl Acad Sci U S A* (1997) 94(10):5320–5. doi: 10.1073/pnas.94.10.5320
102. Holyoake TL, Nicolini FE, Eaves CJ. Functional differences between transplantable human hematopoietic stem cells from fetal liver, cord blood, and adult marrow. *Exp Hematol* (1999) 27(9):1418–27. doi: 10.1016/S0301-472X(99)00078-8
103. Hao Q, Shah A, Thiemann F, Smogorzewska E, Crooks G. A functional comparison of CD34 + CD38- cells in cord blood and bone marrow. *Blood* (1995) 86(10):3745–53. doi: 10.1182/blood.V86.10.3745.bloodjournal86103745

104. Larochelle A, Vormoor J, Hanenberg H, Wang JCY, Bhatia M, Lapidot T, et al. Identification of primitive human hematopoietic cells capable of repopulating NOD/SCID mouse bone marrow: Implications for gene therapy. *Nat Med* (1996) 2(12):1329–37. doi: 10.1038/nm1296-1329
105. Ueda T, Yoshino H, Kobayashi K, Kawahata M, Ebihara Y, Ito M, et al. Hematopoietic repopulating ability of cord blood CD34(+) cells in NOD/Shi-scid mice. *Stem Cells* (2000) 18(3):204–13. doi: 10.1634/stemcells.18-3-204
106. Yahata T, Ando K, Nakamura Y, Ueyama Y, Shimamura K, Tamaoki N, et al. Functional human T lymphocyte development from cord blood CD34+ cells in nonobese diabetic/Shi-scid, IL-2 receptor gamma null mice. *J Immunol (Baltimore Md 1950)* (2002) 169(1):204–9. doi: 10.4049/jimmunol.169.1.204
107. Shultz LD, Lyons BL, Burzenski LM, Gott B, Chen X, Chaleff S, et al. Human Lymphoid and Myeloid Cell Development in NOD/LtSz-scid IL2Rγnull Mice Engrafted with Mobilized Human Hemopoietic Stem Cells. *J Immunol* (2005) 174(10):6477–89. doi: 10.4049/jimmunol.174.10.6477
108. McDermott SP, Eppert K, Lechman ER, Doedens M, Dick JE. Comparison of human cord blood engraftment between immunocompromised mouse strains. *Blood* (2010) 116(2):193–200. doi: 10.1182/blood-2010-02-271841
109. Tanaka T, Kitamura F, Nagasaka Y, Kuida K, Suwa H, Miyasaka M. Selective long-term elimination of natural killer cells in vivo by an anti-interleukin 2 receptor beta chain monoclonal antibody in mice. *J Exp Med* (1993) 178 (3):1103–7. doi: 10.1084/jem.178.3.1103
110. Watanabe S, Terashima K, Ohta S, Horibata S, Yajima M, Shiozawa Y, et al. Hematopoietic stem cell–engrafted NOD/SCID/IL2Rγnull mice develop human lymphoid systems and induce long-lasting HIV-1 infection with specific humoral immune responses. *Blood* (2006) 109(1):212–8. doi: 10.1182/blood-2006-04-017681
111. Watanabe S, Ohta S, Yajima M, Terashima K, Ito M, Mugishima H, et al. Humanized NOD/SCID/IL2Rγnull Mice Transplanted with Hematopoietic Stem Cells under Nonmyeloablative Conditions Show Prolonged Life Spans and Allow Detailed Analysis of Human Immunodeficiency Virus Type 1 Pathogenesis. *J Virol* (2007) 81(23):13259–64. doi: 10.1128/JVI.01353-07
112. Nie C, Sato K, Misawa N, Kitayama H, Fujino H, Hiramatsu H, et al. Selective infection of CD4+ effector memory T lymphocytes leads to preferential depletion of memory T lymphocytes in R5 HIV-1-infected humanized NOD/SCID/IL-2Rgammanull mice. *Virology* (2009) 394(1):64–72. doi: 10.1016/j.virol.2009.08.011
113. Sato K, Izumi T, Misawa N, Kobayashi T, Yamashita Y, Ohmichi M, et al. Remarkable Lethal G-to-A Mutations in vif-Proficient HIV-1 Provirus by Individual APOBEC3 Proteins in Humanized Mice. *J Virol* (2010) 84 (18):9546–56. doi: 10.1128/JVI.00823-10
114. Sato K, Nie C, Misawa N, Tanaka Y, Ito M, Koyanagi Y. Dynamics of memory and naïve CD8+ T lymphocytes in humanized NOD/SCID/IL-2Rgammanull mice infected with CCR5-tropic HIV-1. *Vaccine* (2010) 28 Suppl 2:B32–7. doi: 10.1016/j.vaccine.2009.10.154
115. Berges BK, Akkina SR, Folkvord JM, Connick E, Akkina R. Mucosal transmission of R5 and X4 tropic HIV-1 via vaginal and rectal routes in humanized Rag2-/- gammac -/- (RAG-hu) mice. *Virology* (2008) 373 (2):342–51. doi: 10.1016/j.virol.2007.11.020
116. Akkina R, Berges BK, Palmer BE, Remling L, Neff CP, Kuruvilla J, et al. Humanized Rag1-/- γc-/- mice support multilineage hematopoiesis and are susceptible to HIV-1 infection via systemic and vaginal routes. *PloS One* (2011) 6(6):e20169. doi: 10.1371/journal.pone.0020169
117. Van Duyne R, Cardenas J, Easley R, Wu W, Kehn-Hall K, Klase Z, et al. Effect of transcription peptide inhibitors on HIV-1 replication. *Virology* (2008) 376 (2):308–22. doi: 10.1016/j.virol.2008.02.036
118. Cheng L, Ma J, Li G, Su L. Humanized Mice Engrafted With Human HSC Only or HSC and Thymus Support Comparable HIV-1 Replication, Immunopathology, and Responses to ART and Immune Therapy. *Front Immunol* (2018) 9:817–. doi: 10.3389/fimmu.2018.00817
119. Satheesan S, Li H, Burnett JC, Takahashi M, Li S, Wu SX, et al. HIV Replication and Latency in a Humanized NSG Mouse Model during Suppressive Oral Combinational Antiretroviral Therapy. *J Virol* (2018) 92 (7):e02118–17. doi: 10.1128/JVI.02118-17
120. Kumar P, Ban HS, Kim SS, Wu H, Pearson T, Greiner DL, et al. T cell-specific siRNA delivery suppresses HIV-1 infection in humanized mice. *Cell* (2008) 134(4):577–86. doi: 10.1016/j.cell.2008.06.034
121. Gorantla S, Makarov E, Finke-Dwyer J, Gebhart CL, Domm W, Dewhurst S, et al. CD8+ Cell Depletion Accelerates HIV-1 Immunopathology in Humanized Mice. *J Immunol* (2010) 184(12):7082–91. doi: 10.4049/jimmunol.1000438
122. Gorantla S, Makarov E, Finke-Dwyer J, Castanedo A, Holguin A, Gebhart CL, et al. Links between progressive HIV-1 infection of humanized mice and viral neuropathogenesis. *Am J Pathol* (2010) 177(6):2938–49. doi: 10.2353/ajpath.2010.100536
123. Holt N, Wang J, Kim K, Friedman G, Wang X, Taupin V, et al. Human hematopoietic stem/progenitor cells modified by zinc-finger nucleases targeted to CCR5 control HIV-1 in vivo. *Nat Biotechnol* (2010) 28(8):839–47. doi: 10.1038/nbt.1663
124. Dash PK, Gorantla S, Gendelman HE, Knibbe J, Casale GP, Makarov E, et al. Loss of neuronal integrity during progressive HIV-1 infection of humanized mice. *J Neurosci* (2011) 31(9):3148–57. doi: 10.1523/JNEUROSCI.5473-10.2011
125. Kim J, Peachman KK, Jobe O, Morrison EB, Allam A, Jagodzinski L, et al. Tracking Human Immunodeficiency Virus-1 Infection in the Humanized DRAG Mouse Model. *Front Immunol* (2017) 8:1405–. doi: 10.3389/fimmu.2017.01405
126. Allam A, Majji S, Peachman K, Jagodzinski L, Kim J, Ratto-Kim S, et al. TFH cells accumulate in mucosal tissues of humanized-DRAG mice and are highly permissive to HIV-1. *Sci Rep* (2015) 5(1):10443. doi: 10.1038/srep10443
127. Denton PW, Estes JD, Sun Z, Othieno FA, Wei BL, Wege AK, et al. Antiretroviral pre-exposure prophylaxis prevents vaginal transmission of HIV-1 in humanized BLT mice. *PloS Med* (2008) 5(1):e16. doi: 10.1371/journal.pmed.0050016
128. Sun Z, Denton PW, Estes JD, Othieno FA, Wei BL, Wege AK, et al. Intrarectal transmission, systemic infection, and CD4+ T cell depletion in humanized mice infected with HIV-1. *J Exp Med* (2007) 204(4):705–14. doi: 10.1084/jem.20062411
129. Denton PW, Othieno F, Martinez-Torres F, Zou W, Krisko JF, Fleming E, et al. One percent tenofovir applied topically to humanized BLT mice and used according to the CAPRISA 004 experimental design demonstrates partial protection from vaginal HIV infection, validating the BLT model for evaluation of new microbicide candidates. *J Virol* (2011) 85(15):7582–93. doi: 10.1128/JVI.00537-11
130. Long BR, Stoddart CA. Alpha Interferon and HIV Infection Cause Activation of Human T Cells in NSG-BLT Mice. *J Virol* (2012) 86 (6):3327–36. doi: 10.1128/JVI.06676-11
131. Dudek TE, No DC, Seung E, Vrbanac VD, Fadda L, Bhoumik P, et al. Rapid Evolution of HIV-1 to Functional CD8+ T Cell Responses in Humanized BLT Mice. *Sci Trans Med* (2012) 4(143):143ra98–ra98. doi: 10.1126/scitranslmed.3003984
132. Chang H, Biswas S, Tallarico AS, Sarkis PTN, Geng S, Panditrao MM, et al. Human B-cell ontogeny in humanized NOD/SCID γc(null) mice generates a diverse yet auto/poly- and HIV-1-reactive antibody repertoire. *Genes Immun* (2012) 13(5):399–410. doi: 10.1038/gene.2012.16
133. Seung E, Tager AM. Humoral immunity in humanized mice: a work in progress. *J Infect Dis* (2013) 208Suppl 2(Suppl 2):S155–S9. doi: 10.1093/infdis/jit448
134. Martinez-Torres F, Nochi T, Wahl A, Garcia JV, Denton PW. Hypogammaglobulinemia in BLT Humanized Mice – An Animal Model of Primary Antibody Deficiency. *PloS One* (2014) 9(10):e108663. doi: 10.1371/journal.pone.0108663
135. Denton PW, Olesen R, Choudhary SK, Archin NM, Wahl A, Swanson MD, et al. Generation of HIV Latency in Humanized BLT Mice. *J Virol* (2012) 86 (1):630–4. doi: 10.1128/JVI.06120-11
136. Takenaka K, Prasolava TK, Wang JCY, Mortin-Toth SM, Khalouei S, Gan OI, et al. Polymorphism in Sirpa modulates engraftment of human hematopoietic stem cells. *Nat Immunol* (2007) 8(12):1313–23. doi: 10.1038/ni1527
137. Yamauchi T, Takenaka K, Urata S, Shima T, Kikushige Y, Tokuyama T, et al. Polymorphic Sirpa is the genetic determinant for NOD-based mouse lines to achieve efficient human cell engraftment. *Blood* (2013) 121(8):1316–25. doi: 10.1182/blood-2012-06-440354

138. Oldenborg P-A, Zheleznyak A, Fang Y-F, Lagenaur CF, Gresham HD, Lindberg FP. Role of CD47 as a Marker of Self on Red Blood Cells. *Sci (N Y NY)* (2000) 288(5473):2051–4. doi: 10.1126/science.288.5473.2051
139. Blazar BR, Lindberg FP, Ingulli E, Panoskaltsis-Mortari A, Oldenborg PA, Iizuka K, et al. CD47 (integrin-associated protein) engagement of dendritic cell and macrophage counterreceptors is required to prevent the clearance of donor lymphohematopoietic cells. *J Exp Med* (2001) 194(4):541–9. doi: 10.1084/jem.194.4.541
140. Greenblatt MB, Vrbanac V, Tivey T, Tsang K, Tager AM, Aliprantis AO. Graft versus host disease in the bone marrow, liver and thymus humanized mouse model. *PloS One* (2012) 7(9):e44664. doi: 10.1371/journal.pone.0044664
141. Barton K, Winckelmann A, Palmer S. HIV-1 Reservoirs During Suppressive Therapy. *Trends Microbiol* (2016) 24(5):345–55. doi: 10.1016/j.tim.2016.01.006
142. Siliciano RF. The Challenge of Viral Reservoirs in HIV-1 Infection. *Annu Rev Med* (2002) 53(1):557–93. doi: 10.1146/annurev.med.53.082901.104024
143. Murray AJ, Kwon KJ, Farber DL, Siliciano RF. The Latent Reservoir for HIV-1: How Immunologic Memory and Clonal Expansion Contribute to HIV-1 Persistence. *J Immunol* (2016) 197(2):407–17. doi: 10.4049/jimmunol.1600343
144. Migueles SA, Connors M. Success and failure of the cellular immune response against HIV-1. *Nat Immunol* (2015) 16(6):563–70. doi: 10.1038/ni.3161
145. Archin NM, Liberty AL, Kashuba AD, Choudhary SK, Kuruc JD, Crooks AM, et al. Administration of vorinostat disrupts HIV-1 latency in patients on antiretroviral therapy. *Nature* (2012) 487(7408):482–5. doi: 10.1038/nature11286
146. Rasmussen TA, Tolstrup M, Brinkmann CR, Olesen R, Erikstrup C, Solomon A, et al. Panobinostat, a histone deacetylase inhibitor, for latent-virus reactivation in HIV-infected patients on suppressive antiretroviral therapy: a phase 1/2, single group, clinical trial. *Lancet HIV* (2014) 1(1):e13–21. doi: 10.1016/S2352-3018(14)70014-1
147. Søgaard OS, Graversen ME, Leth S, Olesen R, Brinkmann CR, Nissen SK, et al. The Depsipeptide Romidepsin Reverses HIV-1 Latency In Vivo. *PloS Pathog* (2015) 11(9):e1005142. doi: 10.1371/journal.ppat.1005142
148. Bouchat S, Gatot JS, Kabeya K, Cardona C, Colin L, Herbein G, et al. Histone methyltransferase inhibitors induce HIV-1 recovery in resting CD4(+) T cells from HIV-1-infected HAART-treated patients. *AIDS* (2012) 26 (12):1473–82. doi: 10.1097/QAD.0b013e32835535f5
149. Spivak AM, Bosque A, Balch AH, Smyth D, Martins L, Planelles V. Ex Vivo Bioactivity and HIV-1 Latency Reversal by Ingenol Dibenzoate and Panobinostat in Resting CD4+ T Cells from Aviremic Patients. *Antimicrobial Agents Chemother* (2015) 59(10):5984–91. doi: 10.1128/AAC.01077-15
150. Banerjee C, Archin N, Michaels D, Belkina AC, Denis GV, Bradner J, et al. BET bromodomain inhibition as a novel strategy for reactivation of HIV-1. *J Leukoc Biol* (2012) 92(6):1147–54. doi: 10.1189/jlb.0312165
151. Doyon G, Zerbato J, Mellors JW, Sluis-Cremer N. Disulfiram reactivates latent HIV-1 expression through depletion of the phosphatase and tensin homolog. *AIDS* (2013) 27(2):F7–f11. doi: 10.1097/QAD.0b013e3283570620
152. Lim S-Y, Osuna CE, Hraber PT, Hesselgesser J, Gerold JM, Barnes TL, et al. TLR7 agonists induce transient viremia and reduce the viral reservoir in SIV-infected rhesus macaques on antiretroviral therapy. *Sci Trans Med* (2018) 10 (439):eaao4521. doi: 10.1126/scitranslmed.aao4521
153. Watson DC, Moysi E, Valentin A, Bergamaschi C, Devasundaram S, Fortis SP, et al. Treatment with native heterodimeric IL-15 increases cytotoxic lymphocytes and reduces SHIV RNA in lymph nodes. *PloS Pathog* (2018) 14 (2):e1006902. doi: 10.1371/journal.ppat.1006902
154. Tsai P, Wu G, Baker CE, Thayer WO, Spagnuolo RA, Sanchez R, et al. In vivo analysis of the effect of panobinostat on cell-associated HIV RNA and DNA levels and latent HIV infection. *Retrovirology* (2016) 13(1):36. doi: 10.1186/s12977-016-0268-7
155. Laird GM, Bullen CK, Rosenbloom DI, Martin AR, Hill AL, Durand CM, et al. Ex vivo analysis identifies effective HIV-1 latency-reversing drug combinations. *J Clin Invest* (2015) 125(5):1901–12. doi: 10.1172/JCI80142
156. Jiang G, Dandekar S. Targeting NF-κB signaling with protein kinase C agonists as an emerging strategy for combating HIV latency. *AIDS Res Hum Retroviruses* (2015) 31(1):4–12. doi: 10.1089/aid.2014.0199
157. Rice AP. Cyclin-dependent kinases as therapeutic targets for HIV-1 infection. *Expert Opin Ther Targets* (2016) 20(12):1453–61. doi: 10.1080/14728222.2016.1254619
158. Wender PA, Kee J-M, Warrington JM. Practical Synthesis of Prostratin, DPP, and Their Analogs, Adjuvant Leads Against Latent HIV. *Sci (N Y NY)* (2008) 320(5876):649–52. doi: 10.1126/science.1154690
159. Gutiérrez C, Serrano-Villar S, Madrid-Elena N, Pérez-Elías MJ, Martín ME, Barbas C, et al. Bryostatin-1 for latent virus reactivation in HIV-infected patients on antiretroviral therapy. *AIDS* (2016) 30(9):1385–92. doi: 10.1097/QAD.0000000000001064
160. Marsden MD, Loy BA, Wu X, Ramirez CM, Schrier AJ, Murray D, et al. In vivo activation of latent HIV with a synthetic bryostatin analog effects both latent cell "kick" and "kill" in strategy for virus eradication. *PloS Pathog* (2017) 13(9):e1006575. doi: 10.1371/journal.ppat.1006575
161. Bobardt M, Kuo J, Chatterji U, Chanda S, Little SJ, Wiedemann N, et al. The inhibitor apoptosis protein antagonist Debio 1143 Is an attractive HIV-1 latency reversal candidate. *PloS One* (2019) 14(2):e0211746–e. doi: 10.1371/journal.pone.0211746
162. Nixon CC, Mavigner M, Sampey GC, Brooks AD, Spagnuolo RA, Irlbeck DM, et al. and SIV latency reversal via non-canonical NF-κB signalling in vivo. *Nature* (2020) 578(7793):160–5. doi: 10.1038/s41586-020-1951-3
163. Garrido C, Abad-Fernandez M, Tuyishime M, Pollara JJ, Ferrari G, Soriano-Sarabia N, et al. Interleukin-15-Stimulated Natural Killer Cells Clear HIV-1-Infected Cells following Latency Reversal Ex Vivo. *J Virol* (2018) 92(12): e00235–18. doi: 10.1128/JVI.00235-18
164. Seay K, Church C, Zheng JH, Deneroff K, Ochsenbauer C, Kappes JC, et al. In Vivo Activation of Human NK Cells by Treatment with an Interleukin-15 Superagonist Potently Inhibits Acute In Vivo HIV-1 Infection in Humanized Mice. *J Virol* (2015) 89(12):6264–74. doi: 10.1128/JVI.00563-15
165. McBrien JB, Mavigner M, Franchitti L, Smith SA, White E, Tharp GK, et al. Robust and persistent reactivation of SIV and HIV by N-803 and depletion of CD8+ cells. *Nature* (2020) 578(7793):154–9. doi: 10.1038/s41586-020-1946-0
166. Llewellyn GN, Alvarez-Carbonell D, Chateau M, Karn J, Cannon PM. HIV-1 infection of microglial cells in a reconstituted humanized mouse model and identification of compounds that selectively reverse HIV latency. *J Neurovirol* (2018) 24(2):192–203. doi: 10.1007/s13365-017-0604-2
167. Rasmussen TA, Lewin SR. Shocking HIV out of hiding: where are we with clinical trials of latency reversing agents? *Curr Opin HIV AIDS* (2016) 11 (4):394–401. doi: 10.1097/COH.0000000000000279
168. Shan L, Deng K, Shroff NS, Durand CM, Rabi SA, Yang H-C, et al. Stimulation of HIV-1-specific cytolytic T lymphocytes facilitates elimination of latent viral reservoir after virus reactivation. *Immunity* (2012) 36(3):491–501. doi: 10.1016/j.immuni.2012.01.014
169. Mikulak J, Oriolo F, Zaghi E, Di Vito C, Mavilio D. Natural killer cells in HIV-1 infection and therapy. *AIDS* (2017) 31(17):2317–30. doi: 10.1097/QAD.0000000000001645
170. Nabatanzi R, Bayigga L, Cose S, Rowland-Jones S, Canderan G, Joloba M, et al. Aberrant natural killer (NK) cell activation and dysfunction among ART-treated HIV-infected adults in an African cohort. *Clin Immunol* (2019) 201:55–60. doi: 10.1016/j.clim.2019.02.010
171. Costanzo MC, Kim D, Creegan M, Lal KG, Ake JA, Currier JR, et al. Transcriptomic signatures of NK cells suggest impaired responsiveness in HIV-1 infection and increased activity post-vaccination. *Nat Commun* (2018) 9(1):1212. doi: 10.1038/s41467-018-03618-w
172. Deng K, Pertea M, Rongvaux A, Wang L, Durand CM, Ghiaur G, et al. Broad CTL response is required to clear latent HIV-1 due to dominance of escape mutations. *Nature* (2015) 517(7534):381–5. doi: 10.1038/nature14053
173. Gorny MK, Conley AJ, Karwowska S, Buchbinder A, Xu JY, Emini EA, et al. Neutralization of diverse human immunodeficiency virus type 1 variants by an anti-V3 human monoclonal antibody. *J Virol* (1992) 66(12):7538–42. doi: 10.1128/JVI.66.12.7538-7542.1992
174. Burton DR, Pyati J, Koduri R, Sharp SJ, Thornton GB, Parren PW, et al. Efficient neutralization of primary isolates of HIV-1 by a recombinant human monoclonal antibody. *Sci (N Y NY)* (1994) 266(5187):1024–7. doi: 10.1126/science.7973652
175. Trkola A, Purtscher M, Muster T, Ballaun C, Buchacher A, Sullivan N, et al. Human monoclonal antibody 2G12 defines a distinctive neutralization

epitope on the gp120 glycoprotein of human immunodeficiency virus type 1. *J Virol* (1996) 70(2):1100–8. doi: 10.1128/JVI.70.2.1100-1108.1996
176. Zwick MB, Labrijn AF, Wang M, Spenlehauer C, Saphire EO, Binley JM, et al. Broadly neutralizing antibodies targeted to the membrane-proximal external region of human immunodeficiency virus type 1 glycoprotein gp41. *J Virol* (2001) 75(22):10892–905. doi: 10.1128/JVI.75.22.10892-10905.2001
177. Trkola A, Kuster H, Rusert P, Joos B, Fischer M, Leemann C, et al. Delay of HIV-1 rebound after cessation of antiretroviral therapy through passive transfer of human neutralizing antibodies. *Nat Med* (2005) 11(6):615–22. doi: 10.1038/nm1244
178. Mehandru S, Vcelar B, Wrin T, Stiegler G, Joos B, Mohri H, et al. Adjunctive Passive Immunotherapy in Human Immunodeficiency Virus Type 1-Infected Individuals Treated with Antiviral Therapy during Acute and Early Infection. *J Virol* (2007) 81(20):11016–31. doi: 10.1128/JVI.01340-07
179. Walker LM, Burton DR. Passive immunotherapy of viral infections: 'super-antibodies' enter the fray. *Nat Rev Immunol* (2018) 18(5):297–308. doi: 10.1038/nri.2017.148
180. Caskey M, Klein F, Nussenzweig MC. Broadly neutralizing anti-HIV-1 monoclonal antibodies in the clinic. *Nat Med* (2019) 25(4):547–53. doi: 10.1038/s41591-019-0412-8
181. Caskey M, Klein F, Lorenzi JC, Seaman MS, West AP Jr., Buckley N, et al. Viraemia suppressed in HIV-1-infected humans by broadly neutralizing antibody 3BNC117. *Nature* (2015) 522(7557):487–91. doi: 10.1038/nature14411
182. Scheid JF, Horwitz JA, Bar-On Y, Kreider EF, Lu C-L, Lorenzi JCC, et al. HIV-1 antibody 3BNC117 suppresses viral rebound in humans during treatment interruption. *Nature* (2016) 535(7613):556–60. doi: 10.1038/nature18929
183. Lu C-L, Murakowski DK, Bournazos S, Schoofs T, Sarkar D, Halper-Stromberg A, et al. Enhanced clearance of HIV-1–infected cells by broadly neutralizing antibodies against HIV-1 in vivo. *Sci (N Y NY)* (2016) 352 (6288):1001–4. doi: 10.1126/science.aaf1279
184. Caskey M, Schoofs T, Gruell H, Settler A, Karagounis T, Kreider EF, et al. Antibody 10-1074 suppresses viremia in HIV-1-infected individuals. *Nat Med* (2017) 23(2):185–91. doi: 10.1038/nm.4268
185. Bar-On Y, Gruell H, Schoofs T, Pai JA, Nogueira L, Butler AL, et al. Safety and antiviral activity of combination HIV-1 broadly neutralizing antibodies in viremic individuals. *Nat Med* (2018) 24(11):1701–7. doi: 10.1038/s41591-018-0186-4
186. Mendoza P, Gruell H, Nogueira L, Pai JA, Butler AL, Millard K, et al. Combination therapy with anti-HIV-1 antibodies maintains viral suppression. *Nature* (2018) 561(7724):479–84. doi: 10.1038/s41586-018-0531-2
187. Cohen YZ, Butler AL, Millard K, Witmer-Pack M, Levin R, Unson-O'Brien C, et al. Safety, pharmacokinetics, and immunogenicity of the combination of the broadly neutralizing anti-HIV-1 antibodies 3BNC117 and 10-1074 in healthy adults: A randomized, phase 1 study. *PloS One* (2019) 14(8):e0219142. doi: 10.1371/journal.pone.0219142
188. Niessl J, Baxter AE, Mendoza P, Jankovic M, Cohen YZ, Butler AL, et al. Combination anti-HIV-1 antibody therapy is associated with increased virus-specific T cell immunity. *Nat Med* (2020) 26(2):222–7. doi: 10.1038/s41591-019-0747-1
189. Park JH, Geyer MB, Brentjens RJ. CD19-targeted CAR T-cell therapeutics for hematologic malignancies: interpreting clinical outcomes to date. *Blood* (2016) 127(26):3312–20. doi: 10.1182/blood-2016-02-629063
190. Zhang WY, Wang Y, Guo YL, Dai HR, Yang QM, Zhang YJ, et al. Treatment of CD20-directed Chimeric Antigen Receptor-modified T cells in patients with relapsed or refractory B-cell non-Hodgkin lymphoma: an early phase IIa trial report. *Signal Transduct Targ Ther* (2016) 1:16002. doi: 10.1038/sigtrans.2016.2
191. Fry TJ, Shah NN, Orentas RJ, Stetler-Stevenson M, Yuan CM, Ramakrishna S, et al. CD22-targeted CAR T cells induce remission in B-ALL that is naive or resistant to CD19-targeted CAR immunotherapy. *Nat Med* (2018) 24 (1):20–8. doi: 10.1038/nm.4441
192. Zhen A, Kitchen S. Stem-cell-based gene therapy for HIV infection. *Viruses* (2013) 6(1):1–12. doi: 10.3390/v6010001
193. Scholler J, Brady TL, Binder-Scholl G, Hwang W-T, Plesa G, Hege KM, et al. Decade-Long Safety and Function of Retroviral-Modified Chimeric Antigen Receptor T Cells. *Sci Trans Med* (2012) 4(132):132ra53–ra53. doi: 10.1126/scitranslmed.3003761
194. Bar KJ, Sneller MC, Harrison LJ, Justement JS, Overton ET, Petrone ME, et al. Effect of HIV Antibody VRC01 on Viral Rebound after Treatment Interruption. *New Engl J Med* (2016) 375(21):2037–50. doi: 10.1056/NEJMoa1608243
195. Hutter G, Nowak D, Mossner M, Ganepola S, Mussig A, Allers K, et al. Long-term control of HIV by CCR5 Delta32/Delta32 stem-cell transplantation. *New Engl J Med* (2009) 360(7):692–8. doi: 10.1056/NEJMoa0802905
196. Gupta RK, Abdul-Jawad S, McCoy LE, Mok HP, Peppa D, Salgado M, et al. HIV-1 remission following CCR5Delta32/Delta32 haematopoietic stem-cell transplantation. *Nature* (2019) 568(7751):244–8. doi: 10.1038/s41586-019-1027-4
197. Drake MJ, Bates P. Application of gene-editing technologies to HIV-1. *Curr Opin HIV AIDS* (2015) 10(2):123–7. doi: 10.1097/COH.0000000000000139
198. Tebas P, Stein D, Tang WW, Frank I, Wang SQ, Lee G, et al. Gene Editing of CCR5 in Autologous CD4 T Cells of Persons Infected with HIV. *New Engl J Med* (2014) 370(10):901–10. doi: 10.1056/NEJMoa1300662
199. Ishino Y, Shinagawa H, Makino K, Amemura M, Nakata A. Nucleotide sequence of the iap gene, responsible for alkaline phosphatase isozyme conversion in Escherichia coli, and identification of the gene product. *J Bacteriol* (1987) 169(12):5429–33. doi: 10.1128/JB.169.12.5429-5433.1987
200. Jansen R, Embden JD, Gaastra W, Schouls LM. Identification of genes that are associated with DNA repeats in prokaryotes. *Mol Microbiol* (2002) 43 (6):1565–75. doi: 10.1046/j.1365-2958.2002.02839.x
201. Barrangou R, Fremaux C, Deveau H, Richards M, Boyaval P, Moineau S, et al. CRISPR provides acquired resistance against viruses in prokaryotes. *Sci (N Y NY)* (2007) 315(5819):1709–12. doi: 10.1126/science.1138140
202. Jinek M, Chylinski K, Fonfara I, Hauer M, Doudna JA, Charpentier E. A Programmable Dual-RNA–Guided DNA Endonuclease in Adaptive Bacterial Immunity. *Sci (N Y NY)* (2012) 337(6096):816–21. doi: 10.1126/science.1225829
203. Ebina H, Misawa N, Kanemura Y, Koyanagi Y. Harnessing the CRISPR/Cas9 system to disrupt latent HIV-1 provirus. *Sci Rep* (2013) 3(1):2510. doi: 10.1038/srep02510
204. Qu X, Wang P, Ding D, Li L, Wang H, Ma L, et al. Zinc-finger-nucleases mediate specific and efficient excision of HIV-1 proviral DNA from infected and latently infected human T cells. *Nucleic Acids Res* (2013) 41(16):7771–82. doi: 10.1093/nar/gkt571
205. Hu W, Kaminski R, Yang F, Zhang Y, Cosentino L, Li F, et al. RNA-directed gene editing specifically eradicates latent and prevents new HIV-1 infection. *Proc Natl Acad Sci U States America* (2014) 111(31):11461–6. doi: 10.1073/pnas.1405186111
206. Adams Waldorf KM, Stencel-Baerenwald JE, Kapur RP, Studholme C, Boldenow E, Vornhagen J, et al. Fetal brain lesions after subcutaneous inoculation of Zika virus in a pregnant nonhuman primate. *Nat Med* (2016) 22(11):1256–9. doi: 10.1038/nm.4193
207. Mousseau G, Kessing CF, Fromentin R, Trautmann L, Chomont N, Valente ST. The Tat Inhibitor Didehydro-Cortistatin A Prevents HIV-1 Reactivation from Latency. *mBio* (2015) 6(4):e00465. doi: 10.1128/mBio.00465-15
208. Laspia MF, Rice AP, Mathews MB. HIV-1 Tat protein increases transcriptional initiation and stabilizes elongation. *Cell* (1989) 59(2):283–92. doi: 10.1016/0092-8674(89)90290-0
209. Mancebo HS, Lee G, Flygare J, Tomassini J, Luu P, Zhu Y, et al. P-TEFb kinase is required for HIV Tat transcriptional activation in vivo and in vitro. *Genes Dev* (1997) 11(20):2633–44. doi: 10.1101/gad.11.20.2633
210. Wei P, Garber ME, Fang S-M, Fischer WH, Jones KA. A Novel CDK9-Associated C-Type Cyclin Interacts Directly with HIV-1 Tat and Mediates Its High-Affinity, Loop-Specific Binding to TAR RNA. *Cell* (1998) 92 (4):451–62. doi: 10.1016/S0092-8674(00)80939-3
211. Mahmoudi T, Parra M, Vries RG, Kauder SE, Verrijzer CP, Ott M, et al. The SWI/SNF chromatin-remodeling complex is a cofactor for Tat transactivation of the HIV promoter. *J Biol Chem* (2006) 281(29):19960–8. doi: 10.1074/jbc.M603336200
212. Tréand C, du Chéné I, Brès V, Kiernan R, Benarous R, Benkirane M, et al. Requirement for SWI/SNF chromatin-remodeling complex in Tat-mediated activation of the HIV-1 promoter. *EMBO J* (2006) 25(8):1690–9. doi: 10.1038/sj.emboj.7601074

213. Benkirane M, Chun RF, Xiao H, Ogryzko VV, Howard BH, Nakatani Y, et al. Activation of integrated provirus requires histone acetyltransferase. p300 and P/CAF are coactivators for HIV-1 Tat. *J Biol Chem* (1998) 273(38):24898–905. doi: 10.1074/jbc.273.38.24898
214. Col E, Caron C, Seigneurin-Berny D, Gracia J, Favier A, Khochbin S. The histone acetyltransferase, hGCN5, interacts with and acetylates the HIV transactivator, Tat. *J Biol Chem* (2001) 276(30):28179–84. doi: 10.1074/jbc.M101385200
215. Marzio G, Tyagi M, Gutierrez MI, Giacca M. HIV-1 Tat transactivator recruits p300 and CREB-binding protein histone acetyltransferases to the viral promoter. *Proc Natl Acad Sci* (1998) 95(23):13519–24. doi: 10.1073/pnas.95.23.13519
216. Mousseau G, Clementz MA, Bakeman WN, Nagarsheth N, Cameron M, Shi J, et al. An analog of the natural steroidal alkaloid cortistatin A potently suppresses Tat-dependent HIV transcription. *Cell Host Microbe* (2012) 12 (1):97–108. doi: 10.1016/j.chom.2012.05.016
217. Mousseau G, Aneja R, Clementz MA, Mediouni S, Lima NS, Haregot A, et al. Resistance to the Tat Inhibitor Didehydro-Cortistatin A Is Mediated by Heightened Basal HIV-1 Transcription. *mBio* (2019) 10(4):e01750–18. doi: 10.1128/mBio.01750-18
218. Huntington ND, Legrand N, Alves NL, Jaron B, Weijer K, Plet A, et al. IL-15 trans-presentation promotes human NK cell development and differentiation in vivo. *J Exp Med* (2009) 206(1):25–34. doi: 10.1084/jem.20082013
219. Katano I, Nishime C, Ito R, Kamisako T, Mizusawa T, Ka Y, et al. Long-term maintenance of peripheral blood derived human NK cells in a novel human IL-15-transgenic NOG mouse. *Sci Rep* (2017) 7(1):17230. doi: 10.1038/s41598-017-17442-7
220. Matsuda M, Ono R, Iyoda T, Endo T, Iwasaki M, Tomizawa-Murasawa M, et al. Human NK cell development in hIL-7 and hIL-15 knockin NOD/SCID/IL2rgKO mice. *Life Sci Alliance* (2019) 2(2):e201800195. doi: 10.26508/lsa.201800195
221. Demetrius L. Of mice and men. When it comes to studying ageing and the means to slow it down, mice are not just small humans. *EMBO Rep* (2005) 6 Spec No(Suppl 1):S39–44. doi: 10.1038/sj.embor.7400422
222. Perlman RL. Mouse models of human disease: An evolutionary perspective. *Evol Med Public Health* (2016) 2016(1):170–6. doi: 10.1093/emph/eow014
223. Nguyen TL, Vieira-Silva S, Liston A, Raes J. How informative is the mouse for human gut microbiota research? *Dis Model Mech* (2015) 8(1):1–16. doi: 10.1242/dmm.017400
224. Hugenholtz F, de Vos WM. Mouse models for human intestinal microbiota research: a critical evaluation. *Cell Mol Life Sci* (2018) 75(1):149–60. doi: 10.1007/s00018-017-2693-8
225. Saxena D, Li Y, Yang L, Pei Z, Poles M, Abrams WR, et al. Human microbiome and HIV/AIDS. *Curr HIV/AIDS Rep* (2012) 9(1):44–51. doi: 10.1007/s11904-011-0103-7
226. Zilberman-Schapira G, Zmora N, Itav S, Bashiardes S, Elinav H, Elinav E. The gut microbiome in human immunodeficiency virus infection. *BMC Med* (2016) 14(1):83. doi: 10.1186/s12916-016-0625-3
227. Liu J, Williams B, Frank D, Dillon SM, Wilson CC, Landay AL. Inside Out: HIV, the Gut Microbiome, and the Mucosal Immune System. *J Immunol (Baltimore Md 1950)* (2017) 198(2):605–14. doi: 10.4049/jimmunol.1601355
228. Crakes KR, Jiang G. Gut Microbiome Alterations During HIV/SIV Infection: Implications for HIV Cure. *Front Microbiol* (2019) 10:1104–. doi: 10.3389/fmicb.2019.01104
229. Daharsh L, Zhang J, Ramer-Tait A, Li Q. A Double Humanized BLT-mice Model Featuring a Stable Human-Like Gut Microbiome and Human Immune System. *J Vis Exp* (2019) (150):10.3791/59773. doi: 10.3791/59773

Conflict of Interest: The authors declare that the research was conducted in the absence of any commercial or financial relationships that could be construed as a potential conflict of interest.

frontiers in Immunology

CORRECTION
published: 06 December 2021
doi: 10.3389/fimmu.2021.808068

Corrigendum: Humanized Mice for the Evaluation of Novel HIV-1 Therapies

Shawn Abeynaike[1,2] *and Silke Paust*[1,2]*

[1] Department of Immunology and Microbiology, The Scripps Research Institute, La Jolla, CA, United States, [2] The Skaggs Graduate Program in Chemical and Biological Sciences, The Scripps Research Institute, La Jolla, CA, United States

OPEN ACCESS

Edited and reviewed by:
Qingfeng Chen,
Institute of Molecular and Cell Biology (A*STAR), Singapore

***Correspondence:**
Silke Paust
paust@scripps.edu

Specialty section:
This article was submitted to Viral Immunology, a section of the journal Frontiers in Immunology

Received: 03 November 2021
Accepted: 08 November 2021
Published: 06 December 2021

Citation:
Abeynaike S and Paust S (2021) Corrigendum: Humanized Mice for the Evaluation of Novel HIV-1 Therapies. Front. Immunol. 12:808068. doi: 10.3389/fimmu.2021.808068

Keywords: humanized mice, BLT, DRAG, HIV-1 infection, viral latency, latency reversal, immunotherapy, gene therapy

A Corrigendum on:

Humanized Mice for the Evaluation of Novel HIV-1 Therapies
By Abeynaike S and Paust S (2021). Front. Immunol. 12:636775. doi: 10.3389/fimmu.2021.636775

In the original article, there was a mistake in **Table 1** as published. The authors incorrectly categorized thy/liv implanted SCID-hu mice as showing no multilineage hematopoeisis. To clarify, Namikawa 1990, showed that SCID mice implanted with both Thy/Liv displayed multilineage hematopoiesis. Specifically, they showed in addition to T cells (CD3, CD4 and CD8), the presence of mature and immature forms of myelomonocytic cells which stained positive for human CD15, as well as progenitors for erythroids and megakaryocytic lineages (1).

The corrected **Table 1** appears below.

The authors apologize for this error and state that this does not change the scientific conclusions of the article in any way. The original article has been updated.

TABLE 1 | Summary of humanized mouse models and their tissue-based chimerism.

	SCID-hu	hu-PBL	hu-HSC	BLT	TKO-BLT
Mouse Model					
Genetic Background	C.B17scid/scid (SCID)	SCID NOD-SCID NSG BRG NCG	SCID NOD-SCID NSG BRG NRG DRAG	SCID NOD-SCID NSG NRG	C57BL/6 Rag2 $^{-/-}$ $\gamma_c^{-/-}$
Humanization Method	Subcapsular Coimplantation of human fetal thymus and liver fragments 	Intraperitoneal Injection of human PBMCs 	Injection of CD34+ cells from cord blood/fetal liver 	Coimplantation human fetal thy/liv with i.v. injection of CD34+ cells from fetal liver 	Coimplantation human fetal thy/liv with i.v. injection of CD34+ cells from fetal liver 
Immune Reconstitution	T cell engraftment Multilineage hematopoiesis No primary immune response	T cell engraftment No multilineage hematopoiesis No primary immune response	Multilineage hematopoiesis Primary immune response No HLA restriction	Multilineage hematopoiesis Primary immune response Human HLA T cell restriction	Multilineage hematopoiesis Primary immune response Human HLA T cell restriction
References	McCune Namikawa (11), Namikawa Weilbaecher (12)	Moiser, Gulizia (13), Hesselton. Greiner (14), van Rijn, Simonetti (15), Ali, Flutter (16)	Kamei-Reid and Dick (17), Peault, Weissman (18), Hiramatsu, Nishikomori (19), Danner, Chaudhari (20)	Lan, Tonomura (21), Melkus, Estes (22), Brainard, Seung (23), Stoddart, Maidji (24)	Lavender, Messer (25), Lavender, Pang (26), Lavander, Pace (27)

Created with BioRender.com.

REFERENCE

1. Namikawa R, Weilbaecher K, Kaneshima H, Yee E, Mccune J. Long-Term Human Hematopoiesis in the SCID-hu Mouse. *J Exp Med* (1990) 172 (4):1055–63.

frontiers in Immunology

ORIGINAL RESEARCH
published: 18 May 2021
doi: 10.3389/fimmu.2021.672143

TLR9- and CD40-Targeting Vaccination Promotes Human B Cell Maturation and IgG Induction *via* pDC-Dependent Mechanisms in Humanized Mice

Liang Cheng[1,2*], *Guangming Li*[1,3], *Caroline Marnata Pellegry*[1], *Fumihiko Yasui*[1,4], *Feng Li*[1,5], *Sandra M. Zurawski*[6], *Gerard Zurawski*[6], *Yves Levy*[7,8], *Jenny P.-Y. Ting*[1,9,10] *and Lishan Su*[1,3*]

[1] Lineberger Comprehensive Cancer Center, University of North Carolina at Chapel Hill, Chapel Hill, NC, United States, [2] Frontier Science Center for Immunology and Metabolism, Medical Research Institute, Wuhan University, Wuhan, China, [3] Division of Virology, Pathogenesis and Cancer, Institute of Human Virology, Department of Pharmacology, University of Maryland School of Medicine, Baltimore, MD, United States, [4] Department of Microbiology and Cell Biology, Tokyo Metropolitan Institute of Medical Science, Tokyo, Japan, [5] Guangzhou Eighth People's Hospital, Guangzhou Medical University, Guangzhou, China, [6] Baylor Institute for Immunology Research, Vaccine Research Institute, INSERM U955, Dallas, TX, United States, [7] Assistance Publique-Hôpitaux de Paris, Groupe Henri-Mondor Albert-Chenevier, Service Immunologie Clinique, Créteil, France, [8] Vaccine Research Institute, Université Paris-Est Créteil, Faculté de Médecine, INSERM U955, Créteil, France, [9] Department of Genetics, University of North Carolina at Chapel Hill, Chapel Hill, NC, United States, [10] Department of Microbiology-Immunology, University of North Carolina at Chapel Hill, Chapel Hill, NC, United States

Mice reconstituted with a human immune system (humanized mice) provide a robust model to study human immunology, vaccinology, and human infectious diseases. However, the development and function of B cells in humanized mice is impaired. B cells from humanized mice are immature and are impaired in IgM to IgG isotype switch in response to infection or vaccination. In the present study we report that Toll-like receptor 9 (TLR9) agonist CpG-B combined with CD40-targeting vaccination triggered human B cell immunoglobin class-switch from IgM^+ to IgG^+ B cells in humanized mice. Human B cells from mice vaccinated with CpG-B as adjuvant were more mature in phenotype and produced significant levels of both total IgG and antigen-specific IgG. We found that CpG-B treatment activated human pDCs (plasmacytoid dendritic cells) *in vivo* to induce interferon-alpha (IFN-α)expression in humanized mice. Pre-depletion of human pDC *in vivo* abrogated the adjuvant effect of CpG-B. Our results indicate that TLR9 and CD40-targeting vaccination triggers human B cell maturation and immunoglobulin class-switch in a pDC-dependent manner in humanized mice. The findings also shed light on induction of human IgG antibodies in humanized mouse models.

Keywords: plasmacytoid dendritic cell, IFN-alpha, immunoglobin class-switch, IgG induction, CD40-targeting vaccination, B cell maturation, CpG-B

OPEN ACCESS

Edited by:
*Qingfeng Chen, Institute of Molecular and Cell Biology (A*STAR), Singapore*

Reviewed by:
Amy L. MacNeill, Colorado State University, United States
Johan Van Weyenbergh, KU Leuven, Belgium

***Correspondence:**
Liang Cheng
liangcheng@whu.edu.cn
Lishan Su
lsu@ihv.umaryland.edu

Specialty section:
This article was submitted to Viral Immunology, a section of the journal Frontiers in Immunology

Received: *25 February 2021*
Accepted: *27 April 2021*
Published: *18 May 2021*

Citation:
Cheng L, Li G, Pellegry CM, Yasui F, Li F, Zurawski SM, Zurawski G, Levy Y, Ting JP-Y and Su L (2021) TLR9- and CD40-targeting Vaccination Promotes Human B Cell Maturation and IgG Induction via pDC-Dependent Mechanisms in Humanized Mice. Front. Immunol. 12:672143. doi: 10.3389/fimmu.2021.672143

INTRODUCTION

Recent development of humanized mice provides robust models to study infection, pathogenesis, and therapy of human viruses (1, 2). We and others have shown before that a functional human immune system was developed in immunodeficient mice after adoptive transfer of human hematopoietic stem cells (HSCs) (3–8). Major human immune subtype such as pDC, mDC, monocyte, T and B cells can be detected in peripheral blood and lymphoid organs 3 months after HSCs transfer (7). Humanized mice can initiate innate immunity and antigen-specific T cell response to vaccine or infection (9–12). However, although B cell are developed in humanized mice, those cells are immature (13). B cells from humanized mice shows $CD24^{int/hi}CD38^{hi}$ immature phenotype and express high levels of CD10, another immature B cell marker (14). Moreover, B cells from humanized mice are predominately IgM^+ with few IgG^+ B cells (15). The cells are impaired in IgM to IgG isotype switch in response to infection or vaccination (14, 15).

Toll like receptor (TLRs) are expressed by various immune cells such as plasmacytoid dendritic cells (pDCs), monocytes and myeloid dendritic cells (mDCs) and B cells (16, 17). They can sense the microbial components named pathogen-associated molecular patterns (PAMPs) (16, 17). Stimulation of TLR signaling by synthetic or natural TLR ligands (TLR-Ls) results in up-regulation of MHC class II molecules, co-stimulatory molecules, and cytokines in different kind of cells in the immune system, especially innate immune cells (18, 19). These synthetic or natural agonists for TLRs are potential new vaccine adjuvants (20, 21). We and others have shown before that TLR-Ls can efficiently activate human innate immune cells from humanized mice both *in vitro* and *in vivo* (9, 11). Importantly, we proved that CpG-B, R848 and Poly I:C can enhance antigen-specific T cells response to a CD40-targeting HIV vaccine in humanized mice (9). Moreover, we recently reported that therapeutic treatment with a CD40-targeting HIV vaccine plus poly I:C as adjuvant can significantly reduce HIV-1 reservoir in HIV-infected humanized mice (12). These results indicated that humanized mice serve as a relevant model to develop and evaluate novel vaccines and adjuvants to human infectious disease.

As B cells from humanized mice fails to efficiently transition from IgM^+ to IgG^+ B cells, it is still questionable to use humanized mouse model to evaluate humoral immune response to vaccines (13). Efforts have been made to improve B cell IgM to IgG class-switch and antigen-specific antibody production in humanized mice in recent years. It was reported that GM-CSF and IL-4 stimulate humoral responses in humanized mice by promoting dendritic cell, T and B cell maturation (22). Transgenes expressing human stem cell factor, granulocyte-macrophage colony stimulating factor and interleukin-3 was reported to improve B cell development in humanized mice (23). The expression of human IL-6 by knocking-in human IL-6 gene to its respective mouse locus also increased class switched memory B cells and serum immunoglobulin G (IgG) after HSCs reconstitution (24). Stimulation of TLR signaling by synthetic or natural TLR ligands (TLR-Ls) results in cytokines induction, as well as up-regulation of MHC class II molecules and co-stimulatory molecules in innate immune cells (9, 11). Synthetic CpG oligodeoxynucleotides (CpG ODNs), which signal through TLR9, are approved by FDA (DYNAVAX) as HBV vaccine adjuvants after human clinical trials. The principal TLR9-expressing cells in humans are plasmacytoid DCs (pDCs) and B cells (25, 26). We speculated that targeting TLR9 would serve as a good stratagem to improve humoral immune response to vaccines in humanized mice. However, knowledge about how CpG ODNs activate pDC and enhance B cell response *in vivo* in humans is still limited.

In the present study we tested whether targeting TLR9 by CpG-B can overcome the deficiency of B cell response in humanized mice. We found that CpG-B combined with CD40-targeting vaccination enhanced B cell maturation, triggered human B cell immunoglobin class-switch from IgM^+ to IgG^+ B cells, and induced antigen-specific IgG response. Furthermore, we found that pDCs were essential for the adjuvant activity of CpG-B. Our results indicate that TLR9 and CD40-targeting vaccination triggers human B cell maturation, IgM to IgG immunoglobulin class-switch in a pDC-dependent manner in humanized mice.

MATERIALS AND METHODS

Construction of Humanized Mice

We constructed humanized NRG (NOD-$Rag2^{-/-}$ $\gamma_C^{-/-}$) mice by reconstitution with human fetal liver (17 to 22 weeks of gestational age) derived $CD34^+$ hematopoietic progenitor cells (Advanced Bioscience Resources, Alameda, CA) as previously reported (27). Briefly, $CD34^+$ hematopoietic progenitor cells purified from fetal liver were injected into the liver of newborn (1-3 day) NRG mice. Human immune reconstitution was detected by flow cytometry 12 weeks after transplantation. All animal studies were approved by the University of North Carolina Institutional Animal Care and Use Committee (IACUC).

Ethics Statement

Human fetal liver was obtained from elective or medically indicated termination of pregnancy through a non-profit intermediary working with outpatient clinics (Advanced Bioscience Resources, Alameda, CA). Informed consent of the maternal donor is obtained in all cases, under regulation governing the clinic. The use of the tissue in the research had no influence on the decision regarding termination of the pregnancy. The project was reviewed by the University's Office of Human Research Ethics, which has determined that this submission does not constitute human subjects research as defined under federal regulations [45 CFR 46.102 (d or f) and 21 CFR 56.102(c)(e)(l)] and does not require IRB approval. All animal experiments were conducted following NIH guidelines for housing and care of laboratory animals and in accordance with The University of North Carolina at Chapel Hill with protocols approved by the institution's Institutional Animal Care and Use Committee (IACUC ID: 14-100).

Vaccination

Recombinant anti-human CD40 antibody fused to 5 HIV-1 long peptide regions (αCD40-HIV5pep) was produced as previously reported (28), except that the flexible linker and HIV peptide sequences were reconfigured and the variable regions CD40 antibody were changed to a human framework. Humanized mice were intramuscularly (half dose) and intraperitoneally (half dose) injected with 10 μg αCD40-HIV5pep or recombinant hemagglutinin protein alone or with 50 μg of CpG-B at week0, week3 and week6. Splenocytes from vaccinated humanized mice were collected 7 days after the third vaccination.

Detection of Cytokines

Human IFN-α was detected by enzyme-linked immunosorbent assay using the human IFN-α pan ELISA kits purchased from Mabtech. A high sensitivity immunology multiplex assay (Luminex) (Millipore, Billerica, Massachusetts, USA) was used to measure human IL-6 in plasma of humanized mice according to the manufacturer's instructions.

Flow Cytometry

Single cell suspensions prepared from peripheral blood, spleen of humanized mice was stained with surface markers and analyzed on a CyAn ADP (Dako). FITC-conjugated anti-human CD40, CD24, PE-conjugated anti-human CD303, CD38, PE/Cy5-conjugated anti-human CD86, IgG, PE/Cy7-conjugated anti-human HLA-DR, PB-conjugated anti-human CD4, IgM, APC-conjugated anti-human CD10 and APC/Cy7-conjugated anti-human CD45 were purchased from Biolegend. Pacific orange-conjugated anti-mouse CD45, PE/Texas red-conjugated anti-human CD19 and LIVE/DEAD Fixable Aqua (LD7) Dead Cell Stain Kit were purchased from Invitrogen. Data were analyzed using Summit4.3 software (Dako).

Total IgM and IgG Detection

Total IgM and IgG were detected by ELISA kits, purchased from Bethyl Laboratories,int.(Cat. No. E80-104 and Cat. No. E80-100) according to the protocols.

Detection of Total and Antigen-Specific IgG-Secreting Cells by ELISpot

IgG-secreting cells were detected by using ELISpot^{PLUS} for Human IgG kits (Product Code: 3850-2HW-Plus) according to the protocols. In brief, 96-well ELISpot plates were coated with an IgG capture antibody (for total IgG detection) or antigen (αCD40-HIV5pep, for specific IgG detection) in PBS overnight at 4°C. Then the plate was blocked with 200 μl/well of medium containing 10% FBS for at least 30 minutes at room temperature. The pre-activated splenocytes (splenocyte from humanized mice cultured ex vivo in the present of R848(1μg/ml) and IL-2 (10 u/ml) for 48hours) were then added to the ELISpot plate and incubated in a 37°C incubator with 5% CO_2 for 16-24 hours. Plates were washed 5 times with PBS and incubated with IgG detection mAbs for 2 hours at room temperature. Then, 1:1,000 dilution of streptavidin-HRP was added and incubated for 1 hour at room temperature. Followed by washing 5 times, the plates were developed with TMB substrate solution until distinct spots emerge. The spots were inspected and counted by using an ELISpot reader.

Antigen-Specific IgG Detection in Serum

96-well ELISA plates were coated with antigen (αCD40-HIV5pep, 10 μg/ml or HA protein, 10μg/ml) in PBS overnight at 4°C. Then the plate was blocked with 200 μl/well of medium containing 10% FBS for at least 30 minutes at room temperature. Then 50 μl of serum from vaccinated mice was added into the plate and incubated for 2 hours. Plates were washed 5 times with PBS and incubated with IgG detection mAbs for 2 hours at room temperature. Then, 1:1,000 dilution of streptavidin-HRP was added and incubated for 1 hour at room temperature. Followed by washing 5 times, the plates were developed with TMB substrate solution. The reaction was stopped with ELISA Stop Solution (Cat. No. E115), and the plate was read at 450 nm.

pDC Depletion *In Vivo*

A mAB specific to BDCA2, clone 15B, was used to deplete pDCs in humanized mice through i.p. injection (4 mg/kg). In brief, 15B was applied to mice at 3 and 1 day before each vaccination. At day0, the mice were either treated with CpG-B or received vaccination treatment.

Statistical Analysis

In all experiments, significance levels of data were determined by using Prism5 (GraphPad Software). Experiments were analyzed by two-tailed Student's t-test, one-way analysis of variance (ANOVA) and Tukey's multiple comparisons test, or Spearman rank correlation test as indicated in figure legends. A p value less than 0.05 was considered significant. The number of animals was specified in each figure legend.

RESULTS

TLR9 and CD40-Targeting Vaccination Promotes IgG Induction in Humanized Mice

Human B cell development and function are compromised in humanized mice, and B cells are impaired to undergo immunoglobin class switch from IgM to IgG. We tested whether targeting TLR-9 by CpG-B combined with a CD40-targeting vaccine can enhance B cell immunity in humanized mice. Humanized mice were immunized with αCD40-HIV5pep protein with or without CpG-B. B cell responses were evaluated one week after the boost vaccination. As reported (15), we found that B cells from PBMCs and spleen of PBS-treated humanized mice did not express surface IgG (**Figures 1A, B**). Vaccination with αCD40-HIV5pep protein alone failed to induce IgG expression on B cells (**Figures 1A, B**). Impressively, we found that, in humanized mice vaccinated with CpG-B together with αCD40-HIV5pep protein, around 12% (7.0% to 21.3%) of B cells from PBMCs and 5% (3.2% to 6.3%) of B cells from the spleens of humanized mice were IgG^+ B

cells (**Figures 1A, B**). CpG-B together with αCD40-HIV5pep vaccination also increased total human IgM level by-2 fold (**Figure 1C**). Human IgG, which is rarely detectable in humanized mice, reached 100 μg/ml in 75% (3/4) humanized mice after CpG-B together with CD40-targeting vaccination (**Figure 1C**). We also detected by ELISpot assay around 1,500 cells per million B cells from spleens of 75% (3/4) humanized mice received CpG-B plus CD40-targeting vaccination that were producing IgG, while no IgG-producing cells were detected in control groups (**Figure 1D**).

We next tested whether antigen-specific IgG was induced by CD40-targeting vaccination together with CpG-B. We found that 75% (3/4) mice from CpG-B/CD40-targeting vaccine group produced specific IgG, while no antigen specific IgG was detectable in control groups (**Figure 1E**). Expression of activation-induced cytidine deaminase (AID) by germinal center (GC) B cells is important for class switch and recombination (29). We found that AID expression was significantly increased (> 3-fold) in splenocytes from CpG-B plus CD40-targeting vaccination mice than cells from control groups (**Figure 1F**).

Together, our data indicate that TLR9 agonist CpG-B with a CD40-targeting vaccine induces immunoglobulin class-switch and enhances Ag-specific IgG responses in 75% (3/4) humanized mice tested.

CpG-B Promotes Maturation and Activation of B Cells in Humanized Mice

We next detected the phenotype of human B cells after vaccination. As reported (14), we found that most B cells from control mice were $CD24^{high}CD38^{high}$ which indicated immature phenotype (**Figures 2A, B**). CD40-targeting vaccination alone

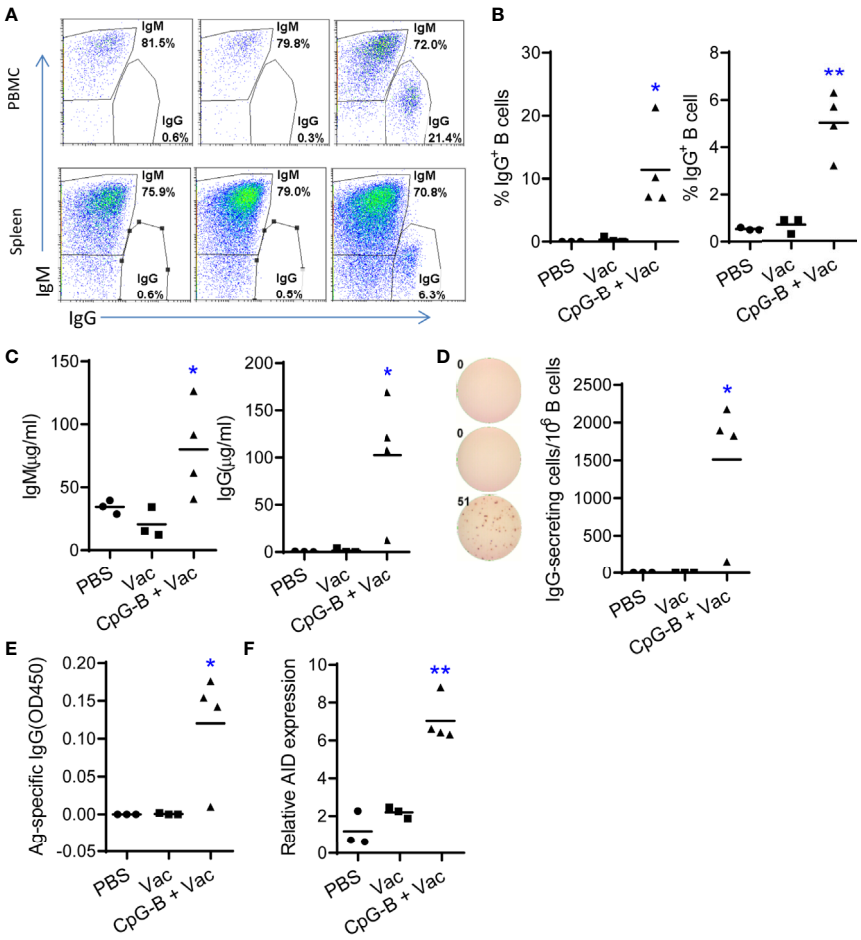

FIGURE 1 | TLR9 agonist CpG-B promotes IgG responses in humanized mice vaccinated with CD40-targeting vaccine. Humanized mice were treated with PBS control (n=3) or vaccinated with αCD40-HIV5pep (n=3) alone or vaccinated with αCD40-HIV5pep plus CpG-B (n=4) at week0, week3 and week6. At week 7, mice were sacrificed. **(A, B)** The expression of IgM and IgG on B cells from PBMCs and spleens was detected by FACS. **(C)** The total level of IgM and IgG in the plasma was detected by ELISA. **(D)** Splenocyte from humanized mice were cultured ex vivo in the present of R848(1μg/ml) and IL-2(10 u/ml) for 48hours, the cells were used for total IgG detection by ELISpot. **(E)** Antigen specific IgG level in the plasma was detected by ELISA. **(F)** The expression of activation-induced cytidine deaminase (AID) in spleen cells was detected by RT-PCR. Each dot represents one individual mouse, bars indicate mean. *P < 0.05, **P < 0.01, by unpaired, two-tailed Student's t-test comparing the two vaccinated groups.

did not change the percentage of $CD38^{high}CD24^{high}$ immature B cells. CpG-B together with CD40-targeting vaccination decreased the percentage of $CD38^{high}CD24^{high}$ B cells and increased the percentage of mature B cells with $CD38^{int}CD24^{int}$ or $CD38^{low}CD24^{int}$ phenotype (**Figures 2A, B**). We also find that CpG-B together with CD40-targeting vaccination increased the percentage of $CD10^-$ B cells (**Figures 2C, D**). In addition, CpG-B together with CD40-targeting

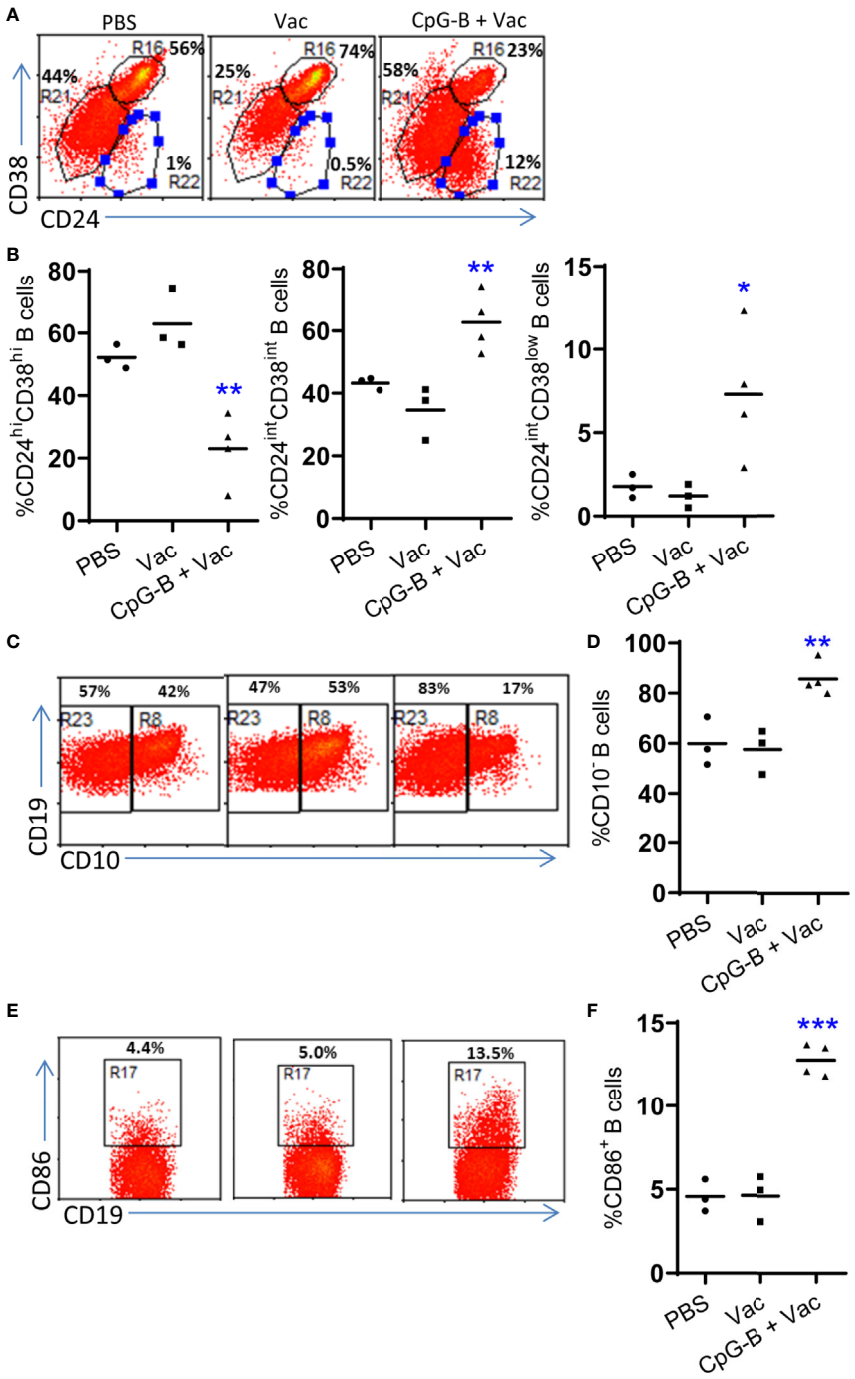

FIGURE 2 | CpG-B promotes maturation and activation of B cells in humanized mice. Humanized mice were vaccinated as in **Figure 1**. The phenotype of human B cells ($hCD45^+CD19^+$) from spleens of mice was detected by FACS. Representative dot plot **(A, C, E)** and Summarized data **(B, D, F)** showing the expression of CD38and CD24, CD10 and CD86 on human B cells. Each dot represents one individual mouse with n=3 in PBS group, n=4 in Vac group and n=4 in CpG-B plus Vac group. Bars indicate mean. *P < 0.05, **P < 0.01, ***P < 0.001, by unpaired, two-tailed Student's t-test comparing the two vaccinated groups.

vaccination induced CD86$^+$ activated B cells (**Figures 2E, F**). These data indicated that CpG-B plus CD40-targeting vaccination induce B cells maturation and activation.

CpG-B Induces IFN- α Production in pDC Dependent Manner in Humanized Mice

Dendritic cells are key to initiate and control immune responses. Plasmacytoid dendritic cells (pDC) represent a unique dendritic cell subtype and are specialized to produce large amount of IFN-α upon viral infection (30). It was reported that pDCs, through IFN-α and IL-6, are critical for the induction of IgG from human blood mononuclear cells in response to influenza virus (31). We found that CpG-B treatment activated human pDCs (**Figure 3A**) and induced IFN-α and IL-6 production in humanized mice (**Figure 3B**). TLR9, the receptor for CpG-B, is preferentially expressed by pDC and B cells of human immune system. To investigate whether pDC contributed to IFN-α production after CpG-B treatment, we used a monoclonal antibody which can efficiently and specifically deplete pDC *in vivo* in humanized mice (32) (**Figure 3C**). We found that pre-depletion of pDC abrogated IFN-α production after CpG-B treatment (**Figure 3D**). The results indicate that CpG-B treatment in humanized mice induces IFN-α expression thought a pDC dependent manner.

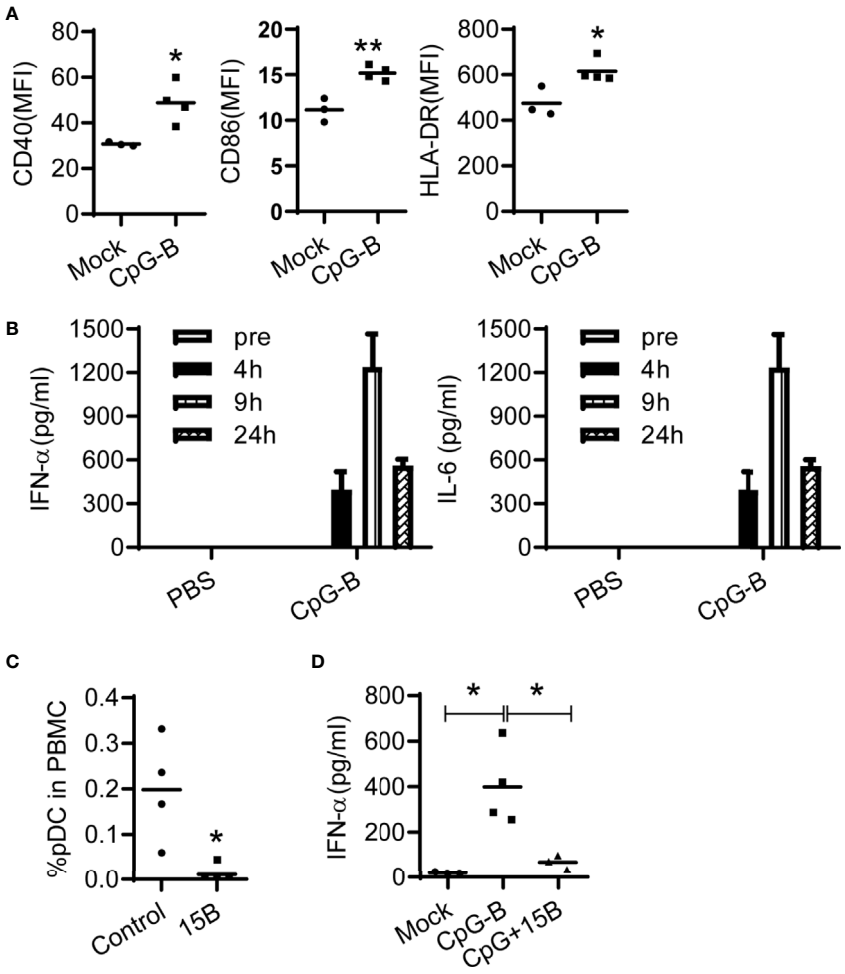

FIGURE 3 | CpG-induced IFN-a production *in vivo* is dependent on human pDCs in humanized mice. **(A, B)** Humanized mice were treated with PBS (n=3) or CpG-B (50ug/mouse, i.p., n=4). **(A)** IFN-α and IL-6 level in plasma at indicated timepoint post treatment were detected by ELISA. **(B)** The expression of CD40, CD86 and HLA-DR on pDC (CD4$^+$CD303$^+$) from spleens at 24 hours post-treatment was detected by FACS. **(C)** Humanized mice were pretreated with either isotype control (n=3) or pDC depletion monoclonal antibody (clone 15B, 200 μg/mouse, i.p., n=4) at day -3 and -1. The percentage of pDC in human CD45+ cells from blood were detected by FACS. **(D)** Humanized mice were pretreated with either isotype control (n=4) or pDC depletion monocolonal antibody (clone 15B, 200 μg/mouse, i.p., n=3) at day -3 and -1. At day0, mice were treated PBS (Mock, n=4) with CpG-B (n=4). IFN-a level in plasma was detected 24 hours after CpG-B treatment. Each dot represents one individual mouse, bars indicate mean. *P < 0.05, **P < 0.01, by unpaired, two-tailed Student's t-test **(A, C)** or by one-way analysis of variance (ANOVA) and Tukey's multiple comparisons test **(D)**.

TLR9 and CD40-Targeting Vaccination Depends on pDC to Promote Human B Cell Maturation and IgG Induction in Humanized Mice

We next investigated whether CpG-B and CD40-targeting vaccination induced B cell maturation and IgG production *in vivo* dependent on pDC. We vaccinated humanized mice with CpG-B and CD40-targeting vaccine in the presence or absence of pDC and then detected B cell phenotype and antibody response. As expected, pre-depletion of pDC by monoclonal antibody abrogated CpG-B induced IFN-α production (**Figure 4A**). Interestingly, CpG-B and CD40-targeting vaccine induced B cell maturation was also abrogated in the absence of pDC (**Figure 4B**). In the absence of pDC, CpG-B and CD40-targeting vaccination also failed to induce total IgG (**Figure 4C**) and antigen-specific IgG (**Figure 4D**). Furthermore, we found that the IFN-α level in plasma of mice correlated with total and specific IgG production in vaccinated hu-mice (**Figures 4E, F**).

CD40-Targeting Is Important for the Vaccine to Induce Class-Switch and IgG Production

CD40 is a co-stimulatory receptor expressed by a range of APCs, including DCs (33). Thus, targeting CD40 offers the potential advantage of inducing DC maturation and delivery of antigen to CD40 induced antigen-specific humoral and cellular immune response (34, 35). We next determined whether CD40-targeting is important to induce class-switch and IgG production in humanized mice. Humanized mice were immunized with recombinant hemagglutinin protein (HA) with or without CpG-B. HA protein alone failed to induce specific IgG (**Figure 5**). HA with CpG-B as adjuvant, although induce IFN-α production and CD86 expression on pDC, also did not induce specific IgG response to HA protein (**Figure 5**). These results indicate that CD40-targeting is important for the vaccine to induce class-switch and IgG production.

Taken together, we conclude that TLR9- and CD40-targeting vaccination promotes human B cell maturation and IgG response *via* pDCs dependent mechanisms in humanized mice.

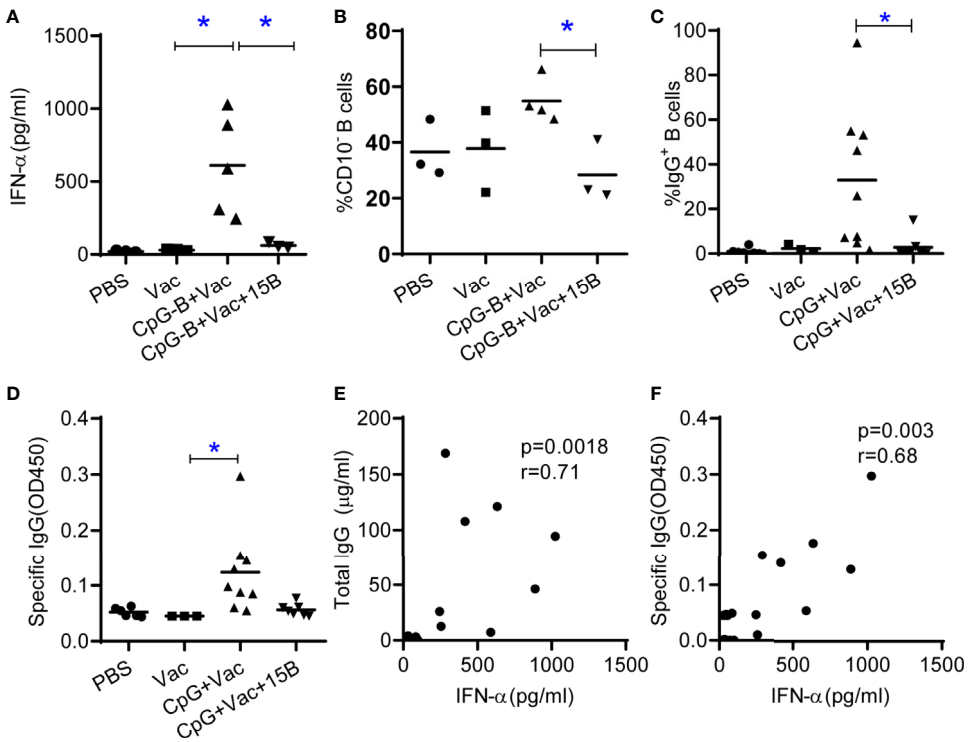

FIGURE 4 | TLR9 and CD40-targeting vaccination depends on pDC to promote human B cell maturation and IgG induction in humanized mice. Humanized mice were vaccinated as in **Figure1** except one group of the mice were treated with pDC depletion Ab before vaccination **(A)** IFN-α in the plasma 24 hours after vaccination. **(B)** Expression of CD10 on B cells from spleen at termination. **(C)** Total IgG level in serum was detected by ELISA. **(D)** Antigen specific IgG level in the plasma was detected by ELISA. Each dot represents one individual mouse, bars indicate mean. Shown are representative data (PBS, n=3; Vac, n=3; CpG-B+Vac, n=4; CpG+Vac+15B, n=3, for A and B) or combined data (PBS, n=6; Vac, n=3; CpG-B+Vac, n=9; CpG+Vac+15B, n=7, for C and D) of two independent experiments with mean values. *P < 0.05, by one-way analysis of variance (ANOVA) and Tukey's multiple comparisons test. **(E, F)** Correlation analysis between the IFN-α levels in plasma and total IgG **(E)** and specific IgG **(F)** levels in plasma (Spearman rank correlation test). r, correlation coefficient.

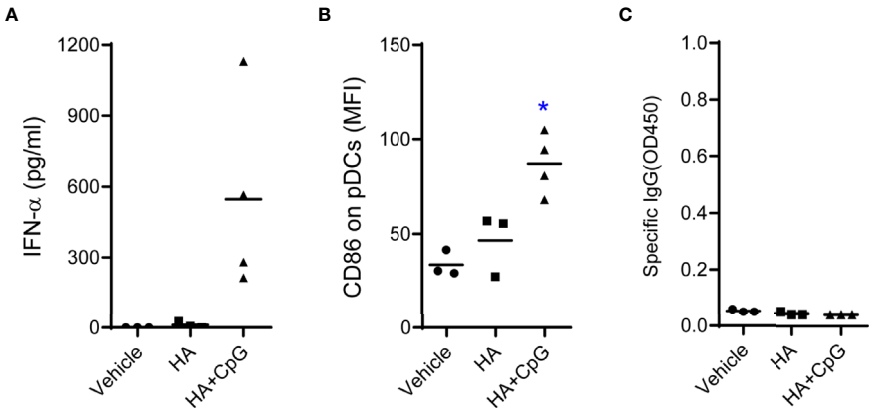

FIGURE 5 | CD40-targeting vaccination is required to induce IgG-response in humanized mice. Humanized mice were treated with PBS control (Vehicle, n=3) or vaccinated with recombinant hemagglutinin protein (HA, n=3, 10μg/mouse) alone or vaccinated with HA plus CpG-B (n=4) at week0, week3 and week6. **(A)** IFN-a levels in plasma in plasma at 24 hours post first vaccination was detected by ELISA. **(B)** The expression of CD86 on pDC ($CD4^+CD303^+$) from PBMC at 24 hours post-treatment was detected by FACS. **(C)** Antigen specific IgG level in the plasma was detected by ELISA. Each dot represents one individual mouse, bars indicate mean. *P < 0.05 by unpaired, two-tailed Student's t-test comparing the two vaccinated groups.

The study also provides insights for using humanized mouse models for vaccine development and induction of human IgG antibodies in humanized mice.

DISCUSSION

Humoral immunity is compromised in humanized mice (13). In the present study we reported that CpG-B adjuvant combined with a CD40-targeting vaccination enhanced antigen-specific IgG response. Furthermore, we proved that pre-depletion of human pDC *in vivo* abrogated the adjuvant effect of CpG-B. Our results indicated that CpG-B and CD40-targeting vaccination promoted B cell maturation, triggered human B cell immunoglobulin class-switch and induced IgG production in a pDC-dependent manner in humanized mice. The findings also shed light on induction of human IgG antibodies in humanized mouse models.

Mice reconstituted with human immune system provides a useful model to study human immunology and vaccinology. Although B cells are developed in humanized mice reconstituted with human HSCs, the cells are immature (13–15, 22–24). The circulating antibody levels, especially IgG levels, are significantly lower compared to adult humans (13). Moreover, the generation of antigen-specific IgG responses in humanized mice, are weak, limiting their application in testing candidate vaccines (13). It was reported that the immunoglobulin gene repertoires of human B cells from humanized mice are similar to those of B cells from human peripheral blood, suggesting that B cells from humanized mice have the genetic potential to produce antibody responses with broad isotype and high affinity (36). Studies have suggested that an absence of human cytokines and the disorganized secondary lymphoid structures might contribute to the defects in B cells (37–39). Signaling TLR results in large amount of cytokines induction in humanized mice. It was reported that pDC-derived IFN-α and IL-6 were critical for the induction of IgG from human blood mononuclear cells in response to influenza virus (31). pDC preferentially express TLR9 and TLR7 (25). We have previously shown that stimulation of pDC by TLR-9 agonist CpG-B induces IFN-α as well as IL-6 production *in vivo* in humanized mice (9). In the present study, we found that CpG-B adjuvant combined with CD40-targeting vaccination induced IgG^+ B cells in spleen and PBMCs of humanized mice and induced antigen-specific IgG in serum. This indicated that CpG-B and CD40-targeting vaccination triggers human B cell immunoglobulin class-switch in humanized mice. We also observed that B cells from mice receiving CpG-B plus CD40-targeting vaccination were more mature in phenotype and express a higher level of the activation marker CD86. The results together suggest that with proper adjuvant, human B cells in this model can produce specific IgG to a vaccine treatment. We also performed CpG-B plus non-CD40 targeting recombinant protein and showed that it did not induce significant IgG response. Thus CD40-targeting, as well as TLR9 activation, was also important for the vaccine to induce class-switch and IgG production. This could be due to CD40 activation of targeted APCs or prolonged antigen-presentation as was observed for T cell epitopes (40).

To prove whether pDCs are important for the IgG induction *in vivo*, we used a pDC-specific antibody to deplete pDC before vaccination. Our results showed that depletion of human pDC *in vivo* abrogated the B cell maturation and IgG production in response to CpG-B/CD40-targeting vaccination. The results suggest that human pDCs are essential to mediate the adjuvant effect of CpG-B *in vivo*. This is consistent with the report that pDC-derived IFN-α and IL-6 were critical for the induction of IgG from human blood mononuclear cells in response to influenza virus (31). We found that pDCs were required for CpG-B treatment in humanized mice to induce IFN-α and IL-6 production. We speculate that IFN-α and IL-6 from pDC enhanced B cell maturation and IgG-class switch in response to CpG-B plus CD40-targeting vaccination. It is also

important to state that there were shortcomings in our study. The antigen we used in this study was not HIV envelop protein so that we were not able to evaluate the neutralization activity of antibody induced by our vaccination stratagem. In another recent study, we proved that TLR-9 agonist plus CD40-targeting HIV envelop vaccination induced HIV-1 envelop-specific IgG with a diversified immunoglobulin repertoire and circulating Env-specific IgG-switched memory human B cells that exhibit clear signs of antigen-driven antibody affinity maturation (41).

In summary, we report that CpG-B as an adjuvant promoted human IgG induction through pDC-dependent mechanisms. The proof-of-concept study sheds light on specific induction of human IgG antibodies in humanized mice.

DATA AVAILABILITY STATEMENT

The original contributions presented in the study are included in the article/supplementary material. Further inquiries can be directed to the corresponding authors.

ETHICS STATEMENT

The animal study was reviewed and approved by University of North Carolina Institutional Animal Care and Use Committee.

AUTHOR CONTRIBUTIONS

LC and LS conceived the study and designed the experiments. GL, FL, FY, and CP performed the experiments. LC performed the analyses. LC, JT, and LS interpreted the data, wrote the manuscript, and supervised the study. GZ and SZ provided key reagents. YL helped conceive the overall program for studying anti-CD40 targeting in humanized mice. All authors contributed to the article and approved the submitted version.

FUNDING

This study was supported in part by NIH grants R01AI136990 (to LS), AI141333 (to JT), AI109784 (to JT and LS), and the Vaccine Research Institute *via* the ANR-10-LABX-77 grant funded part of this work.

ACKNOWLEDGMENTS

We thank Liqun Chi for technical support, Ning Jenny Jiang for helping with analyzing B cell maturation, and Qiuchen Zhao and Lulu Shi for editing the manuscript. Lineberger Comprehensive Cancer Center cores, UNC flow cytometry core, DLAM and UNC CFAR for support.

REFERENCES

1. Lai F, Chen Q. Humanized Mouse Models for the Study of Infection and Pathogenesis of Human Viruses. *Viruses* (2018) 10(11):643. doi: 10.3390/v10110643
2. Marsden MD, Zack JA. Humanized Mouse Models for Human Immunodeficiency Virus Infection. *Annu Rev Virol* (2017) 4:393–412. doi: 10.1146/annurev-virology-101416-041703
3. Shultz LD, Lyons BL, Burzenski LM, Gott B, Chen X, Chaleff S, et al. Human Lymphoid and Myeloid Cell Development in NOD/Ltsz-Scid IL2R Gamma Null Mice Engrafted With Mobilized Human Hemopoietic Stem Cells. *J Immunol* (2005) 174:6477–89. doi: 10.4049/jimmunol.174.10.6477
4. Zhang L, Kovalev GI, Su L. HIV-1 Infection and Pathogenesis in a Novel Humanized Mouse Model. *Blood* (2007) 109:2978–81. doi: 10.1182/blood-2006-07-033159
5. Ishikawa F, Yasukawa M, Lyons B, Yoshida S, Miyamoto T, Yoshimoto G, et al. Development of Functional Human Blood and Immune Systems in NOD/SCID/IL2 Receptor {Gamma} Chain(Null) Mice. *Blood* (2005) 106:1565–73. doi: 10.1182/blood-2005-02-0516
6. Traggiai E, Chicha L, Mazzucchelli L, Bronz L, Piffaretti JC, Lanzavecchia A, et al. Development of a Human Adaptive Immune System in Cord Blood Cell-Transplanted Mice. *Science* (2004) 304:104–7. doi: 10.1126/science.1093933
7. Cheng L, Ma J, Li G, Su L. Humanized Mice Engrafted With Human HSC Only or HSC and Thymus Support Comparable Hiv-1 Replication, Immunopathology, and Responses to ART and Immune Therapy. *Front Immunol* (2018) 9:817. doi: 10.3389/fimmu.2018.00817
8. Li Y, Masse-Ranson G, Garcia Z, Bruel T, Kok A, Strick-Marchand H, et al. A Human Immune System Mouse Model With Robust Lymph Node Development. *Nat Methods* (2018) 15:623–30. doi: 10.1038/s41592-018-0071-6
9. Cheng L, Zhang Z, Li G, Li F, Wang L, Zhang L, et al. Human Innate Responses and Adjuvant Activity of TLR Ligands in Vivo in Mice Reconstituted With a Human Immune System. *Vaccine* (2017) 35:6143–53. doi: 10.1016/j.vaccine.2017.09.052
10. Melkus MW, Estes JD, Padgett-Thomas A, Gatlin J, Denton PW, Othieno FA, et al. Humanized Mice Mount Specific Adaptive and Innate Immune Responses to EBV and TSST-1. *Nat Med* (2006) 12:1316–22. doi: 10.1038/nm1431
11. Meixlsperger S, Leung CS, Ramer PC, Pack M, Vanoaica LD, Breton G, et al. CD141+ Dendritic Cells Produce Prominent Amounts of IFN-Alpha After Dsrna Recognition and Can Be Targeted Via DEC-205 in Humanized Mice. *Blood* (2013) 121:5034–44. doi: 10.1182/blood-2012-12-473413
12. Cheng L, Wang Q, Li G, Banga R, Ma J, Yu H, et al. TLR3 Agonist and CD40-Targeting Vaccination Induces Immune Responses and Reduces HIV-1 Reservoirs. *J Clin Invest* (2018) 128:4387–96. doi: 10.1172/JCI99005
13. Seung E, Tager AM. Humoral Immunity in Humanized Mice: A Work in Progress. *J Infect Dis* (2013) 208 Suppl 2:S155–9. doi: 10.1093/infdis/jit448
14. Watanabe Y, Takahashi T, Okajima A, Shiokawa M, Ishii N, Katano I, et al. The Analysis of the Functions of Human B and T Cells in Humanized NOD/Shi-Scid/Gammac(Null) (NOG) Mice (Hu-HSC NOG Mice). *Int Immunol* (2009) 21:843–58. doi: 10.1093/intimm/dxp050
15. Biswas S, Chang H, Sarkis PT, Fikrig E, Zhu Q, Marasco WA. Humoral Immune Responses in Humanized BLT Mice Immunized With West Nile Virus and HIV-1 Envelope Proteins are Largely Mediated Via Human CD5+ B Cells. *Immunology* (2011) 134:419–33. doi: 10.1111/j.1365-2567.2011.03501.x
16. Beutler BA. TLRS and Innate Immunity. *Blood* (2009) 113:1399–407. doi: 10.1182/blood-2008-07-019307
17. Kawai T, Akira S. The Role of Pattern-Recognition Receptors in Innate Immunity: Update on Toll-Like Receptors. *Nat Immunol* (2010) 11:373–84. doi: 10.1038/ni.1863
18. O'Neill LA, Bowie AG. Sensing and Signaling in Antiviral Innate Immunity. *Curr Biol CB* (2010) 20:R328–33. doi: 10.1016/j.cub.2010.01.044
19. Iwasaki A, Medzhitov R. Regulation of Adaptive Immunity by the Innate Immune System. *Science* (2010) 327:291–5. doi: 10.1126/science.1183021
20. Coffman RL, Sher A, Seder RA. Vaccine Adjuvants: Putting Innate Immunity to Work. *Immunity* (2010) 33:492–503. doi: 10.1016/j.immuni.2010.10.002
21. Mbow ML, De Gregorio E, Valiante NM, Rappuoli R. New Adjuvants for Human Vaccines. *Curr Opin Immunol* (2010) 22:411–6. doi: 10.1016/j.coi.2010.04.004

22. Chen Q, He F, Kwang J, Chan JK, Chen J. Gm-CSF and IL-4 Stimulate Antibody Responses in Humanized Mice by Promoting T, B, and Dendritic Cell Maturation. *J Immunol* (2012) 189:5223–9. doi: 10.4049/jimmunol.1201789
23. Jangalwe S, Shultz LD, Mathew A, Brehm MA. Improved B Cell Development in Humanized NOD-Scid IL2Rgamma(Null) Mice Transgenically Expressing Human Stem Cell Factor, Granulocyte-Macrophage Colony-Stimulating Factor and Interleukin-3. *Immun Inflamm Dis* (2016) 4:427–40. doi: 10.1002/iid3.124
24. Yu H, Borsotti C, Schickel JN, Zhu S, Strowig T, Eynon EE, et al. A Novel Humanized Mouse Model With Significant Improvement of Class-Switched, Antigen-Specific Antibody Production. *Blood* (2017) 129:959–69. doi: 10.1182/blood-2016-04-709584
25. Hornung V, Rothenfusser S, Britsch S, Krug A, Jahrsdorfer B, Giese T, et al. Quantitative Expression of Toll-Like Receptor 1-10 Mrna in Cellular Subsets of Human Peripheral Blood Mononuclear Cells and Sensitivity to Cpg Oligodeoxynucleotides. *J Immunol* (2002) 168:4531–7. doi: 10.4049/jimmunol.168.9.4531
26. Kadowaki N, Ho S, Antonenko S, Malefyt RW, Kastelein RA, Bazan F, et al. Subsets of Human Dendritic Cell Precursors Express Different Toll-Like Receptors and Respond to Different Microbial Antigens. *J Exp Med* (2001) 194:863–9. doi: 10.1084/jem.194.6.863
27. Zhang L, Jiang Q, Li G, Jeffrey J, Kovalev GI, Su L. Efficient Infection, Activation, and Impairment of Pdcs in the BM and Peripheral Lymphoid Organs During Early HIV-1 Infection in Humanized Rag2(-)/(-)Gamma C(-)/(-) Mice in Vivo. *Blood* (2011) 117:6184–92. doi: 10.1182/blood-2011-01-331173
28. Flamar AL, Xue Y, Zurawski SM, Montes M, King B, Sloan L, et al. Targeting Concatenated HIV Antigens to Human CD40 Expands a Broad Repertoire of Multifunctional CD4+ and CD8+ T Cells. *AIDS* (2013) 27:2041–51. doi: 10.1097/QAD.0b013e3283624305
29. Muramatsu M, Kinoshita K, Fagarasan S, Yamada S, Shinkai Y, Honjo T. Class Switch Recombination and Hypermutation Require Activation-Induced Cytidine Deaminase (AID), a Potential RNA Editing Enzyme. *Cell* (2000) 102:553–63. doi: 10.1016/S0092-8674(00)00078-7
30. Liu YJ. IPC: Professional Type 1 Interferon-Producing Cells and Plasmacytoid Dendritic Cell Precursors. *Annu Rev Immunol* (2005) 23:275–306. doi: 10.1146/annurev.immunol.23.021704.115633
31. Jego G, Palucka AK, Blanck JP, Chalouni C, Pascual V, Banchereau J. Plasmacytoid Dendritic Cells Induce Plasma Cell Differentiation Through Type I Interferon and Interleukin 6. *Immunity* (2003) 19:225–34. doi: 10.1016/S1074-7613(03)00208-5
32. Li G, Cheng M, Nunoya J, Cheng L, Guo H, Yu H, et al. Plasmacytoid Dendritic Cells Suppress HIV-1 Replication But Contribute to HIV-1 Induced Immunopathogenesis in Humanized Mice. *PloS Pathog* (2014) 10:e1004291. doi: 10.1371/journal.ppat.1004291
33. Grewal IS, Flavell RA. CD40 and CD154 in Cell-Mediated Immunity. *Annu Rev Immunol* (1998) 16:111–35. doi: 10.1146/annurev.immunol.16.1.111
34. Barr TA, McCormick AL, Carlring J, Heath AW. A Potent Adjuvant Effect of CD40 Antibody Attached to Antigen. *Immunology* (2003) 109:87–92. doi: 10.1046/j.1365-2567.2003.01634.x
35. Hangalapura BN, Oosterhoff D, Aggarwal S, Wijnands PG, van de Ven R, Santegoets SJ, et al. Selective Transduction of Dendritic Cells in Human Lymph Nodes and Superior Induction of High-Avidity Melanoma-Reactive Cytotoxic T Cells by a CD40-Targeted Adenovirus. *J Immunother* (2010) 33:706–15. doi: 10.1097/CJI.0b013e3181eccbd4
36. Ippolito GC, Hoi KH, Reddy ST, Carroll SM, Ge X, Rogosch T, et al. Antibody Repertoires in Humanized NOD-Scid-IL2Rgamma(Null) Mice and Human B Cells Reveals Human-Like Diversification and Tolerance Checkpoints in the Mouse. *PloS One* (2012) 7:e35497. doi: 10.1371/journal.pone.0035497
37. Vuyyuru R, Patton J, Manser T. Human Immune System Mice: Current Potential and Limitations for Translational Research on Human Antibody Responses. *Immunol Res* (2011) 51:257–66. doi: 10.1007/s12026-011-8243-9
38. Chen Q, Khoury M, Chen J. Expression of Human Cytokines Dramatically Improves Reconstitution of Specific Human-Blood Lineage Cells in Humanized Mice. *Proc Natl Acad Sci U.S.A.* (2009) 106:21783–8. doi: 10.1073/pnas.0912274106
39. Matsumura T, Kametani Y, Ando K, Hirano Y, Katano I, Ito R, et al. Functional Cd5+ B Cells Develop Predominantly in the Spleen of NOD/SCID/Gammac(Null) (NOG) Mice Transplanted Either With Human Umbilical Cord Blood, Bone Marrow, or Mobilized Peripheral Blood CD34+ Cells. *Exp Hematol* (2003) 31:789–97. doi: 10.1016/S0301-472X(03)00193-0
40. Yin W, Gorvel L, Zurawski S, Li D, Ni L, Duluc D, et al. Functional Specialty of CD40 and Dendritic Cell Surface Lectins for Exogenous Antigen Presentation to CD8(+) and CD4(+) T Cells. *EBioMedicine* (2016) 5:46–58. doi: 10.1016/j.ebiom.2016.01.029
41. Godot V, Tcherakian C, Gil L, Cervera-Marzal I, Li G, Cheng L, et al. TLR-9 Agonist and CD40-Targeting Vaccination Induces HIV-1 Envelope-Specific B Cells With a Diversified Immunoglobulin Repertoire in Humanized Mice. *PloS Pathog* (2020) 16:e1009025. doi: 10.1371/journal.ppat.1009025

Conflict of Interest: GZ, SZ, and YL are named inventors on patent applications relevant to αCD40-HIV5pep held by INSERM Transfert.

The remaining authors declare that the research was conducted in the absence of any commercial or financial relationships that could be construed as a potential conflict of interest.

frontiers in Immunology

REVIEW
published: 17 June 2021
doi: 10.3389/fimmu.2021.663328

Humanized Mouse Models for the Study of Periodontitis: An Opportunity to Elucidate Unresolved Aspects of Its Immunopathogenesis and Analyze New Immunotherapeutic Strategies

Carolina Rojas[1†], *Michelle P. García*[1†], *Alan F. Polanco*[1†], *Luis González-Osuna*[1†], *Alfredo Sierra-Cristancho*[1,2†], *Samanta Melgar-Rodríguez*[1,3†], *Emilio A. Cafferata*[1,4*†] *and Rolando Vernal*[1,3*†]

[1] Periodontal Biology Laboratory, Faculty of Dentistry, Universidad de Chile, Santiago, Chile, [2] Faculty of Dentistry, Universidad Andres Bello, Santiago, Chile, [3] Department of Conservative Dentistry, Faculty of Dentistry, Universidad de Chile, Santiago, Chile, [4] Department of Periodontology, School of Dentistry, Universidad Científica del Sur, Lima, Perú

OPEN ACCESS

Edited by:
Qingfeng Chen,
Institute of Molecular and Cell Biology (A*STAR), Singapore

Reviewed by:
Christopher W. Cutler,
Augusta University, United States
Sharvan Sehrawat,
Indian Institute of Science Education and Research Mohali, India

***Correspondence:**
Rolando Vernal
rvernal@uchile.cl
Emilio A. Cafferata
ecafferata@cientifica.edu.pe

†ORCID:
Carolina Rojas
orcid.org/0000-0003-4004-3999
Michelle P. García
orcid.org/0000-0002-4283-7269
Alan F. Polanco
orcid.org/0000-0002-3883-7733
Luis González-Osuna
orcid.org/0000-0002-8456-6372
Alfredo Sierra-Cristancho
orcid.org/0000-0003-0952-9835
Samanta Melgar-Rodríguez
orcid.org/0000-0003-1480-5734
Emilio A. Cafferata
orcid.org/0000-0001-9243-1382
Rolando Vernal
orcid.org/0000-0002-1391-320X

Specialty section:
This article was submitted to Microbial Immunology, a section of the journal Frontiers in Immunology

Received: 02 February 2021
Accepted: 10 May 2021
Published: 17 June 2021

Periodontitis is an oral inflammatory disease in which the polymicrobial synergy and dysbiosis of the subgingival microbiota trigger a deregulated host immune response, that leads to the breakdown of tooth-supporting tissues and finally tooth loss. Periodontitis is characterized by the increased pathogenic activity of T helper type 17 (Th17) lymphocytes and defective immunoregulation mediated by phenotypically unstable T regulatory (Treg), lymphocytes, incapable of resolving the bone-resorbing inflammatory milieu. In this context, the complexity of the immune response orchestrated against the microbial challenge during periodontitis has made the study of its pathogenesis and therapy difficult and limited. Indeed, the ethical limitations that accompany human studies can lead to an insufficient etiopathogenic understanding of the disease and consequently, biased treatment decision-making. Alternatively, animal models allow us to manage these difficulties and give us the opportunity to partially emulate the etiopathogenesis of periodontitis by inoculating periodontopathogenic bacteria or by placing bacteria-accumulating ligatures around the teeth; however, these models still have limited translational application in humans. Accordingly, humanized animal models are able to emulate human-like complex networks of immune responses by engrafting human cells or tissues into specific strains of immunodeficient mice. Their characteristics enable a viable time window for the study of the establishment of a specific human immune response pattern in an *in vivo* setting and could be exploited for a wider study of the etiopathogenesis and/or treatment of periodontitis. For instance, the antigen-specific response of human dendritic cells against the periodontopathogen *Porphyromonas gingivalis* favoring the Th17/Treg response has already been tested in humanized mice models. Hypothetically, the proper emulation of periodontal dysbiosis in a humanized animal could give insights into the subtle molecular characteristics of a human-like local and systemic immune response during periodontitis and support the design of novel

immunotherapeutic strategies. Therefore, the aims of this review are: To elucidate how the microbiota-elicited immunopathogenesis of periodontitis can be potentially emulated in humanized mouse models, to highlight their advantages and limitations in comparison with the already available experimental periodontitis non-humanized animal models, and to discuss the potential translational application of using these models for periodontitis immunotherapeutics.

Keywords: periodontitis, animal model, humanized mice, immunopathogenesis, immunotherapy

INTRODUCTION

The oral mucosa is a place of immense antigenic diversity that demands a tightly balanced immune surveillance, capable of maintaining the balance between host and microbial interactions. Indeed, a plethora of signals, including food antigens, airborne particles, commensal microbiota, and ongoing damage from mastication, finely tune the oral mucosal barrier immunity (1, 2). Moreover, the existence of an incredibly thin and highly-permeable epithelium located at the bottom of the gingival crevice, composed of 3-5 layers of cells and harboring diverse microbial communities between the tooth and the gingiva, allows the continuous transmigration of immune cells against the microbial challenge, thus making this scenario particularly challenging for a balanced immune response (1, 3).

ETIOPATHOGENESIS OF PERIODONTITIS: MICROBIOTA AND HOST INTERACTIONS

Certainly, constant environmental stimuli given by oral anatomical features and their functions, as well as the salivary flow and composition, directly influence the tooth-adherent microbiota. Hence, the orchestrated stability of at least 700 different taxa colonizing these distinct oral meta-niches has been a permanent matter of attention for dentists (4). In a healthy periodontium, the symbiosis between the resident eubiotic microorganisms and the host's immune response commands this equilibrium. However, ill-defined factors, such as plaque accumulation, diet, stress, smoking, genetic predisposition, chronic inflammation, among others, contribute to a disequilibrium within bacterial communities, favoring the emergence of highly virulent bacteria, including *Porphyromonas gingivalis*, *Aggregatibacter actinomycetemcomitans*, and *Fusobacterium nucleatum*, as well as the reduction of health-compatible commensal bacteria.

For instance, *P. gingivalis* pathogenicity relies on its capability of expressing a variety of virulence factors, such as lipopolysaccharide, extracellular capsule, gingipains, and fimbriae, which, despite its low relative abundance, can both over-activate and subvert the immune response in mice or human periodontium (5, 6). Furthermore, different strains of this keystone pathogen have been detected in active periodontal lesions of teeth with poor prognosis and have demonstrated the capacity of eliciting a differential osteo-destructive immune response (7–9). Otherwise, the pathobiont *A. actinomycetemcomitans*, associated with more severe forms of periodontitis, is also armed with a variety of virulence factors such as lipopolysaccharide, leukotoxin, and fimbriae, which induce leukocyte lysis, favor periodontal colonization and provoke a dysregulated immune response during periodontal inflammation (10–12). In this context, the polymicrobial synergy of a dysbiotic bacterial consortium, frequently including the interplay between *P. gingivalis*, *A. actinomycetemcomitans*, and/or *F. nucleatum*, leads to a cycle of pathogenic inflammation, which perpetuates a nutrient-rich environment that promotes their expansion and deeper invasion of periodontal tissues; thus, provoking inflammatory alveolar bone loss in a susceptible host (13, 14).

Apart from other mucosal barriers entirely dependent on microbial commensals, gingival immune homeostasis is distinctly influenced by physiological damage during mastication. In fact, chewing elicits the production of interleukin (IL)-6 by fibroblasts, which promotes oral barrier protection *via* T-helper type 17 (Th17)-mediated immunity (15). Indeed, Th17 lymphocytes are key players in the maintenance of oral integrity by actively recruiting neutrophils to the teeth/mucosa interface and controlling opportunistic fungal infections (16); however, they are also key drivers of osteolytic inflammation during periodontitis. Thus, the amplification and dysregulation of Th17 lymphocyte activity mediated by Th17-related cytokines, including IL-6, IL-17A, IL-21, IL-23, and the osteolytic factor termed receptor activator of nuclear factor κB ligand (RANKL), lead to the breakdown of soft tooth-supporting tissues and alveolar bone resorption in susceptible individuals (16–18).

Contrarily, the maintenance of tolerance, prevention of autoimmunity, and inhibition of chronic inflammation required in the healthy periodontium has been attributed to T regulatory (Treg) lymphocyte activity (19–21). Treg lymphocytes are mainly characterized by their sustained surface expression of the IL-2 receptor α chain, termed CD25, and their signature transcription factor forkhead box P3 (Foxp3), and by having an armament of molecular strategies for, as its name implies, regulate both the innate and adaptive immune response (22). Treg lymphocytes control, at least in part, periodontal inflammation *via* the production of immunoregulatory cytokines, such as transforming growth factor (TGF)-β1, IL-10, and IL-35, which inhibit the expansion and activity of effector T lymphocytes such as Th1 and Th17 cells (21, 23). Periodontitis-affected tissues show enrichment in Treg lymphocyte activity demonstrated by the increased expression of their associated immune-regulatory/suppressive molecules like cytotoxic T-lymphocyte antigen 4 (CTLA-4), glucocorticoid-induced TNF-related protein (GITR) and Foxp3 (24). On the

other hand, systemic ablation of Treg lymphocytes, by inoculating anti-GITR, increases the periodontal levels of tumor necrosis factor (TNF)-α, RANKL, and alveolar bone loss (25). However, for these immune-regulatory properties to be effective, the maintenance of their regulatory phenotype, mediated by the expression of Foxp3, is mandatory (20, 26). During periodontitis, Treg lymphocytes show a reduced Foxp3 expression and, instead, produce IL-17A and RANKL (20, 27); thus, making the inflammatory milieu highly enriched in inflammatory cytokines like IL-6, pivotal in dictating Treg lymphocyte fate in periodontal lesions.

The antagonistic relationship between bone-resorptive Th17 lymphocytes and immunoregulatory Treg lymphocytes dictates the delicate balance of alveolar bone remodeling (17, 20). On the one hand, osteoclasts differentiate and activate in the presence of macrophage colony-stimulating factor (M-CSF) and RANKL, which increase during periodontitis mainly by Th17 activity; while on the other hand, osteoblasts produce osteoprotegerin (OPG), the RANKL soluble decoy, which is partly mediated by Treg lymphocyte activity during periodontitis (17, 23, 27–31). Therefore, the cooperative action between bone-resorbing osteoclasts and bone-forming osteoblasts, regulated by the immune response, defines the dynamic maintenance of alveolar bone homeostasis.

CURRENT ANIMAL MODELS FOR EXPERIMENTAL PERIODONTITIS

The complexity and diversity of factors that contribute to periodontitis pathogenesis, including the combination of polymicrobial synergy and dysbiosis, chronic inflammatory dysregulation, and genetic predisposition factors have done the search for an ideal animal model of periodontitis difficult and challenging. Nevertheless, several authors have managed to mimic how these factors influence the development of periodontal diseases by separating them into different phases, including the formation of biofilms, bacterial colonization and invasion of periodontal tissues, induction of a deregulated host immune response, and breakdown of soft tooth-supporting tissues and alveolar bone resorption (32). **Table 1** summarizes the different methods that have been used to generate experimental periodontitis in mice. In general terms, the advantages of using mice models include a known microbiota and immune composition, diverse genetically engineered strains, and rapid availability of reagents for the investigation of recently described molecules (59). However, conditions such as substantially small mouths require highly skilled operators and a large number of animals (60).

Experimental mice models developed for the study of periodontitis have been substantially beneficial and important to examine diverse biologic hypotheses related to disease pathogenesis, host-bacteria interactions, and therapeutic approaches, being able to, at least in part, finely reproduce the clinical, molecular, and histologic features of human periodontitis. Besides, the animals used to generate periodontitis are relatively inexpensive, easy to handle, have a short gestation period, and are characterized by developing a highly reproducible periodontal inflammatory process (33, 61). Among the various methods employed to mimic periodontitis in mice, currently, the most commonly used are oral gavage, periodontal inoculation, and ligature.

Oral Gavage

The oral gavage model consists of the inoculation of human bacterial strains with an oral-esophageal gauge or a micropipette, usually using 10^9 colony-forming units in a viscous suspension, prepared with 2% carboxymethylcellulose (62). The bacteria that have been most frequently used to induce periodontitis by oral gavage are *P. gingivalis*, *A. actinomycetemcomitans*, and *F. nucleatum*, as well as combinations of different bacterial strains (63–66). This method has been used successfully to establish the relationship between periodontitis and systemic conditions. For instance, the inoculation of *P. gingivalis* in hyperlipidemic mice *via* oral gavage provoked the accelerated formation of atherosclerotic plaques (67).

However, this experimental design can last at least 4 and up to 8 weeks until clear and significant evidence of alveolar bone resorption is achieved. Moreover, the magnitude of bone loss is not always reproducible, and the frequent inconsistency of the results is attributable to various factors, being the systemic nature of the infection caused the main factor (33, 34, 61). In consequence, oral gavage has been established as not fully effective to induce periodontitis (34).

Periodontal Inoculation

The periodontal inoculation model comprises the localized microinjection of bacteria or some isolated bacterial component, such as lipopolysaccharide, directly into the palatal interproximal gingiva between the first, second, and third maxillary molar (18, 35). This method promotes significant periodontal inflammation, characterized by an increased expression of pro-inflammatory cytokines, apical migration of the junctional epithelium, and activation of osteoclastogenesis, consistently resulting in alveolar bone resorption (36, 40). Regarding the injection regimen, evidence commonly shows that the injections are performed two or three times per week under general anesthesia, generally using isoflurane (61, 68). The experimental period for this methodology may vary according to the purpose of the study, being generally between 20 and 30 days, although significant evidence of alveolar bone loss can be verified 7 days after initiation of the injections (18, 69).

This model has been used to evaluate different hypotheses regarding the mechanisms of periodontal inflammation and alveolar bone loss, due to the fact that it allows a reliable characterization of the immune response induced in the periodontal tissues and the cervical lymph nodes that drain the infected periodontium (6, 40). Since the mono-infection with a known bacterium allows great experimental control over the pathogenic stimulus, this model has been shown to be useful for analyzing pathogenic differences between different periodontal bacteria, their different serotypes, or bacteria defective in a certain virulence factor (6, 7, 18, 40, 41).

Ligature

Ligature-induced periodontitis is an efficient model capable of inducing predictable alveolar bone loss within few days in

TABLE 1 | The most widely used models to generate experimental periodontitis in mice.

Experimental Periodontitis Model	Description	Requirements	Advantages and Biological Approaches		Limitations	References
			Technical Advantages	Biological Application and Plausibility		
Oral gavage/oral infection	Inoculation of live human bacteria, such as *Pg*, *Aa, and/or Fn*, via an oral-esophageal-gastric cannula or a micropipette into the mouse digestive system. • Gut microbiota dysbiosis and bacteremia favors chronic low-grade inflammation similar to periodontitis.	1) Anaerobic/capnophilic culture and bacteria-compatible animal facilities. 2) Constant monitoring and standarization of bacteria MOI. There is no consensus regarding the ideal concentration or quantity of inoculated bacteria.	1) Allows the precise enteric administration of bacteria. 2) It can be performed without anesthesia.*	1) Promotes periodontal inflammation and progressive alveolar bone resorption consistent with a chronic form of periodontitis. 2) Allows the bacterial invasion of mice oral tissues and bacteremia during a relatively long period of time (4-8 weeks). 3) The sustained systemic microbial challenge and low-grade systemic inflammation resembles the chronicity of periodontitis. 4) Enables the study of the association between systemic conditions and periodontitis-associated bacterial strains. Depending on the MOI and bacterial strain, it can also favor gut dysbiosis, joint inflammation, atheroma formation, and neuroinflammation.	1) Not fully effective to induce periodontal lesions. It generates less alveolar bone loss compared with other models. 2) Multiple inoculations in a long period of time (4-8 weeks) are needed until disease development. Increased animal stress and risk of esophageal lesions. 3) Effectiveness depends on the used bacterial strain and its virulence. 4) Not fully compatible with immunocompromised mice strains and humanized mice models.	(7, 25, 33–39)
Periodontal inoculation of bacteria	Localized microinjection of live human bacteria into mouse vestibular or palatal mucosa. • Mucosal infection and local bacterial challenge induce a local immune response capable of generating periodontal lesions.	1) Anaerobic/capnophilic culture and bacteria-compatible animal facilities. 2) Constant monitoring and standardization of bacteria MOI. 3) Constant anesthesia supplementation and post-intervention animal surveillance. There is no consensus regarding the ideal concentration or quantity of inoculated bacteria.	1) Semi-precise local administration of bacteria.	1) Promotes periodontal inflammation and alveolar bone resorption consistent with a chronic form of periodontitis. 2) Enables the study of specific periodontal host-bacteria interactions associated to infection, such as PRR-antigen interaction. 3) Useful for the study of virulence/immunogenic/pathogenic differences between periodontitis-associated bacteria.	1) Not fully effective to induce periodontal lesions. It generates less alveolar bone loss and inflammatory response compared with other models, such as ligature. 2) Repetitive injection regimen (2-3 per week) and mid-long experimental period until disease development (20-45 days).	(6, 18, 35, 40–42)
Oral and anal inoculation of periodontitis-associated bacteria	Topical administration of a mixture of 3%CMC and periodontitis-associated bacteria, such as *Pg*, into the mouse oral cavity and anus. • Mice coprophagia promotes continuous re-infection and establishment of chronic oral microbial challenge.	1) Anaerobic/capnophilic culture and bacteria-compatible animal facilities. 2) Constant monitoring and standarization of bacteria MOI.	1) Minimal or no trauma to the mouse mucosa. 2) It can be performed without anesthesia.*	1) Allows the bacterial invasion of mice oral tissues and bacteremia during a relatively long period of time (4-8 weeks). 2) Promotes periodontal inflammation and alveolar bone resorption consistent with a chronic form of periodontitis. 3) The sustained systemic microbial challenge and low-grade systemic inflammation resembles chronicity of periodontitis. 4) Enables the study of the association between systemic affections and periodontitis-associated bacterial strains.	1) Unprecise administration of bacteria. 2) Gut dysbiosis and faecal bacteria can be confounding factors. 3) Consecutive application regimen (8 days) and mid-long experimental period until disease development (8 weeks). 4) Not fully compatible with immunocompromised mice strains and humanized mice models.	(43–45)

(Continued)

TABLE 1 | Continued

Experimental Periodontitis Model	Description	Requirements	Advantages and Biological Approaches		Limitations	References
			Technical Advantages	Biological Application and Plausibility		
Periodontal inoculation of isolated bacterial antigens	Local microinjection of known bacterial components, derived or not from periodontitis-associated bacteria, such as LPS. The inoculation is carried out into mouse vestibular or palatal mucosa. • Bacterial antigens directly elicit the mouse immune response.	1) Skilled operator. 2) Constant anesthesia supplementation and post-intervention animal surveillance. There is no consensus regarding the ideal concentration or quantity of inoculated bacterial antigen for the model.	1) It does not need bacterial culture† or their inoculation. 2) Compatible with immunocompromised mice strains and humanized mice models.	1) Promotes periodontal inflammation and alveolar bone resorption consistent with an acute/aggresive form of periodontitis. 2) Induces low-grade systemic inflammation (in the case of LPS) when applied for at least 2 weeks. It can provoke cortical lesions, neuroinflammation, and arthritic lesions. 3) Enables the study of the specific interaction of PAMPs with the host immune response.	1) Repetitive injection regimen (2-3 per week). 2) It does not emulate bacteria-host interaction, essential during periodontitis.	(18, 46–50)
Chemically-induced periodontitis	TNBS and/or DSS are orally delivered weekly and/or biweekly. • DDS targets the innate immune response by undermining the epithelial barrier and inducing ROS production. TNBS induces a T-cell mediated response.	1) Experiment can last between 7 to 18 weeks, with weekly or biweekly interventions.	1) It does not need anesthesia nor bacterial culture. 2) Compatible with immunocompromised mice strains and humanized mice models.	1) Promotes periodontal inflammation and progressive alveolar bone resorption consistent with a chronic form of periodontitis. 2) Induces low-grade systemic inflammation, including colon and liver lesions. 3) Allows the study of the association between gut mucosal and oral mucosal inflammation.	1) It does not emulate bacteria-host interaction, essential during periodontitis. 2) Not fully effective to induce periodontal lesions. It generates less alveolar bone loss compared with other models, such as ligature.	(51, 52)
Ligature-induced periodontitis	Placement of a retentive ligature, usually silk, around or at the interproximal spaces of the mouse tooth. • Accumulation of bacterial biomass favors the development of a dysbiotic microbiota capable of inducing a local mucosal immune response and periodontal lesions.	1) Highly skilled operator, with optional magnification devices. 2) Most models use silk sutures around maxillary second molars, though there is no consensus regarding the place or width/length of the ligature or the need of its renewal.	1) Compatible with immunocompromised mice and humanized mice models. 2) Minimal trauma to the mouse mucosa. 3) Allows the collection of mouse gingival crevicular fluid.	1) Promotes acute periodontal inflammation and rapid alveolar bone resorption resembling an acute/aggresive form of periodontitis. 2) Compatible with the current oral dysbiosis-associated periodontitis pathogenesis paradigm. 3) Induces low-grade systemic inflammation, also compatible with periodontitis definition. 4) Allows the study of local immune response against inespecific bacterial challenge and alveolar bone regeneration after ligature removal. 5) When combined with oral gavage or periodontal inoculation, it can be useful for the study of virulence/immunogenic/pathogenic differences between periodontitis-associated bacteria.	1) Risk of mechanical trauma if not performed by calibrated operator. 2) Animals need to be constantly checked for ligature position. 3) No sustained bone loss after prolonged periods of time, unless combined with bacteria inoculation or gavage; thus, not resembling periodontitis chronicity.	(20, 23, 29, 32–35, 53, 54)
Calvaria inoculation of periodontitis-associated bacteria	Subcutaneous inoculation of periodontitis-associated bacteria, mostly *Pg*, at the skull midline between the ears and eyes. • The injection induces the formation of an abscess, acute local inflammation, and adjacent bone resorption.	1) Anaerobic/capnophilic culture and bacteria-compatible animal facilities. 2) Constant monitoring and standarization of bacteria MOI. There is no consensus regarding the ideal concentration or quantity of inoculated bacteria.	1) Semi-precise local administration of bacteria. 2) Does not require a skilled operator.	1) Promotes acute subcutaneous inflammation and rapid alveolar bone resorption, resembling an acute/aggresive form of infection/inflammation-induced bone resorption. 2) Allows the study of the immunogenic and pathogenic potential of bacteria.	1) Abscess formation does not resemble a periodontitis lesion. 2) Not fully compatible with immunocompromised mice strains and humanized mice models.	(55–58)

Aa, Aggregatibacter actinomycetemcomitans; CMC, carboxymethyl cellulose; DSS, dextrane sulfate sodium; Fn, Fusobacterium nucleatum; LPS, lipopolysaccharide; MOI, multiplicity of infection; PAMPs, pathogen-associated molecular patterns; Pg, Porphyromonas gingivalis; PRR, pattern recognition receptor; ROS, reactive oxygen species; TNBS, 2,4,6-Trinitrobenzene sulfonic acid.

**The use of isofluorane anesthesia is recommended in some publications to reduce the provoked stress and the incidence of esophageal lesions during oral gavage.*

†Some authors would prefer to extract bacterial components, such as LPS, from their own bacteria cultures.

mice (70). Besides, the removal of ligatures allows the study of lesion healing and resolution of inflammation (53). The main procedure involves placing silk, nylon, or cotton ligatures around maxillary or mandibular molars under anesthesia so that the retentive ligatures facilitate the accumulation of bacteria and thus, provoke periodontal inflammation and alveolar bone loss (53, 61, 71). Indeed, the occurrence of these bacteria-host interactions is compatible with the current paradigm of periodontitis pathogenesis, in which the development of dysbiotic oral microbiota provokes a bone-destructive immune response (28, 72).

The use of ligatures to induce periodontitis in mice has permitted the kinetic analysis of the morphologic characteristics of bone resorption (53). Differences between control and ligated mice alveolar bone loss become evident after just 5 days and gradually increase their differences at day 10 and 15 (20). Apart from that, the characterization of bacterial accumulation in ligatures has revealed that mice oral commensal communities go through extensive structural and composition changes, leading to microbial dysbiosis (28). Meanwhile, differential immune responses can be appreciated at subsequent time points; for instance, myeloperoxidase-producing cells, such as neutrophils, can be seen since day 3, and genes related to the critical adaptive immune response in periodontitis have expression peaks in periodontal lesions after 9 days, including markers for Th1, Th2, Th17, and Treg lymphocyte activity (32).

The ligature-induced periodontitis model has been extensively reported in mice (20, 23, 29, 32–35, 53, 54, 60); however, the extremely small mice oral cavity and the minuscule interproximal space between the maxillary or mandibular molars represent a not minor technical difficulty in placing the ligatures (73). Moreover, this placement can get even harder when dealing with immunodeficient mice when working in sterile conditions; thus, reinforcing the idea that experienced and highly skilled operators are needed. In response to this, simpler ligature models have been proposed, including the use of a 0.2-mm orthodontic ligature wire, after filing the molar interproximal surfaces with a curved C+ nickel-titanium root canal file, and the use of already tied ligature knots and 3D-printed devices (32, 74). These preformed ligatures would allow their atraumatic positioning in any molar interdental space, accumulating plaque and provoking a local immune response followed by bone resorption, in a similar way to its predecessors (32).

TRANSLATIONAL LIMITATIONS OF THE CURRENT ANIMAL MODELS FOR EXPERIMENTAL PERIODONTITIS

Even though the above-described animal models have proven to be particularly useful to study the molecular mechanisms associated with the onset, progression, and recovery from periodontitis, different challenges also arise when we try to translate these results to human contexts. Despite the similarities between mice and human immune systems, including molecular mediators and cell subpopulations that interact during both innate and adaptive immune responses (59), there are still discrepancies that must be considered. Indeed, substantial molecular differences between murine and human growth factors and cytokines influence the course of their hematopoietic and immune system development (75). Among the most relevant differences, gingival microbiota, key molecular mediators, including immunoglobulins, cytokines, chemokines, co-stimulatory molecules, Toll-like receptors, and T-cell signaling pathways should be considered when a translational projection of results obtained in animal models of periodontitis is desired (28, 75, 76). For instance, human effector $CD4^+$ T lymphocytes express human leukocyte antigen (HLA) molecules and regulate Foxp3 expression without necessarily acquiring an immunoregulatory phenotype, while mouse $Foxp3^+$ T lymphocytes are mostly defined as regulatory (75, 76); thus, displaying variations that could be important in the study of periodontitis. Furthermore, the ethical and technical constraints that severely limit *in vivo* studies of human biology, constant evolution of human-specific diseases, resistance to microbial infections, and pharmacodynamic interactions have led to increasing demand for translationally enhanced animal models. In this context, the limitations that hinder the direct replication of outcomes predicted by murine studies into human diseases support the requirement for the generation of humanized mouse models for the study of periodontitis (77).

HUMANIZED MICE MODELS

Humanized mice models, or mouse/human chimeras, have been defined as immuno-deficient mice engrafted with human primary hematopoietic cells and/or tissues capable of reconstituting a functional human immune system (HIS) (75); thus, providing an opportunity for the study of live human biological processes and affections. There are three main humanized mice models: the human peripheral blood lymphocytes (hu-PBL) model, the human stem cells (hu-HSC) model, and the human bone marrow/fetal liver/thymus (BLT) model (**Figure 1**), each with its distinctive advantages and limitations (**Table 2**).

Human Peripheral Blood Lymphocytes (hu-PBL) Model

The hu-PBL model consists of the inoculation and engraftment of human leukocytes isolated from peripheral blood, also termed peripheral blood mononuclear cells (PBMCs), *via* intravenous (i.v.), intraperitoneal (i.p.), intrafemoral (i.f.), intracardiac (i.c.), or intrahepatic (i.h.) injection. This is the easiest and most cost-efficient method of animal humanization due to the large quantities of human leukocytes that can be isolated from peripheral blood. Also, this model has fast engraftment kinetics, as human leukocytes can be found circulating in murine peripheral blood within days and up to 4 to 6 weeks (75, 76). Human T lymphocytes with an activated effector and memory phenotype are the main population present in this model, whereas B lymphocytes and myeloid cells are present but at much lower quantities, probably due to the dominant expansion of T lymphocytes and the lack of human cytokines required for their survival (76, 85, 86).

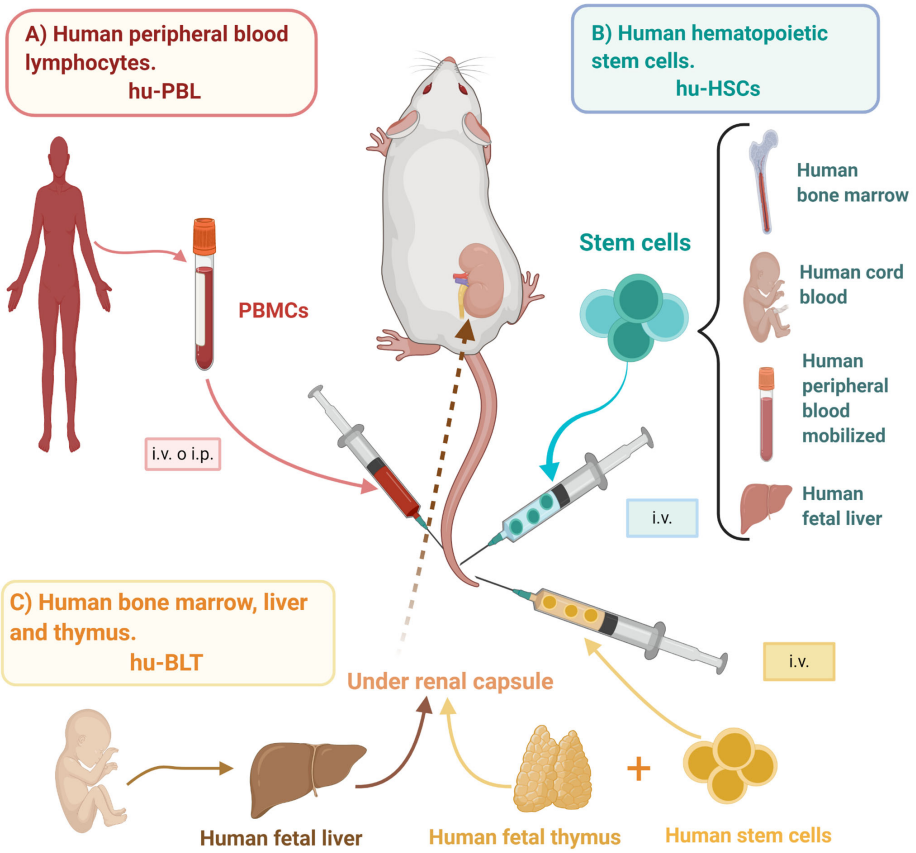

FIGURE 1 | Mice humanization strategies. Mice/human chimeras originate from immunodeficient mice engrafted with different sources of human cells or tissues able to reconstitute a human-like immune response, such as **(A)** hu-PBL: PBMCs are obtained from healthy donors and i.v. or i.p. inoculated, **(B)** hu-HSCs: HSCs may be obtained from bone marrow, umbilical cord blood, peripheral blood, or fetal liver, and i.v. inoculated into either adult or newborn mice, and **(C)** hu-BLT: Bone marrow stem cells and tissues from fetal liver and thymus are transplanted into previously irradiated mice, specifically under the renal capsule. hu-BLT, human bone marrow, liver, and thymus; hu-HSCs, human hematopoietic stem cells; hu-PBL, human peripheral blood lymphocytes; i.p., intraperitoneal; i.v., intravenous; PBMCs, peripheral blood mononuclear cells. Created with BioRender.com.

Technically, mice may be preconditioned with a sublethal dose of irradiation, which has been reported to facilitate engraftment and colonization of human PBMCs. Nonetheless, this step is not completely necessary for all mice platforms because the PBMC inoculum contains already mature human leukocytes that do not need to undergo differentiation in the mouse environment. Moreover, irradiation accelerates the occurrence of xenogeneic graft-*versus*-host-disease (GvHD), which results in reduced animal survival (87). In this context, rapid onset of GvHD is the main disadvantage of the hu-PBL model, generated by the elevated levels of activated human T lymphocytes due to MHC I and II mismatch. However, new strains of mice deficient in MHC I and/or II delay GvHD development and increase animal survival, thus widening the available experimental window (88).

Human Stem Cells (hu-HSC) Model

In the hu-HSC model, human hematopoietic stem cells (HSC) are injected and engrafted into either adult or newborn immunodeficient mice (89, 90). The $CD34^+$ HSCs may be obtained from bone marrow, cord blood, fetal liver, or mobilized human HSCs and are injected i.v. or i.f. into adult mice or i.v. (facial vein), i.c., or i.h. into newborn mice (91, 92). Additionally, for this model to achieve effective levels of HSC engraftment, myelosuppression preconditioning with sublethal irradiation is necessary to deplete mouse HSCs. However, new mouse strains with mutations in c-Kit, a stem cell factor (SCF) receptor critical for HSC engraftment, or with transgenic expression of membrane-bound human SCF allow the successful engraftment of human HSCs without previous irradiation (93, 94). After preconditioning and inoculation, a diverse repertoire of cell populations differentiates into multiple lineages of human cells and engrafts the murine tissues. Those cells include erythrocytes, platelets, T lymphocytes, natural killer (NK) cells, dendritic cells, monocytes/macrophages, and granulocytes (89, 90, 95–97). Nevertheless, this model presents some important disadvantages, such as the lack of a functional B lymphocyte compartment, in part due to inadequate $CD4^+$ T lymphocyte function and impaired antigen response. This is associated with the lack of HLA on the thymic epithelium and

TABLE 2 | The most widely used models for mice humanization.

Humanized Mice Model	Description	Requirements	Advantages and Biological Approaches		Limitations	References of its use in periodontitis studies
			Advantages	Biological Application and Plausibility		
Human peripheral blood lymphocytes (hu-PBL) model.	Inoculation and engraftment of PBMCs, via intravenous, intraperitoneal, intrafemoral, intracardiac, or intrahepatic injection.	Preconditioning with a sublethal dose of irradiation facilitates human cell engraftment (Optional).	1) The easiest and most cost-efficient method for mice humanization. 2) Abundance of human PBMCs available for mice engraftment. 3) Fast human cell engraftment kinetics. Human cells are observed in mice blood within days and up to 4 to 6 weeks after their inoculation.	1) Effector and memory T lymphocytes are the main human cell populations present in this model. Method of choice for the analysis of $CD3^+$ T lymphocytes. • T lymphocytes, particularly Th17 lymphocytes, have a vital role during oral mucosal immune surveillance and periodontitis immune response, by producing IL-17A, chemoattracting neutrophils, and promoting RANKL upregulation.	1) Short experimental window, due to rapid onset of GvHD (4 to 8 weeks). 2) GvHD is faster if preconditioning irradiation is performed. 3) Low engraftment of primary immune response cells.	(78–84)
Human stem cells (hu-HSC) model.	Inoculation and engraftment of $CD34^+$ HSCs obtained from bone marrow, cord blood, or fetal liver, via intravenous, intrafemoral, intracardiac, or intrahepatic injection.	Preconditioning with a sublethal dose of irradiation allows the depletion of mouse HSCs and facilitates human HSCs engraftment (Conditional to mouse strain).	1) Allows the humanization of adult and newborn mice. 2) Mouse strains with mutations in receptor c-Kit or transgenic expression of SCF allow the successful engraftment of human HSCs without the necessity of preconditioning irradiation.	1) Allows the engraftment of human erythrocytes, platelets, T lymphocytes, NK cells, dendritic cells, monocytes/macrophages, and granulocytes. • The granulocyte (neutrophil)/Th17 lymphocyte axis is vital during oral mucosal immune surveillance and periodontitis immune response. • Monocyte/macrophage subpopulations, including subsets M1 and M2, have a role in pro-inflammatory cytokine production and inflammation resolution/healing during periodontitis. • Dendritic cells are the major antigen-presenting cells during periodontitis. • NK cells have a role during periodontal inflammation.	1) Limited engraftment of B lymphocytes, and if it occurs, they are generally non-functional. 2) Impaired immune cell differentiation due to lack of thymic HLA.	No study.
Human bone marrow/fetal liver/thymus (BLT) model.	Surgical transplantation of human fetal liver and thymus fragments under the kidney capsule of mice, followed by an intravenous injection of human HSCs.	Preconditioning with a sublethal dose of irradiation allows the depletion of mouse HSCs and facilitates human HSCs engraftment (Necessary).	1) Development of a robust mucosal human immune system. 2) Promotes an enhanced reconstitution of secondary lymphoid organs. 3) Reconstitution of lymph nodes allows the constant repopulation of human immune cells.	1) Allows the engraftment of human T lymphocytes, B lymphocytes, monocytes, macrophages, and dendritic cells. 2) Very useful for the study of human T lymphocytes, due to the fact that these cells maturate in the transplanted autologous thymic tissues. • The development of a robust human-like mucosal immune system could be compatible to emulate an intricate network of human-like periodontal immune responses, with a constant expansion and activation of resident and infiltrating immune cells, similar to human periodontitis lesions.	1) High incidence of GvHD, that limits the time window for experimentation.	No study.

GvHD, xenogeneic graft-versus-host-disease; HLA, human leukocyte antigen; PBMCs, peripheral blood mononuclear cells; SCF, stem cell factor; NK, natural killer.

the absence of human primary lymphoid organs, and consequently, the limited differentiation of human cells inside the model.

Human Bone Marrow, Liver, and Thymus (hu-BLT) Model

The hu-BLT model consists of the surgical transplantation of human fetal liver and thymus fragments under the kidney capsule of sublethally irradiated immunocompromised mice, followed by an i.v. injection of autologous HSCs (98). This model has been described as superior to the others, as it promotes an enhanced reconstitution of secondary lymphoid organs, which contributes to HIS education and allows the systemic repopulation of multiple human immune cell lineages, including T and B lymphocytes, monocytes, macrophages, and dendritic cells. This model has been an important tool to study human T lymphocyte development, as these cells are educated in autologous thymic tissues (99, 100). Nevertheless, the hu-BLT model presents higher GvHD incidence compared with the hu-SRC model, sometimes earlier than 20 weeks after transplantation (101).

IMMUNODEFICIENT MURINE HOSTS AS PLATFORMS FOR HUMANIZATION

Besides the humanization strategy, successful engraftment largely relies on the features of the animal recipient host. In this context, the development of immunodeficient mice hosts, capable of engrafting human cells or tissues, has implied a progressive succession of genetic modifications in order to avoid xenogeneic graft rejection and enable a stable reconstitution of human cells (76, 102). In brief, one of the first groundbreaking achievements was the *Prkdc*^{scid} (protein kinase, DNA activated, catalytic polypeptide) mutation on the CB17 mouse strain, commonly named as SCID (severe combined immunodeficiency) (103). This mutation results in a reduced number of functional T and B lymphocytes, enabling transient engraftment of human PBMCs, HSCs, or fetal hematopoietic tissues (92, 104). Nevertheless, with aging, these mice generate autologous T and B lymphocytes, an event termed leakiness. Moreover, this animal host still presents high levels of NK cells and other innate immune cells that hinder proper human cell engraftment (76, 102).

Another approach implied the targeted mutation of the recombination-activating genes 1 and 2 (*Rag1* and *Rag2*), which impedes the development of functional T and B lymphocytes in mice and prevents leakiness (105, 106). However, Rag1/2-deficient mice maintain a high NK cell activity, allowing limited engraftment of HSCs (76). Afterward, NOD-SCID mice were developed by crossing NOD (for non-obese diabetic) mice with the SCID strains (107). This animal host presents additional defects in innate immunity, such as the lack of complement C5, and impaired macrophage cytokine production, antigen presentation, and NK function (76, 107, 108). Even though this approach provides enhanced human HSC and PBMC engraftments (109, 110), the model also has a limited life span due to the early development of lymphomas and innate immunity residual activity mice strain (76).

NSG, NOG, and BRG Mice

Fortunately, another immunodeficient mouse strain with a targeted mutation of the *Il2rg* gene, which encodes IL-2 receptor γ-chain (IL-2Rγ), has been developed (89, 90, 95, 111, 112) (**Figure 2**). IL-2Rγ is an essential component for IL-2, IL-4, IL-7, IL-9, IL-15, and IL-21 signaling and its absence in *Il2rg*^{null} mice leads to defective lymph nodes, deficient T and B lymphocyte development, affects innate immunity, and completely abolishes NK cell generation (113, 114). Besides, this mutation has promoted enhanced support of both human HSC and PBMC engraftments as compared with the previously described immunodeficient mice (76). After an extensive succession of mutations, the main immunodeficient mouse strains currently used are NOD-SCID *Il2rg*^{null} mice, which includes NOD.Cg-*Prkdc*^{scid}*Il2rg*^{tm1Wjl} (NSG mice), NODShi.Cg-*Prkdc*^{scid}*Il2rg*^{tm1Sug} (NOG mice), NOD-*Rag1*^{null} *Il2rg*^{null} (NRG), and BALB/c-*Rag2*^{null}*Il2rg*^{null} or *Rag2*^{tm1Flv}*Il2rg*^{tm1Flv} (BRG mice). All these mice strains are able to support human tissue and cell engraftment (86, 90, 95). The characteristics, advantages, and disadvantages of each immunodeficient mouse model derived from *Il2rg*^{null} mice have been extensively reviewed in detail by Shultz et al. (75, 76).

Altogether, these animal models comprise an important opportunity for the study of multiple biological processes and diseases, including periodontitis. Importantly, the selection of a model or another depends on the scientific question and experimental settings; thus, it is highly recommended to consider that the levels of functional HIS engraftment differs depending on the recipient mouse strain and humanization strategy used.

CURRENT CHALLENGES FOR MICE HUMANIZATION

Notwithstanding the accumulated successes achieved along with the development of new and more refined immunodeficient murine platforms, the development of a vigorous functional HIS following engraftment, necessary for transferable humanized models, has remained challenging. This is due to species specificity of MHC antigens, homing molecules that may impede appropriate trafficking of human immune cells, discrepancies between hematopoietic growth factors and cytokines, poor development of lymphoid architecture, and impaired class switching and affinity maturation of immunoglobulins (115).

In this context, mice humanization protocols that involve the transference of human cells into severely immunodeficient mice strains may initiate an alloreactive response in which T lymphocytes react against HLA disparities and minor antigens, resulting in the initiation of GvHD. This potentially life-threatening complication consists in the acute anti-host effector response of human T lymphocytes recognizing foreign murine MHC expressed by host recipient cells (88). While the rapid development of this disease enables preclinical testing of human immunosuppressive agents, the relatively short survival of engrafted animals given by GvHD could prevent the realization of long-term *in vivo* studies and the proper emulation of chronic diseases (101, 115).

In other words, as mature CD4$^+$ T lymphocytes have been educated in the human thymic stroma, they are not tolerized to the murine antigenic environment, which leads to the rapid-onset of xenogeneic GvHD. In fact, during engraftment of human cells, GvHD onset and severity vary between donors, which seem to depend on the number of CD4$^+$ T lymphocytes within the transferred human cells (116). Another important influencing factor is the mice strain, from which NSG mice provide a faster expansion of the human CD45$^+$ compartment and higher engraftment levels of CD3$^+$ T lymphocytes; however, they also have a faster rate of GvHD than, for example, BRG mice (117). Also, HSC-reconstituted mice might not be able to recognize antigens presented by HLA-DR human dendritic cells in the periphery because they are specific for murine MHC class II molecules. This negatively affects the induction of an efficient immune response, resulting in reduced Th lymphocyte activity and insufficient interactions between T and B lymphocytes, which are required for class-switch recombination (116). Thus, substantial considerations should be taken into account when selecting the ideal model to assess the immunopathogenesis and the efficacy of novel immunotherapies for periodontitis.

Despite these limitations, a significant improvement has been accomplished by the transgenic introduction of human HLA molecules into immunodeficient mice strains. For example, transgenic expression of HLA-DR4 in NRG mice has enabled the proper development of CD4$^+$ T lymphocytes and completely

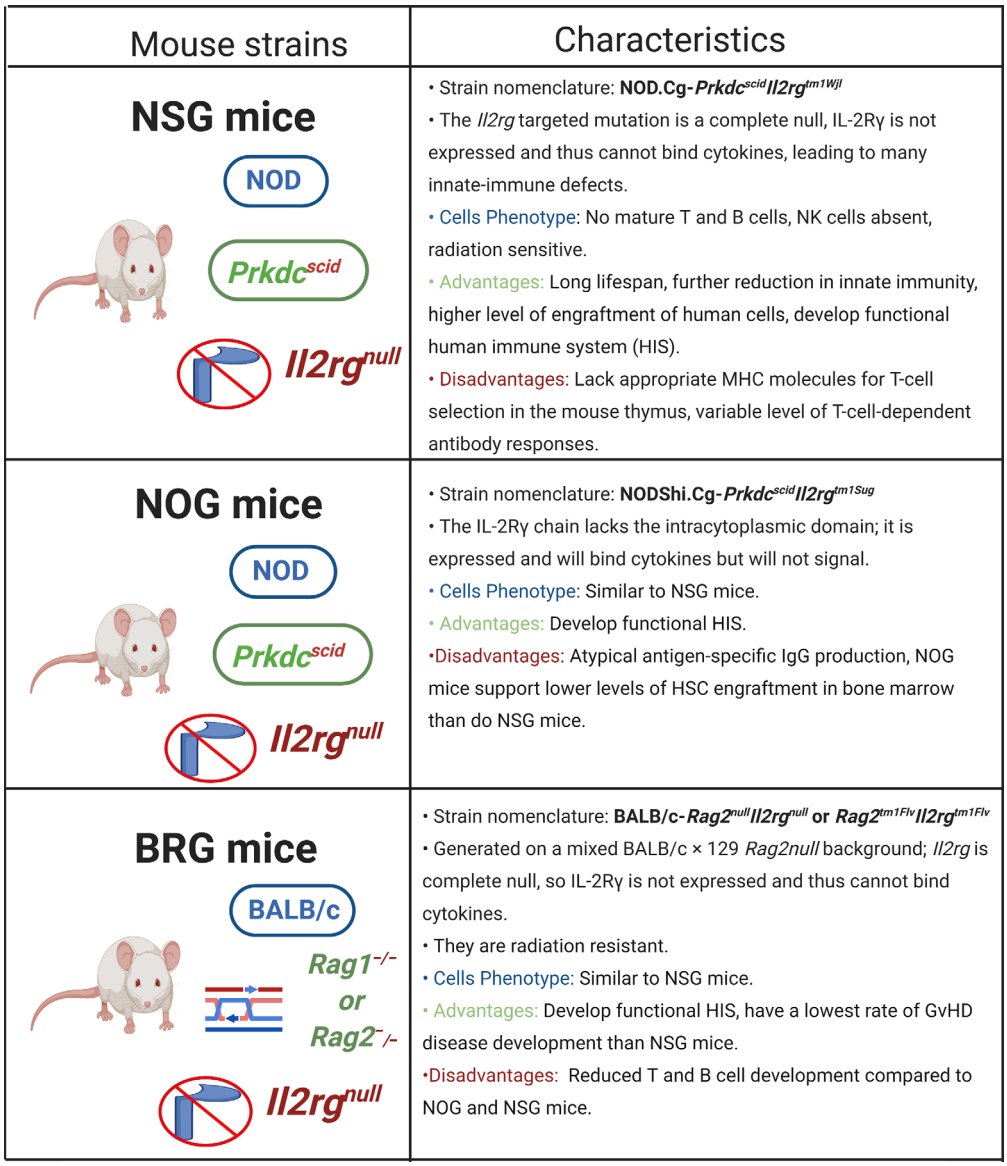

FIGURE 2 | Immunodeficient mice strains prone to humanization. Several genetic modifications have enabled that immunodeficient host mice be capable of engrafting human cells or tissues without immediate xenogeneic rejection and allow a stable reconstitution of human cells. These immunodeficient mice include NSG mice, NOG mice, and BRG mice, each one with its own advantages and disadvantages summarized in the Figure. *il2rg*, interleukin-2 receptor subunit gamma; MHC, major histocompatibility complex; NOD, non-obese diabetic. Created with BioRender.com.

functional B lymphocytes from infused HSCs of HLA-DR-matched donors (118). In addition, the complimentary removal of murine MHC class II molecules, the main target of human $CD4^+$ T lymphocyte-mediated GvHD responses, further improved the generation of human antigen-specific immune responses in immunodeficient mice reconstituted with human cells while reducing the risk of xenogeneic GvHD development (119). Therefore, the diversity of humanized model systems represents an important set of tools for modeling pathogen interactions with human cells and tissues *in vivo* (120), so the consecutive overcome of their punctual limitations enlightens their potential application for the study of immunopathologies characterized by T lymphocyte-mediated aberrant responses, such as periodontitis.

CHARACTERIZATION OF THE HUMANIZED MICE MODELS

Following the transplantation of human cells, an extensive engraftment characterization is often required. Indeed, clinical features of the recipient host, donor cell source, and engraftment technique have a great influence on the kinetics, extent, composition,

and morphological aspects of the graft reconstitution in the different organs and, consequently, its consistency. For instance, NSG mice exhibit small, poorly developed primary and secondary lymphoid organs, which lack typical lymphoid structures and are solely composed of reticular stromal cells (75, 121). Consequently, grafted human cells, which form variably sized aggregates, are not capable of recreating the typical lymphoid tissue architecture of immunocompetent organisms (75, 121, 122). Therefore, extensive immune profiling across innate and adaptive immune cell subpopulations, including human T lymphocytes ($CD3^+$, $CD4^+$, and $CD8^+$ cells), B lymphocytes ($CD19^+$ cells), macrophages ($CD68^+$ cells), and neutrophils ($CD15^+$ cells), among others, should be characterized before studying the development periodontitis or any proposed therapeutic approach (123, 124).

To analyze human cell engraftment in immunosuppressed mice, flow cytometry is a cost-effective method for the characterization of cell populations through the identification of lineage-specific markers using fluorochrome-coupled antibodies (**Figure 3A**). Indeed, flow cytometry allows the analysis of isolated cells from different tissues or organs by quantifying the percentages and the absolute number of murine and human immune cells on each sample, starting with $CD45^+$ cytometric gating strategy for immune cells subpopulations. Nowadays, flow cytometry technology has advanced to the capacity of measuring up to 50 parameters on a single cell; however, most flow cytometers are limited to 12-18 parameters per sample, and spectral overlap makes its analysis complex. Apart from that, immunohistochemistry analysis contributes with the tissue-specific spatial context to better understand engrafted human cell homing and distribution in mice tissues (**Figure 3B**), additionally helping to identify the GvHD inflammatory lesions dominated by T lymphocytes and macrophages (125–127).

Despite the important information that flow cytometry and immunohistochemistry provide for the characterization of humanized mice, new high-dimensional parameter analysis tools have been introduced to accurately describe and understand the complexity of these models (128). For instance, mass cytometry offers a single-cell analysis that couples flow cytometry with mass spectrometry and is able to evaluate up to 50 simultaneous parameters without spectral overlap using markers coupled with metal isotopes (129, 130). Another novel tool is imaging mass cytometry, which also uses metal-tagged antibodies, enhancing the imaging of up to 37 protein markers on fresh-frozen or formalin-fixed paraffin-embedded tissue sections (131). These and other complemental high throughput platforms could allow the performance of a multidimensional data analysis that could allow the identification of subtle changes in periodontal immune populations (132).

HUMANIZED MICE MODELS: CHALLENGES FOR THEIR APPLICATION AND OPPORTUNITIES FOR THE STUDY OF PERIODONTITIS

In the periodontal disease research arena, the use of humanized mice models has been increasingly gaining interest for their potential translational applicability. The first proposed model demonstrated that the engraftment of immunodeficient mice with hu-PBLs provided a conceivable animal model to study human immune responses towards periodontitis-associated antigens/pathogens (78–83).

Indeed, to characterize the human leukocyte response against the periodontopathogen *A. actinomycetemcomitans*, formerly termed *Actinobacillus actinomycetemcomitans*, a humanized animal model named *Aa*-hu-PBL-NOD/SCID was designed (83). NOD-SCID mice were reconstituted with periodontitis-affected patients-derived hu-PBLs and then orally inoculated with *A. actinomycetemcomitans*. From this experiment, relevant findings were obtained, including: i) The achievement of significant engraftment, between 30-60%, of human leukocytes (80); ii) After bacteria challenge, an increase in the number of B lymphocytes, $CD4^+$ and $CD8^+$ T lymphocytes, and monocytes/macrophages was observed in the periodontal compartment; however, without bacteria inoculation, human leukocytes were almost exclusively observed around bone marrow blood vessels in the proximity to the periodontium (80); iii) When $CD4^+$ T lymphocytes were isolated from the mice oral mucosa, they revealed significantly higher activation and proliferation levels in response to bacterial infection, with a phenotype distribution similar to that observed in T-cells isolated from the periodontitis-affected donors (79); iv) An important *A. actinomycetemcomitans*-specific IgG antibody response was achieved and maintained over a 6 to 8 week period after bacteria inoculation (78); and v) A significant increment in the RANKL expression and alveolar bone resorption, as well as decreased OPG expression, was detected in response to *A. actinomycetemcomitans* infection, as compared with the absence of bacteria inoculation (82). Interestingly, when OPG was administered as a therapeutic strategy to protect mice against periodontitis, the levels of alveolar bone resorption were significantly reduced even after bacterial infection (78).

Afterward, Zhang et al. (83) assessed the role of suppressor of cytokine signaling (SOCS) molecules in *A. actinomycetemcomitans*-induced osteoclastogenesis by using a humanized model in which NOD/SCID mice were engrafted with hu-PBLs derived from periodontitis patients or age-matched healthy subjects. They achieved engraftment of ~30% of Hu-PBLs and concluded that the RANKL-mediated dendritic cell-related osteoclastogenesis was associated with an upregulation of SOCS and downregulation of SOCS3, the dominant-negative form of SOCS (83). Moreover, by using an HLA-DR1 humanized C57BL/6 mice model of periodontitis infected with *P. gingivalis*, the development of rheumatoid arthritis and its impact on bone density and systemic cytokine production were also analyzed (133). *P. gingivalis* gingival infection promoted a transient increase in the number of Th17 lymphocytes and higher systemic cytokine activity, femoral bone density loss, and production of anti-citrullinated protein antibodies, as compared with sham-infected mice controls (133). On the other hand, when human monocyte-derived dendritic cells were reconstituted in NSG mice to induce humanization, the exposure to a fimbriae-expressing mutant strain of *P. gingivalis* led to the formation of anti-apoptotic dendritic cells, which drove dampened Th1/Th17 responses and promoted a potent indoleamine-2,3-dioxygenase-dependent Treg response (84). In this context, the

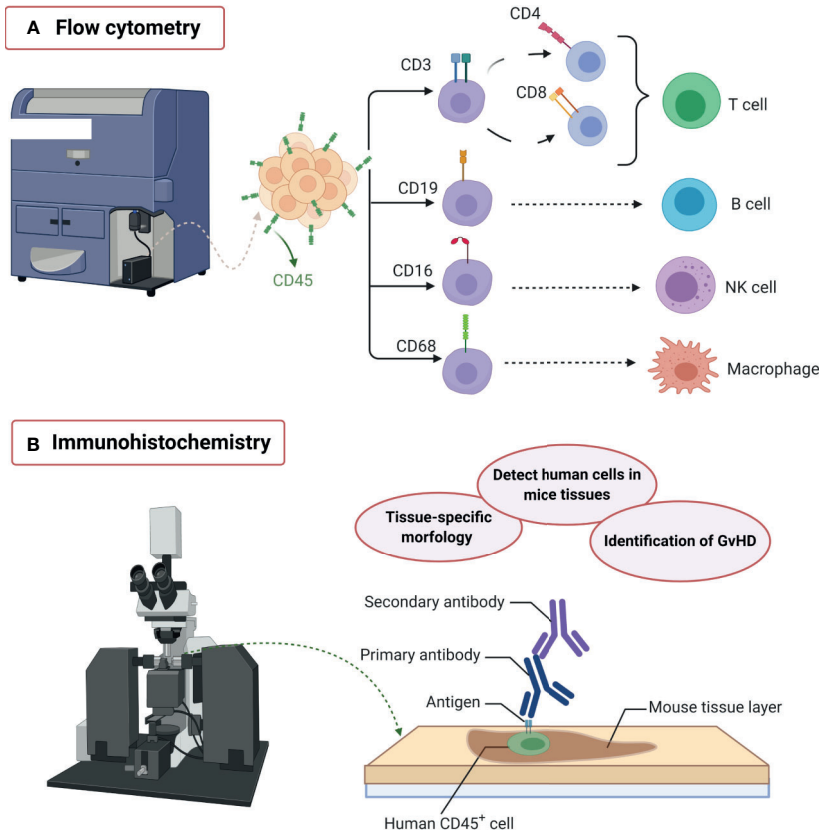

FIGURE 3 | Humanized mice model characterization. The diversity of graft sources and receptors for humanization often needs an extensive immune cell subpopulations' profiling in order to discriminate the desired human-like immune response from the graft-*versus*-host-disease (GvHD) xenogeneic immune response. For this purpose, flow cytometry and immunohistochemistry have been used. **(A)** Flow cytometry: The use of multiple fluorochrome-labeled antibodies allows the identification of different immune cell lineages at the same time. The $CD45^+$ peripheral blood mononuclear cells (PBMCs) can be further classified, for example, into $CD3^+CD4^+/CD8^+$ T cells, $CD19^+$ B cells, $CD16^+$ natural killer cells, or $CD68^+$ macrophages, which are characteristic of a human-like periodontal immune response. **(B)** Immunohistochemistry: Tissue labeling allows the spatial identification of human cells in mice tissues, the visualization of their interaction with periodontal tissue-specific morphology, and the identification of GvHD lesions. Created with BioRender.com.

use of the humanized mice model accompanied by the *in vivo* tracking of pathogen-loaded dendritic cells contributed to validate the *P. gingivalis*-induced immunomodulation of dendritic cells and the intracellular bacteria persistence in distant organs. Particularly, *P. gingivalis*-primed dendritic cells promoted Treg activity to evade effector immune responses, by preventing the apoptosis of carrier dendritic cells and thus, favoring its systemic dissemination and survival (84).

Despite the huge progress achieved on revealing the pathogenesis of periodontitis using rodent models, the precise roles of human immune cells and molecular mediators have not been fully elucidated yet. Wild-type animal models have been extensively used to study the nature of immune response against periodontopathogens; nevertheless, oral mucosa colonizers in mice are not the same microorganisms found in human periodontal tissues (28, 134). In this context, human periodontopathogens inoculated in wild-type rodents or the induction of bacterial dysbiosis by the ligature placement around mice molars may not exactly reflect the host-microbiota interactions described in humans; thus, making the extrapolation of the findings to the human framework difficult and limited. Taking these antecedents into account, humanized mice models could provide robust physiological systems available to be exploited in the periodontal arena.

Indeed, the intricate inflammatory nature of periodontitis opens the possibility to propose the use of humanized mice models to specifically address scientific questions that might not be fully explained with conventional mice models. For instance, the first stages of the inflammatory response against periodontopathogens are enriched in mediators belonging to the innate arm of the immune response, which could be evaluated using the hu-HSCs model, as it allows the engraftment of hematopoietic precursors and further differentiation of a vast repertoire of immune cell populations (89, 90, 95–97). Nevertheless, if antigen presentation or dendritic cells are a matter of interest, this model may be inadequate as it lacks the HLA expression necessary for cell differentiation. Conversely, hu-PBLs mice models comprise a graft in which an important percentage of immune cells have already gone through a differentiation process (75, 76). Particularly, $CD4^+$ T lymphocytes, the main cell population that settles into host tissues

with this strategy, have an activated effector or memory phenotype, which means that they do not need to undergo cell differentiation into the mouse environment. In the case of periodontitis, $CD4^+$ T lymphocytes have been identified as key cells that mediate the alveolar bone resorption (16–18); therefore, the hu-PBLs mice model would be useful to analyze committed immune-phenotype cells, not so for primary immune responses. In all these models, it is noteworthy that xenogeneic mismatch should be considered. Although it has been described from the first assays that an antigen-specific human immune response (both humoral and cell-mediated) can be achieved in SCID or NOD/SCID systems even in the presence of ongoing GvHD (135–137), the non-specific activation of human immune cells, detected, for example, as an IL-2 background production, could also occur (80). For this, MHC knockout and/or HLA transgenic mice platforms could represent a great opportunity to prevent or diminish any confounding factors given by GvHD development.

On the basis of the studies mentioned above, the use of humanized mice models for the study of the virulence of periodontal bacteria and the immunopathogenesis of periodontitis has proven to be feasible and particularly relevant (**Figure 4**). To ensure the success of this experimental strategy, it is highly recommended to adequately select both the murine platform and the humanization strategy, taking into account their advantages and limitations in the context of the study aims. In addition, a detailed characterization of the graft is necessary prior to any other experimental intervention, in order to ensure the standardization of humanization kinetics, adequate experimental work window, and reproducibility of the immunological findings developed in the host animal (115). Regarding therapeutic approaches, humanized animal models are an emerging topic in the field of periodontal research, so their development could be an important step in the search for innovative immunotherapeutic strategies applicable to periodontitis-affected patients.

CONCLUDING REMARKS

The enhanced translational application and diversity of humanized mice models could innovate the way we study periodontal immune responses and consequently, prompt the designing of novel immunotherapeutics. However, there is an evolving need to overcome the complications related to the xenogeneic transfer of cells to immunodeficient hosts, which could compromise the study of this chronic disease and drug dynamics. Therefore, the proper characterization of the periodontitis humanized mice model should entail a high throughput analysis of the grafted human immune cells that

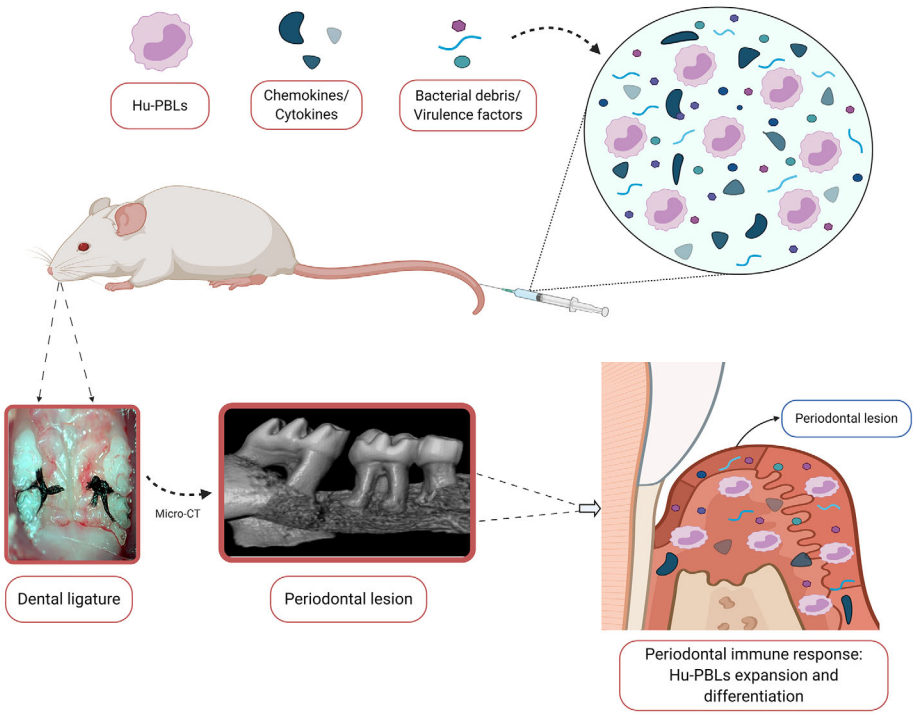

FIGURE 4 | Proposal for a humanized mouse model for the study of periodontitis. The placement of bilateral silk ligatures around the second maxillary molars of hu-PBL-NSG mice provokes local bacteria accumulation, periodontal microbiota dysbiosis, and bacteremia. Consequently, this bacterial insult results in systemic dissemination of antigens, bacterial debris, virulence factors, cytokines, and chemokines. In turn, they are capable of being recognized by the engrafted human peripheral blood mononuclear cells (PBMCs), which ultimately leads to the orchestration of a human-like immune response within the periodontal tissues and lymph nodes that drain them. The resulting local expansion and differentiation of the human PBMCs would lead to the formation of a periodontal lesion, characterized by the presence of a dense inflammatory infiltrate and alveolar bone resorption. Hu-PBLs, human peripheral blood lymphocytes. Created with BioRender.com.

repopulate the mice periodontium, potential antigen-presenting sites, and the remaining local and distal lymphoid organs. In this way, they could ensure staged profiling of the periodontitis-like immune response and avoid to the minimum its confusion with the GvHD-provoked immune response.

AUTHOR CONTRIBUTIONS

CR, EAC, and RV conceived the review. CR, EAC, and AP were involved in drafting the manuscript. MG designed and prepared the figures. LG-O, AS-C, and SM-R critically evaluated and supplemented the manuscript. EAC and RV revised and prepared the manuscript for submission. All authors contributed to the article and approved the submitted version.

FUNDING

This study was financially supported by grant FONDECYT 1181780 (RV) from the Agencia Nacional de Investigación y Desarrollo (ANID), Chile. EAC, AS-C, and SM-R were the recipients of Ph.D. scholarships from the Faculty of Dentistry, Universidad de Chile, Chile. CR and LG-O were the recipients of Ph.D. scholarships Fondecyt 21180841 and 21190087, respectively, from ANID.

REFERENCES

1. Moutsopoulos NM, Konkel JE. Tissue-Specific Immunity at the Oral Mucosal Barrier. *Trends Immunol* (2018) 39(4):276–87. doi: 10.1016/j.it.2017.08.005
2. Moutsopoulos NM, Konkel JE. Healthy Mouth, Healthy Gut: A Dysbiotic Oral Microbiome Exacerbates Colitis. *Mucosal Immunol* (2020) 13(6):852–4. doi: 10.1038/s41385-020-00341-y
3. Acar B, Çağdaş D, Tan C, Özbek B, Yaz I, Yildirim YD, et al. Evaluation of Periodontal Status and Cytokine/Chemokine Profile of GCF in Patients With Severe Congenital Neutropenia. *Odontology* (2021) 109(2):474–82. doi: 10.1007/s10266-020-00565-1
4. Seidel CL, Gerlach RG, Wiedemann P, Weider M, Rodrian G, Hader M, et al. Defining Metaniches in the Oral Cavity According to Their Microbial Composition and Cytokine Profile. *Int J Mol Sci* (2020) 21(21):8218. doi: 10.3390/ijms21218218
5. Dashper SG, Mitchell HL, Seers CA, Gladman SL, Seemann T, Bulach DM, et al. *Porphyromonas Gingivalis* Uses Specific Domain Rearrangements and Allelic Exchange to Generate Diversity in Surface Virulence Factors. *Front Microbiol* (2017) 8:48. doi: 10.3389/fmicb.2017.00048
6. Monasterio G, Fernández B, Castillo F, Rojas C, Cafferata EA, Rojas L, et al. Capsular-Defective *Porphyromonas Gingivalis* Mutant Strains Induce Less Alveolar Bone Resorption Than W50 Wild-Type Strain Due to a Decreased Th1/Th17 Immune Response and Less Osteoclast Activity. *J Periodontol* (2019) 90(5):522–34. doi: 10.1002/JPER.18-0079
7. Boyer E, Leroyer P, Malherbe L, Fong SB, Loreal O, Bonnaure Mallet M, et al. Oral Dysbiosis Induced by *Porphyromonas Gingivalis* Is Strain-Dependent in Mice. *J Oral Microbiol* (2020) 12(1):1832837. doi: 10.1080/20002297.2020.1832837
8. Vernal R, Diaz-Guerra E, Silva A, Sanz M, Garcia-Sanz JA. Distinct Human T-Lymphocyte Responses Triggered by *Porphyromonas Gingivalis* Capsular Serotypes. *J Clin Periodontol* (2014) 41(1):19–30. doi: 10.1111/jcpe.12176
9. Vernal R, Díaz-Zúñiga J, Melgar-Rodríguez S, Pujol M, Díaz-Guerra E, Silva A, et al. Activation of RANKL-Induced Osteoclasts and Memory T Lymphocytes by *Porphyromonas Gingivalis* Is Serotype Dependant. *J Clin Periodontol* (2014) 41(5):451–9. doi: 10.1111/jcpe.12236
10. Díaz-Zúñiga J, Melgar-Rodríguez S, Alvarez C, Monasterio G, Benítez A, Ciuchi P, et al. T-Lymphocyte Phenotype and Function Triggered by *Aggregatibacter Actinomycetemcomitans* Is Serotype-Dependent. *J Periodontal Res* (2015) 50(6):824–35. doi: 10.1111/jre.12270
11. Fine DH, Karched M, Furgang D, Sampathkumar V, Velusamy S, Godboley D. Colonization and Persistence of Labeled and "Foreign" Strains of *Aggregatibacter Actinomycetemcomitans* Inoculated Into the Mouths of Rhesus Monkeys. *J Oral Biol* (2015) 2(1):10.13188/2377-987X.1000005. doi: 10.13188/2377-987X.1000005
12. Melgar-Rodríguez S, Díaz-Zúñiga J, Alvarez C, Rojas L, Monasterio G, Carvajal P, et al. Serotype B of *Aggregatibacter Actinomycetemcomitans* Increases Osteoclast and Memory T-Lymphocyte Activation. *Mol Oral Microbiol* (2015) 31(2):162–74. doi: 10.1111/omi.12112
13. Polak D, Shapira L, Weiss EI, Houri-Haddad Y. The Role of Coaggregation Between *Porphyromonas Gingivalis* and *Fusobacterium Nucleatum* on the Host Response to Mixed Infection. *J Clin Periodontol* (2012) 39(7):617–25. doi: 10.1111/j.1600-051X.2012.01889.x
14. Ebbers M, Lübcke PM, Volzke J, Kriebel K, Hieke C, Engelmann R, et al. Interplay Between *P. Gingivalis*, *F. Nucleatum* and *A. Actinomycetemcomitans* in Murine Alveolar Bone Loss, Arthritis Onset and Progression. *Sci Rep* (2018) 8(1):15129. doi: 10.1038/s41598-018-33129-z
15. Dutzan N, Abusleme L, Bridgeman H, Greenwell-Wild T, Zangerle-Murray T, Fife ME, et al. On-Going Mechanical Damage From Mastication Drives Homeostatic Th17 Cell Responses at the Oral Barrier. *Immunity* (2017) 46(1):133–47. doi: 10.1016/j.immuni.2016.12.010
16. Dutzan N, Abusleme L. T Helper 17 Cells as Pathogenic Drivers of Periodontitis. *Adv Exp Med Biol* (2019) 1197:107–17. doi: 10.1007/978-3-030-28524-1_9
17. Alvarez C, Monasterio G, Cavalla F, Córdova LA, Hernández M, Heymann D, et al. Osteoimmunology of Oral and Maxillofacial Diseases: Translational Applications Based on Biological Mechanisms. *Front Immunol* (2019) 10:1664. doi: 10.3389/fimmu.2019.01664
18. Monasterio G, Castillo F, Ibarra JP, Guevara J, Rojas L, Alvarez C, et al. Alveolar Bone Resorption and Th1/Th17-Associated Immune Response Triggered During *Aggregatibacter Actinomycetemcomitans*-Induced Experimental Periodontitis Are Serotype-Dependent. *J Periodontol* (2018) 89(10):1249–61. doi: 10.1002/JPER.17-0563
19. Alvarez C, Rojas C, Rojas L, Cafferata EA, Monasterio G, Vernal R. Regulatory T Lymphocytes in Periodontitis: A Translational View. *Mediators Inflamm* (2018) 2018:7806912. doi: 10.1155/2018/7806912
20. Alvarez C, Suliman S, Almarhoumi R, Vega ME, Rojas C, Monasterio G, et al. Regulatory T Cell Phenotype and Anti-Osteoclastogenic Function in Experimental Periodontitis. *Sci Rep* (2020) 10(1):19018. doi: 10.1038/s41598-020-76038-w
21. Cafferata EA, Jerez A, Vernal R, Monasterio G, Pandis N, Faggion CMJr. The Therapeutic Potential of Regulatory T Lymphocytes in Periodontitis: A Systematic Review. *J Periodontal Res* (2019) 54(3):207–17. doi: 10.1111/jre.12629
22. Barbi J, Pardoll D, Pan F. Treg Functional Stability and Its Responsiveness to the Microenvironment. *Immunol Rev* (2014) 259(1):115–39. doi: 10.1111/imr.12172
23. Cafferata EA, Terraza-Aguirre C, Barrera R, Faúndez N, González N, Rojas C, et al. Interleukin-35 Inhibits Alveolar Bone Resorption by Modulating the Th17/Treg Imbalance During Periodontitis. *J Clin Periodontol* (2020) 47(6):676–88. doi: 10.1111/jcpe.13282
24. Nakajima T, Ueki-Maruyama K, Oda T, Ohsawa Y, Ito H, Seymour GJ, et al. Regulatory T-Cells Infiltrate Periodontal Disease Tissues. *J Dent Res* (2005) 84(7):639–43. doi: 10.1177/154405910508400711
25. Garlet GP, Cardoso CR, Mariano FS, Claudino M, de Assis GF, Campanelli AP, et al. Regulatory T Cells Attenuate Experimental Periodontitis Progression in Mice. *J Clin Periodontol* (2010) 37(7):591–600. doi: 10.1111/j.1600-051X.2010.01586.x

26. Dutzan N, Gamonal J, Silva A, Sanz M, Vernal R. Over-Expression of Forkhead Box P3 and Its Association With Receptor Activator of Nuclear Factor-Kappa B Ligand, Interleukin (IL)-17, IL-10 and Transforming Growth Factor-Beta During the Progression of Chronic Periodontitis. *J Clin Periodontol* (2009) 36(5):396–403. doi: 10.1111/j.1600-051X.2009.01390.x
27. Tsukasaki M, Komatsu N, Nagashima K, Nitta T, Pluemsakunthai W, Shukunami C, et al. Host Defense Against Oral Microbiota by Bone-Damaging T Cells. *Nat Commun* (2018) 9(1):701. doi: 10.1038/s41467-018-03147-6
28. Dutzan N, Kajikawa T, Abusleme L, Greenwell-Wild T, Zuazo CE, Ikeuchi T, et al. Dysbiotic Microbiome Triggers T_H17 Cells to Mediate Oral Mucosal Immunopathology in Mice and Humans. *Sci Transl Med* (2018) 10(463):eaat0797. doi: 10.1126/scitranslmed.aat0797
29. Cafferata EA, Castro-Saavedra S, Fuentes-Barros G, Melgar-Rodríguez S, Rivera F, Carvajal P, et al. Boldine Inhibits the Alveolar Bone Resorption During Ligature-Induced Periodontitis by Modulating the Th17/Treg Imbalance. *J Periodontol* (2021) 92(1):123–36. doi: 10.1002/JPER.20-0055
30. Kikuta J, Wada Y, Kowada T, Wang Z, Sun-Wada GH, Nishiyama I, et al. Dynamic Visualization of RANKL and Th17-Mediated Osteoclast Function. *J Clin Invest* (2013) 123(2):866–73. doi: 10.1172/JCI65054
31. Bi CS, Wang J, Qu HL, Li X, Tian BM, Ge S, et al. Calcitriol Suppresses Lipopolysaccharide-Induced Alveolar Bone Damage in Rats by Regulating T Helper Cell Subset Polarization. *J Periodontal Res* (2019) 54(6):612–23. doi: 10.1111/jre.12661
32. Marchesan J, Girnary MS, Jing L, Miao MZ, Zhang S, Sun L, et al. An Experimental Murine Model to Study Periodontitis. *Nat Protoc* (2018) 13(10):2247–67. doi: 10.1038/s41596-018-0035-4
33. Saadi-Thiers K, Huck O, Simonis P, Tilly P, Fabre JE, Tenenbaum H, et al. Periodontal and Systemic Responses in Various Mice Models of Experimental Periodontitis: Respective Roles of Inflammation Duration and *Porphyromonas Gingivalis* Infection. *J Periodontol* (2013) 84(3):396–406. doi: 10.1902/jop.2012.110540
34. de Molon RS, Mascarenhas VI, de Avila ED, Finoti LS, Toffoli GB, Spolidorio DM, et al. Long-Term Evaluation of Oral Gavage With Periodontopathogens or Ligature Induction of Experimental Periodontal Disease in Mice. *Clin Oral Investig* (2016) 20(6):1203–16. doi: 10.1007/s00784-015-1607-0
35. de Molon RS, de Avila ED, Boas Nogueira AV, Chaves de Souza JA, Avila-Campos MJ, de Andrade CR, et al. Evaluation of the Host Response in Various Models of Induced Periodontal Disease in Mice. *J Periodontol* (2014) 85(3):465–77. doi: 10.1902/jop.2013.130225
36. Garlet GP, Cardoso CR, Silva TA, Ferreira BR, Avila-Campos MJ, Cunha FQ, et al. Cytokine Pattern Determines the Progression of Experimental Periodontal Disease Induced by *Actinobacillus Actinomycetemcomitans* Through the Modulation of MMPs, RANKL, and Their Physiological Inhibitors. *Oral Microbiol Immunol* (2006) 21(1):12–20. doi: 10.1111/j.1399-302X.2005.00245.x
37. Garlet GP, Cardoso CR, Campanelli AP, Garlet TP, Avila-Campos MJ, Cunha FQ, et al. The Essential Role of IFN-γ in the Control of Lethal *Aggregatibacter Actinomycetemcomitans* Infection in Mice. *Microbes Infect* (2008) 10(5):489–96. doi: 10.1016/j.micinf.2008.01.010
38. Palioto DB, Finoti LS, Kinane DF, Benakanakere M. Epigenetic and Inflammatory Events in Experimental Periodontitis Following Systemic Microbial Challenge. *J Clin Periodontol* (2019) 46(8):819–29. doi: 10.1111/jcpe.13151
39. Hamamoto Y, Ouhara K, Munenaga S, Shoji M, Ozawa T, Hisatsune J, et al. Effect of *Porphyromonas Gingivalis* Infection on Gut Dysbiosis and Resultant Arthritis Exacerbation in Mouse Model. *Arthritis Res Ther* (2020) 22(1):249. doi: 10.1186/s13075-020-02348-z
40. Monasterio G, Budini V, Fernández B, Castillo F, Rojas C, Alvarez C, et al. IL-22-Expressing $CD4^+Ahr^+$ T Lymphocytes Are Associated With RANKL-Mediated Alveolar Bone Resorption During Experimental Periodontitis. *J Periodontal Res* (2019) 54(5):513–24. doi: 10.1111/jre.12654
41. Monasterio G, Castillo F, Astorga J, Hoare A, Terraza-Aguirre C, Cafferata EA, et al. O-Polysaccharide Plays a Major Role on the Virulence and Immunostimulatory Potential of *Aggregatibacter Actinomycetemcomitans* During Periodontal Infection. *Front Immunol* (2020) 11:591240. doi: 10.3389/fimmu.2020.591240
42. Garlet GP, Avila-Campos MJ, Milanezi CM, Ferreira BR, Silva JS. *Actinobacillus Actinomycetemcomitans*-Induced Periodontal Disease in Mice: Patterns of Cytokine, Chemokine, and Chemokine Receptor Expression and Leukocyte Migration. *Microbes Infect* (2005) 7(4):738–47. doi: 10.1016/j.micinf.2005.01.012
43. Hao L, Chen J, Zhu Z, Reddy MS, Mountz JD, Chen W, et al. Odanacatib, A Cathepsin K-Specific Inhibitor, Inhibits Inflammation and Bone Loss Caused by Periodontal Diseases. *J Periodontol* (2015) 86(8):972–83. doi: 10.1902/jop.2015.140643
44. Wei W, Ren J, Yin W, Ding H, Lu Q, Tan L, et al. Inhibition of Ctsk Modulates Periodontitis With Arthritis *Via* Downregulation of TLR9 and Autophagy. *Cell Prolif* (2020) 53(1):e12722. doi: 10.1111/cpr.12722
45. Pan W, Yin W, Yang L, Xue L, Ren J, Wei W, et al. Inhibition of Ctsk Alleviates Periodontitis and Comorbid Rheumatoid Arthritis Via Downregulation of the TLR9 Signalling Pathway. *J Clin Periodontol* (2019) 46(3):286–96. doi: 10.1111/jcpe.13060
46. Wang X, Tong Y, Zhang J, Khan N, Zhang K, Bai H, et al. Neuroinflammation Changes With Periodontal Inflammation Status During Periodontitis in Wild-Type Mice. *Oral Dis* (2021) 27(4):1001–11. doi: 10.1111/odi.13618
47. Scanu A, Giraudo C, Galuppini F, Lazzarin V, Pennelli G, Sivolella S, et al. Periodontal Injection of Lipopolysaccharide Promotes Arthritis Development in Mice. *Inflammation* (2019) 42(3):1117–28. doi: 10.1007/s10753-019-00975-6
48. Chi L, Cheng X, He X, Sun J, Liang F, Pei Z, et al. Increased Cortical Infarction and Neuroinflammation in Ischemic Stroke Mice With Experimental Periodontitis. *Neuroreport* (2019) 30(6):428–33. doi: 10.1097/WNR.0000000000001220
49. Souza JAC, Magalhães FAC, Oliveira G, RS DEM, Zuanon JA, Souza PPC. Pam2CSK4 (TLR2 Agonist) Induces Periodontal Destruction in Mice. *Braz Oral Res* (2020) 34:e012. doi: 10.1590/1807-3107bor-2020.vol34.0012
50. Zhang J, Yu C, Zhang X, Chen H, Dong J, Lu W, et al. *Porphyromonas Gingivalis* Lipopolysaccharide Induces Cognitive Dysfunction, Mediated by Neuronal Inflammation *Via* Activation of the TLR4 Signaling Pathway in C57BL/6 Mice. *J Neuroinflamm* (2018) 15(1):37. doi: 10.1186/s12974-017-1052-x
51. Oz HS, Chen T, Ebersole JL. A Model for Chronic Mucosal Inflammation in IBD and Periodontitis. *Dig Dis Sci* (2010) 55(8):2194–202. doi: 10.1007/s10620-009-1031-x
52. Oz HS, Ebersole JL. A Novel Murine Model for Chronic Inflammatory Alveolar Bone Loss. *J Periodontal Res* (2010) 45(1):94–9. doi: 10.1111/j.1600-0765.2009.01207.x
53. Abe T, Hajishengallis G. Optimization of the Ligature-Induced Periodontitis Model in Mice. *J Immunol Methods* (2013) 394(1-2):49–54. doi: 10.1016/j.jim.2013.05.002
54. Alvarez C, Abdalla H, Suliman S, Rojas P, Wu Y-C, Almarhoumi R, et al. RvE1 Impacts the Gingival Inflammatory Infiltrate by the T Cell Response in Experimental Periodontitis. *Front Immunol* (2021) 12:664756. doi: 10.3389/fimmu.2021.664756
55. Huck O, Mulhall H, Rubin G, Kizelnik Z, Iyer R, Perpich JD, et al. *Akkermansia Muciniphila* Reduces *Porphyromonas Gingivalis*-Induced Inflammation and Periodontal Bone Destruction. *J Clin Periodontol* (2020) 47(2):202–12. doi: 10.1111/jcpe.13214
56. Batool F, Stutz C, Petit C, Benkirane-Jessel N, Delpy E, Zal F, et al. A Therapeutic Oxygen Carrier Isolated From *Arenicola Marina* Decreased *P. Gingivalis* Induced Inflammation and Tissue Destruction. *Sci Rep* (2020) 10(1):14745. doi: 10.1038/s41598-020-71593-8
57. Huck O, Al-Hashemi J, Poidevin L, Poch O, Davideau JL, Tenenbaum H, et al. Identification and Characterization of microRNA Differentially Expressed in Macrophages Exposed to *Porphyromonas Gingivalis* Infection. *Infect Immun* (2017) 85(3):e00771–16. doi: 10.1128/IAI.00771-16
58. Ishihara Y, Anan H, Yoneda M, Maeda K, Hirofuji T. Susceptibility of Type 2 Diabetic Mice to Low-Virulence Bacterial Infection: Induction of Abscess Formation by Gingipain-Deficient *Porphyromonas Gingivalis*. *J Periodontal Res* (2007) 42(3):253–8. doi: 10.1111/j.1600-0765.2006.00941.x

59. Rydell-Törmänen K, Johnson JR. The Applicability of Mouse Models to the Study of Human Disease. *Methods Mol Biol* (2019) 1940:3–22. doi: 10.1007/978-1-4939-9086-3_1
60. Graves DT, Kang J, Andriankaja O, Wada K, Rossa CJr. Animal Models to Study Host-Bacteria Interactions Involved in Periodontitis. *Front Oral Biol* (2012) 15:117–32. doi: 10.1159/000329675
61. de Molon RS, de Avila ED, Cirelli JA. Host Responses Induced by Different Animal Models of Periodontal Disease: A Literature Review. *J Investig Clin Dent* (2013) 4(4):211–8. doi: 10.1111/jicd.12018
62. Wiebe CB, Adkins CA, Putnins EE, Hakkinen L, Larjava HS. Naturally Occurring Periodontal Bone Loss in the Wild Deer Mouse, Genus. *Peromyscus J Periodontol* (2001) 72(5):620–5. doi: 10.1902/jop.2001.72.5.620
63. Polak D, Wilensky A, Shapira L, Halabi A, Goldstein D, Weiss EI, et al. Mouse Model of Experimental Periodontitis Induced by *Porphyromonas Gingivalis/Fusobacterium Nucleatum* Infection: Bone Loss and Host Response. *J Clin Periodontol* (2009) 36(5):406–10. doi: 10.1111/j.1600-051X.2009.01393.x
64. Glowacki AJ, Yoshizawa S, Jhunjhunwala S, Vieira AE, Garlet GP, Sfeir C, et al. Prevention of Inflammation-Mediated Bone Loss in Murine and Canine Periodontal Disease Via Recruitment of Regulatory Lymphocytes. *Proc Natl Acad Sci USA* (2013) 110(46):18525–30. doi: 10.1073/pnas.1302829110
65. Barros SP, Arce RM, Galloway P, Lawter R, Offenbacher S. Therapeutic Effect of a Topical CCR2 Antagonist on Induced Alveolar Bone Loss in Mice. *J Periodontal Res* (2011) 46(2):246–51. doi: 10.1111/j.1600-0765.2010.01340.x
66. Nahid MA, Rivera M, Lucas A, Chan EK, Kesavalu L. Polymicrobial Infection With Periodontal Pathogens Specifically Enhances microRNA miR-146a in ApoE$^{-/-}$ Mice During Experimental Periodontal Disease. *Infect Immun* (2011) 79(4):1597–605. doi: 10.1128/IAI.01062-10
67. Lalla E, Lamster IB, Hofmann MA, Bucciarelli L, Jerud AP, Tucker S, et al. Oral Infection With a Periodontal Pathogen Accelerates Early Atherosclerosis in Apolipoprotein E-null Mice. *Arterioscler Thromb Vasc Biol* (2003) 23(8):1405–11. doi: 10.1161/01.ATV.0000082462.26258.FE
68. Garcia de Aquino S, Manzolli Leite FR, Stach-Machado DR, Francisco da Silva JA, Spolidorio LC, Rossa CJr. Signaling Pathways Associated With the Expression of Inflammatory Mediators Activated During the Course of Two Models of Experimental Periodontitis. *Life Sci* (2009) 84(21-22):745–54. doi: 10.1016/j.lfs.2009.03.001
69. Nakamura H, Fukusaki Y, Yoshimura A, Shiraishi C, Kishimoto M, Kaneko T, et al. Lack of Toll-Like Receptor 4 Decreases Lipopolysaccharide-Induced Bone Resorption in C3H/HeJ Mice *In Vivo*. *Oral Microbiol Immunol* (2008) 23(3):190–5. doi: 10.1111/j.1399-302X.2007.00410.x
70. de Molon RS, Park CH, Jin Q, Sugai J, Cirelli JA. Characterization of Ligature-Induced Experimental Periodontitis. *Microsc Res Tech* (2018) 81 (12):1412–21. doi: 10.1002/jemt.23101
71. Graves DT, Fine D, Teng YT, Van Dyke TE, Hajishengallis G. The Use of Rodent Models to Investigate Host-Bacteria Interactions Related to Periodontal Diseases. *J Clin Periodontol* (2008) 35(2):89–105. doi: 10.1111/j.1600-051X.2007.01172.x
72. Hajishengallis G. Periodontitis: From Microbial Immune Subversion to Systemic Inflammation. *Nat Rev Immunol* (2015) 15(1):30–44. doi: 10.1038/nri3785
73. Häärä O, Harjunmaa E, Lindfors PH, Huh SH, Fliniaux I, Äberg T, et al. Ectodysplasin Regulates Activator-Inhibitor Balance in Murine Tooth Development Through Fgf20 Signaling. *Development* (2012) 139 (17):3189–99. doi: 10.1242/dev.079558
74. Li D, Feng Y, Tang H, Huang L, Tong Z, Hu C, et al. A Simplified and Effective Method for Generation of Experimental Murine Periodontitis Model. *Front Bioeng Biotechnol* (2020) 8:444. doi: 10.3389/fbioe.2020.00444
75. Shultz LD, Brehm MA, Garcia-Martinez JV, Greiner DL. Humanized Mice for Immune System Investigation: Progress, Promise and Challenges. *Nat Rev Immunol* (2012) 12(11):786–98. doi: 10.1038/nri3311
76. Shultz LD, Ishikawa F, Greiner DL. Humanized Mice in Translational Biomedical Research. *Nat Rev Immunol* (2007) 7(2):118–30. doi: 10.1038/nri2017
77. Walsh NC, Kenney LL, Jangalwe S, Aryee KE, Greiner DL, Brehm MA, et al. Humanized Mouse Models of Clinical Disease. *Annu Rev Pathol* (2017) 12:187–215. doi: 10.1146/annurev-pathol-052016-100332
78. Teng YT, Nguyen H, Gao X, Kong YY, Gorczynski RM, Singh B, et al. Functional Human T-Cell Immunity and Osteoprotegerin Ligand Control Alveolar Bone Destruction in Periodontal Infection. *J Clin Invest* (2000) 106 (6):59–67. doi: 10.1172/jci10763
79. Gao X, Teng YT. T-Cell-Receptor Gene Usage of *Actinobacillus Actinomycetemcomitans*-Reactive Periodontal CD4$^+$ T Cells From Localized Juvenile Periodontitis Patients and Human Peripheral Blood Leukocyte-Reconstituted NOD/SCID Mice. *J Periodontal Res* (2002) 37 (5):399–404. doi: 10.1034/j.1600-0765.2002.01006.x
80. Teng YT, Nguyen H, Hassanloo A, Ellen RP, Hozumi N, Gorczynski RM. Periodontal Immune Responses of Human Lymphocytes in *Actinobacillus Actinomycetemcomitans*-Inoculated NOD/SCID Mice Engrafted With Peripheral Blood Leukocytes of Periodontitis Patients. *J Periodontal Res* (1999) 34(1):54–61. doi: 10.1111/j.1600-0765.1999.tb02222.x
81. Shenker BJ, Wannberg S, Vitale L, Kieba I, Lally ET. Reconstruction of Severe Combined Immunodeficient Mice With Lymphocytes From Patients With Localized Juvenile Periodontitis. *J Periodontal Res* (1993) 28(6 Pt 2):487–90. doi: 10.1111/j.1600-0765.1993.tb02109.x
82. Teng YT. Mixed Periodontal Th1-Th2 Cytokine Profile in *Actinobacillus Actinomycetemcomitans*-Specific Osteoprotegerin Ligand (or RANK-L)-Mediated Alveolar Bone Destruction *In Vivo*. *Infect Immun* (2002) 70 (9):5269–73. doi: 10.1128/iai.70.9.5269-5273.2002
83. Zhang X, Alnaeeli M, Singh B, Teng YT. Involvement of SOCS3 in Regulation of CD11c$^+$ Dendritic Cell-Derived Osteoclastogenesis and Severe Alveolar Bone Loss. *Infect Immun* (2009) 77(5):2000–9. doi: 10.1128/IAI.01070-08
84. Tyagi RK, Miles B, Parmar R, Garg NK, Dalai SK, Baban B, et al. Human IDO-Competent, Long-Lived Immunoregulatory Dendritic Cells Induced by Intracellular Pathogen, and Their Fate in Humanized Mice. *Sci Rep* (2017) 7:41083. doi: 10.1038/srep41083
85. Woodland RT, Schmidt MR. Homeostatic Proliferation of B Cells. *Semin Immunol* (2005) 17(3):209–17. doi: 10.1016/j.smim.2005.02.006
86. King M, Pearson T, Shultz LD, Leif J, Bottino R, Trucco M, et al. A New Hu-PBL Model for the Study of Human Islet Alloreactivity Based on NOD-scid Mice Bearing a Targeted Mutation in the IL-2 Receptor Gamma Chain Gene. *Clin Immunol* (2008) 126(3):303–14. doi: 10.1016/j.clim.2007.11.001
87. King MA, Covassin L, Brehm MA, Racki W, Pearson T, Leif J, et al. Human Peripheral Blood Leucocyte Non-Obese Diabetic-Severe Combined Immunodeficiency Interleukin-2 Receptor Gamma Chain Gene Mouse Model of Xenogeneic Graft-*Versus*-Host-Like Disease and the Role of Host Major Histocompatibility Complex. *Clin Exp Immunol* (2009) 157 (1):104–18. doi: 10.1111/j.1365-2249.2009.03933.x
88. Brehm MA, Kenney LL, Wiles MV, Low BE, Tisch RM, Burzenski L, et al. Lack of Acute Xenogeneic Graft-*Versus*-Host Disease, But Retention of T-Cell Function Following Engraftment of Human Peripheral Blood Mononuclear Cells in NSG Mice Deficient in MHC Class I and II Expression. *FASEB J* (2019) 33(3):3137–51. doi: 10.1096/fj.201800636R
89. Ito M, Hiramatsu H, Kobayashi K, Suzue K, Kawahata M, Hioki K, et al. Nod/Scid/γ_c^{null} Mouse: An Excellent Recipient Mouse Model for Engraftment of Human Cells. *Blood* (2002) 100(9):3175–82. doi: 10.1182/blood-2001-12-0207
90. Ishikawa F, Yasukawa M, Lyons B, Yoshida S, Miyamoto T, Yoshimoto G, et al. Development of Functional Human Blood and Immune Systems in NOD/SCID/IL2 Receptor γ Chain^{null} Mice. *Blood* (2005) 106(5):1565–73. doi: 10.1182/blood-2005-02-0516
91. Holyoake TL, Nicolini FE, Eaves CJ. Functional Differences Between Transplantable Human Hematopoietic Stem Cells From Fetal Liver, Cord Blood, and Adult Marrow. *Exp Hematol* (1999) 27(9):1418–27. doi: 10.1016/s0301-472x(99)00078-8
92. Lapidot T, Pflumio F, Doedens M, Murdoch B, Williams DE, Dick JE. Cytokine Stimulation of Multilineage Hematopoiesis From Immature Human Cells Engrafted in SCID Mice. *Science* (1992) 255(5048):1137–41. doi: 10.1126/science.1372131
93. Brehm MA, Racki WJ, Leif J, Burzenski L, Hosur V, Wetmore A, et al. Engraftment of Human HSCs in Nonirradiated Newborn NOD-*scid Il2rγ*^{null} Mice Is Enhanced by Transgenic Expression of Membrane-Bound Human SCF. *Blood* (2012) 119(12):2778–88. doi: 10.1182/blood-2011-05-353243

94. McIntosh BE, Brown ME, Duffin BM, Maufort JP, Vereide DT, Slukvin II, et al. Nonirradiated NOD,B6.SCID *Il2rγ*$^{-/-}$ *Kit*$^{W41/W41}$ (NBSGW) Mice Support Multilineage Engraftment of Human Hematopoietic Cells. *Stem Cell Rep* (2015) 4(2):171–80. doi: 10.1016/j.stemcr.2014.12.005
95. Shultz LD, Lyons BL, Burzenski LM, Gott B, Chen X, Chaleff S, et al. Human Lymphoid and Myeloid Cell Development in NOD/LtSz-*scid Il2rγ*^{null} Mice Engrafted With Mobilized Human Hemopoietic Stem Cells. *J Immunol* (2005) 174(10):6477–89. doi: 10.4049/jimmunol.174.10.6477
96. Traggiai E, Chicha L, Mazzucchelli L, Bronz L, Piffaretti JC, Lanzavecchia A, et al. Development of a Human Adaptive Immune System in Cord Blood Cell-Transplanted Mice. *Science* (2004) 304(5667):104–7. doi: 10.1126/science.1093933
97. Hiramatsu H, Nishikomori R, Heike T, Ito M, Kobayashi K, Katamura K, et al. Complete Reconstitution of Human Lymphocytes From Cord Blood CD34^{+} Cells Using the *NOD/SCID/*γ_c^{null}Mice Model. *Blood* (2003) 102 (3):873–80. doi: 10.1182/blood-2002-09-2755
98. Lan P, Tonomura N, Shimizu A, Wang S, Yang YG. Reconstitution of a Functional Human Immune System in Immunodeficient Mice Through Combined Human Fetal Thymus/Liver and CD34^{+} Cell Transplantation. *Blood* (2006) 108(2):487–92. doi: 10.1182/blood-2005-11-4388
99. Durost PA, Aryee KE, Manzoor F, Tisch RM, Mueller C, Jurczyk A, et al. Gene Therapy With an Adeno-Associated Viral Vector Expressing Human Interleukin-2 Alters Immune System Homeostasis in Humanized Mice. *Hum Gene Ther* (2018) 29(3):352–65. doi: 10.1089/hum.2017.072
100. Onoe T, Kalscheuer H, Danzl N, Chittenden M, Zhao G, Yang YG, et al. Human Natural Regulatory T Cell Development, Suppressive Function, and Postthymic Maturation in a Humanized Mouse Model. *J Immunol* (2011) 187(7):3895–903. doi: 10.4049/jimmunol.1100394
101. Greenblatt MB, Vrbanac V, Tivey T, Tsang K, Tager AM, Aliprantis AO. Graft *Versus* Host Disease in the Bone Marrow, Liver and Thymus Humanized Mouse Model. *PLoS One* (2012) 7(9):e44664. doi: 10.1371/journal.pone.0044664
102. Shultz LD, Pearson T, King M, Giassi L, Carney L, Gott B, et al. Humanized NOD/LtSz-*scid* IL2 Receptor Common Gamma Chain Knockout Mice in Diabetes Research. *Ann N Y Acad Sci* (2007) 1103:77–89. doi: 10.1196/annals.1394.002
103. Bosma GC, Custer RP, Bosma MJ. A Severe Combined Immunodeficiency Mutation in the Mouse. *Nature* (1983) 301(5900):527–30. doi: 10.1038/301527a0
104. Mosier DE, Gulizia RJ, Baird SM, Wilson DB. Transfer of a Functional Human Immune System to Mice With Severe Combined Immunodeficiency. *Nature* (1988) 335(6187):256–9. doi: 10.1038/335256a0
105. Shinkai Y, Rathbun G, Lam KP, Oltz EM, Stewart V, Mendelsohn M, et al. Rag-2-Deficient Mice Lack Mature Lymphocytes Owing to Inability to Initiate V(D)J Rearrangement. *Cell* (1992) 68(5):855–67. doi: 10.1016/0092-8674(92)90029-c
106. Mombaerts P, Iacomini J, Johnson RS, Herrup K, Tonegawa S, Papaioannou VE. Rag-1-Deficient Mice Have No Mature B and T Lymphocytes. *Cell* (1992) 68(5):869–77. doi: 10.1016/0092-8674(92)90030-g
107. Shultz LD, Schweitzer PA, Christianson SW, Gott B, Schweitzer IB, Tennent B, et al. Multiple Defects in Innate and Adaptive Immunologic Function in NOD/LtSz-*scid* Mice. *J Immunol* (1995) 154(1):180–91.
108. Serreze DV, Gaskins HR, Leiter EH. Defects in the Differentiation and Function of Antigen Presenting Cells in NOD/Lt Mice. *J Immunol* (1993) 150(6):2534–43.
109. Hesselton RM, Greiner DL, Mordes JP, Rajan TV, Sullivan JL, Shultz LD. High Levels of Human Peripheral Blood Mononuclear Cell Engraftment and Enhanced Susceptibility to Human Immunodeficiency Virus Type 1 Infection in NOD/LtSz-*scid/scid* Mice. *J Infect Dis* (1995) 172(4):974–82. doi: 10.1093/infdis/172.4.974
110. Lowry PA, Shultz LD, Greiner DL, Hesselton RM, Kittler EL, Tiarks CY, et al. Improved Engraftment of Human Cord Blood Stem Cells in NOD/LtSz-*scid/scid* Mice After Irradiation or Multiple-Day Injections Into Unirradiated Recipients. *Biol Blood Marrow Transplant* (1996) 2(1):15–23.
111. Liao W, Lin JX, Leonard WJ. IL-2 Family Cytokines: New Insights Into the Complex Roles of IL-2 as a Broad Regulator of T Helper Cell Differentiation. *Curr Opin Immunol* (2011) 23(5):598–604. doi: 10.1016/j.coi.2011.08.003
112. Yahata T, Ando K, Nakamura Y, Ueyama Y, Shimamura K, Tamaoki N, et al. Functional Human T Lymphocyte Development From Cord Blood CD34^{+} Cells in Nonobese Diabetic/Shi-*Scid*, IL-2 Receptor γ Null Mice. *J Immunol* (2002) 169(1):204–9. doi: 10.4049/jimmunol.169.1.204
113. DiSanto JP, Müller W, Guy-Grand D, Fischer A, Rajewsky K. Lymphoid Development in Mice With a Targeted Deletion of the Interleukin 2 Receptor γ Chain. *Proc Natl Acad Sci USA* (1995) 92(2):377–81. doi: 10.1073/pnas.92.2.377
114. Cao X, Shores EW, Hu-Li J, Anver MR, Kelsall BL, Russell SM, et al. Defective Lymphoid Development in Mice Lacking Expression of the Common Cytokine Receptor γ Chain. *Immunity* (1995) 2(3):223–38. doi: 10.1016/1074-7613(95)90047-0
115. Allen TM, Brehm MA, Bridges S, Ferguson S, Kumar P, Mirochnitchenko O, et al. Humanized Immune System Mouse Models: Progress, Challenges and Opportunities. *Nat Immunol* (2019) 20(7):770–4. doi: 10.1038/s41590-019-0416-z
116. Schinnerling K, Rosas C, Soto L, Thomas R, Aguillón JC. Humanized Mouse Models of Rheumatoid Arthritis for Studies on Immunopathogenesis and Preclinical Testing of Cell-Based Therapies. *Front Immunol* (2019) 10:203. doi: 10.3389/fimmu.2019.00203
117. Ali N, Flutter B, Sanchez Rodriguez R, Sharif-Paghaleh E, Barber LD, Lombardi G, et al. Xenogeneic Graft-*Versus*-Host-Disease in NOD-*scid* Il-2rγ^{null} Mice Display a T-Effector Memory Phenotype. *PLoS One* (2012) 7(8): e44219. doi: 10.1371/journal.pone.0044219
118. Danner R, Chaudhari SN, Rosenberger J, Surls J, Richie TL, Brumeanu TD, et al. Expression of HLA Class II Molecules in Humanized NOD.Rag1KO.IL2RgcKO Mice Is Critical for Development and Function of Human T and B Cells. *PLoS One* (2011) 6(5):e19826. doi: 10.1371/journal.pone.0019826
119. Covassin L, Laning J, Abdi R, Langevin DL, Phillips NE, Shultz LD, et al. Human Peripheral Blood CD4 T Cell-Engrafted Non-Obese Diabetic-*Scid IL2rγ*^{null} $H_2 - Ab_1^{tm1Gru}$ Tg (Human Leucocyte Antigen D-Related 4) Mice: A Mouse Model of Human Allogeneic Graft-*Versus*-Host Disease. *Clin Exp Immunol* (2011) 166(2):269–80. doi: 10.1111/j.1365-2249.2011.04462.x
120. Sarkar S, Heise MT. Mouse Models as Resources for Studying Infectious Diseases. *Clin Ther* (2019) 41(10):1912–22. doi: 10.1016/j.clinthera.2019.08.010
121. Seymour R, Sundberg JP, Hogenesch H. Abnormal Lymphoid Organ Development in Immunodeficient Mutant Mice. *Vet Pathol* (2006) 43 (4):401–23. doi: 10.1354/vp.43-4-401
122. Santagostino SF, Arbona RJR, Nashat MA, White JR, Monette S. Pathology of Aging in NOD *Scid* Gamma Female Mice. *Vet Pathol* (2017) 54(5):855–69. doi: 10.1177/0300985817698210
123. Gonzalez L, Strbo N, Podack ER. Humanized Mice: Novel Model for Studying Mechanisms of Human Immune-Based Therapies. *Immunol Res* (2013) 57(1-3):326–34. doi: 10.1007/s12026-013-8471-2
124. Misharin AV, Haines GKIII, Rose S, Gierut AK, Hotchkiss RS, Perlman H. Development of a New Humanized Mouse Model to Study Acute Inflammatory Arthritis. *J Transl Med* (2012) 10:190. doi: 10.1186/1479-5876-10-190
125. Guo J, Li Y, Shan Y, Shu C, Wang F, Wang X, et al. Humanized Mice Reveal an Essential Role for Human Hepatocytes in the Development of the Liver Immune System. *Cell Death Dis* (2018) 9(6):667. doi: 10.1038/s41419-018-0720-9
126. Arrey F, Löwe D, Kuhlmann S, Kaiser P, Moura-Alves P, Krishnamoorthy G, et al. Humanized Mouse Model Mimicking Pathology of Human Tuberculosis for *In Vivo* Evaluation of Drug Regimens. *Front Immunol* (2019) 10:89. doi: 10.3389/fimmu.2019.00089
127. Vudattu NK, Waldron-Lynch F, Truman LA, Deng S, Preston-Hurlburt P, Torres R, et al. Humanized Mice as a Model for Aberrant Responses in Human T Cell Immunotherapy. *J Immunol* (2014) 193(2):587–96. doi: 10.4049/jimmunol.1302455
128. Herndler-Brandstetter D, Shan L, Yao Y, Stecher C, Plajer V, Lietzenmayer M, et al. Humanized Mouse Model Supports Development, Function, and Tissue Residency of Human Natural Killer Cells. *Proc Natl Acad Sci USA* (2017) 114(45):E9626–E34. doi: 10.1073/pnas.1705301114
129. Bendall SC, Nolan GP, Roederer M, Chattopadhyay PK. A Deep Profiler's Guide to Cytometry. *Trends Immunol* (2012) 33(7):323–32. doi: 10.1016/j.it.2012.02.010
130. Bandura DR, Baranov VI, Ornatsky OI, Antonov A, Kinach R, Lou X, et al. Mass Cytometry: Technique for Real Time Single Cell Multitarget Immunoassay Based on Inductively Coupled Plasma Time-of-Flight

Mass Spectrometry. *Anal Chem* (2009) 81(16):6813–22. doi: 10.1021/ac901049w
131. Chang Q, Ornatsky O, Hedley D. Staining of Frozen and Formalin-Fixed, Paraffin-Embedded Tissues With Metal-Labeled Antibodies for Imaging Mass Cytometry Analysis. *Curr Protoc Cytom* (2017) 82:12.47.1–12.47.8. doi: 10.1002/cpcy.29
132. Curran M, Mairesse M, Matas-Céspedes A, Bareham B, Pellegrini G, Liaunardy A, et al. Recent Advancements and Applications of Human Immune System Mice in Preclinical Immuno-Oncology. *Toxicol Pathol* (2020) 48(2):302–16. doi: 10.1177/0192623319886304
133. Sandal I, Karydis A, Luo J, Prislovsky A, Whittington KB, Rosloniec EF, et al. Bone Loss and Aggravated Autoimmune Arthritis in HLA-Drβ1-Bearing Humanized Mice Following Oral Challenge With *Porphyromonas Gingivalis*. *Arthritis Res Ther* (2016) 18(1):249. doi: 10.1186/s13075-016-1143-6
134. Abusleme L, Hong BY, Hoare A, Konkel JE, Diaz PI, Moutsopoulos NM. Oral Microbiome Characterization in Murine Models. *Bio Protoc* (2017) 7 (24):e2655. doi: 10.21769/BioProtoc.2655
135. Sandhu J, Shpitz B, Gallinger S, Hozumi N. Human Primary Immune Response in SCID Mice Engrafted With Human Peripheral Blood Lymphocytes. *J Immunol* (1994) 152(8):3806–13.
136. Hozumi N, Gorczynski R, Peters W, Sandhu JS. A SCID Mouse Model for Human Immune Response and Disease. *Res Immunol* (1994) 145(5):370–9. doi: 10.1016/s0923-2494(94)80202-5
137. Tary-Lehmann M, Saxon A, Lehmann PV. The Human Immune System in hu-PBL-SCID Mice. *Immunol Today* (1995) 16(11):529–33. doi: 10.1016/0167-5699(95)80046-8

Conflict of Interest: The authors declare that the research was conducted in the absence of any commercial or financial relationships that could be construed as a potential conflict of interest.

Citation: *Rojas C, García MP, Polanco AF, González-Osuna L, Sierra-Cristancho A, Melgar-Rodríguez S, Cafferata EA and Vernal R (2021) Humanized Mouse Models for the Study of Periodontitis: An Opportunity to Elucidate Unresolved Aspects of Its Immunopathogenesis and Analyze New Immunotherapeutic Strategies. Front. Immunol. 12:663328. doi: 10.3389/fimmu.2021.663328*

frontiers in Immunology

ORIGINAL RESEARCH
published: 27 July 2021
doi: 10.3389/fimmu.2021.671648

Generation of Novel Human Red Blood Cell-Bearing Humanized Mouse Models Based on C3-Deficient NOG Mice

Takuya Yamaguchi[1†], *Ikumi Katano*[1], *Iyo Otsuka*[1], *Ryoji Ito*[1], *Misa Mochizuki*[2], *Motohito Goto*[3] *and Takeshi Takahashi*[1*]

[1] Laboratory Animal Research Department, Central Institute for Experimental Animals (CIEA), Kawasaki, Japan, [2] Pathological Analysis Center, CIEA, Kawasaki, Japan, [3] Animal Resource & Technical Research Center, CIEA, Kawasaki, Japan

OPEN ACCESS

Edited by:
Yan Li,
Nanjing University, China

Reviewed by:
Yong-Guang Yang,
Jilin University, China
Liang Shan,
Washington University in St. Louis, United States

***Correspondence:**
Takeshi Takahashi
takeshi-takahashi@ciea.or.jp

[†]Present address:
Takuya Yamaguchi,
Laboratory of Veterinary Pharmacology, Department of Veterinary Medicine, College of Bioresource Sciences, Nihon University, Fujisawa, Japan

Specialty section:
This article was submitted to Microbial Immunology, a section of the journal Frontiers in Immunology

Received: *24 February 2021*
Accepted: *12 July 2021*
Published: *27 July 2021*

Citation:
Yamaguchi T, Katano I, Otsuka I, Ito R, Mochizuki M, Goto M and Takahashi T (2021) Generation of Novel Human Red Blood Cell-Bearing Humanized Mouse Models Based on C3-Deficient NOG Mice. Front. Immunol. 12:671648. doi: 10.3389/fimmu.2021.671648

Despite recent advances in immunodeficient mouse models bearing human red blood cells (hRBCs), the elimination of circulating hRBCs by residual innate immune systems remains a significant challenge. In this study, we evaluated the role of mouse complement C3 in the elimination of circulating hRBCs by developing a novel NOG substrain harboring a truncated version of the murine C3 gene (NOG-C3$^{\Delta MG2\text{-}3}$). Genetic C3 deletion prolonged the survival of transfused hRBCs in the circulation. Chemical depletion and functional impairment of mouse macrophages, using clodronate liposomes (Clo-lip) or gadolinium chloride ($GdCl_3$), respectively, further extended the survival of hRBCs in NOG-C3$^{\Delta MG2\text{-}3}$ mice. Low $GdCl_3$ toxicity allowed the establishment of hRBC-bearing mice, in which hRBCs survived for more than 4 weeks with transfusion once a week. In addition, erythropoiesis of human hematopoietic stem cells (hHSCs) was possible in NOG-C3$^{\Delta MG2\text{-}3}$/human GM-CSF-IL-3 transgenic mice with Clo-lip treatment. These findings indicate that mouse models harboring hRBCs can be achieved using NOG-C3$^{\Delta MG2\text{-}3}$ mice, which could facilitate studies of human diseases associated with RBCs.

Keywords: humanized mouse, red blood cell, complements, NOG, macrophage, gadolinium chloride

INTRODUCTION

Xenotransplantation in immunodeficient mice has become an essential *in vivo* model for studying human hematopoietic cell development and hematological diseases (1, 2). The most commonly used immunocompromised mouse strains are NOD/Shi-scid/IL-2Rγ^{null} (NOG) (3), NOD/LtSz-scid/IL-2Rγ^{null} (NSG) (4), and BALB/c-Rag2^{null}/IL-2Rγ^{null} (5). In the last two decades, significant efforts have been made to expand the repertoire of cell lineages (6–10) and engraft human cells to establish a functional humanized immune system (11–14). As a result, numerous mouse strains recapitulating human diseases are now available for drug discovery (15–18). However, some human hematopoietic lineages cannot be generated using the current humanized mouse models.

Human red blood cells (hRBCs) are the most abundant cells in the blood, comprising approximately 40% of the hematocrit. However, hRBCs are short-lived in experimental models, hindering progress in malaria research (19–21). The rate of differentiation of hematopoietic stem

cells (HSCs) to mature hRBCs is extremely low in humanized mouse models, even though immature human erythrocytes can be found in the bone marrow (BM) of human hematopoietic stem cell (hHSC)-reconstituted NOG or NSG mice (Dr. Tatsutoshi Nakahata, personal communication) (22). The absence of mature hRBCs in the peripheral blood (PB) was also reported in the novel NSG-W41 model, which has an enhanced ability for human hematopoiesis (7, 22). Although the success of induction of hRBCs was reported in a dual humanized mouse model with human liver and hematopoietic systems during the submission of this manuscript, the frequency in total RBCs remained not more than 5% (23).

In addition, when immunodeficient mice are transfused with large amounts of mature hRBCs (i.e., when 20–40% of erythrocytes in the blood circulation are human-derived), the erythrocytes are rapidly eliminated within a few days (24, 25). Repeated injections of hRBCs every 1–2 days are necessary to overcome the poor hRBC retention and establish hRBC-bearing mice (20, 26–28). Hu et al. aimed to produce an improved hRBC-bearing mouse model by depleting macrophages and suppressing macrophage-mediated hRBCs phagocytosis. Selective depletion of macrophages using clodronate liposomes (Clo-lip) not only prolonged the survival of injected hRBCs but also allowed the development of circulating hRBCs from hHSCs in the blood of NOD/SCID and NSG mice (24). Although this model can be used for hRBC studies, repeated injections of Clo-lip are toxic or even lethal. In addition, the frequent replenishment of hRBCs by repeated daily transfusion may not recapitulate the physiology of hRBCs, indicating that current mouse models are not always suitable for long-term studies, such as modeling the life cycle of malaria parasites.

The fact that murine macrophages rapidly eliminate transfused mature hRBCs suggests that hRBCs are recognized by host innate immune cells as foreign substances by either direct or indirect mechanisms. Glycans, such as oligomannoside- and N-acetyllactosamine-type glycans, have been suggested to play a role in the recognition of hRBCs by mouse innate immune cells (29). Ishihara et al. demonstrated that mouse C3 can deposit on hRBCs and suggested the role of C3 in the elimination of hRBCs (30). In addition, Chen et al. reported that, in hRBC-transplanted NOD/SCID mice, the complement induces hRBC adherence to murine phagocytes (25), suggesting that hRBCs are opsonized by the murine complement, leading to hRBC recognition by murine macrophages.

In this study, we investigated the role of murine complement C3 in the recognition and rejection of hRBCs *in vivo* by establishing a novel NOG substrain harboring a truncated version of the murine C3 gene (NOG-C3$^{\Delta MG2\text{-}3}$). The lack of C3 prolonged the survival of exogenous hRBCs in the circulation. Gadolinium chloride ($GdCl_3$) was reported to inhibit macrophages in the rat (31, 32) and mouse liver (33). To develop an improved method for depleting or suppressing mouse macrophages, we compared the ability of $GdCl_3$ and Clo-lip to inhibit macrophages in NOG-C3$^{\Delta MG2\text{-}3}$ and NOG mice. $GdCl_3$ and Clo-lip significantly prolonged the survival of transfused hRBCs in NOG-C3$^{\Delta MG2\text{-}3}$ mice. Although the effects of $GdCl_3$ were weak compared with Clo-lip, $GdCl_3$ was less toxic than Clo-lip; thus, transfusion of hRBCs with $GdCl_3$ treatments once a week maintained hRBCs for an extended period. Finally, induction of hRBCs from hHSCs was achieved in hHSC-reconstituted NOG-C3$^{\Delta MG2\text{-}3}$/human (h) GM-CSF-IL-3 (GM3) transgenic (Tg) mice after Clo-lip treatment.

The results indicate that NOG-C3$^{\Delta MG2\text{-}3}$ mice practically facilitate the production of humanized mice with hRBCs and they will be a novel model to study malaria infection and other human erythrocyte-related diseases.

MATERIALS AND METHODS

Mice

NOG (NOD.Cg-Prkdc^{scid} Il2rg^{tm1Sug}/ShiJic) (3) and NOG-C3$^{\Delta MG2\text{-}3}$ (NOD.Cg-Prkdc^{scid} Il2rg^{tm1Sug}C3^{em1}/Jic) mice were maintained at the Central Institute for Experimental Animals (CIEA) under specific pathogen-free conditions. To generate NOG-C3$^{\Delta MG2\text{-}3}$ mice, we used the CRISPR/Cas9 system for genome editing (34, 35). Four different guide RNA (gRNA) sequences were designed to target exons 5, 6, and 7 of the complement 3 gene. All gRNAs were cloned into the PX330 plasmid (36) and cleavage activity was confirmed using the reporter construct pCAGGS-EGxxFP (37). Both plasmids were obtained from Addgene (Watertown, MA). The genomic region containing the target exons was inserted in the middle of the EGFP gene, and the plasmid was transfected into HEK293T cells together with each gRNA-PX330 plasmid. Genome-editing success was evaluated *via* GFP signal rescue after cleavage of the targeted exon. Two gRNAs (gRNA1 and -4) were selected, and a mixture of the two was used for microinjection into fertilized eggs of NOG mice. The sequences of the gRNAs were as follows: gRNA1 targeting exon 5, 5'-CTTGACAGGAATGCCATCGG-3'gRNA4 targeting exon 7, 5'-CATCGATGACCCAAATGGCC-3'.

Ethics Statement

All studies involving human participants were reviewed and approved by the research ethics committee of the CIEA. Study participants provided written informed consent. All animal experiments were performed in accordance with institutional guidelines (14038, 17024, and 20043) and were approved by the animal experimentation committee of the CIEA.

Flow Cytometry and Antibodies

Murine PB was collected from the retro-orbital venous plexus using heparinized pipettes periodically under anesthesia. BM cells were obtained by flushing femurs with 1 mL phosphate-buffered saline (PBS). PB and BM samples were diluted 10- and 5-fold with PBS, respectively, and 10 µL of the diluted sample was mixed with an equal volume of antibody mixture (described below). After 20–30 min of incubation in the dark at room temperature, the samples were further diluted 15–20-fold with PBS and analyzed on a FACSCanto™ or LSRFortessa™ flow cytometer (BD Biosciences, San Jose, CA). Flow cytometry data were analyzed using FlowJo (ver. 10.7.1, BD Biosciences).

Anti-human CD235a (glycophorin A)-allophycocyanin/cyanine 7 (APC/Cy7), anti-human CD71-APC and anti-mouse TER-119-phycoerythrin (PE) were purchased from BioLegend (San Diego, CA). Fluorescent isothiocyanate (FITC)-labeled goat anti-mouse complement C3 polyclonal antibody was purchased from MP Biomedicals (Santa Ana, CA). Anti-mouse complement component C1q-PE and anti-mouse complement component C4-biotin antibodies were purchased from Cedarlane (Burlington, ON). Streptavidin-PE (StAv-PE) was purchased from BD Bioscience.

Enzyme-Linked Immunosorbent Assay (ELISA)

C3 levels in the plasma were measured using an anti-mouse complement C3 ELISA kit (Abcam, Cambridge, UK) according to the manufacturer's instructions.

Transplantation of hRBCs

We collected PB from healthy donors to obtain hRBCs for transfusion. The plasma and buffy coat were removed after centrifugation (400 × g for 5 min). The pellets were washed with PBS, and the RBCs were adjusted to a concentration of 1×10^{10} cells/mL. Mice were intravenously (i.v.) injected with hRBCs *via* the tail vein. For long-term experiments, the hRBCs were intraperitoneally (i.p.) injected once a week for maintenance after the initial transfusion.

Transplantation of hHSCs

To reconstitute the human hematopoietic system, 6–8-week-old NOG-C3$^{\Delta MG2-3}$, NOG/hGM3 Tg, and NOG-C3$^{\Delta MG2-3}$/hGM3 Tg mice were irradiated with X-rays at 160 cGy (MBR-1520R-4; Hitachi, Hitachi, Japan). Then, 5.0 x 10^4 or 2.5×10^4 umbilical cord blood-derived CD34$^+$ cells (StemExpress, Folsom, CA), for NOG-C3$^{\Delta MG2-3}$ mice or for NOG/hGM3 Tg and NOG-C3$^{\Delta MG2-3}$/hGM3 Tg mice, respectively, were transplanted by i.v. injection the next day; hHSC-NOG-C3$^{\Delta MG2-3}$, hHSC-NOG/hGM3 Tg, and hHSC-NOG-C3$^{\Delta MG2-3}$/hGM3 Tg mice were thus obtained.

Chemical Treatment

Clo-lip (400 μL/kg; Hygieia Bioscience, Osaka, Japan) and $GdCl_3$ (30 mg/kg; G7532, Sigma Aldrich, St. Louis, MO) were i.v.-injected into 6–10-week-old NOG or NOG-C3$^{\Delta MG2-3}$ mice *via* the tail vein. The injection volume was adjusted to 200 μL with saline. Control mice were injected with 200 μL of saline. Mice were injected with Clo-lip, $GdCl_3$, or saline four times at 3–4-day intervals and were transfused with hRBCs on the day after the last injection. For long-term experiments, Clo-lip was i.v.-injected as the first treatment to ensure macrophage depletion. Thereafter, $GdCl_3$ was administered three times by i.v. injection, at 3–4-day intervals. After the first transfusion of hRBCs, $GdCl_3$ was administered by i.p. injection every 4–6 days for maintenance. For the induction of hRBC from hHSCs, hHSC-transplanted mice were treated with Clo-lip as described above with 3-4-days intervals at 8 weeks after hHSC-transplantation.

In Vitro C3 Deposition Assay

The mouse PB (5 μL) was diluted with 50 μL of PBS containing heparin; 3 μL of the solution was mixed with 30 μL of mouse serum from NOG or NOG-C3$^{\Delta MG2-3}$ mice and incubated for 30 min at 37°C. Subsequently, samples were stained with FITC-labeled goat anti-C3 polyclonal antibody for 20 min at room temperature. Then, the cells were washed with PBS and analyzed using a FACSCanto flow cytometer.

In Vivo C3 Deposition Assay

Mice were administered hRBCs ($2–5 \times 10^9$) by i.v. injection and the PB was collected 3 h after the injection. The blood (10 μL) was immediately transferred to a tube containing 100 μL of cold PBS with 5 IU/mL heparin and 10 mM EDTA (PBS/heparin/EDTA) to prevent complement activation. The diluted blood (10 μL) was stained with APC/Cy7-anti-human CD235a and FITC-anti-mouse C3 polyclonal antibodies, or APC/Cy7-CD235a and biotin-anti-mouse C1q or -C4 antibodies, followed by StAv-PE for 20 min on ice. After staining, the cells were suspended in 100 μL of cold PBS/EDTA and analyzed using flow cytometry.

Histology

Tissues from mice were fixed in 10% neutralized formalin (Mildform, FUJIFILM Wako Pure Chemical, Osaka, Japan). Formalin-fixed tissues were embedded in paraffin and analyzed with either hematoxylin and eosin staining or immunohistochemistry using anti-mouse CD68 antibody (Cell Signaling Technology, Danvers, MA) or anti-F4/80 antibody (BIO-RAD, Hercules, CA). Sections were stained using a fully automated BOND-MAX system (Leica Biosystems, Mount Waverley, Australia). The images were captured using a NanoZoomer S60 scanner (Hamamatsu Photonics, Hamamatsu, Japan).

Statistical Analysis

The statistical significance of the results was determined using two-way repeated-measures ANOVA or Mixed-effects analysis using GraphPad Prism software (ver. 9.0; GraphPad Software Inc., San Diego, CA).

RESULTS

Deposition of Mouse Complement on hRBC Surfaces in NOG Mice

To examine the fate of transfused hRBCs in NOG mice, we i.v.-injected fresh hRBCs into NOG mice and investigated their dynamics in the circulation using flow cytometry. We found that hRBCs were rapidly eliminated from the circulation of NOG mice, even when 5.0×10^9 hRBCs (equivalent to 25%–35% of total RBCs) were administered (**Figures 1A, B**). Mouse innate immune cells, especially macrophages, have been implicated in the rapid clearance of hRBCs (24); hence, we investigated the role of mouse complement molecules in the elimination of hRBCs by mouse innate immune cells. To evaluate the deposition of mouse complement molecules on the hRBC surfaces, PB was collected 3 h after hRBC injection and stained with polyclonal anti-mouse C1q, C3, or C4b antibodies. Significant amounts of mouse C3 fragments were detected on the transfused hRBC surfaces, whereas C1q and C4 were modest (**Figure 1C**).

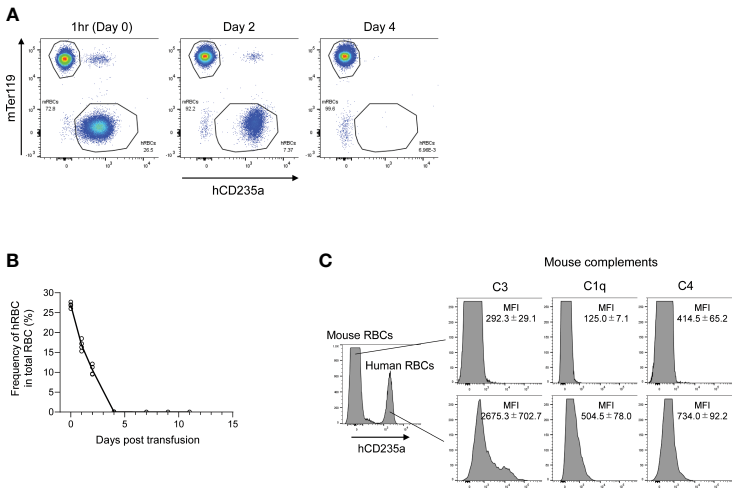

FIGURE 1 | The fate of hRBCs in NOG mice. **(A)** PB was collected from NOG mice at 1 h, 2 days, and 4 days after hRBC transfusion. Human and mouse RBCs were distinguished based on hCD235a (glycophorin A) and Ter119 expression. A representative FACS plot is shown. **(B)** Kinetics of transfused hRBCs in NOG mice. PB was collected at the indicated time points, and the presence of hRBCs was assessed using flow cytometry. The value on day 0 represents the frequency of hRBCs relative to total RBCs at 1 h after transfusion. Each dot represents a value from each mouse, and the line indicates the time course of the means. **(C)** Deposition of murine C3 on the surfaces of transfused hRBCs. PB was collected from hRBC-transfused NOG mice at 3 h post-transfusion, stained with anti-human CD235a and anti-mouse C3, C1q, or C4 antibodies, and analyzed using flow cytometry. The upper histogram represents mouse (hCD235a$^-$) RBCs; human (hCD235a$^+$) RBCs are shown in the lower histogram.

Generation of C3-Deficient NOG Mice

The deposition of mouse C3 on the surfaces of hRBCs indicates that murine C3 may function as an opsonin to facilitate the recognition of hRBCs by mouse innate immune cells. To evaluate the relevance of C3 to hRBC recognition, we disrupted the mouse C3 gene using CRISPR/Cas9. Among five founder mice, one mouse had a 252-nucleotide (nt) deletion resulting in the total exclusion of exon 6 and exclusion of large parts of exons 5 and 7 (nt 614–865; **Supplementary Figure 1**). The resulting 84-amino-acid (aa) truncation (aa 172–255 in pro C3 molecules) corresponded to a part spanning the MG2-MG3 domains in the C3α chain (38). Despite the in-frame deletion, mouse C3 protein was not detected in the plasma by ELISA (**Supplementary Figure 2A**), indicating the absence of mature functional mouse C3 molecules in the circulation. Indeed, when the serum from NOG or mutant (NOG-C3$^{\Delta MG2\text{-}3}$) mice was incubated with hRBCs *in vitro*, large amounts of mouse C3 or its derivative fragments were deposited on the hRBC surfaces with the NOG mouse serum. By contrast, no signal was detected when hRBCs were incubated with NOG-C3$^{\Delta MG2\text{-}3}$ mouse serum (**Supplementary Figure 2B**), confirming that NOG-C3$^{\Delta MG2\text{-}3}$ are C3-deficient.

Prolonged Survival of hRBCs in NOG-C3$^{\Delta MG2\text{-}3}$ Mice

We then assessed the survival of transfused hRBCs in NOG and NOG-C3$^{\Delta MG2\text{-}3}$ mice. To this end, we transfused 5.0×10^9 hRBCs into NOG and NOG-C3$^{\Delta MG2\text{-}3}$ mice and evaluated their dynamics in the circulation using flow cytometry. In NOG mice, the frequency of circulating hRBCs decreased dramatically within a few days (**Figures 1** and **2**). The survival rates of hRBCs were 64.8% ± 11.2% at 1 day post-transfusion (dpt), 36.5% ± 16.3% at 2 dpt, and 7.7% ± 5.9% at 3 dpt; no hRBCs were detected after 4 dpt (**Figure 2B**). The elimination of transfused hRBCs was slower in NOG-C3$^{\Delta MG2\text{-}3}$ mice than in NOG mice, with hRBC survival rates of 88.8% ± 2.0% at 1 dpt, 73.7% ± 1.2% at 2 dpt, and 59.5% ± 3.4% at 3 dpt (**Figure 2B**). Remarkably, 44.0% ± 5.8% of the transfused hRBCs (equivalent to ~12% of the total RBCs in the mouse blood) were maintained at 4 dpt in NOG-C3$^{\Delta MG2\text{-}3}$ mice (**Figure 2A**); a significant amount of hRBCs could still be detected up to 7 days after a single transfusion (**Figure 2B**). The transfusion of a smaller number of hRBCs (2.5×10^8) was also tested. The frequency of hRBCs 30 min after transfusion was 1.15% ± 0.21% in NOG mice and 3.53% ± 0.42% in NOG-C3$^{\Delta MG2\text{-}3}$ mice, which was statistically significant. At 6 hours post transfusion, there were a few hRBCs in NOG mice, whereas 2.43% ± 0.44% of the total RBCs were hRBCs in NOG-C3$^{\Delta MG2\text{-}3}$ mice (**Figure 2C**). The decrease of the survival rate of hRBCs was more rapid in NOG mice than in NOG-C3$^{\Delta MG2\text{-}3}$ mice (**Figure 2D**), suggesting that C3-dependent elimination mechanisms are independent of the number of hRBCs. The prolonged survival of human RBCs in NOG-C3$^{\Delta MG2\text{-}3}$ mice was observed irrespective of the donor blood type because we obtained similar results with different donor blood types (A-type, O-type and AB-type, data not shown).

Depletion of Mouse Macrophages by Clo-lip Extends the Survival of hRBCs in NOG and NOG-C3$^{\Delta MG2\text{-}3}$ Mice

Despite the extended hRBC survival in NOG-C3$^{\Delta MG2\text{-}3}$ mice, the survival period of erythrocytes was significantly shorter than

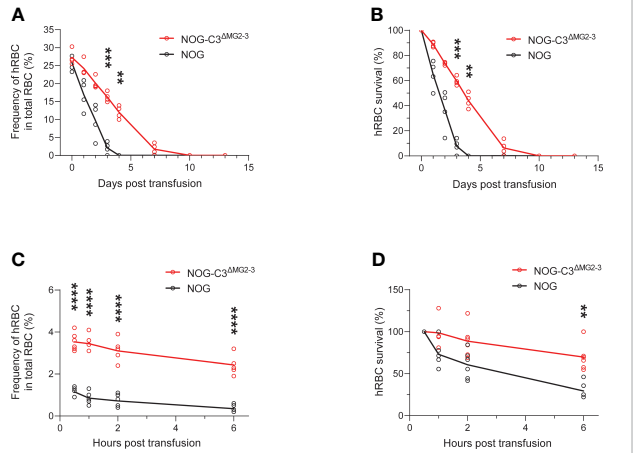

FIGURE 2 | Elimination of hRBCs in NOG and NOG-C3$^{\Delta MG2-3}$ mice. **(A, C)** Changes in the frequencies of hRBCs relative to total RBCs over time. PB samples from NOG and NOG-C3$^{\Delta MG2-3}$ mice were collected and analyzed at the indicated time points (same as in **Figure 1**). Each group (red line for NOG-C3$^{\Delta MG2-3}$ and black line for NOG) consisted of four mice **(A)** or six mice **(C)**. The numbers of transfused hRBCs were 5.0 x 10^9 **(A)** and 2.5 x 10^8 **(C)**. **(B, D)** Survival rates of hRBCs. The values in **(B, D)** were calculated from **(A, C)**, respectively, as percentages relative to the value on day 0. Asterisks indicate statistically significant differences between NOG-C3$^{\Delta MG2-3}$ and NOG mice as determined by two-way repeated-measures ANOVA (****p < 0.0001, ***p < 0.001 and **p < 0.01).

their natural lifespan. Hence, we depleted mouse macrophages by treating NOG and NOG-C3$^{\Delta MG2-3}$ mice with Clo-lip, which has been previously shown to extend hRBC survival. After four Clo-lip injections at 3–4-day intervals, we transfused hRBCs into NOG and NOG-C3$^{\Delta MG2-3}$ mice. Consistent with the previous reports, Clo-lip extended the survival of hRBCs in NOG mice. We detected 34.7% ± 16.8% and 13.5% ± 12.1% of the initial amount of hRBCs at 4 and 7 dpt, respectively (**Figures 3A, B**). The half-life of hRBCs extended from 1–2 days to 2–3 days in NOG mice; nevertheless, the difference between Clo-lip-treated NOG mice and saline-treated control mice was not statistically significant (**Figure 3B**). By contrast, the extension of hRBC survival was profound in NOG-C3$^{\Delta MG2-3}$ mice. The survival rates of hRBCs were 71.9% ± 5.6% at 7 dpt, 38.9% ± 12.0% at 13 dpt, and 18.9% ± 10.1% at 21 dpt (**Figure 3C**); hRBC half-life was extended from 3–4 days to 10–13 days (**Figure 3D**). Notably, a significant number of hRBCs could be detected up to 1 month after a single transfusion of hRBCs.

$GdCl_3$ Prolongs hRBC Survival Without Causing Phenotypic Abnormalities

Despite the prolonged hRBC survival in NOG and NOG-C3$^{\Delta MG2-3}$ mice after Clo-lip treatment, Clo-lip caused significant toxicity. Two of four NOG mice and two of five NOG-C3$^{\Delta MG2-3}$ mice died during the experiments (**Figure 3**), and the remaining mice exhibited aberrant phenotypes, including ruffled hair, weight loss, and a hunched posture (data not shown). Hence, alternative chemicals are required to either deplete or suppress mouse macrophages.

$GdCl_3$ has been shown to deplete or suppress macrophages in rats (31) and mice (33). In this study, we administered 30 mg/kg of $GdCl_3$ four times at 3–4-day intervals. This dosing was determined based on preliminary results from titration experiments (data not shown). Immunohistochemistry showed that Clo-lip induced severe depletion of F4/80-positive macrophages in the spleen and liver of NOG mice (**Figure 4**). Recovery of hepatic macrophages was detected at 7 days post Clo-lip treatment, and a few macrophages were detected in the spleen. In contrast to Clo-lip, $GdCl_3$ did not deplete macrophages in the liver of NOG mice, although there were some morphological changes such as swelling (**Figure 4A**). $GdCl_3$ also induced a mild reduction of macrophages in the spleen (**Figure 4B**). Notably, $GdCl_3$ treatment did not cause significant toxicity, in sharp contrast to Clo-lip. $GdCl_3$-treated mice did not develop overt phenotypic abnormalities, and, although the mice experienced a slight weight loss early after $GdCl_3$ treatment, mouse weight returned to physiological levels at 1 week after treatment (**Supplementary Figure 3**).

Importantly, $GdCl_3$ treatment of NOG and NOG-C3$^{\Delta MG2-3}$ mice before hRBC transfusion significantly extended the survival of hRBCs. In NOG mice, hRBC half-life was extended from 1–2 days to approximately 4 days after transfusion (**Figures 5A, B**). The extension of hRBC survival was confirmed in NOG-C3$^{\Delta MG2-3}$ mice, where $GdCl_3$ increased hRBC half-life from 2–4 days to nearly 8 days. At 12 dpt, 18.3% ± 6.6% of the initial hRBC count was retained, which was equivalent to ~5% of the total RBC count in the mouse blood (**Figures 5C, D**). The effects of $GdCl_3$ were also

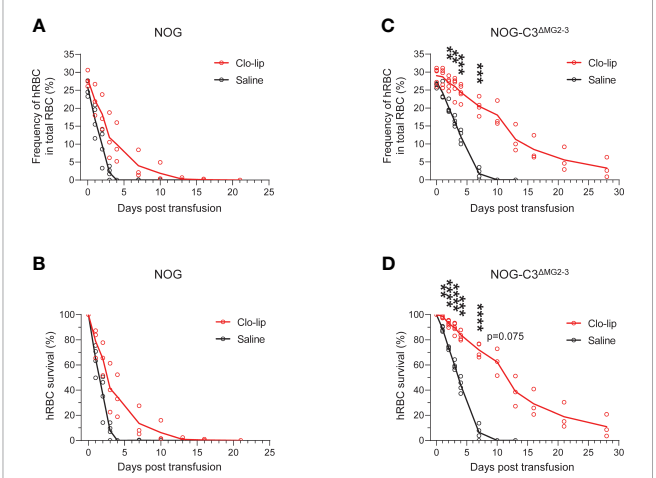

FIGURE 3 | Prolonged survival of hRBCs after Clo-lip treatment. NOG and NOG-C3$^{\Delta MG2-3}$ mice were treated with Clo-lip four times at 3–4-day intervals. Mice were transfused with hRBCs at 1 day after the last Clo-lip treatment. Frequencies **(A, C)** and survival rates **(B, D)** of transfused hRBCs in NOG mice **(A, B)** and NOG-C3$^{\Delta MG2-3}$ mice **(C, D)**. The NOG group consisted of four saline-treated and four Clo-lip-treated mice. The NOG-C3$^{\Delta MG2-3}$ group consisted of four saline-treated and five Clo-lip-treated mice. Two Clo-lip-injected NOG mice (on days 0 and 28) and two Clo-lip-injected NOG-C3$^{\Delta MG2-3}$ mice (on days 7 and 10) died during the experiment. Asterisks indicate statistically significant differences between Clo-lip-injected mice and saline-injected mice as determined using Mixed-effects analysis (****p < 0.0001, ***p < 0.001, and **p < 0.01).

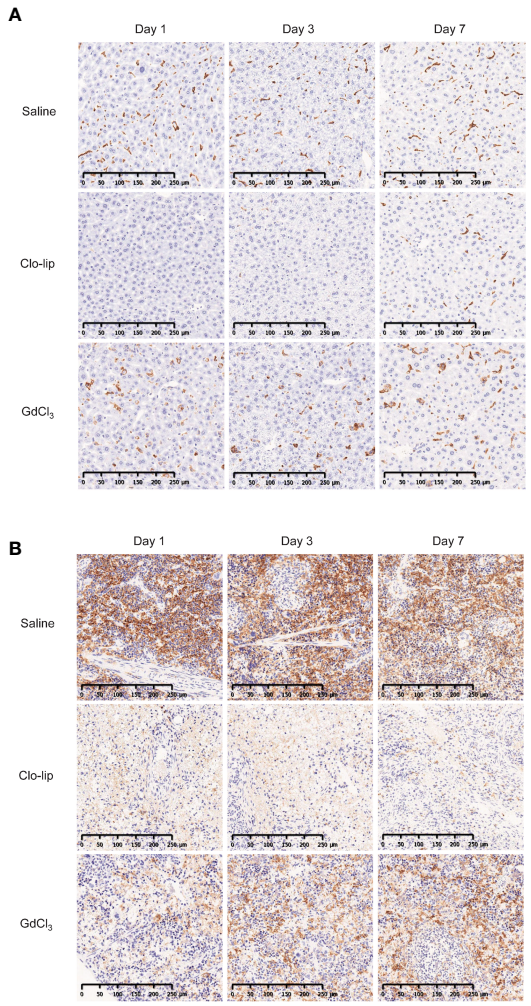

FIGURE 4 | Effects of Clo-lip and $GdCl_3$ on macrophages in NOG mice. NOG mice were administered saline, Clo-lip, or $GdCl_3$ four times at 3–4-day intervals. Livers **(A)** and spleens **(B)** were excised at 1, 3, or 7 days after the last treatment. Tissue macrophages were detected with anti-F4/80 antibody and visualized using diaminobenzidine (brown). Representative images are shown.

confirmed in NOG mice with a smaller number of hRBCs (2.5×10^8) (**Supplementary Figure 4**).

Notably, $GdCl_3$ did not cause significant toxicity in NOG or NOG-C3$^{\Delta MG2\text{-}3}$ mice, and no deaths occurred during the experiments (data not shown).

Long-Term Maintenance of hRBCs by Multiple Injections in NOG-C3$^{\Delta MG2\text{-}3}$ Mice

After confirming prolonged survival of hRBCs in NOG-C3$^{\Delta MG2\text{-}3}$ mice, multiple injections of hRBCs and $GdCl_3$ were administered to maintain the level of hRBCs in the circulation for an extended period. To ensure initial elimination of mouse macrophages, Clo-lip was administered as the initial treatment, followed by three $GdCl_3$ treatments at 3–4-day intervals. After pretreatment, 5.0×10^9 hRBCs were administered to NOG mice on day 0, and $GdCl_3$ was administered on days 2, 5, and 8 by i.p. injection. Consecutive administration of $GdCl_3$ did not prolong the survival of hRBCs in NOG mice. The additional administration of 5.0×10^9 hRBCs by i.p. injection on day 5 transiently increased the amount of hRBCs on the following day; however, they rapidly decreased thereafter (**Supplementary Figure 5**). NOG-C3$^{\Delta MG2\text{-}3}$ mice showed better results. After pretreatment, 5.0×10^9 hRBCs were administered both by i.v. and i.p. injections on day 0, to increase the initial loading amount. Thereafter, $GdCl_3$ was i.p.-injected every 4–6 days, and 5.0×10^9 hRBCs were administered by i.p. injection once a week for 3 weeks. The proportion of hRBCs in PB was around 25% after the first injection of hRBCs, and gradually increased with every hRBC injection (**Figure 6**). The proportion of hRBCs in two mice reached nearly 100% by day 15 and was maintained for 2 weeks. The other two mice showed about 80% chimerism by day 28. During the experiment, one mouse died on day 20; all of the other mice were healthy. These results indicate that NOG-C3$^{\Delta MG2\text{-}3}$ mice are significantly superior with respect to the maintenance of hRBCs compared with NOG mice.

Induction of Human RBCs From Human HSCs

Long-term maintenance of transfused hRBCs in NOG-C3$^{\Delta MG2\text{-}3}$ mice allowed for examination of the differentiation of hRBCs from hHSCs. Our preliminary experiments suggested that Clo-lip, but not $GdCl_3$, induced a few hRBCs (not greater than 1% in

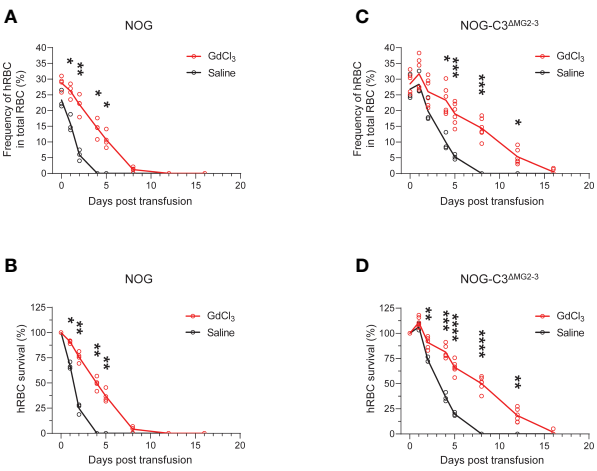

FIGURE 5 | Prolonged survival of hRBCs in NOG-C3$^{\Delta MG2\text{-}3}$ mice treated with $GdCl_3$. NOG and NOG-C3$^{\Delta MG2\text{-}3}$ mice were treated with $GdCl_3$ four times at 3–4-day intervals. Mice were then transfused with hRBCs at 1 day after the last Clo-lip treatment. Frequencies **(A, C)** and survival rates **(B, D)** of transfused hRBCs in NOG mice **(A, B)** and NOG-C3$^{\Delta MG2\text{-}3}$ mice **(C, D)**. The NOG group consisted of three saline-treated and four Clo-lip-treated mice. The NOG-C3$^{\Delta MG2\text{-}3}$ group consisted of three saline-treated and six Clo-lip-treated mice. Asterisks indicate statistically significant differences between Clo-lip-injected mice and saline-injected mice as determined using two-way repeated-measures ANOVA (****$p < 0.0001$, ***$p < 0.001$, **$p < 0.01$, and *$p < 0.05$).

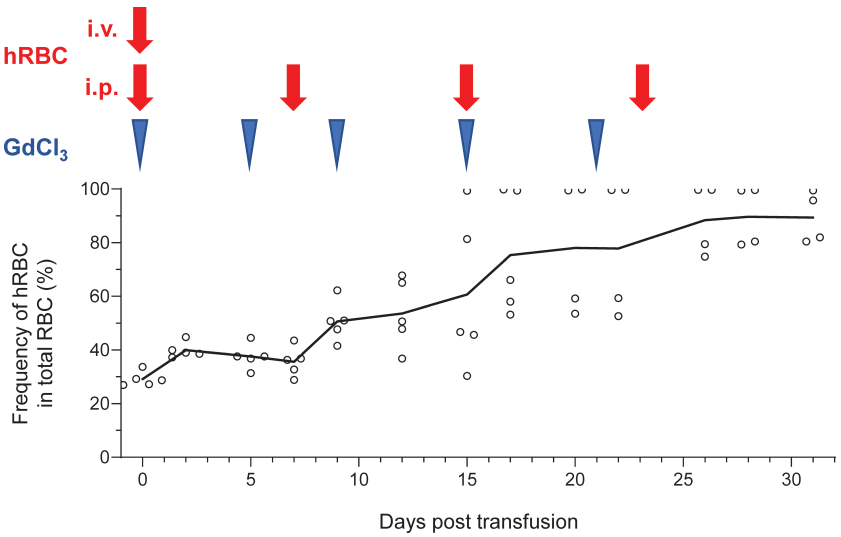

FIGURE 6 | Long-term stable maintenance of hRBCs by repeated administration of hRBCs and $GdCl_3$ in NOG-C3$^{\Delta MG2-3}$ mice. NOG-C3$^{\Delta MG2-3}$ mice were treated with Clo-lip once, and subsequently with $GdCl_3$ three times at 3–4-day intervals. Mice were transfused with i.v. (5.0×10^9) and i.p. (5.0×10^9) injections of hRBCs on the next day of the pretreatment cycle, to increase the initial number of hRBCs and avoid transient polycythemia. $GdCl_3$ was administered every 4–6 days to suppress murine macrophages. hRBCs were i.p.- injected every 7–8 days. The NOG-C3$^{\Delta MG2-3}$ group consisted of five mice. The average numbers of hRBCs at the indicated time points are shown, along with the values from each individual mouse. Blue arrow heads and red arrow represent administration of $GdCl_3$ and hRBC supplementation, respectively.

PB) in hHSC-NOG-C3$^{\Delta MG2-3}$ mice. Thus, we used NOG-C3$^{\Delta MG2-3}$/hGM-CSF-IL-3 (hGM3) Tg mice to enhance erythropoiesis and human myelopoiesis (15). The proportion of hRBCs in some hHSC-NOG-C3$^{\Delta MG2-3}$/hGM3 Tg mice reached approximately 8-10% in PB after three-time injections of Clo-lip. However, nearly half of the mice both in the NOG-C3$^{\Delta MG2-3}$/hGM3 Tg and hHSC-NOG/hGM3 Tg groups died during the experiments, resulting in a large variance and the absence of a statistical significance between these two groups (**Figure 7A**). The BM analysis showed an enhanced development of human erythrocytes in the NOG-C3$^{\Delta MG2-3}$/hGM3 Tg and hHSC-NOG/hGM3 Tg mice (**Figure 7B**). About 40% of them were CD71$^+$ CD235a$^+$ immature erythrocytes, indicating the erythropoiesis from hHSC in the BM (**Figure 7C**).

DISCUSSION

In this study, we investigated the molecular mechanisms underlying the rapid elimination of hRBCs from mouse circulation and identified mouse C3 as a critical mediator of hRBC depletion. We generated a C3-deficient NOG mouse strain, NOG-C3$^{\Delta MG2-3}$, in which clearance of transfused hRBCs was significantly slower than in NOG mice. Chemical depletion or suppression of mouse macrophages in NOG-C3$^{\Delta MG2-3}$ mice further extended the survival of transfused hRBCs; thus, repeated administration of less toxic $GdCl_3$ and hRBCs produced stable hRBC-bearing NOG-C3$^{\Delta MG2-3}$ mice for more than 4 weeks.

The intolerance to hRBCs of NOG mice highlights the ability of innate immune cells to recognize xenogeneic cells and tissue. The innate immune system captures a wide variety of exogenous and "self-derived" antigens *via* multi-layered molecular systems involving Toll-like, lectin, and scavenger receptors. We hypothesized that the transfused hRBCs were exposed to soluble innate factors in the circulation, thereby contributing to their rapid clearance. The results showed deposition of mouse complement molecules on hRBCs, indicating that these molecules act as opsonins covering the surfaces of transfused hRBCs. A role of complement factors in hRBC elimination has previously been suggested (30). Chen et al. also recently reported that murine complement depletion by cobra venom factor (CVF) significantly prolonged the survival of infused hRBCs in NOD/SCID and NOD/SCID β2m-deficient mice treated with Clo-lip (25). In our NOG-C3$^{\Delta MG2-3}$ mice, genetic C3 depletion was sufficient to significantly extend the survival of hRBCs without Clo-lip treatment. CVF treatment may not completely eliminate complement molecules in mice.

Despite the prolonged survival of hRBCs in NOG-C3$^{\Delta MG2-3}$ and macrophage-depleted NOG mice, the hRBC lifespan in the mice was significantly shorter than the natural lifespan of hRBCs (up to 120 days). Notably, there was a synergistic effect between C3 deficiency and depletion of mouse macrophages. This was most evident during the initial 4 days after hRBC transfusion. NOG-C3$^{\Delta MG2-3}$ and Clo-lip-treated NOG mice showed a 50% reduction of hRBCs at 4 dpt, while there was a 15–20% reduction in Clo-lip-treated NOG-C3$^{\Delta MG2-3}$ mice; this synergy indicates that two major mechanisms, macrophage-dependent and C3-

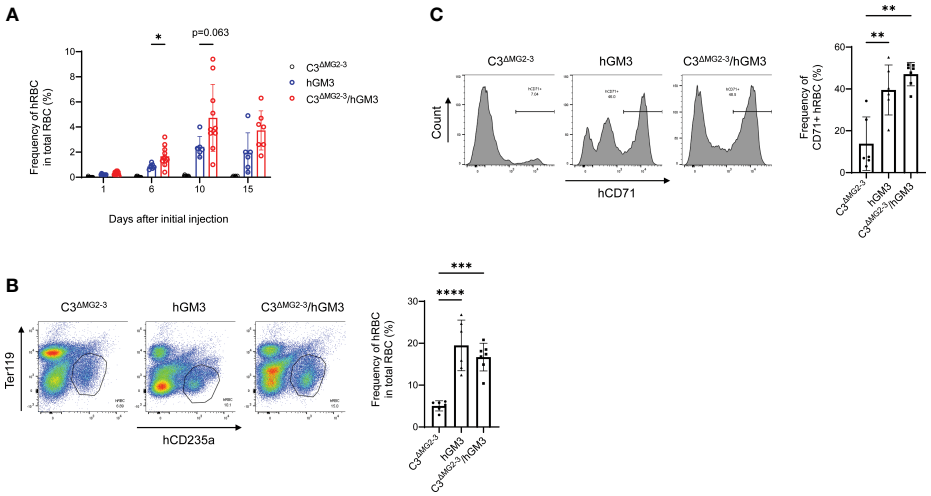

FIGURE 7 | Induction of hRBCs from hHSCs in NOG-C3$^{\Delta MG2\text{-}3}$/hGM3 Tg mice. **(A)** Development of hRBCs in hHSC engrafted mice. hHSC-NOG-C3$^{\Delta MG2\text{-}3}$/hGM3 Tg (n=13), hHSC-NOG-C3$^{\Delta MG2\text{-}3}$ (n=15), or hHSC-NOG/hGM3 Tg (n=10) mice were treated with Clo-lip 8 weeks after HSC transplantation. PB was collected at the indicated time points and analyzed using flow cytometry. Note that six, nine and four in the hHSC-NOG-C3$^{\Delta MG2\text{-}3}$/hGM3 Tg, hHSC-NOG-C3$^{\Delta MG2\text{-}3}$, or hHSC-NOG/hGM3 Tg died during the experiments. Asterisks indicate statistically significant differences between hHSC-NOG-C3$^{\Delta MG2\text{-}3}$ and hHSC-NOG/hGM3 Tg mice as determined using Mixed-effects analysis (****$p < 0.0001$, **$p < 0.01$, and *$p < 0.05$). **(B, C)** Analysis of BM. BM cells from mice in **(A)** were collected 15 days after the initial Clo-lip treatment and stained with anti-hCD235a and anti-hCD71 antibodies. Representative FACS plots are shown with the frequency of human CD235a$^+$ cells in total RBC **(B)**. The frequencies of CD71$^+$ immature hRBC in human CD235a$^+$ hRBCs are shown with the representative FACS histograms **(C)**.

dependent, independently promote hRBC elimination in NOG mice. Considering the expression of C3 receptors in macrophages, these two mechanisms would be partially, but not totally, overlapped. In addition, a significant decay of hRBCs in Clo-lip-treated NOG-C3$^{\Delta MG2\text{-}3}$ mice in the early phase after Clo-lip treatment indicates that mechanisms independent of C3 or macrophages are likely involved to some extent. Because macrophages recover around 7 days after depletion by Clo-lip, hRBCs would be exposed to macrophage-dependent mechanisms and eliminated in the later phase.

The histological analysis of hRBC distribution in NOG mice showed engulfment of hRBCs by mouse CD68$^+$ macrophages in the spleen and liver at 24 hours after hRBC transfusion (**Supplementary Figure 6**), indicating that transfused hRBCs are trapped in the reticuloendothelial system. The molecular mechanisms underlying the engulfment by macrophages remain to be clarified. Humoral molecules, including C3, may facilitate phagocytosis as opsonins. In addition, macrophages may have unique receptors that directly recognize surface antigens on hRBCs. Siglec-1 was previously reported to bind xenogeneic RBCs (39, 40) and this mechanism may be responsible for the elimination of hRBCs. Regarding C3-dependent mechanisms, because NOD mice lack a functional C5 gene due to the hemolytic complement (*Hc*) mutation (41, 42), the effects of C3 on hRBC clearance could be mediated by cellular mechanisms rather than complement cascade-dependent lysis, which requires the activation of C5–C9 molecules. C3 may induce phagocytic cells, including both macrophages and non-macrophages, to eliminate hRBCs. Alternatively, C3-dependent mechanisms may sequester hRBCs in some tissues independent of phagocytosis, although this remains to be clarified.

Treatment with chemical compounds to suppress mouse macrophages is required to maximize the utility of hRBC-infused NOG-C3$^{\Delta MG2\text{-}3}$ mouse models. In the present study, hRBCs were maintained in NOG-C3$^{\Delta MG2\text{-}3}$ mice for nearly one month by weekly injections of hRBCs and $GdCl_3$. Since, current protocols for maintaining hRBCs in immunodeficient mice require daily injections of hRBCs, our model practically facilitates the production and handling of hRBC-engrafted mouse models. In addition, the time required for replenishment of hRBCs in NOG-C3$^{\Delta MG2\text{-}3}$ mice is significantly longer than that in conventional NOG mice, which facilitates recapitulation of the erythrocytic cycle of malaria parasites, in which infection and rupture of hRBCs occur repeatedly.

The comparison of three different mouse strains with hHSCs indicates that there are several requirements for establishing hRBC-engrafted models. Firstly, the enhanced difference of human erythropoiesis in NOG-C3$^{\Delta MG2\text{-}3}$/hGM3 Tg or NOG/hGM3Tg mice compared to NOG-C3$^{\Delta MG2\text{-}3}$ mice indicates that human GM-CSF and IL-3 play a dominant role in human erythropoiesis in the BM. Secondly, the relatively higher frequency of mature hRBCs in the PB in NOG-C3$^{\Delta MG2\text{-}3}$/hGM3 Tg than in NOG/hGM3Tg mice showed the importance of C3 deficiency. Considering the similar level of erythropoiesis in the BM in these two strains, however, C3 deficiency would facilitate accumulation of hRBCs in the periphery rather than promoting erythropoiesis. In addition to these two requirements, strong elimination of mouse macrophages is essential. It would

be supportive that a paper by Song demonstrated that simultaneous transplantation of human liver and HSC achieved the development of hRBC from human HSC in MISTRG mice with the additive genetic deficiency in the fumarylacetoacetate hydrolase gene (*Fah*$^{-/-}$) (23). This model strongly enhances human hematopoiesis by human M-CSF, IL-3, GM-CSF, and thrombopoietin (9). In addition, after reconstitution of human liver, the dual chimera mice with human liver had decrease amounts of mouse C3 and mouse Kupffer cells. Hence, this model and ours have some similarities. Indeed, chimeric ratio of hRBC in the PB was close between these two models.

In conclusion, NOG-C3$^{\Delta MG2-3}$ mice were shown to be suitable for producing a long-term hRBC-bearing mouse model. Further studies are needed to identify the molecular mechanisms underlying macrophage-mediated hRBC elimination, for the generation of better mouse models in which hRBCs can survive for an extended period, ideally close to their natural life span, without using Clo-lip or $GdCl_3$.

DATA AVAILABILITY STATEMENT

The raw data supporting the conclusions of this article will be made available by the authors, without undue reservation.

ETHICS STATEMENT

The studies involving human participants were reviewed and approved by The research ethics committee of the CIEA. The participants provided their written informed consent to participate in this study.

AUTHOR CONTRIBUTIONS

TY, IO and TT designed the project, conducted experiments, and completed the manuscript. MM performed the pathological examinations. MG performed the embryo manipulation. IK and RI contributed to the critical reading of the manuscript. All authors contributed to the article and approved the submitted version,

FUNDING

This work was supported in part by a Grant-in-Aid for Scientific Research (B) (18H02368 to TT) and Grant-in-Aid for Early-Career Scientists (20K15704 to TY). This project was commissioned by a Grant-in-Aid for Research on Hepatitis from the Japan Agency for Medical Research and Development.

ACKNOWLEDGMENTS

We thank Mr. Kenji Kawai for contributing her histology expertise, Ms. Yoko Esaki for mouse embryo manipulation, and Ms. Kayo Tomiyama and Mr. Yasuhiko Ando for animal generation and care. We acknowledge our colleagues at the CIEA for their helpful suggestions and discussions.

SUPPLEMENTARY MATERIAL

The Supplementary Material for this article can be found online at: https://www.frontiersin.org/articles/10.3389/fimmu.2021.671648/full#supplementary-material

REFERENCES

1. Shultz LD, Ishikawa F, Greiner DL. Humanized Mice in Translational Biomedical Research. *Nat Rev Immunol* (2007) 7(2):118–30. doi: 10.1038/nri2017
2. Ito R, Takahashi T, Katano I, Ito M. Current Advances in Humanized Mouse Models. *Cell Mol Immunol* (2012) 9(3):208–14. doi: 10.1038/cmi.2012.2
3. Ito M, Hiramatsu H, Kobayashi K, Suzue K, Kawahata M, Hioki K, et al. NOD/SCID/γ C Null Mouse: An Excellent Recipient Mouse Model for Engraftment of Human Cells. *Blood J Am Soc Hematol* (2002) 100(9):3175–82. doi: 10.1182/blood-2001-12-0207
4. Shultz LD, Lyons BL, Burzenski LM, Gott B, Chen X, Chaleff S, et al. Human Lymphoid and Myeloid Cell Development in NOD/LtSz-Scid IL2Rγnull Mice Engrafted With Mobilized Human Hemopoietic Stem Cells. *J Immunol* (2005) 174(10):6477–89. doi: 10.4049/jimmunol.174.10.6477
5. Traggiai E, Chicha L, Mazzucchelli L, Bronz L, Piffaretti J-C, Lanzavecchia A, et al. Development of a Human Adaptive Immune System in Cord Blood Cell-Transplanted Mice. *Science* (2004) 304(5667):104–7. doi: 10.1126/science.1093933
6. Katano I, Takahashi T, Ito R, Kamisako T, Mizusawa T, Ka Y, et al. Predominant Development of Mature and Functional Human NK Cells in a Novel Human IL-2–Producing Transgenic NOG Mouse. *J Immunol* (2015) 194(7):3513–25. doi: 10.4049/jimmunol.1401323
7. McIntosh BE, Brown ME, Duffin BM, Maufort JP, Vereide DT, Slukvin II, et al. Nonirradiated NOD, B6. SCID Il2rγ–/– KitW41/W41 (NBSGW) Mice Support Multilineage Engraftment of Human Hematopoietic Cells. *Stem Cell Rep* (2015) 4(2):171–80. doi: 10.1016/j.stemcr.2014.12.005
8. Billerbeck E, Barry WT, Mu K, Dorner M, Rice CM, Ploss A. Development of Human CD4+ Foxp3+ Regulatory T Cells in Human Stem Cell Factor–, Granulocyte-Macrophage Colony-Stimulating Factor–, and Interleukin-3–Expressing NOD-SCID Il2rγnull Humanized Mice. *Blood J Am Soc Hematol* (2011) 117(11):3076–86. doi: 10.1182/blood-2010-08-301507
9. Rongvaux A, Willinger T, Martinek J, Strowig T, Gearty SV, Teichmann LL, et al. Development and Function of Human Innate Immune Cells in a Humanized Mouse Model. *Nat Biotechnol* (2014) 32(4):364–72. doi: 10.1038/nbt.2858
10. Mathews S, Woods AB, Katano I, Makarov E, Thomas MB, Gendelman HE, et al. Human Interleukin-34 Facilitates Microglia-Like Cell Differentiation and Persistent HIV-1 Infection in Humanized Mice. *Mol Neurodegeneration* (2019) 14(1):1–15. doi: 10.1186/s13024-019-0311-y
11. Danner R, Chaudhari SN, Rosenberger J, Surls J, Richie TL, Brumeanu T-D, et al. Expression of HLA Class II Molecules in Humanized NOD. Rag1KO. IL2RgcKO Mice Is Critical for Development and Function of Human T and B Cells. *PloS One* (2011) 6(5):e19826. doi: 10.1371/journal.pone.0019826
12. Harui A, Kiertscher SM, Roth MD. Reconstitution of huPBL-NSG Mice With Donor-Matched Dendritic Cells Enables Antigen-Specific T-Cell Activation. *J Neuroimmune Pharmacol* (2011) 6(1):148–57. doi: 10.1007/s11481-010-9223-x
13. Katano I, Nishime C, Ito R, Kamisako T, Mizusawa T, Ka Y, et al. Long-Term Maintenance of Peripheral Blood Derived Human NK Cells in a Novel Human IL-15-Transgenic NOG Mouse. *Sci Rep* (2017) 7(1):1–14. doi: 10.1038/s41598-017-17442-7

14. Perdomo-Celis F, Medina-Moreno S, Davis H, Bryant J, Taborda NA, Rugeles MT, et al. High Activation and Skewed T Cell Differentiation Are Associated With Low IL-17A Levels in a Hu-PBL-NSG-SGM3 Mouse Model of HIV Infection. *Clin Exp Immunol* (2020) 200(2):185–98. doi: 10.1111/cei.13416
15. Ito R, Takahashi T, Katano I, Kawai K, Kamisako T, Ogura T, et al. Establishment of a Human Allergy Model Using Human IL-3/GM-CSF–Transgenic NOG Mice. *J Immunol* (2013) 191(6):2890–9. doi: 10.4049/jimmunol.1203543
16. Belarif L, Danger R, Kermarrec L, Nerrière-Daguin V, Pengam S, Durand T, et al. IL-7 Receptor Influences Anti-TNF Responsiveness and T Cell Gut Homing in Inflammatory Bowel Disease. *J Clin Invest* (2019) 129(5):1910–25. doi: 10.1172/JCI121668
17. Goettel JA, Gandhi R, Kenison JE, Yeste A, Murugaiyan G, Sambanthamoorthy S, et al. AHR Activation Is Protective Against Colitis Driven by T Cells in Humanized Mice. *Cell Rep* (2016) 17(5):1318–29. doi: 10.1016/j.celrep.2016.09.082
18. Ito R, Maruoka S, Soda K, Katano I, Kawai K, Yagoto M, et al. A Humanized Mouse Model to Study Asthmatic Airway Inflammation *via* the Human IL-33/IL-13 Axis. *JCI Insight* (2018) 3(21):e121580. doi: 10.1172/jci.insight.121580
19. Minkah NK, Schafer C, Kappe SH. Humanized Mouse Models for the Study of Human Malaria Parasite Biology, Pathogenesis, and Immunity. *Front Immunol* (2018) 9:807. doi: 10.3389/fimmu.2018.00807
20. Soulard V, Bosson-Vanga H, Lorthiois A, Roucher C, Franetich J-F, Zanghi G, et al. Plasmodium Falciparum Full Life Cycle and Plasmodium Ovale Liver Stages in Humanized Mice. *Nat Commun* (2015) 6(1):1–9. doi: 10.1038/ncomms8690
21. Kaushansky A, Mikolajczak SA, Vignali M, Kappe SH. Of Men in Mice: The Success and Promise of Humanized Mouse Models for Human Malaria Parasite Infections. *Cell Microbiol* (2014) 16(5):602–11. doi: 10.1111/cmi.12277
22. Rahmig S, Kronstein-Wiedemann R, Fohgrub J, Kronstein N, Nevmerzhitskaya A, Bornhäuser M, et al. Improved Human Erythropoiesis and Platelet Formation in Humanized NSGW41 Mice. *Stem Cell Rep* (2016) 7 (4):591–601. doi: 10.1016/j.stemcr.2016.08.005
23. Song Y, Shan L, Gbyli R, Liu W, Strowig T, Patel A, et al. Combined Liver–Cytokine Humanization Comes to the Rescue of Circulating Human Red Blood Cells. *Science* (2021) 371(6533):1019–25. doi: 10.1126/science.abe2485
24. Hu Z, Van Rooijen N, Yang Y-G. Macrophages Prevent Human Red Blood Cell Reconstitution in Immunodeficient Mice. *Blood J Am Soc Hematol* (2011) 118(22):5938–46. doi: 10.1182/blood-2010-11-321414
25. Chen B, Fan W, Zou J, Zhang S, He J, Shu C, et al. Complement Depletion Improves Human Red Blood Cell Reconstitution in Immunodeficient Mice. *Stem Cell Rep* (2017) 9(4):1034–42. doi: 10.1016/j.stemcr.2017.08.018
26. Tsuji M, Ishihara C, Arai S, Hiratai R, Azuma I. Establishment of a SCID Mouse Model Having Circulating Human Red Blood Cells and a Possible Growth of Plasmodium Falciparum in the Mouse. *Vaccine* (1995) 13 (15):1389–92. doi: 10.1016/0264-410X(95)00081-B
27. Saito-Ito A, Tsuji M, Wei Q, He S, Matsui T, Kohsaki M, et al. Transfusion-Acquired, Autochthonous Human Babesiosis in Japan: Isolation of Babesia Microti-Like Parasites With Hu-RBC-SCID Mice. *J Clin Microbiol* (2000) 38 (12):4511–6. doi: 10.1128/JCM.38.12.4511-4516.2000
28. Angulo-Barturen I, Jiménez-Díaz MB, Mulet T, Rullas J, Herreros E, Ferrer S, et al. A Murine Model of Falciparum-Malaria by *In Vivo* Selection of Competent Strains in Non-Myelodepleted Mice Engrafted With Human Erythrocytes. *PloS One* (2008) 3(5):e2252. doi: 10.1371/journal.pone.0002252
29. Ishihara C, Hiratai R, Tsuji M, Yagi K, Nose M, Azuma I. Mannan Decelerates the Clearance of Human Red Blood Cells in SCID Mouse. *Immunopharmacology* (1998) 38(3):223–8. doi: 10.1016/S0162-3109(97)00054-4
30. Ishihara C, Tsuji M, Hagiwara K, Hioki K, Arikawa J, Azuma I. Transfusion With Xenogeneic Erythrocytes Into SCID Mice and Their Clearance From the Circulation. *J Veterinary Med Sci* (1994) 56(6):1149–54. doi: 10.1292/jvms.56.1149
31. Vollmar B, Rüttinger D, Wanner GA, Leiderer R, Menger MD. Modulation of Kupffer Cell Activity by Gadolinium Chloride in Endotoxemic Rats. *Shock (Augusta Ga)* (1996) 6(6):434–41. doi: 10.1097/00024382-199612000-00008
32. Zhu R, Guo W, Fang H, Cao S, Yan B, Chen S, et al. Kupffer Cell Depletion by Gadolinium Chloride Aggravates Liver Injury After Brain Death in Rats. *Mol Med Rep* (2018) 17(5):6357–62. doi: 10.3892/mmr.2018.8646
33. Nishioka T, Kuroishi T, Sugawara Y, Yu Z, Sasano T, Endo Y, et al. Induction of Serum IL-18 With Propionibacterium Acnes and Lipopolysaccharide in Phagocytic Macrophage-Inactivated Mice. *J Leukocyte Biol* (2007) 82(2):327–34. doi: 10.1189/jlb.1006598
34. Ran FA, Hsu PD, Wright J, Agarwala V, Scott DA, Zhang F. Genome Engineering Using the CRISPR-Cas9 System. *Nat Protoc* (2013) 8(11):2281–308. doi: 10.1038/nprot.2013.143
35. Hsu PD, Lander ES, Zhang F. Development and Applications of CRISPR-Cas9 for Genome Engineering. *Cell* (2014) 157(6):1262–78. doi: 10.1016/j.cell.2014.05.010
36. Cong L, Ran FA, Cox D, Lin S, Barretto R, Habib N, et al. Multiplex Genome Engineering Using CRISPR/Cas Systems. *Science* (2013) 339(6121):819–23. doi: 10.1126/science.1231143
37. Mashiko D, Fujihara Y, Satouh Y, Miyata H, Isotani A, Ikawa M. Generation of Mutant Mice by Pronuclear Injection of Circular Plasmid Expressing Cas9 and Single Guided RNA. *Sci Rep* (2013) 3:3355. doi: 10.1038/srep03355
38. Schuster MC, Ricklin D, Papp K, Molnar KS, Coales SJ, Hamuro Y, et al. Dynamic Structural Changes During Complement C3 Activation Analyzed by Hydrogen/Deuterium Exchange Mass Spectrometry. *Mol Immunol* (2008) 45 (11):3142–51. doi: 10.1016/j.molimm.2008.03.010
39. Waldman JP, Vogel T, Burlak C, Coussios C, Dominguez J, Friend P, et al. Blocking Porcine Sialoadhesin Improves Extracorporeal Porcine Liver Xenoperfusion With Human Blood. *Xenotransplantation* (2013) 20(4):239–51. doi: 10.1111/xen.12043
40. Waldman JP, Brock LG, Rees MA. A Human-Specific Mutation Limits Nonhuman Primate Efficacy in Preclinical Xenotransplantation Studies. *Transplantation* (2014) 97(4):385. doi: 10.1097/01.TP.0000441321.87915.82
41. Baxter AG, Cooke A. Complement Lytic Activity has No Role in the Pathogenesis of Autoimmune Diabetes in NOD Mice. *Diabetes* (1993) 42 (11):1574–8. doi: 10.2337/diab.42.11.1574
42. Wetsel R, Fleischer DT, Haviland D. Deficiency of the Murine Fifth Complement Component (C5). A 2-Base Pair Gene Deletion in a 5'-Exon. *J Biol Chem* (1990) 265(5):2435–40. doi: 10.1016/S0021-9258(19)39817-5

Conflict of Interest: The authors declare that the research was conducted in the absence of any commercial or financial relationships that could be construed as a potential conflict of interest.

Advantages of publishing in Frontiers

OPEN ACCESS
Articles are free to read for greatest visibility and readership

FAST PUBLICATION
Around 90 days from submission to decision

HIGH QUALITY PEER-REVIEW
Rigorous, collaborative, and constructive peer-review

TRANSPARENT PEER-REVIEW
Editors and reviewers acknowledged by name on published articles

Frontiers
Avenue du Tribunal-Fédéral 34
1005 Lausanne | Switzerland

Visit us: www.frontiersin.org
Contact us: frontiersin.org/about/contact

REPRODUCIBILITY OF RESEARCH
Support open data and methods to enhance research reproducibility

DIGITAL PUBLISHING
Articles designed for optimal readership across devices

FOLLOW US
@frontiersin

IMPACT METRICS
Advanced article metrics track visibility across digital media

EXTENSIVE PROMOTION
Marketing and promotion of impactful research

LOOP RESEARCH NETWORK
Our network increases your article's readership